Sepsis-induced cardiac dysfunction:
Pathophysiology and experimental treatments

A thesis presented by

Dr Jianmin Chen

registered at

Barts and The London School of Medicine and Dentistry

Queen Mary

University of London

for the degree of

Doctor of Philosophy

Centre for Translational Medicine & Therapeutics,

The William Harvey Research Institute

John Vane Science Centre, Charterhouse Square,

London EC1M 6BQ, United Kingdom

| ABSTRACT

The severity of cardiac dysfunction predicts mortality in septic patients. In this thesis, I have investigated the pathophysiology and the novel therapeutic strategy to attenuate cardiac dysfunction in experimental sepsis.

I have developed a model of cardiac dysfunction caused by lipopolysaccharide (LPS)/peptidoglycan (PepG) co-administration or polymicrobial sepsis in young and old, male and female mice. There is good evidence that females tolerate sepsis better than males. Here, I have demonstrated for the first time that the cardiac dysfunction caused by sepsis was less pronounced in female than in male mice; this protection was associated with cardiac activation of a pro-survival pathway [Akt and endothelial nitric oxide synthase], and the decreased activation of a pro-inflammatory signalling pathway [nuclear factor (NF)-κB].

Patients with chronic kidney disease (CKD) requiring dialysis have a higher risk of sepsis and a 100-fold higher mortality. Activation of NF-κB is associated with sepsis-induced cardiac dysfunction and NF-κB is activated by IκB kinase (IKK). Here, I have shown that 5/6th nephrectomy for 8 weeks caused a small, but significant, cardiomyopathy, cardiac activation of NF-κB and expression of inducible nitric oxide synthase (iNOS). When subjected to LPS or polymicrobial sepsis, CKD mice exhibited exacerbation of cardiac dysfunction and cardiac activation of NF-κB and iNOS expression, which were attenuated by a specific IKK inhibitor (IKK 16). Thus, selective inhibition of IKK may represent a novel therapeutic approach for the sepsis-induced cardiac dysfunction in CKD patients.

Activation of transient receptor potential vanilloid receptor type 1 (TRPV1) improves outcome in sepsis/endotoxaemia. The identity of the endogenous activators of TRPV1 and the role of the channel in the cardiac dysfunction caused by sepsis/endotoxaemia is unknown. Here, I have shown that activation of TRPV1 by 12-(S)-HpETE and 20-HETE (potent ligands of TRPV1) leads to the release of calcitonin gene-related peptide (downstream mediator of TRPV1 activation), which protects the heart against the cardiac dysfunction caused by LPS.

| ACKNOWLEDGEMENTS

I would first like to express my enormous gratitude to my brilliant PhD supervisor, Prof Christoph Thiemermann, for his great support, encouragement, mentoring and guidance in my study as well as my personal life throughout the last four years, and I could not thank him more, and he continues to be my great mentor.

I would also like to acknowledge China Scholarship Council for granting me a PhD scholarship, and many colleagues who made this thesis possible. In particular, I would like to thank Dr Nimesh Patel, as my secondary supervisor, for the enlightening discussions and his help. I would also like to thank Dr Sina Coldewey and Dr Areeg Khan for teaching me the echocardiography, CLP and myocardial infarction models during my early PhD, Mr Julius Kieswich for his help with CKD model, Dr Thomas Gobbetti for his support with macrophage study and bacterial counting, Mr Alexander Hamers and Dr Michaela Finsterbusch for working together with me on TRPV1 project, Prof Amrita Ahluwalia for sharing her knowledge and always lending a helping hand, Prof Magdi Yaqoob for his enthusiastic support, and at last, but not least, Prof Massimo Collino and Mr Fausto Chiazza for their support with signalling analysis, and for accommodating me in the Department of Drug Science and Technology, University of Turin to learn western blot and MPO assays.

During my PhD in William Harvey Research Institute, I have had the great pleasure developing a number of friendships; in particular, I would like to thank Flow and Regina for sharing life stories and being great supporters.

Finally, I would like to express a heartfelt thank you to my family - my Mum, Dad, Brother, Sister-in-law, Nephew and Niece - and friends - Cindy, Irina and Beeny for their love, encouragement and unending support.

| DECLARATION

I declare that this thesis is a presentation of my original research.

I acknowledge that Dr Thomas Gobbetti has carried out the macrophage study and the bacterial counting of the peritoneal lavage samples I have generated (chapter III). I also acknowledge that Mr Alexander Hamers and Dr Michaela Finsterbusch have carried out the western blot analysis on TRPV1 phosphorylation and the neuropeptides measurements of the samples I have generated (chapter IV).

Name: Dr Jianmin Chen

Signature:

Supervisor: Prof Christoph Thiemermann

Signature:

Date: London, 28/07/2016

| LIST OF PUBLISHED PAPERS

Jianmin Chen*, Alexander J.P. Hamers*****, Michaela Finsterbusch, Maleeha Zafar, Roger Corder, Romain A. Colas, Jesmond Dalli, Christoph Thiemermann*****, Amrita Ahluwalia***** (2016). Endogenously generated arachidonate-derived ligands for TRPV1 underlie cardiac protection in sepsis. *Nature Communication*, under review. (*****These authors contributed equally to this work)

Jianmin Chen, Julius Kieswich, Fausto Chiazza, Amie J. Moyes, Thomas Gobbetti, Nimesh S.A. Patel, Mauro Perretti, Adrian J. Hobbs, Massimo Collino, Muhammad M. Yaqoob, Christoph Thiemermann (2016). IκB kinase inhibitor attenuates sepsis-induced cardiac dysfunction in CKD. *Journal of the American Society of Nephrology*, DOI: 10.1681/ASN.2015060670.

Jianmin Chen, Christoph Thiemermann. (2016). Selenium and niacin for sepsis therapy: The sum is greater than its parts. *Critical Care Medicine,* 44(6):1256-7. doi: 10.1097/CCM.0000000000001493.

Jianmin Chen, Fausto Chiazza, Massimo Collino, Nimesh S.A. Patel, Sina M. Coldewey, Christoph Thiemermann. (2014). Gender dimorphism of the cardiac dysfunction in murine sepsis: Signalling mechanisms and age-dependency. *PLoS ONE*, 9(6): e100631.

Thomas Gobbetti, Sina M Coldewey, **Jianmin Chen**, Simon McArthur, Pauline le Fauder, Nicolas Cenac, Roderick J Flower, Christoph Thiemermann, Mauro Perretti. (2014). Non-redundant protective properties of FPR2/ALX in polymicrobial murine sepsis. *Proceedings of the National Academy of Sciences*, 111(52):18685-90.

| LIST OF PUBLISHED ABSTRACTS

Jianmin Chen, Alexander J.P. Hamers, Michaela Finsterbusch, Christoph Thiemermann, Amrita Ahluwalia. Activation of TRPV1 by 12(s)-HpETE and 20-HETE releases CGRP and protects the heart against the cardiac dysfunction caused by LPS. Experimental Biology 2016 Congress, 2nd-6th April 2016, San Diego, USA (Oral presentation). **ASIP Trainee Travel Award winner**

Jianmin Chen, Julius Kieswich, Fausto Chiazza, Thomas Gobbetti, Nimesh S.A. Patel, Mauro Perretti, Massimo Collino, Muhammad M. Yaqoob, Christoph Thiemermann. The cardiac dysfunction caused by sepsis in animals with chronic kidney disease is attenuated by inhibiting IκB kinase. *Shock*, 2015, 44(Supplement 2): 16. 16th Congress of the European Shock Society, 24th-26th September 2015, Cologne, Germany (Oral presentation). **European New Investigator Award, Travel Award winner**

Jianmin Chen, Julius Kieswich, Fausto Chiazza, Thomas Gobbetti, Nimesh S.A. Patel, Mauro Perretti, Massimo Collino, Muhammad M. Yaqoob, Christoph Thiemermann. The cardiac dysfunction caused by sepsis in animals with chronic kidney disease is attenuated by inhibiting IκB kinase. *Shock*, 2015, 43(Supplement 1): 92. Thirty-Eighth Annual Conference on Shock, 6th-9th June 2015, Denver, USA (Poster presentation). **Travel Award winner**

Jianmin Chen, Julius Kieswich, Fausto Chiazza, Nimesh S.A. Patel, Massimo Collino, Muhammad M. Yaqoob, Christoph Thiemermann. Pre-existing chronic kidney disease worsens the myocardial dysfunction caused by sepsis in mice. *pA2 online, E-journal of the British Journal of Pharmacology*, 2015, http://www.pa2online.org/abstract/abstract.jsp?abid=32407&author=J%20Chen&cat= -1&period=-1. Pharmocology 2014, 16th-18th Dec 2014, London (Oral presentation).

Jianmin Chen, Julius Kieswich, Muhammad M. Yaqoob, Christoph Thiemermann. Effects of pre-existing chronic kidney disease on pathophysiology of sepsis. *Shock*, 2014, 41(Supplement 2): 40. Thirty-Seventh Annual Conference on Shock, 7th-10th June 2014, Westin Charlotte, USA (Poster presentation). **Travel Award winner**

Jianmin Chen, Fausto Chiazza, Massimo Collino, Sina M. Coldewey, Nimesh S.A. Patel, Christoph Thiemermann. Gender dimorphism of the cardiac dysfunction in sepsis. *Shock*, 2014, 41(Supplement 2): 35. Thirty-Seventh Annual Conference on Shock, 7th-10th June 2014, Westin Charlotte, USA (Poster presentation).

Jianmin Chen, Julius Kieswich, Fausto Chiazza, Thomas Gobbetti, Nimesh S.A. Patel, Mauro Perretti, Massimo Collino, Muhammad M. Yaqoob, Christoph Thiemermann. The cardiac dysfunction caused by sepsis in animals with chronic kidney disease is attenuated by inhibiting IκB kinase. Czech Medical Mission to the UK, 4th September 2015, London (Invited lecture).

Jianmin Chen, Julius Kieswich, Fausto Chiazza, Nimesh S.A. Patel, Massimo Collino, Muhammad M. Yaqoob, Christoph Thiemermann. Pre-existing chronic kidney disease worsens the myocardial dysfunction caused by sepsis in mice. William Harvey Research Institute New Year Celebration, 13th Feb 2015, London (Oral presentation). **Best oral presentation by a PhD student, William Harvey Medal**

Jianmin Chen, Julius Kieswich, Fausto Chiazza, Nimesh S.A. Patel, Massimo Collino, Muhammad M. Yaqoob, Christoph Thiemermann. Pre-existing chronic kidney disease worsens the myocardial dysfunction caused by sepsis in mice. Pharmocology 2014, 16th-18th Dec 2014, London (Oral presentation).

Jianmin Chen, Fausto Chiazza, Massimo Collino, Sina M. Coldewey, Nimesh S.A. Patel, Christoph Thiemermann. Gender dimorphism of the cardiac dysfunction in sepsis. William Harvey Research Institute Research Review, 1st July 2014, London (Poster presentation).

Jianmin Chen, Julius Kieswich, Muhammad M. Yaqoob, Christoph Thiemermann. Pre-existing chronic kidney disease worsens the myocardial dysfunction caused by sepsis in mice. William Harvey Research Institute Research Review, 1st July 2014, London (Poster presentation).

Jianmin Chen, Nimesh S.A. Patel, Sina M. Coldewey, Christoph Thiemermann. Gender differences in the myocardial dysfunction caused by co-administration of LPS and peptidoglycan in mice. William Harvey Day 2013. 16th October 2013, London (Poster presentation).

Jianmin Chen, Nimesh S.A. Patel, Sina M. Coldewey, Christoph Thiemermann. Gender differences in the myocardial dysfunction caused by co-administration of LPS and peptidoglycan in mice. Young Life Scientists Symposium 2013 Cardiovascular medicine: Bridging clinical and basic researchers. 6th September 2013, London (Poster presentation).

| ABBREVIATIONS

12-(S)-HpETE	12-(S)-hydroperoxyeicosatetraenoic acid
17ODYA	17 octadecynoic acid
20-HETE	20-hydroxyeicosatetraenoic acid
ACCP	American College of Chest Physicians
ALT	alanine aminotransferase
ATS	American Thoracic Society
ASA	acetyl salicylic acid
ASC	apoptosis-associated speck-like protein containing a CARD
AST	serum aspartate aminotransferase
AWERB	Animal Welfare Ethics Review Board
BCA	Bicinchoninic Acid
BIR	baculoviral inhibitory repeat
CAD	coronary artery disease
CARD	caspase recruitment domain
CDC	cinnamyl-3, 4-dihydroxy-a-cyanocinnamate
CGRP	calcitonin gene-related peptide
CHF	congestive heart failure
CI	confidence interval
CKD	chronic kidney disease
CLP	caecal ligation and puncture
CLRs	C-type lectin receptors
CpG	cytosine phosphate guanidine
CRP	C-reactive protein
C-SOM	cyclo-somatostatin
CT	computed tomography
CVD	cardiovascular disease
CVP	central venous pressure
DRGs	dorsal root ganglions
ds	double-stranded
DTT	DL-Dithiethrectol
ECG	electrocardiography

ECSIT	evolutionarily conserved signalling intermediate in Toll pathways
eNOS	endothelial NOS
EPIC	European Prevalence of Infection in Intensive Care
ERK	extracellular signal-regulated kinase
ESBL	extended-spectrum β-lactamases
ESICM	European Society of Intensive Care Medicine
ESRD	end-stage renal disease
ET-1	endothelin-1
FAC	fractional area change
FcRγ	Fc receptor IgE high-affinity I gamma polypeptide
FiO_2	fraction of inspired oxygen
FS	fractional shortening
GFR	glomerular filtration rate
GRADE	Grading of Recommendations Assessment Development and Evaluation
HRP	horseradish peroxidase
KC	keratinocyte-derived cytokine
LBP	LPS binding protein
ICU	intensive care unit
IκB	inhibitor of κB
IKK	IκB kinase
IL	interleukin
iNOS	inducible NOS
IRAK	IL-1 receptor-associated kinase
IRFs	interferon regulatory factors
ISF	International Sepsis Forum
IVS	interventricular septum
JNK	c-Jun amino-terminal kinase
LAD	left anterior descending coronary artery
LPS	lipopolysaccharide
LRR	leucine-rich repeats
LTA	lipoteichoic acid

LVEDV	left ventricular end-diastolic volume
LVEF	left ventricular ejection fraction
LVH	left ventricular hypertrophy
LVID	LV internal dimension
LVPW	LV posterior wall
MAP	mean arterial pressure
MAPK	mitogen-activated protein kinase
MD2	myeloid differentiation protein-2
MDA5	melanoma differentiation-associated protein 5
MEKK	MAPK/extracellular signal-regulated kinases (ERK) kinase kinase
MINCLE	macrophage-inducible C-type lectin
MKKs	MAP kinase kinases
MODS	multiple organ dysfunction syndrome
MPO	myeloperoxidase
MRSA	methicillin-resistant *Staphylococcus aureus*
MyD88	myeloid differentiation primary response gene 88
NACHT	nucleotide-binding oligomerisation
NF	nuclear factor
nNOS	neuronal NO synthase
NO	nitric oxide
NOD	nucleotide-binding oligomerisation domain
NLRC	NLR family CARD-domain–containing protein
NLRP	NOD leucine-rich-repeat and pyrin domain–containing protein
NLRs	nucleotide-binding oligomerisation domain (NOD)-like receptors
NOS	nitric oxide synthases
PaCO2	partial pressure of carbon dioxide
PAMPs	pathogen-associated molecular patterns
PaO$_2$	partial pressure of oxygen
PC	pro-caspase
PepG	peptidoglycan

PI3K	phosphoinositide 3-kinases
PIC	Proteinase Inhibitor cocktail
PIP2	phosphatidylinositol-4,5-bisphosphate
PROWESS	rhAPC Worldwide Evaluation in Severe Sepsis
PRRs	pattern recognition receptors
PVDF	polyvinyldenedifluoride
PYD	pyrin domain
rhAPC	recombinant human activated protein C
RIG-I	retinoic acid inducible gene I protein
RIP	receptor interacting protein
RLRs	retinoic acid inducible gene I-like receptors
ROS	reactive oxygen species
SCCM	Society of Critical Care Medicine
SD	standard deviation
SDS-PAGE	sodium dodecyl sulphatepolyacrylamide gel electrophoresis
SEM	standard error of the mean
SIRS	systemic inflammatory response syndrome
SIS	Surgical Infection Society
SNX	subtotal (5/6th) nephrectomy
SOFA	sequential organ failure assessment
ss	single-stranded
SSC	Surviving Sepsis Campaign
TAB	TAK1-binding protein
TAK	transforming growth factor-β-activated kinase
TBK	TRAF family member-associated NF-κB activator-binding kinase
TIR	Toll/IL-1R
TIRAP	TIR-containing adaptor protein
TLR2-1	TLR2–TLR1 heterodimers
TLR2-2	TLR2–TLR2 heterodimers
TLR2-6	TLR2–TLR6 heterodimers
TLRs	Toll-like receptors
TM	transmembrane domains

TMB	tetramethylbenzidine
TNF	tumor necrosis factor
TRAM	TRIF-related adaptor molecule
TRAF	TNF-α receptor associated factor
TRIF	Toll/interleukin 1 receptor domain-containing adapter inducing IFN-β
TRPV1	transient receptor potential vanilloid receptor type 1
UBC13	ubiquitin conjugating enzymes ubiquitin C13
UEV1A	ubiquitin conjugating enzyme variant 1A
UG	ungraded
VR1	vanilloid receptor type 1
VRE	vancomycin-resistant *Enterococcus*
VSE	vancomycin-sensitive *Enterococcus*
WT	wild-type

Measurements and Units

%	percentage
bpm	beats per min
°C	degrees Celsius
EC50	dose, which elicits 50 % of the maximum response
g	gram
h	hour
HR	heart rate
IC50	concentration, which produces 50 % of the max inhibition
IU	international units
mg/kg	milligram per kilogram
mg/ml	milligram per millilitre
min	min
ml	millilitre
μl	microlitre
ml/kg	millilitre per kilogram

mM	millimolar
µM	micromolar
µmol/L	micromol per litre
mm Hg	millimetres of mercury
n	number
nM	nanomolar
OD	optical density
sec	seconds
w	weeks
y	years

| TABLE OF CONTENTS

| INDEX OF FIGURES

| INDEX OF TABLES

CHAPTER I | GENERAL INTRODUCTION

1.1 Sepsis

1.1.1   Definitions and Diagnosis

The word sepsis originates from the Greek word "σηψις", which refers to decomposition of organic matter in the presence of bacteria [1]. Germ theory was the basis of the initial view of sepsis, in which pathogens were believed to be the only cause of sepsis [2, 3]. However, the failure of decades of intensive efforts to treat sepsis with antibiotic therapy alone, led to the new hypothesis that an excessive systemic inflammatory response of the host importantly contributes to the pathophysiology of sepsis [4]. In 1991, a consensus conference held in Chicago by the American College of Chest Physicians (ACCP) and the Society of Critical Care Medicine (SCCM) proposed a new definition of sepsis as a systemic inflammatory response syndrome (SIRS) as a result of a presumed or proven infectious process (Table 1.1) [5]. SIRS is a description of an inflammatory process caused by a wide variety of insults (not limited to infection), such as trauma, burns, pancreatitis or surgery. The diagnostic criteria for SIRS are based on the presence of two or more of the following clinical manifestations: abnormal body temperature, greater heart rate, greater respiratory rate, and/or alternated peripheral leukocyte count [5]. Based on cardiovascular response and altered organ function, the severity of sepsis was graded as severe sepsis, septic shock, multiple organ dysfunction syndrome (MODS) (Table 1.1) [5]. These concepts have been adopted by clinicians and researchers worldwide and have greatly facilitated the written and verbal communications relating to sepsis, improved clinical care and served as the foundation for establishing entry criteria for clinical trials. However, the diagnostic criteria for SIRS were regarded to be overly sensitive and not specific to sepsis. The criteria did not include elevated circulating levels of biomarkers for sepsis, such as plasma C-reactive protein (CRP) or procalcitonin [6].

Table 1.1 Definitions based on 1991 ACCP/ SCCM Consensus Conference.

Term	Definition
SIRS	Inflammatory process caused by a wide variety of severe insults. It is diagnosed by the presence of two or more of the following clinical manifestations: (1) body temperature > 38.3ºC or < 36ºC (hyperthermia or hypothermia); (2) heart rate > 90 beats/min (tachycardia); (3) respiratory rate > 20 breaths/min (tachypnea) or PaCO2 < 32 mm Hg; (4) peripheral leukocyte count > 12.000/mm^3 or < 4.000/ mm^3 or > 10% immature forms (bands) (leukocytopenia or leukocytosis).
Sepsis	The SIRS due to presumed or proven infectious process.
Severe sepsis	Sepsis accompanied by organ dysfunction, hypoperfusion or hypotension.
Septic shock	Sepsis accompanied by circulatory collapse evidenced by hypotension despite adequate fluid resuscitation. Sepsis-induced hypotension is defined as a systolic blood pressure < 90 mm Hg or a reduction of ≥40 mm Hg from baseline.
MODS	Manifestation of organ dysfunction in acutely ill patients, so that intervention is needed to sustain homeostasis.

The table displays the definitions of SIRS, sepsis, severe sepsis, septic shock and MODS based on 1991 ACCP/SCCM Consensus Conference. PaCO2 = partial pressure of carbon dioxide; SIRS = Systemic inflammatory response syndrome. Table modified from Bone et al., 1992.

A second consensus conference was held in Washington D.C. in 2001 sponsored by SCCM, ACCP, the European Society of Intensive Care Medicine (ESICM), the American Thoracic Society (ATS), and the Surgical Infection Society (SIS), with the aim to improve the definitions leading to the diagnosis of sepsis. In order to improve the specificity for prompt recognition of sepsis and to better reflect the host response to infection, a more comprehensive list of symptoms and signs commonly seen in sepsis was added to the diagnostic criteria for sepsis, including the possible clinical manifestations and altered biochemical parameters (Table 1.2) [6]. However, it was emphasised that none of the listed clinical symptoms or biochemical parameters is adequate and/or specific for diagnosing sepsis. For example, increased cardiac output can be induced by major surgical interventions or multi-site trauma. Arterial hypotension may accompany other conditions, such as haemorrhage or acute myocardial infarction. Therefore, it is important for clinicians to include only the findings that cannot be explained by other explicit causes when making the assessment and diagnosis [6]. Concepts and criteria of severe sepsis and septic shock outlined in the 1991 consensus conference remain unchanged and are still valid [6]. There are several assessment scales to define organ dysfunction, but the sequential organ failure assessment (SOFA) score system was recommended to assess the evolving nature of organ dysfunction [7].

Table 1.2 Diagnostic criteria for sepsis based on 2001 ACCP/SCCM/ATS/ ESICM/SIS Consensus Conference.

Infection
Documented or suspected, and some of the following clinical or biochemical criteria:

General parameters
Body temperature > 38.3ºC or < 36ºC (hyperthermia or hypothermia)
Heart rate > 90 bpm or > 2 SD above the normal value for age (tachycardia)
Respiratory rate > 20 breaths/min (tachypnea)
Altered mental status
Significant edema or positive fluid balance (> 20 mL/kg over 24 h)
Hyperglycemia (plasma glucose > 110 mg/dL or 7.7 mM/L) in the absence of diabetes

Inflammatory parameters
Peripheral leukocyte count > 12.000/mm^3 or < 4.000/ mm^3 or > 10% immature forms (bands) (leukocytopenia or leukocytosis)
Plasma C-reactive protein > 2 SD above the normal value
Plasma procalcitonin > 2 SD above the normal value

Hemodynamic parameters
Arterial hypotension (systolic blood pressure < 90 mm Hg, mean arterial pressure < 70 mm Hg, or a systolic blood pressure decrease > 40 mm Hg in adults or < 2 SD below normal for age)
Mixed venous oxygen saturation > 70 %
Cardiac index > 3.5 L min^{-1} m^{-2}

Organ dysfunction parameters
Arterial hypoxaemia (PaO_2/FiO_2 < 300)
Acute decreased urine output (urine output < 0.5 mL kg^{-1} h^{-1} or 45 mM/L for at least 2 h)
Creatinine increase ≥ 0.5 mg/dL
Coagulation abnormalities (international normalized ratio >1.5 or activated partial thromboplastin time > 60 s)
Ileus (absent bowl sounds)
Thrombocytopenia (platelet count < 100 000 /μL)
Hyperbilirubinaemia (plasma total bilirubin > 4 mg/dL or 70 μmoll/L)

Tissue perfusion parameters
Hyperlactatemia (> 3 mmol/L)
Decreased capillary refill or mottling

The table displays the diagnostic criteria for sepsis based on 2001 SCCM/ACCP/ATS/ESCIM/SIS Consensus Conference, this serves as a supplement for the diagnostic definition of sepsis outlined by 1991 ACCP/SCCM Consensus Conference. FiO_2 = fraction of inspired oxygen; PaO_2 = partial pressure of oxygen; SD = standard deviation. Table modified from Levy et al., 2003.

In addition to modifying the diagnostic criteria of sepsis, the 2001 conference proposed a staging system for sepsis - the PIRO concept – that is based on patients' __P__*redisposing conditions,* the nature and severity of the infectious __i__*nsult*, the host __r__*esponse*, and the presence of __o__*rgan dysfunction* (Table 1.3). This concept attempted to incorporate host baseline factors and their response to both infectious insults and therapy, factors that would impact on sepsis outcome, in characterising the severity of sepsis [6].

Table 1.3 PIRO concept based on 2001 SCCM/ACCP/ATS/ESCIM/SIS Consensus Conference.

	Clinical aspects	Other tests
P (predisposing conditions)	Age, alcohol abuse, steroid or immunosuppressive therapy	Immunologic monitoring, genetic factors
I (insult)	Site-specific (e.g., pneumonia, peritonitis)	X-rays, CT scan, bacteriology
R (response)	Malaise, temperature, heart rate, respiratory rate	White blood cell count, C-reactive protein, procalcitonin, modified activated partial thromboplastin time
O (organ dysfunction)	Arterial pressure, urine output, Glasgow coma score	PaO_2/FIO_2, creatinine, bilirubin, platelets

The table displays the staging system for sepsis - the PIRO concept - proposed by 2001 SCCM/ACCP/ATS/ESCIM/SIS Consensus Conference. CT = computed tomography; FiO_2 = fraction of inspired oxygen; PaO_2 = partial pressure of oxygen. Table modified from Silva et al., 2008.

1.1.2 Epidemiology

Sepsis has been recognised as one of the most common causes of morbidity and mortality among admissions to the intensive care unit (ICU). Epidemiological studies of both incidence and mortality of sepsis showed remarkably constant high rates worldwide. An unacceptably high mortality rate of 46% was reported in patients with severe sepsis admitted to intensive care units between 1995 and 2000 in Britain [8]. A study based on the data from the Intensive Care National Audit & Research Centre Case Mix Programme Database in Britain identified an increase in the percentage of patients with severe sepsis admitted to ICU from 23.5% in 1996 to 28.7% in 2004. Although the in-hospital mortality rate for patients with severe sepsis decreased from 48.3% in 1996 to 44.7% in 2004, the total number of patients that died from sepsis has risen by 55.6% due to the increase in the incidence of sepsis at the same time [9]. The incidence of severe sepsis in the United States was estimated as being 300 cases per 100,000 people annually (751,000 cases per year) with a death rate of 28.6%. The incidence of severe sepsis was shown to increase by 1.5% annually [10]. Similarly, another study on sepsis incidence in the United States estimated 240 cases of sepsis per 100,000 people with a mortality rate of 17.9% [11]. In European countries, septic patients were reported to account for 37.4% of overall admissions to ICU [12]. A French study reported that 8.4% of ICU admissions were diagnosed as septic shock and the death rate was 60% [13]. A study conducted in Brazil showed incidence of admissions to the ICU with sepsis, severe sepsis and septic shock were 61.4, 35.6 and 30.0 per 1000 patient-days, respectively, with the mortality rate progressing from 34.7% to 47.3% and 52.2%, respectively [14]. The increase in incidence and mortality of sepsis is thought to be due to aging of the population, increased incidence of comorbidities, more widely used immunosuppressive treatments, increased accessibility to invasive medical procedures and increased chance of multidrug-resistant infections [15].

A Spanish epidemiological study provided clear evidence of the impact of organ dysfunction on morbidity and mortality in sepsis [16]. The authors reported that 78% of patients had MODS at the time of the diagnosis of sepsis, and both persistence and evolution of organ dysfunction were major contributors to mortality in these patients, which reflected in an increase in SOFA scores over time in non-survivors in

comparison with survivors [16]. Comorbidities were reported to increase the risk and worsen the outcome of sepsis [17], this may be because that pre-existence of comorbidity was correlated with aggravated organ dysfunction [11, 18].

It should be noted that most epidemiological studies were based on the evaluation of septic patients admitted to the ICU, and this may bias the result and underestimate the incidence of sepsis in the general population. The reason is that not all septic patients are treated in ICUs, due to different criteria for eligibility of ICU admission between countries and regions, different availability of critical care resources such as ICU beds and unequal access to medical care facilities caused by cultural or economic factors [19, 20]. These problems should be overcome by studying the incidence, morbidity and mortality of sepsis based on the data recorded from an entire population or correctly weighted samples [15].

1.1.3   Therapeutic Approaches

The speed of identifying sepsis and appropriate intensive care within the first hour after diagnosis will influence morbidity and mortality. In order to provide evidence for the best clinical practice for intensive care treatments of septic patients, the ESICM, the International Sepsis Forum (ISF), and the SCCM developed and initiated the Surviving Sepsis Campaign (SSC) in 2002. In 2004, a group of selected international clinicians, who were regarded as experts in the diagnosis and treatment of infectious disease and sepsis and represented 11 professional societies, published the first internationally accepted, evidence-based guidelines for the therapy of septic patients, aiming at disseminating the knowledge derived from current clinical evidence to bedside practice, improving critical care and decreasing relative risk of death. [21]. Joined by the other 7 international organizations, the group of experts came together again in 2006 and 2007, and updated the guidelines using a new grading system to guide assessment for rating quality of evidence and determining the strength of the recommendations [22]. Based on the most recent clinical evidence, 68 international experts representing 30 professional societies met in 2012 to provide a further update to the guidelines published in 2008 using the same evidence-based grading system. The latest guidelines published in 2013 recommended standardized care for a patient with severe sepsis or septic shock, including procedures of initial resuscitation, control of infection, and other supportive therapy (Table 1.4) [23].

However, it was emphasised by the committee that the clinician's decision-making capability should not be replaced by these guidelines when the clinician is facing a unique set of clinical manifestations in any given patient. In addition, it should be noted that clinicians in some regions or countries might not be able to implement particular recommendations due to limited availability of critical care resources [22].

Table 1.4 Guidelines for management of severe sepsis and septic shock based on SSC, 2012.

A. Initial resuscitation
1. Protocolized, quantitative resuscitation of patients with sepsis-induced tissue hypoperfusion (defined in this document as hypotension persisting after initial fluid challenge or blood lactate concentration $\geq$ 4 mmol/L). Goals during the first 6 h of resuscitation: (a) Central venous pressure 8 - 12 mmHg (b) Mean arterial pressure (MAP) $\geq$ 65 mmHg (c) Urine output $\geq$ 0.5 mL kg^{-1} h (d) Central venous (superior vena cava) or mixed venous oxygen saturation 70 or 65 %, respectively (grade 1C) 2. In patients with elevated lactate levels targeting resuscitation to normalize lactate as rapidly as possible (grade 2C)
B. Screening for sepsis and performance improvement
1. Routine screening of potentially infected seriously ill patients for severe sepsis to allow earlier implementation of therapy (grade 1C)
2. Hospital-based performance improvement efforts in severe sepsis (UG)
C. Diagnosis
1. Cultures as clinically appropriate before antimicrobial therapy if no significant delay ($>$ 45 min) in the start of antimicrobial(s) (grade1C). At least 2 sets of blood cultures (both aerobic and anaerobic bottles) be obtained before antimicrobial therapy with at least 1 drawn percutaneously and 1 drawn through each vascular access device, unless the device was recently ($<$ 48 h) inserted (grade 1C)
2. Use of the 1,3 β-D-glucan assay (grade 2B), mannan and anti-mannan antibody assays (2C), if available and invasive candidiasis is in differential diagnosis of cause of infection.
3. Imaging studies performed promptly to confirm a potential source of infection (UG)
D. Antimicrobial therapy
1. Administration of effective intravenous antimicrobials within the first hour of recognition of septic shock (grade 1B) and severe sepsis without septic shock (grade 1C) as the goal of therapy
2a. Initial empiric anti-infective therapy of one or more drugs that have activity against all likely pathogens (bacterial and/or fungal or viral) and that penetrate in adequate concentrations into tissues presumed to be the source of sepsis (grade 1B)
2b. Antimicrobial regimen should be reassessed daily for potential de-escalation (grade 1B)
3. Use of low procalcitonin levels or similar biomarkers to assist the clinician in the discontinuation of empiric antibiotics in patients who initially appeared septic, but have no subsequent evidence of infection (grade 2C)
4a. Combination empirical therapy for neutropenic patients with severe sepsis (grade 2B) and for patients with difficult to treat, multidrug-resistant bacterial pathogens such as Acinetobacter and Pseudomonas spp. (grade 2B). For patients with severe infections associated with respiratory failure and septic shock, combination therapy with an extended spectrum beta-lactam and either an aminoglycoside or a fluoroquinolone is for P. aeruginosa bacteremia (grade 2B). A combination of beta-lactam and macrolide for patients with septic shock from bacteremic Streptococcus pneumoniae infections (grade 2B)
4b. Empiric combination therapy should not be administered for more than 3 - 5 days. De-escalation to the most appropriate single therapy should be performed as soon as the susceptibility profile is known (grade 2B)
5. Duration of therapy typically 7 - 10 days; longer courses may be appropriate in patients who have a slow clinical response, undrainable foci of infection, bacteremia with S. aureus; some fungal and viral infections or immunologic deficiencies, including neutropenia (grade 2C)
6. Antiviral therapy initiated as early as possible in patients with severe sepsis or septic shock of viral origin (grade 2C)
7. Antimicrobial agents should not be used in patients with severe inflammatory states determined to be of noninfectious cause (UG)
E. Source control
1. A specific anatomical diagnosis of infection requiring consideration for emergent source control be sought and diagnosed or excluded as rapidly as possible, and intervention be undertaken for source control within the first 12 h after the diagnosis is made, if feasible (grade 1C)
2. When infected peri-pancreatic necrosis is identified as a potential source of infection, definitive intervention is best delayed until adequate demarcation of viable and nonviable tissues has occurred (grade 2B)
3. When source control in a severely septic patient is required, the effective intervention associated with the least

physiologic insult should be used (e.g., percutaneous rather than surgical drainage of an abscess) (UG)

4. If intravascular access devices are a possible source of severe sepsis or septic shock, they should be removed promptly after other vascular access has been established (UG)

F. Infection prevention

1a. Selective oral decontamination and selective digestive decontamination should be introduced and investigated as a method to reduce the incidence of ventilator-associated pneumonia; This infection control measure can then be instituted in health care settings and regions where this methodology is found to be effective (grade 2B)

1b. Oral chlorhexidine gluconate be used as a form of oropharyngeal decontamination to reduce the risk of ventilator-associated pneumonia in ICU patients with severe sepsis (grade 2B)

G. Fluid therapy of severe sepsis

1. Crystalloids as the initial fluid of choice in the resuscitation of severe sepsis and septic shock (grade 1B)

2. Against the use of hydroxyethyl starches for fluid resuscitation of severe sepsis and septic shock (grade 1B)

3. Albumin in the fluid resuscitation of severe sepsis and septic shock when patients require substantial amounts of crystalloids (grade 2C)

4. Initial fluid challenge in patients with sepsis-induced tissue hypoperfusion with suspicion of hypovolemia to achieve a minimum of 30 mL/kg of crystalloids (a portion of this may be albumin equivalent). More rapid administration and greater amounts of fluid may be needed in some patients (grade 1C)

5. Fluid challenge technique be applied wherein fluid administration is continued as long as there is hemodynamic improvement either based on dynamic (e.g., change in pulse pressure, stroke volume variation) or static (e.g., arterial pressure, heart rate) variables (UG)

H. Vasopressors

1. Vasopressor therapy initially to target a mean arterial pressure (MAP) of 65 mm Hg (grade 1C)

2. Norepinephrine (NE) as the first choice vasopressor (grade 1B)

3. Epinephrine (added to and potentially substituted for norepinephrine) when an additional agent is needed to maintain adequate blood pressure (grade 2B)

4. Vasopressin 0.03 units/min can be added to norepinephrine with intent of either raising MAP or decreasing NE dosage (UG)

5. Low dose vasopressin is not recommended as the single initial vasopressor for treatment of sepsis-induced hypotension and vasopressin doses higher than 0.03-0.04 units/min should be reserved for salvage therapy (failure to achieve adequate MAP with other vasopressor agents) (UG)

6. Dopamine as an alternative vasopressor agent to NE only in highly selected patients (e.g., patients with low risk of tachyarrhythmias and absolute or relative bradycardia) (grade 2C)

7. Phenylephrine is not recommended in the treatment of septic shock except in circumstances where (a) norepinephrine is associated with serious arrhythmias, (b) cardiac output is known to be high and blood pressure persistently low or (c) as salvage therapy when combined inotrope/vasopressor drugs and low dose vasopressin have failed to achieve MAP target (grade 1C)

8. Low-dose dopamine should not be used for renal protection (grade 1A)

9. All patients requiring vasopressors have an arterial catheter placed as soon as practical if resources are available (UG)

I. Inotropic therapy

1. A trial of dobutamine infusion up to 20 micrograms/kg/min be administered or added to vasopressor (if in use) in the presence of (a) myocardial dysfunction as suggested by elevated cardiac filling pressures and low cardiac output, or (b) ongoing signs of hypoperfusion, despite achieving adequate intravascular volume and adequate MAP (grade 1C)

2. Not using a strategy to increase cardiac index to predetermined supranormal levels (grade 1B)

J. Corticosteroids

1. Not using intravenous hydrocortisone to treat adult septic shock patients if adequate fluid resuscitation and vasopressor therapy are able to restore hemodynamic stability (see goals for Initial Resuscitation). In case this is not achievable, we suggest intravenous hydrocortisone alone at a dose of 200 mg per day (grade 2C)

2. Not using the ACTH stimulation test to identify adults with septic shock who should receive hydrocortisone (grade 2B)

3. In treated patients hydrocortisone tapered when vasopressors are no longer required (grade 2D)

4. Corticosteroids not be administered for the treatment of sepsis in the absence of shock (grade 1D)

5. When hydrocortisone is given, use continuous flow (grade 2D)

K. Blood product administration

1. Once tissue hypoperfusion has resolved and in the absence of extenuating circumstances, such as myocardial ischaemia, severe hypoxemia, acute haemorrhage, or ischemic heart disease, we recommend that red blood cell

transfusion occur only when haemoglobin concentration decreases to $<$ 7.0 g/dL to target a haemoglobin concentration of 7.0 - 9.0 g/dL in adults (grade 1B)

2. Not using erythropoietin as a specific treatment of anaemia associated with severe sepsis (grade 1B)

3. Fresh frozen plasma not be used to correct laboratory clotting abnormalities in the absence of bleeding or planned invasive procedures (grade 2D)

4. Not using anti-thrombin for the treatment of severe sepsis and septic shock (grade 1B)

5. In patients with severe sepsis, administer platelets prophylactically when counts are $\leq$ 10,000/mm^3 (10 x 10^9/L) in the absence of apparent bleeding. We suggest prophylactic platelet transfusion when counts are $\leq$20,000/mm^3 (20 x 10^9/L) if the patient has a significant risk of bleeding. Higher platelet counts ($\geq$ 50,000/mm^3 [50 x 10^9/L]) are advised for active bleeding, surgery, or invasive procedures (grade 2D)

L. Immunoglobulins

1. Not using intravenous immunoglobulins in adult patients with severe sepsis or septic shock (grade 2B)

M. Selenium

1. Not using intravenous selenium for the treatment of severe sepsis (grade 2C)

N. History of Recommendations Regarding Use of Recombinant Activated Protein C (rhAPC)

A history of the evolution of SSC recommendations as to rhAPC (no longer available) is provided.

O. Mechanical ventilation of sepsis-induced acute respiratory distress syndrome (ARDS)

1. Target a tidal volume of 6 mL/kg predicted body weight in patients with sepsis-induced ARDS (grade 1A vs. 12 mL/kg)

2. Plateau pressures be measured in patients with ARDS and initial upper limit goal for plateau pressures in a passively inflated lung be $\leq$ 30 cm H$_2$O (grade 1B)

3. Positive end-expiratory pressure (PEEP) be applied to avoid alveolar collapse at end expiration (atelectotrauma) (grade 1B)

4. Strategies based on higher rather than lower levels of PEEP be used for patients with sepsis - induced moderate or severe ARDS (grade 2C)

5. Recruitment maneuvers be used in sepsis patients with severe refractory hypoxemia (grade 2C)

6. Prone positioning be used in sepsis-induced ARDS patients with a PaO$_2$/FIO$_2$ ratio $\leq$ 100 mm Hg in facilities that have experience with such practices (grade 2B)

7. That mechanically ventilated sepsis patients be maintained with the head of the bed elevated to 30 - 45 degrees to limit aspiration risk and to prevent the development of ventilator-associated pneumonia (grade 1B)

8. That noninvasive mask ventilation (NIV) be used in that minority of sepsis - induced ARDS patients in whom the benefits of NIV have been carefully considered and are thought to outweigh the risks (grade 2B)

9. That a weaning protocol be in place and that mechanically ventilated patients with severe sepsis undergo spontaneous breathing trials regularly to evaluate the ability to discontinue mechanical ventilation when they satisfy the following criteria: a) arousable; b) hemodynamically stable (without vasopressor agents); c) no new potentially serious conditions; d) low ventilatory and end – expiratory pressure requirements; and e) low F$_{IO_2}$ requirements which can be met safely delivered with a face mask or nasal cannula. If the spontaneous breathing trial is successful, consideration should be given for extubation (grade 1A).

10. Against the routine use of the pulmonary artery catheter for patients with sepsis-induced ARDS (grade 1A).

11. A conservative rather than liberal fluid strategy for patients with established sepsis-induced ARDS who do not have evidence of tissue hypoperfusion (grade 1C)

12. In the absence of specific indications such as bronchospasm, not using beta 2 - agonists for treatment of sepsis - induced ARDS (Grade 1B)

P. Sedation, analgesia, and neuromuscular blockade in sepsis

1. Continuous or intermittent sedation be minimized in mechanically ventilated sepsis patients, targeting specific titration endpoints (grade 1B)

2. Neuromuscular blocking agents (NMBAs) be avoided if possible in the septic patient without ARDS due to the risk of prolonged neuromuscular blockade following discontinuation. If NMBAs must be maintained, either intermittent bolus as required or continuous infusion with train - of - four monitoring of the depth of blockade should be used (grade 1C)

3. A short course of NMBA of not greater than 48 h for patients with early sepsis-induced ARDS and a PaO$_2$/FIO$_2$ $<$ 150 mm Hg (grade 2C)

Q. Glucose control

1. A protocolized approach to blood glucose management in ICU patients with severe sepsis commencing insulin dosing when 2 consecutive blood glucose levels are $>$ 180 mg/dL. This protocolized approach should target an upper blood glucose $\leq$ 180 mg/dL rather than an upper target blood glucose $\leq$ 110 mg/dL (grade 1A)

2. blood glucose values be monitored every 1 - 2 hrs until glucose values and insulin infusion rates are stable and

then every 4 hrs thereafter (grade 1C)

3. glucose levels obtained with point - of - care testing of capillary blood be interpreted with caution, as such measurements may not accurately estimate arterial blood or plasma glucose values (UG)

R. Renal replacement therapy

1. Continuous renal replacement therapies and intermittent haemodialysis are equivalent in patients with severe sepsis and acute renal failure (grade 2B)

2. Use continuous therapies to facilitate management of fluid balance in haemodynamically unstable septic patients (grade 2D)

S. Bicarbonate therapy

1. Not using sodium bicarbonate therapy for the purpose of improving haemodynamics or reducing vasopressor requirements in patients with hypoperfusion-induced lactic acidaemia with pH $\geq$ 7.15 (grade 2B)

T. Deep vein thrombosis prophylaxis

1. Patients with severe sepsis receive daily pharmacoprophylaxis against venous thromboembolism (VTE) (grade 1B). This should be accomplished with daily subcutaneous low-molecular weight heparin (LMWH) (grade 1B versus twice daily UFH, grade 2C versus three times daily UFH). If creatinine clearance is $<$ 30 mL/min, use dalteparin (grade 1A) or another form of LMWH that has a low degree of renal metabolism (grade 2C) or UFH (grade 1A)

2. Patients with severe sepsis be treated with a combination of pharmacologic therapy and intermittent pneumatic compression devices whenever possible (grade 2C)

3. Septic patients who have a contraindication for heparin use (e.g, thrombocytopenia, severe coagulopathy, active bleeding, recent intracerebral haemorrhage) not receive pharmacoprophylaxis (grade 1B), but receive mechanical prophylactic treatment, such as graduated compression stockings or intermittent compression devices (grade 2C), unless contraindicated. When the risk decreases start pharmacoprophylaxis (grade 2C)

U. Stress ulcer prophylaxis

1. Stress ulcer prophylaxis using H2 blocker or proton pump inhibitor be given to patients with severe sepsis/septic shock who have bleeding risk factors (grade 1B)

2. When stress ulcer prophylaxis is used, proton pump inhibitors rather than H2RA (grade 2D)

3. Patients without risk factors do not receive prophylaxis (grade 2B)

V. Nutrition

1. Administer oral or enteral (if necessary) feedings, as tolerated, rather than either complete fasting or provision of only intravenous glucose within the first 48 h after a diagnosis of severe sepsis/septic shock (grade 2C)

2. Avoid mandatory full caloric feeding in the first week but rather suggest low dose feeding (e.g., up to 500 calories per day), advancing only as tolerated (grade 2B)

3. Use intravenous glucose and enteral nutrition rather than total parenteral nutrition (TPN) alone or parenteral nutrition in conjunction with enteral feeding in the first 7 days after a diagnosis of severe sepsis/septic shock (grade 2B)

4. Use nutrition with no specific immunomodulating supplementation rather than nutrition providing specific immunomodulating supplementation in patients with severe sepsis (grade 2C)

W. Setting goals of care

1. Discuss goals of care and prognosis with patients and families (grade 1B)

2. Incorporate goals of care into treatment and end-of-life care planning, utilizing palliative care principles where appropriate (grade 1B)

3. Address goals of care as early as feasible, but no later than within 72 h of ICU admission (grade 2C)

The table displays the international guidelines for management of severe sepsis and septic shock recommended by 2012 SSC. The recommendations were made according to the Grading of Recommendations Assessment Development and Evaluation (GRADE) system to guide assessment for rating quality of evidence from high (A) to very low (D) and determining the strength of recommendations as strong (1) or weak (2). UG = ungraded. Table adapted from Dellinger et al., 2013.

In addition to publishing guidelines, the Surviving Sepsis Campaign Management Bundles have been put forward by the committee in 2008, including "the 6-h resuscitation bundle" and "the 24-h management bundle" [22]. Each bundle comprises of 4 to 5 evidence-based procedures, which (when implemented together) are expected to reduce the mortality of sepsis more than the individual interventions alone. Indeed, enhanced compliance with recommended bundles was paralleled with improved sepsis care and a reduction in mortality rate of sepsis by 5% - 7% throughout Europe, America [24] and Spain [25]. An analysis of nearly 32,000 patients from 239 hospitals that distributed in 17 countries in 2011 contributed to an updated version of sepsis bundles in conjunction with the guidelines published in 2013, which dropped the management bundle and divided the resuscitation bundle into two sections (Table 1.5) [23].

Table 1.5 Surviving sepsis campaign care bundles provided by SSC, 2012.

To be completed within 3 h
1) Measure lactate level
2) Obtain blood cultures prior to administration of antibiotics
3) Administer broad spectrum antibiotics
4) Administer 30 mL/kg crystalloid for hypotension or lactate $\geq$ 4 mmol/L
To be completed within 6 h
5) Apply vasopressors (for hypotension that does not respond to initial fluid resuscitation) to maintain a mean arterial pressure (MAP) $\geq$ 65 mm Hg
6) In the event of persistent arterial hypotension despite volume resuscitation (septic shock) or initial lactate $\geq$ 4 mmol/L (36 mg/dL):
- Measure central venous pressure (CVP) (target CVP: $\geq$ 8 mm Hg)
- Measure central venous oxygen saturation (ScvO2) (target ScvO2: $\geq$ 70%)
7) Remeasure lactate if initial lactate was elevated

The table displays the Surviving sepsis campaign care bundles recommended by 2012 SSC. Table adapted from Dellinger et al., 2013.

The recombinant human activated protein C (rhAPC) product - drotrecogin alfa was approved in a number of countries in 2001 for the treatment of patients with severe sepsis which do not have a bleeding risk (contraindication). This decision was based on the rhAPC Worldwide Evaluation in Severe Sepsis (PROWESS) clinical trial, which involved 1,690 patients with severe sepsis and with a high risk of death and demonstrated a reduction in mortality rate by 6% with drotrecogin alfa in comparison with the placebo group [26]. Therefore, the use of rhAPC or drotrecogin alfa was recommended by the SSC guidelines published in 2004 with a quality of evidence of grade B [21]. However, an additional clinical trial in 2005 which enrolled 11,000 septic patients with a low risk of death and single organ dysfunction showed no beneficial treatment effect of drotrecogin alfa, and this lack of effect was associated with an increased bleeding risk [27]. Following this study, the usage of drotrecogin alfa should, according to the 2008 SSC guidelines, be limited to the patients with a high risk of death and multiple organ dysfunction, the quality of evidence was also downgraded from B to C [22]. In line with the previous study, the PROWESS SHOCK trial of 1,696 patients with severe sepsis or septic shock released in 2011 failed to show a survival improvement with the treatment of drotrecogin alfa. Drotrecogin alfa was then withdrawn from the market and the usage of the drug was therefore stopped. (http://www.fda.gov/Drugs/DrugSafety/DrugSafetyPodcasts/ucm277212.htm).

With the progress being made in uncovering the underlying mechanism(s) of sepsis, innovative therapies have been proposed, including a number of interventions that modulate inflammation. Clinical trials trying to block the effects of individual cytokines such as tumor necrosis factor (TNF)-α and interleukin (IL)-1β failed, suggesting that it may be important to develop anti-inflammatory drugs, which suppress multiple inflammatory factors and, thus, blocking general inflammation in sepsis. The other reason for the failure of anti-inflammatory therapies may be due to the fact that a secondary immunosuppressed state was shown to accompany the initially profound pro-inflammatory state in sepsis, which may impair the host response to secondary infections [28]. A third explanation may be that these therapies were simply given too late in man to be effective.

Apart from their lipid-lowering effects, statins have been reported to increase survival in septic patients [29], probably through their pleiotropic anti-inflammatory

properties. Simvastatin improves coronary perfusion and myocardial performance in animals challenged with bacterial toxins [30]. However, further research need to be done before the application of statins becomes accepted in the clinical practice for treating sepsis. A recent large cohort study showed administration of low doses of anti-inflammatory agent acetyl salicylic acid (ASA) within 24 h of the onset of sepsis was strongly associated with lower mortality in ICU patients, but it was also found the treatment might cause increased risk of renal injury [31]. Further studies are needed to elucidate the roles of ASA and other drugs with potential therapeutic effects on sepsis.

1.1.4 Pathophysiology

1.1.4.1 Pathogens

The occurrence of Gram-positive bacterial infection-caused sepsis increased over time [11, 12]. Gram-negative organisms, however, still play a predominant role for as cause of many infections, as has been reported recently in the European Prevalence of Infection in Intensive Care (EPIC II) study [32]. Gram-negative infections accounted for 62% of cases with positive isolates, with the predominant species being *Pseudomonas auruginosa* (19.9%) or *Escherichia coli* (16%); Gram-positive organisms caused 46.8% of all cases, predominated by *Staphylococcus aureus* (20.5%); fungi were identified in 19.4% of cases (Table 1.6). However, blood culture results were negative in approximately 30% of all cases [32]. Gram-negative bacteraemia was also associated with an increased risk of mortality in comparison with Gram-positive bacteraemia [33]. The respiratory tract, especially the lung, is the most common focus of infection in patients with sepsis, and this focus is also associated with the highest risk of death [18]. Abdomen, renal/urinary tract, skin, catheter-related operations and the central nervous system are other common sources of infection [32].

Table 1.6 Types of organisms and infection frequency[a] in microbiological culture-positive infected patients based on the European Prevalence of Infection in Intensive Care (EPIC II) study.

Microorganism	Frequency (%)	Microorganism	Frequency (%)	Microorganism	Frequency (%)
Gram-negative	62.2	**Gram-positive**	46.8	**Fungi**	19.4
Escherichia coli	16.0	*Staphylococcus aureus*	20.5	*Candida*	17
Enterobacter	7.0	MRSA	10.2	*Aspergillus*	1.4
Klebsiella species	12.7	*S epidermidis*	10.8	Other	1
Pseudomonas species	19.9	*Streptococcus pneumoniae*	4.1	**Anaerobes**	4.5
Acinetobacter species	8.8	VSE	7.1	**Other bacteria**	1.5
Other	17.0	VRE	3.8	**Parasites**	0.7
		Other	6.4	**Other organisms**	3.9

ESBL = extended-spectrum β-lactamases; MRSA = methicillin-resistant *Staphylococcus aureus*; VRE = vancomycin-resistant *Enterococcus;* VSE = vancomycin-sensitive *Enterococcus*. [a]Percentages do not necessarily equal 100, because patients may have had more than 1 type of infection or microorganism. Table modified from Vincent et al., 2009.

The innate immune system recognises bacteria via conserved molecular structures. These motifs in bacteria are known as pathogen-associated molecular patterns (PAMPs) and PAMPs are essential for initiating both host immune response and cytokine expression [34]. Lipopolysaccharide (LPS), also known as endotoxin, is a crucial PAMP in Gram-negative bacteria. It presents in the outer membrane of the cell wall of Gram-negative bacteria. The conserved lipid A portion of LPS contributes to its toxicity and is associated with the LPS-induced activation of host cell membranes [35]. In Gram-positive bacteria, peptidoglycan (PepG) and lipoteichoic acid (LTA) play dominant roles, although their activities are much less than that of LPS. They are components of cell walls in the Gram-positive bacteria and can be sensed by host cell-surface receptors, thus initiating inflammatory response [36, 37]. These molecular patterns are also able to act synergistically to cause innate immune cells activation, release of inflammatory cytokines [38] and multiple organ failure [39]. Additionally, bacterial superantigens produced by Staphylococcus aureus and Streptococcus pyogenes stimulate large numbers of T cells and cause a sudden release of cytokines into the blood stream [40].

1.1.4.2 Pattern Recognition Receptors

Pathogens and PAMPs are sensed by families of conserved germline-encoded pattern recognition receptors (PRRs) expressed by innate immune cells, such as macrophages, dendritic cells, and neutrophils [41, 42]. There are several families of PRRs have been characterised, including Toll-like receptors (TLRs) and C-type lectin receptors (CLRs), most of which are located on the cell surface, as well as nucleotide-binding oligomerisation domain (NOD)-like receptors (NLRs) and retinoic acid inducible gene I-like receptors (RLRs), which reside in the cytoplasm [43]. Each PRR detects corresponding PAMPs (Table 1.7). Generally, TLRs and NLRs are primarily crucial in recognising bacteria [44, 45], while RLRs play important roles in recognising viruses [46]. Additionally, CLRs are crucial for recognising fungi and mycobacteria [47, 48]. The recognition of PAMPs by PRRs initiates an innate immune response and induces production of pro-inflammatory and anti-inflammatory mediators via the activation of multiple transcription factors, such as nuclear factor (NF)-κB and interferon regulatory factors (IRFs) [49]. Effective activation of PRRs by PAMPs is essential for killing and elimination of invading pathogens by the host,

however, over-activation of PRRs may cause systemic inflammatory response and elicit harmful damage to the host [50]. Among these four categories of PPRs, TLRs and NLRs are the most extensively studied PPR families.

Table 1.7 Overview of specific ligands for PRRs, according to PRR family.

Recognised PAMP	Origin of the PAMP	Recognised PAMP	Origin of the PAMP
TLRs		**NLRs**	
TLR2-1		**NOD1**	
Triacyl lipopeptides	Bacteria	Muramyl tripeptide peptidoglycans	Gram-negative bacteria
TLR2-2		**NOD2**	
Peptidoglycan	Bacteria	Muramyl dipeptide peptidoglycans	Gram-positive bacteria
Lipoarabinomannan	Mycobacteria		
Phospholipomannan	Candida	**NLRP1**	
Glycosylphosphatidy-linositol	Trypanosoma	Anthrax toxin	Bacillus anthracis
TLR2-6		**NLRP3**	
Diacyl lipopeptides	Mycoplasma	Peptidoglycans	Bacteria
Lipoteichoic acid	Streptococcus	Bacterial toxins	Listeria, staphylococcus
Zymosan	Saccharomyces		
TLR3		**NLRC4**	
ssRNA virus	West Nile virus	Flagellin	Shigella, salmonella, legionella
dsRNA virus	Reovirus		
TLR4		**AIM2**	
Lipopolysaccharide	Gram-negative bacteria	dsDNA	Francisella tularensis
Fungal mannans	Candida		
Envelope proteins	Respiratory syncytial virus		
TLR5		**CLRs**	
Flagellin	Flagellated bacteria	**Mannose receptor**	
TLR7 and TLR8		Fungal mannans	Candida
ssRNA viruses	Influenza virus, vesicular stomatitis virus		
TLR9		**Dectin-1**	
dsDNA viruses	Herpes simplex virus	Beta-1,3-glucans	Fungi
CpG motifs	Bacterial and fungal DNA		
RLRs		**Dectin-2-FcRγ**	
MDA5		Mannans	Candida hyphae
Long dsRNA	Picornaviruses, reoviruses, flaviviruses		
RIG-I		**MINCLE-FcRγ**	
Short dsRNA	Paramyxoviruses, orthomyxoviruses, rhabdoviruses, flaviviruses	Mannans	Candida
		Mycobacterial cord factor	Mycobacteria
5' Triphosphate ssRNA	Paramyxoviruses, orthomyxoviruses, rhabdoviruses, flaviviruses	**Mannose-binding lectin**	
		Repetitive oligosaccharides	Bacteria and fungi

The table displays PRRs and their specific Pathogen-Associated Molecular Pattern (PAMP) Ligands, according to PPR family. CLRs = C-type lectin receptors; CpG = cytosine phosphate guanidine; ds = double-stranded; FcRγ = Fc receptor IgE high-affinity I gamma polypeptide; MDA5 = melanoma differentiation-associated protein 5; MINCLE = macrophage-inducible C-type lectin; NLRs = nucleotide-binding oligomerisation domain (NOD)-like receptors; NLRC4 = NLR family CARD-domain–containing protein 4 (also known as IPAF), NLRP = NOD leucine-rich-repeat and pyrin domain–containing protein; RIG-I = retinoic acid inducible gene I protein; RLRs = retinoic acid inducible gene I-like receptors; ss = single-stranded, TLRs = toll-like receptors, TLR2-1 = TLR2–TLR1 heterodimers; TLR2-2 = TLR2–TLR2 heterodimers; TLR2-6 = TLR2–TLR6 heterodimers. Table modified from Netea et al., 2011.

Toll-Like Receptors

Toll was first described in Drosophila mutant for its effect in controlling dorsal-ventricular polarity during embryogenesis [51]. The Toll gene was later revealed to be able to affect the immune response of Drosophila to fungal infections [52]. To date, 10 functional TLRs have been identified in humans, and 12 have been found in mice. TLR1, TLR2, TLR4, TLR5, and TLR6 reside on the cell surface and are primarily responsible for sensing PAMPs that originate from bacteria and fungi; TLR3, 7, 8 and 9 are expressed in the endosomal compartments, where they play a critical role in sensing nuclear acid originated from bacteria and viruses (see Table 1.7 for receptors and ligands) [41]. The extracellular domain of all TLRs is quite conserved and contains varying numbers of leucine-rich repeats (LRR); this domain is responsible for the recognition of PAMPs. The extracellular domain of TLRs is connected with the cytosolic carboxy-terminal domain known as Toll/IL-1R (TIR) domain via a single transmembrane helix [53]. TIR domain is essential for the transduction of downstream signalling. TLR signalling is initially triggered by the interaction between the activated cytosolic TIR domain and recruited adaptor molecules, which includes myeloid differentiation primary response gene 88 (MyD88), Toll/interleukin 1 receptor domain-containing adapter inducing IFN-β (TRIF), TRIF-related adaptor

molecule (TRAM) and TIR-containing adaptor protein (TIRAP). TLR signalling can be roughly divided into two categories based on the usage of different adaptor molecules, the MyD88-dependent and TRIF-dependent pathways. All TLRs utilize MyD88 as the adaptor molecule, with the exception of TLR3, which recruits TRIF exclusively to initiate downstream signalling [54].

TLR4 is the only receptor among all TLRs, which activates both MyD88-dependent and TRIF-dependent pathways, via recruitment all four adaptor molecules [54]. TLR4 recognises LPS and triggers LPS signalling during endotoxaemia [55]. LPS is first sensed by an endogenous LPS binding protein (LBP). Together they form the LPS-LBP complex, which binds to CD14 on the cell surface. CD14 then transfers LPS to the co-receptor of TLR4, myeloid differentiation protein-2 (MD2), this leads to the formation of a TLR4 homodimer [56]. Once TLR4 homodimerises and is activated, two downstream signalling cascades are initiated by recruitment of two distinct adaptor molecules, MyD88 and TRIF. TLR4 first recruits TIRAP at the cell membrane, followed by the recruitment of MyD88 and, thus, induction of the MyD88-dependent pathway. TLR4 is subsequently trafficked to the endosome followed by its phagocytosis, and recruits TRAM and TRIF to form a signalling complex, which initiates TRIF-dependent pathway [49].

In the MyD88-dependent pathway, the interaction between TLRs and MyD88 leads to the recruitment and activation of IL-1 receptor-associated kinase (IRAK)4, which subsequently activates IRAK1 and IRAK2 [57]. Activated IRAK associates with TNF-α receptor associated factor (TRAF)6, which enables the binding of TRAP6 to E2 ubiquitin conjugating enzymes ubiquitin C13 (UBC13) and ubiquitin conjugating enzyme variant 1A (UEV1A), causing polyubiquitination of TRAF6 modified with K63-ubiquitin linkage. The polyubiquitination subsequently enables the binding of TRAF6 to the ubiquitin-binding domain of IκB kinase (IKK)γ, a subunit of IKK complex critical for activation of NF-κB pathway. Additionally, TRAF6 recruits transforming growth factor-β-activated kinase (TAK)1-binding protein (TAB)2 and binds to the ubiquitin-binding domain of TAB2, leading to the activation of its associated TAK1, which further causes phosphorylation of IKKβ. Pellino 1 can catalyse the synthesis of K63-ubiquitin linkage to IRAK1, which enables IRAK1 to activate IKK directly. The activated IKK complex phosphorylates IκB, followed by

IκB degradation, which further releases subunits of NF-κB to nucleus and thereby initiates production of inflammatory mediators such as TNF-α, IL-6, IL-1β. Moreover, association between TRAF6 and TAK1 leads to the activation of p38 mitogen-activated protein kinase (MAPK) pathway and induces inflammatory cytokines (Figure 1.1) [49, 58].

In the TRIF-dependent pathway, the combination of the intracellular region of TLRs with TRIF activates NF-κB and MAPK through the recruitment of TRAF6 and activation of TAK1 kinase in a way similar to those in the MyD88-dependent pathway. TRIF can also activate these pathways through recruiting receptor interacting protein (RIP)1, which can be modified with K63-ubiquitin linkage [49]. In addition to activating both NF-κB and p38 MAPK pathways, the TRIF-dependent pathway also cooperates the activation of IRF. TRIF activates TRAF3, which is modified with K63-ubiquitin linkage. TRAF3 then further activates TRAF family member-associated NF-κB activator-binding kinase (TBK)1 and IKKε, leading to phosphorylation and nuclear translocation of IRF3 and IRF7 for induction of type I interferon and inflammatory mediators (Figure 1.1) [42, 58].
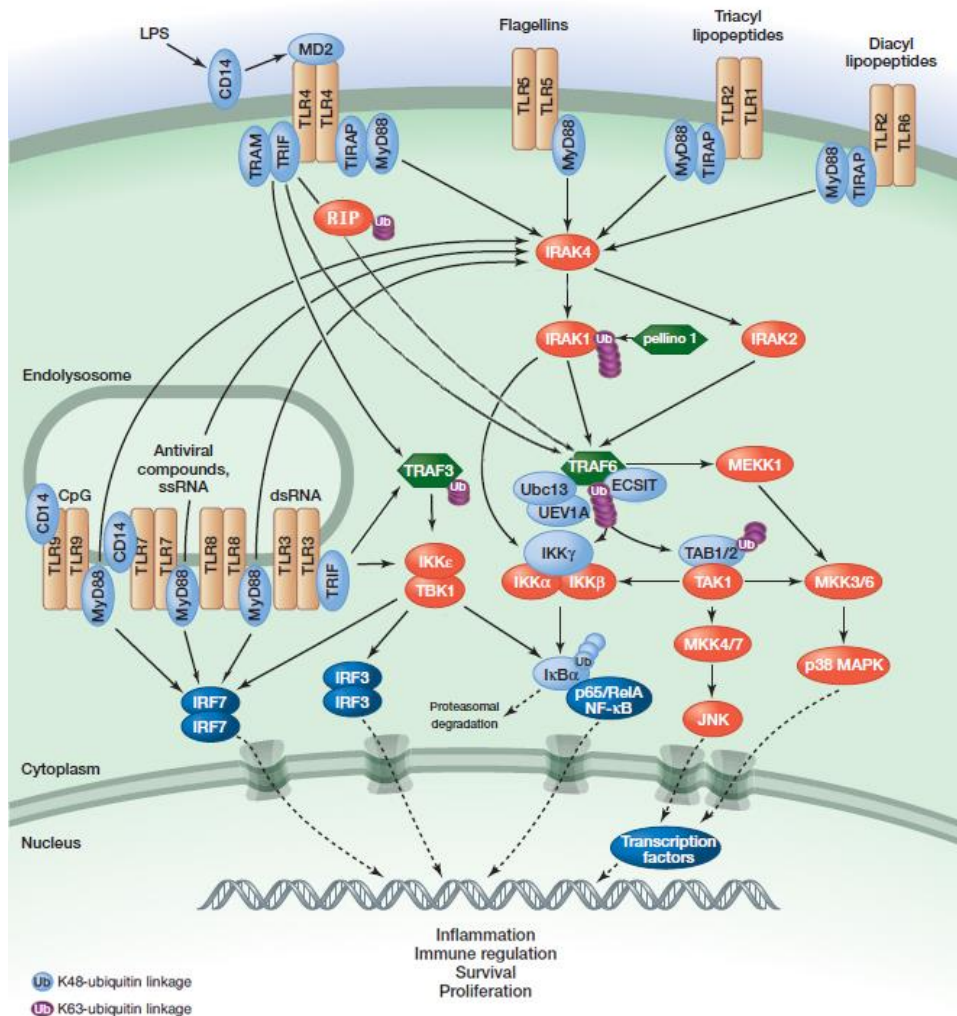
Figure 1.1 Summary of the TLR signalling pathway.

TLR signalling can be roughly divided into two categories based on the usage of different adaptor molecules, the myeloid differentiation primary response gene 88 (MyD88)-dependent and Toll/interleukin 1 receptor domain-containing adapter inducing IFN-β (TRIF)-dependent pathways. In MyD88-dependent pathway, combination of TLR ligands with TLRs leads to the recruitment of MyD88 and Toll/IL-1R-containing adaptor protein (TIRAP). MyD88 activates IL-1 receptor-associated kinase (IRAK)4, which further phosphorylates IRAK1 and IRAK2. Activated IRAK binds to TNF-α receptor associated factor (TRAF)6, which subsequently phosphorylates TAK1-binding protein (TAB)2 and transforming growth factor-β-activated kinase (TAK)1, and thereby initiates production of inflammatory mediators via activation of nuclear factor (NF)-κB and p38 mitogen-activated protein kinase (MAPK) pathway. TRIF-dependent pathway involves the activation of NF-κB and MAPK pathways in a receptor interacting protein (RIP)1 dependent or independent manner. In addition, it also regulates IRF3 and IRF7 through activating TRAF3. JNK = c-Jun amino-terminal kinase; CpG = cytosine phosphate guanidine; ds = double-stranded; ECSIT = evolutionarily

conserved signalling intermediate in Toll pathways; IKK = IκB kinase; LPS = lipopolysaccharide; MKKs = MAP kinase kinases; MD-2 = myeloid differentiation protein-2; MEKK = MAPK/extracellular signal-regulated kinases (ERK) kinase kinase; TBK = TRAF family member-associated NF-κB activator-binding kinase; TRAM = TRIF-related adaptor molecule; UBC13 = ubiquitin conjugating enzymes ubiquitin C13; UEV1A = ubiquitin conjugating enzyme variant 1A. Figure modified from Lim et al., 2013.

NLR Proteins

To date, 22 NLR members have been characterised in humans and more than 30 have been identified in mice [59]. The NLR proteins are composed of C-terminal LRR, which is essential in sensing and binding with PAMPs or other harmful endogenous molecules; a centrally located nucleotide-binding oligomerisation (NACHT) domain, the only region shared by all NLR members, which is believed to mediate self-oligomerisation in an ATP-dependent manner; an N-terminal domain such as a caspase recruitment domain (CARD), a Pyrin domain (PYD) or a baculoviral inhibitory repeat (BIR)-like domain, that is thought to be involved in binding with downstream signalling molecules [60]. The NLR family is subcategorised into two distinct groups according to different N-terminal effector domains, the NLRC group which contains a CARD, such as NOD1 and NOD2; the NLRP group which contains a PYD, such as NLRP1, NLRP3, NLRP4 and NLRP6, etc. The main functions of these N-terminal effector domains are regulating NF-κB, p38 MAPK and caspase-1 activation, thus triggering innate immune response in cytosol [54].

NOD1 and NOD2 mainly recognise cell wall components, PepG and muramyl dipeptide from gram-negative and gram-positive bacteria, respectively (Table 1.7) [48]. NOD1 is universally expressed in host cells, whereas the expression of NOD2 is restricted to monocytes [61] and intestinal epithelial cells [62]. The recognition of their associated PAMPs leads to oligomerisation of these receptors. Once the

receptors oligomerise and are activated, the downstream signalling is initiated by recruiting a CARD-containing adaptor molecule, RIP2, through a haemophilic CARD-CARD interaction [63, 64]. This leads to subsequent activation of NF-κB and, thereby, induces the production of inflammatory mediators such as TNF-α, IL-6, IL-1β. In addition, NOD1 and NOD2 activate MAPK via their association with the CARD-containing molecule, CARD9, which further increases the transcription of various inflammatory cytokines (Figure 1.2) [65]. NODs are also able to synergise with TLRs to augment the inflammatory response [43, 66].

The NLRPs such as NLRP1, NLRP3 and NLRP4 are known to participate in the formation of a multi-protein complex (inflammasome), which consists of NLRPs, apoptosis-associated speck-like protein containing a CARD (ASC), and pro-caspase-1; the most important consequence of the inflammasome formation is the activation of caspase-1 and, thus, release of the IL-1 family of inflammatory cytokines, such as IL-1β and IL-18 [43]. The association of NLRP1, NLRP3 and NLRP4 receptors with their respective PAMPs in immune cells, such as macrophages and dendritic cells, leads to oligomerisation of these receptors, which recruits a cytosolic adaptor molecule known as ASC via haemophilic PYD-PYD interaction. ASC then binds to pro-caspase-1 through haemophilic CARD-CARD interaction, which induces autocatalytic cleavage of pro-caspase-1 into active caspase-1. The activated caspase-1 further converts inactive form of IL-1 family cytokines (production of which is dependent on NF-κB and MAPK pathway) into active form through proteolytical cleavage (Figure 1.2) [43, 64]. In addition to inducing inflammatory cytokines production, caspase-1 activation is also able to initiate a type of inflammatory programmed cell death, which is known as pyroptosis, to eliminate invaded pathogens by killing infected cells [42, 54].
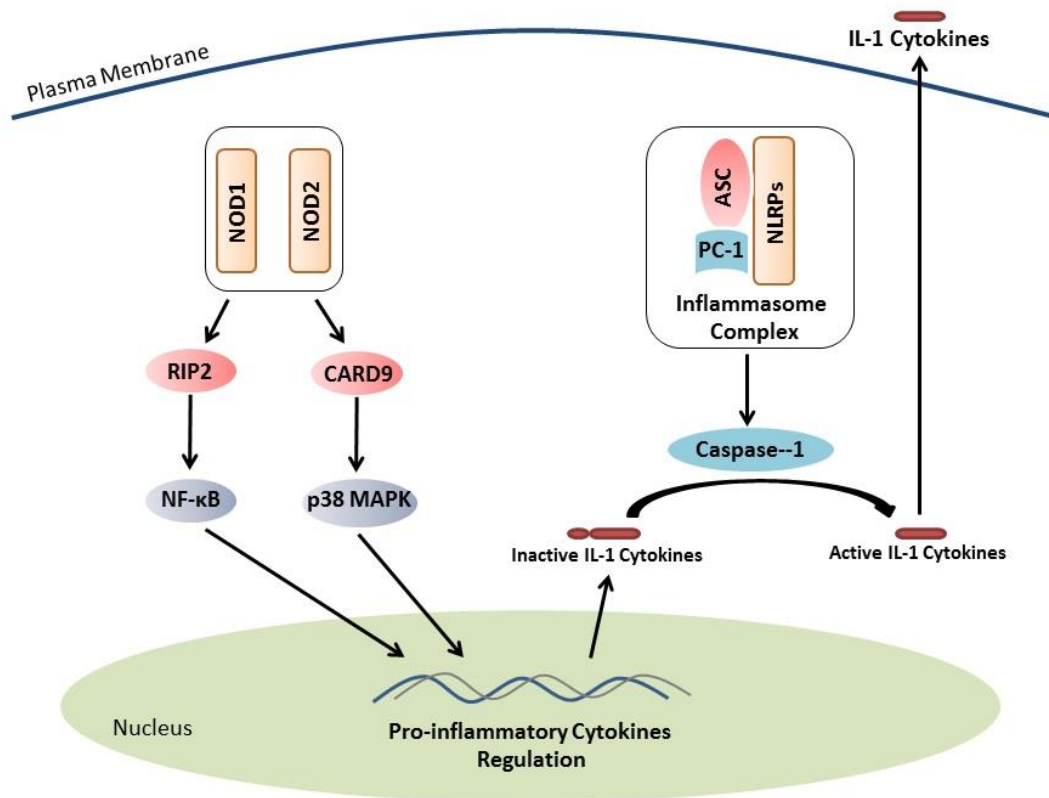
Figure 1.2 Scheme of the NLR signalling pathway.

Recognition of corresponded PAMPs with cytosolic NOD1 and NOD2 leads to the recruitment of receptor interacting protein (RIP)2 for the activation of nuclear factor (NF)-κB, and caspase recruitment domain (CARD)9 for the activation of p38 mitogen-activated protein kinase (MAPK) pathway, which further initiate production of pro-inflammatory mediators. NLRPs such as NLRP1, NLRP3 and NLRP4 assemble inflammasome together with apoptosis-associated speck-like protein containing a CARD (ASC), and pro-caspase (PC)-1 upon the combination with their ligands, leading to the activation of caspase-1. The activated caspase-1 then converts inactive form of IL-1 family cytokines (production of which is dependent on NF-κB and MAPK pathway) into biologically active form.

1.1.5 Gender Dimorphism in Sepsis

A retrospective clinical study of 261 255 septic patients showed a significantly increased mortality rate in male patients which were younger than 50 years of age compared with an age-matched female cohort. This difference was not detected in patients older that 50 years [67]. This 'survival' advantage of the female gender in sepsis is confirmed by data from another prospective clinical trial, which documents an increased survival rate in female patients (74%) when compared with male patients (31%) with sepsis [68]. Additionally, male gender is an independent prognostic variable for survival in patients with sepsis [69]. Experimental studies using various sepsis models also confirmed the gender dimorphism in the outcome of sepsis. Proestrus female mice showed maintained immune responses and a significantly improved survival rate compared with male mice following polymicrobial sepsis induced by caecum ligation and pucture (CLP) [70]. Male gender and age are also associated with higher mortality rates in a model of trauma-haemorrhage followed by a second hit of sepsis [71].

A potential mechanism of this gender dimorphism might involve the gender-specific expression of pro- and anti-inflammatory cytokines. Compared with female patients with sepsis, male patients had elevated levels of IL-6 [72, 73]; IL-6 is an independent predictor for the severity of septic episodes [74]. Experimental studies showed significantly increased level of IL-1 at four hours following LPS injection in male, but not in female, indicating an increased cytokine response of male mice at the early stages of endotoxaemia [75]. Another explanation for the survival advantage in females is that the peritoneal and pleural cavities of females contain a higher number of leukocytes compared with the equivalent group of male mice and rats, comprising greater numbers of macrophages, T and B lymphocytes. The different composition of immune cells in the female peritoneum is due to the increased expression of tissue chemokines and chemokine receptors [76]. Moreover, female resident macrophages have significantly greater TLRs expression and more efficient phagocytosis [76].

In rats with polymicrobial sepsis, treatment with oestradiol exhibited antioxidant properties and attenuated liver and intestine injuries [77]. Testosterone receptor antagonism with flutamide treatment in male mice with trauma-haemorrhage prevented immune deficiency and significantly decreased the mortality rate caused by

a subsequent septic challenge [78]. However, it has been shown that flutamide treatment following trauma increases the activity of enzyme aromatase, which catalyses the conversion of testosterone into oestradiol [79, 80], indicating that the protection afforded by flutamide in male mice may not be mediated by testosterone receptor antagonism, but by increasing the synthesis and the level of oestradiol.

1.1.6 Cardiac Dysfunction in Sepsis

The development of myocardial dysfunction is associated with increased morbidity and mortality of sepsis. More than 40% of cases of sepsis have cardiovascular impairment [81] and the presence of myocardial dysfunction can increase the mortality rate of affected patients to 70% [16]. Due to recognition of the importance of the cardiovascular impairment in sepsis, myocardial dysfunction identified by echocardiography has been included as one of the criteria for diagnosing severe sepsis [38].

Myocardial dysfunction in patients with septic shock was first described by Parker et al. in 1984 [82], who discovered that patients with septic shock showed significant cardiac dysfunction with depressed left ventricular ejection fraction (LVEF) and acute LV dilation. Interestingly, the changes in heart function and cardiac volumes were fully reversed in survivors of septic shock over a 7-10 days period [82]. Before the application of pulmonary artery catheters, it was believed that the cardiovascular involvement associated with sepsis had two distinct phases. In the initial stage of sepsis, patients developed "warm shock" characterised by warm skins and a bounding pulse, resulting from a hyperdynamic state associated with high cardiac output and low systemic vascular resistance. This was followed by "cold shock" due to a hypodynamic state secondary to low cardiac output and high systemic vascular resistance, with clinical signs of cool extremities, a thready pulse, myocardial depression and ultimately death [83, 84]. However, with the application of pulmonary artery catheters (in the clinical or the experimental setting), which can measure haemodynamic changes including cardiac output and LV filling pressures accurately, it was found that patients with septic shock which received sufficient fluid resuscitation consistently exhibited a hyperdynamic state with hot extremities, high cardiac output and low systemic vascular resistance. It was concluded that the previous depiction of a hypodynamic stage of sepsis was the result of inadequate fluid

resuscitation and that the signs of "cold shock" were due to increased systemic vascular resistance compensating for reduced cardiac output [85, 86]. This led to the realisation of the importance of fluid resuscitation in modulating cardiovascular performance in patients with sepsis [87, 88]. However, intrinsic cardiac dysfunction still existed in patients despite of maintained cardiac output and stroke volume [82] with demonstration of depressed EF [89]. Reduction in EF and, hence, myocardial dysfunction was also confirmed by end systolic pressure-volume relationship analysis, a load-independent evaluation of heart function in patients with sepsis [90]. Although the mechanisms underlying the cardiac dysfunction in sepsis are not entirely clear, there is good evidence that a multitude of events including myocardial ischaemia, microcirculation changes, apoptosis, cardiosuppressing factors, nitric oxide (NO) production, calcium trafficking alterations and mitochondrial dysfunction are of pivotal importance (Figure 1.3) [91].
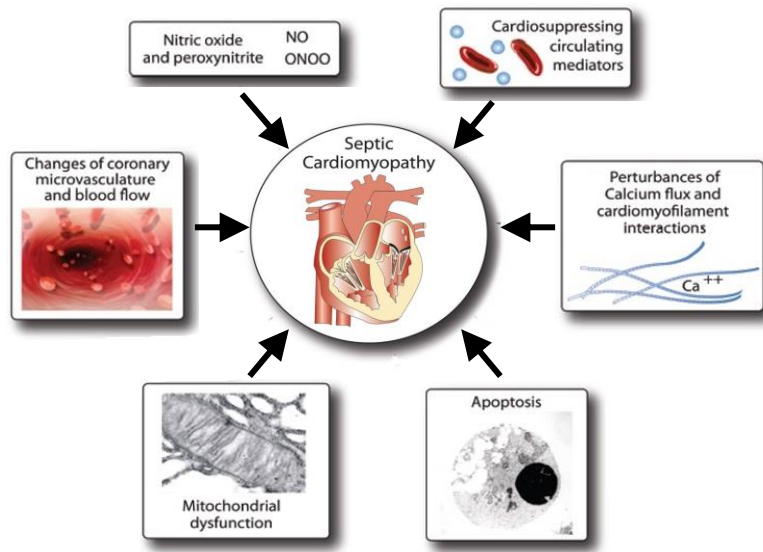
Figure 1.3 A depiction of systemic, cellular, and molecular mechanisms associated with cardiac dysfunction in sepsis. See text for details. Figure modified from Flierl et al., 2008.

1.1.6.1 Systemic, Cellular and Molecular Mechanisms in Sepsis Induced Myocardial dysfunction

Global Ischaemia

A number of early studies suggested that global myocardial ischaemia may be the reason for the cardiac dysfunction observed in sepsis [92]. The theory was abandoned after thermodilution catheters were used in patients with septic shock to assess coronary blood flow and metabolic alterations. These studies demonstrated that patients with sepsis showed preserved or even higher coronary blood flow and decreased coronary artery–coronary sinus oxygen difference [93]. This was confirmed by the observation of markedly dilated coronary arteries and unchanged myocardial lactate production in septic patients [94]. Furthermore, autopsies of patients that had died from sepsis did not reveal any overt signs of cardiac necrosis [95]. However, increased levels of plasma troponin T and troponin I (both biomarkers for myocardial injury) were associated with the depression of left ventricular function in sepsis and septic shock [96]. The reasons for elevation of cardiac troponin in sepsis remains unclear, although it is thought to be due to transiently increased cardiomyocyte membrane permeability caused by increased cytokine levels [97].

Microcirculation Changes

Significant microcirculatory changes have been reported in the heart of patients with sepsis and septic shock, including maldistribution of coronary flow [98], which might be secondary to swollen endothelial cells and non-occlusive intravascular fibrin deposits [99]. Increased migration of activated circulating neutrophils into the interstitium was also reported [100], and these cells may further aggravate myocardial dysfunction via the release of pro-inflammatory cytokines, such as TNF-α [101].

Apoptosis

Many studies report that apoptosis contributes to myocardial dysfunction in sepsis [30, 102] and apoptosis of cardiac myocytes occurs secondary to activation of caspases and mitochondrial cytochrome c release [103]. Application of caspase inhibitors in endotoxin-induced models of shock appeared to decrease cardiac apoptosis and improved cardiac function [104]. However, the reversible myocardial

dysfunction and the rare cardiomyocyte death shown in septic patients [105] support a more important role for functional, rather than structural changes during myocardial depression.

Cardiosupressing Substance

Many studies suggest a potential role for *'cardiosuppressing factors'* in the development of sepsis-induced myocardial dysfunction. Existence of circulating cardiosuppressing substances has been known since the 1970s [106]. In further studies, many factors that are able to act as myocardial depressant mediators were found including TNF-α, IL-1β, IL-6, the complement activation product C5a, endotoxin and endothelin-1 (ET-1), to name but a few. Elevations in the cardiosuppressive cytokines TNF-α, IL-1β and IL-6 were identified in plasma from both septic humans and animals [107]. Infusion of TNF-α in dogs resulted in myocardial dysfunction with depressed EF [108]. The addition of TNF-α to rabbit cardiomyocytes caused a reduction in contractility secondary to suppressed myofilament responsiveness [109]. Direct exposure of myocardial cells to IL-1β led to a decrease of the amplitude and peak velocity of cell shortening in a dose-dependent manner [110]. TNF-α induced myocardial depression might be secondary to the generation of NO [111] and alterations in calcium trafficking [109]. TNF-α and IL-1β also induce mitochondrial injury in sepsis [112]. The addition of recombinant C5a impaired contractility in both sham and septic myocardial cells [113], probably through reacting with its receptor C5aR on myocardial cells [114], which suggests that the activation of complement may play a major role in sepsis-induced myocardial depression. Administration of a blocking antibody of C5a to rodents with sepsis induced by caecal ligation and puncture (CLP) reversed the depression of left ventricular EF resulting in improved survival [114]. Although only a minority of patients with sepsis has detectable levels of endotoxin [115], a potential role of endotoxin in the myocardial dysfunction associated with sepsis should not be neglected. Three hours after the injection of a bolus dose of endotoxin to healthy volunteers, a hyperdynamic circulation associated with high cardiac output and low systemic vascular resistance develops, and this was associated with a reduction in EF after volume loading [116]. The delayed onset of myocardial dysfunction after endotoxin injection suggests that it is unlikely that endotoxin causes myocardial

depression directly, but that LPS mediates the decline in EF through the release of other factors, such as TNF-α [101]. These effects of endotoxin are secondary to its interaction with TLR4, TLR2 [117] and CD14 [117], which are critical links between pathogens and host immune response (see chapter 1.1.4.2.1 Toll Like Receptor for details). The presence of TLR4 in macrophages and neutrophils was necessary for the ability of endotoxin to cause myocardial depression *in vitro* [101]. In addition, both the activation of NF-κB and the increased levels of TNF and IL-1β caused by endotoxin were significantly ameliorated in myocardial cells from CD14-deficient mice [118]. Furthermore, CD14$^{-/-}$ mice were protected from endotoxin-induced myocardial depression compared with wild-type mice [118]. ET-1 was suggested to play a cardiosuppressive role in patients with sepsis [119], and an ET-1-receptor antagonist (SB 234551) attenuates the cardiovascular impairment in endotoxin shock in a dose-dependent manner in rats [120]. Myocardial dysfunction in sepsis is probably not caused by one, but by multiple cardiac suppressive substances, which may act through mediating the activation or inhibition of other factors, eg. NO generation and changes in intracellular calcium trafficking.

Nitric Oxide Production

NO plays a critical role in regulating cardiovascular homeostasis. Most notably, the excessive formation of NO importantly contributes to cardiac dysfunction [121], hypotension and resistance to catecholamines in sepsis [122-125]. NO is produced by NO synthases (NOS) by cell types in the heart. Three forms of NOS enzymes have been identified which are neuronal NO synthase (nNOS, NOS1), inducible NOS (iNOS, NOS2), and endothelial NOS (eNOS, NOS3) [126]. Both *in vivo* and *in vitro* work demonstrated that the level of iNOS in the myocardium increased rapidly after exposure to endotoxin or pro-inflammatory cytokines that are elevated in septic shock [127]. Most notably, mice that are deficient in iNOS protein were protected against the myocardial dysfunction induced by endotoxin [128]. Selected blockade or iNOS-deletion also attenuates the cardiac depression in murine CLP-sepsis by enhancing cardiac norepinephrine responsiveness [129]. The overexpression of eNOS in the myocardium improved myocardial performance, probably through reducing production of reactive oxygen species (ROS) and increasing sarcoplasmic reticulum calcium accumulation, thus illustrating a protective role of myocardial eNOS in sepsis

[130]. The adverse effects of NO on myocardial function may be modulated by peroxynitrite, a by-product produced through interaction between NO and superoxide anions. Peroxynitrite impairs cardiac performance in sepsis through inhibiting mitochondrial respiration, altering calcium transport and denaturing proteins [131, 132]. Removal of peroxynitrite improves myocardial contractility in studies of myocardial dysfunction caused by cytokines [133] and in a rodent model of sepsis [134].

Calcium Trafficking Changes

Alterations in calcium trafficking are also involved in the cardiac depression in sepsis. For instance, intracellular calcium is reduced in myocardial cells after exposure to endotoxin due to decreased L-type channel-dependent calcium flow, leading to suppressed cardiac contractility [135]. Decreased density of ryanodine receptors on the sarcoplasmic reticulum in sepsis is also thought to play an important role in reducing intracellular concentration of calcium by inhibiting calcium release from SR [136]. Moreover, decreased sensitivity of myofilaments to calcium in the septic heart is associated with impaired myocardial contractility [137].

Mitochondrial Dysfunction

There is now good evidence that mitochondrial dysfunction occurs in sepsis and may contribute to organ dysfunction [138]. Sepsis-induced focal mitochondrial injury was observed in both patients dying from sepsis [105] and in septic animals [139]. Mitochondrial DNA is less resistant to the injury induced by LPS when compared with nuclear DNA [140]. Glutathione (an intracellular antioxidant) depletion and NO overproduction observed in skeletal muscle biopsies obtained from septic patients may explain inhibition of oxidative phosphorylation and decreased ATP production by mitochondria [138], which potentially leads to organ failure in sepsis [141]. Mitochondrial permeability transition pore opening is also involved in the myocardial dysfunction induced by sepsis, and preserved myocardial function and decreased mortality rate were obtained through its inhibition [142]. It has been proposed that myocardial depression in sepsis is a protective adaption with the aim to reduce energy consumption (by inhibition of ATP production during the state of mitochondrial dysfunction), which is similar to the hibernation response triggered by myocardial

ischaemia [143].

1.2 Chronic Kidney Disease

1.2.1 Definitions and Diagnosis

Chronic kidney disease (CKD) is caused by reduced renal function and characterised by increases in serum urea and creatinine. Major risk factors for CKD include hypertension, diabetes and old age (>60 years) [144, 145]. The kidney has many functions including excretion of waste products and toxic metabolites, maintenance of haemoglobin synthesis, fluid balance, acid-base and electrolyte balance, and regulation of blood pressure. Therefore, impaired kidney function is associated with a variety of concurrent complications, such as cardiovascular disease (CVD), anaemia and bone diseases, to name but a few [146].

CKD is divided into 5 stages according to the degree of reduction of the glomerular filtration rate (GFR), which describes the volume of fluid filtered by renal glomerular capilllaries into the Bowman's space per unit time. In clinical practice, the most commonly used formula for estimating GFR is that GFR (mL/min/1.73 m^2) = 186 x $(S_{cr})^{-1.154}$ x $(Age)^{-0.203}$ x (0.742 if female) x (1.210 if African-American), where S_{cr} is serum/plasma creatinine in mg/dL [147]. Stage 1 and 2 CKD represents kidney damage with normal or mildly reduced GFR, stages 3-5 CKD represent GFR of 30-59 ml/min/1.73 m^2, 15-29 ml/min/1.73 m^2 and <15 ml/min/1.73 m^2 or on dialysis, respectively (Table 1.8) [145]. Untreated early stages of CKD can lead to end-stage renal disease (ESRD), which requires the initiation of dialysis or renal transplantation. Therefore, once CKD is detected, it is important to identify the cause, concurrent complications and to define the stage of CKD for further management (Table 1.8) [145].

Table 1.8 Stages, stage-specific recommendations for management and prevalence of CKD.

Stage of CKD	Description	GFR	Detection, evaluation, and management
		ml/min/1.73 m^2	
1	Kidney damage* with normal or increased GFR	>90	Diagnosis and treatment Treatment of coexisting conditions Slowing progression Risk reduction for CVD
2	Kidney damage with mild decrease in GFR	60-89	Estimation of progression
3	Moderate decrease in GFR	30-59	Evaluation and treatment of complications
4	Severe decrease in GFR	15-29	Referral to nephrologist and consideration for kidney replacement therapy
5	Kidney failure	<15	Replacement (if uraemia present)

The table displays stages of CKD, stage-specific recommendations for detection, evaluation and management, and prevalence in the United States in 2000. *Kidney damage is defined as persistent albuminuria on two occasions. CI = confidence interval; CVD = cardiovascular disease; GFR = glomerular filtration rate. Table modified from Lesley et al., 2006.

Creatinine clearance is calculated from the creatinine concentration in the collected urine sample, urine flow rate, and the creatinine concentration in the plasma concentration. Creatinine clearance is similar to GFR, and the serum/plasma creatinine level has a reciprocal relationship with GFR [148]. Creatinine clearance exceeds GFR because creatinine is also secreted by proximal tubular cells and also filtered by the glomeruli [145]. Creatinine secretion can be blocked by some drugs, such as trimethoprim and cimetidine, in this case, creatinine clearance is decreased and serum/plasma creatinine concentration is increased without affecting the GFR [149, 150]. The production of creatinine primarily depends on muscle mass and dietary intake, which may have contributed to the variations in the serum/plasma creatinine concentration among different age groups, genders and ethnic groups (Table 1.9) [145].

Table 1.9 Factors affecting creatinine production. *

Factor	Effect on serum/plasma creatinine
Aging	Decreased
Female sex	Decreased
Race or ethnic group †	
Black	Increased
Hispanic	Decreased
Asian	Decreased
Body habitus	
Muscular	Increased
Amputation	Decreased
Obesity	No change
Chronic illness	
Malnutrition, inflammation, deconditioning (e.g., cancer, severe cardiovascular disease, hospitalized patients)	Decreased
Neuromuscular diseases	Decreased
Diet	
Vegetarian diet	Decreased
Ingestion of cooked meat	Increased

The table displays factors contributing to the variations in the serum/plasma creatinine concentration. *Difference in muscle mass accounts for the predominant proportion of serum/plasma creatinine. † White ethnic group served as the reference group. Table adopted from Lesley et al., 2006.

1.2.2 Epidemiology and Outcomes

CKD is a growing health problem worldwide with a global prevalence of around 8%-16% [151]. In 2007, the United Kingdom prevalence of moderate to severe CKD (Stages 3-5) was 8.5% (5.8% in male and 10.6% in female patients), and similar prevalences have been reported in other countries [152, 153]. The prevalence of CKD rises from 8.5% of those under 40 to almost 40% of those that are older than 60 [154]. CKD prevalence in Mexican Americans and non-Hispanic blacks is twice as that in non-Hispanic whites [154]. Low-income status is correlated with an increased risk of albuminuria and progression from CKD to ESRD [155, 156]. Once ESRD has developed, it dramatically increases the clinical and economic burden. In 2011 in the US, the incidence of ESRD was 357 per million population. Nearly 113, 000 patients initiated dialysis, and around 18,000 patients received renal replacement therapy [157]. In developed countries, 2-3% of the overall national health care budget is currently being spent on the treatment of ESRD [158]. In several developing countries, each year around 1 million people die from untreated ESRD, due to lack of accessibility to renal replacement therapy [159].

Premature death caused by CKD is a major contributor to years of life lost in the United States, contributing to 60,000 deaths in 2010 [160]. Among all of the causes of death in CKD patients, CVD remains the number one [161, 162]. CKD caused 560,000 deaths indirectly through CVD in 2010 in the United States [160]. CKD patients not only have higher incidence of ischaemic heart disease, heart failure and cerebrovascular disease, but they also have a higher mortality rate following CV events than non-CKD patients. For example, CKD patients have a 4-5 times higher one-year mortality rate following acute myocardial infarction compared to non-CKD patients [163]. After adjustment for race, gender and age, the mortality of CKD due to CVD is around 10-20 times higher than in an age-matched general population cohort with CVD [161]. This increase in cardiovascular mortality is particularly strong in the younger population, where CKD patients have a 500-times higher cardiovascular mortality compared with non-CKD patients [161].

1.2.3 Uraemic Cardiomyopathy

1.2.3.1 Diagnosis

The CV abnormalities induced by CKD are left ventricular hypertrophy (LVH), coronary artery disease (CAD), and congestive heart failure (CHF) [164]. The diagnosis of CVD consists of clinical symptoms, declinations in physical examination, echocardiography, electrocardiography (ECG), chest X-ray and coronary angiography etc.

Echocardiography is an essential tool for the diagnosis of CVD in CKD patients with symptoms that are suggestive of heart disease. In patients starting dialysis, only 16% patients showed normal echocardiogram; 42% patients showed concentric LVH, 23% showed eccentric LVH, 16% had systolic dysfunction and 4% had isolated LV dilatation [165]. In the United States, LVH is found in about 75% of haemodialysis patients [166]. However, LV mass and LV volume fluctuate due to the fluid accumulation caused by lack of renal excretory capacity and fluid load decreases during dialysis [167]. Therefore it is important that echocardiography is performed when patients are at their dry weight, e.g. on the day after dialysis [164].

The diagnosis of CAD in dialysis patients is difficult. Exercise ECG is unreliable due to i) inability of patients to obtain a sufficient increase in heart rate; ii) existence of electrocardiographic abnormalities at the baseline in CKD patients [168]. Using pharmacological agents to increase heart rate and to induce coronary vasodilation combined with radioisotope e.g. thallium, myocardial imaging has become the standard, non-invasive method for documenting CAD in dialysis patients. However, conflicting data suggest poor sensitivity and specificity of this method [169]. Coronary angiography is the golden standard for detecting CAD in dialysis patients. However, it should be noted that around 50% of dialysis patients with suggestive symptoms of ischaemic heart disease may have a luminal narrowing of less than 50% of coronary artery and, hence, no CAD [170]. This might be due to the combined effects of increased oxygen demanding caused by anaemia and LVH, as well as decreased oxygen supply caused by small vessel coronary disease, reduced capillary density and vascular calcification in CKD patients [164].

1.2.3.2 Risk Factors and Management

The accelerated rate of cardiovascular morbidity and mortality in CKD is undoubtedly ascribed to the high prevalence of traditional risk factors (Table 1.10), e.g., hypertension, dyslipidaemia, diabetes, history of smoking, older age and male gender [164]. Additionally, increased prevalence of other uraemia-related risk factors as renal function declines in subjects with CKD also contributes to the excess risk of CVD. These uraemia-related or non-traditional risk factors include anaemia, abnormal calcium phosphorus metabolism, LVH, inflammation, oxidative stress and hyperhomocysteinaemia, etc (Table 1.10) [171].

Table 1.10 Contribution of traditional and non-traditional risk factors to uraemic cardiomyopathy.

Traditional risk factors	Non-traditional risk factors
Hypertension	Anaemia
Dyslipidaemia	Abnormal calcium and phosphate metabolism
Diabetes	Left ventricular hypertrophy
Smoking	Inflammation
Older age	Oxidative stress
Male gender	Hyperhomocysteinaemia

1.2.3.2.1 Traditional Risk Factors

Hypertension

Hypertension is strongly related to the increased incidence of cardiovascular events in patients with 2-3 stage CKD [172]. More than 70% of ESRD patients have hypertension [147]. Increased pulse pressure has a strong positive relationship with overall mortality of dialysis patients, however, systolic blood pressure is a stronger predictor of cardiovascular death in patients on dialysis [173]. Additionally, dialysis patients have a 48% higher risk of LVH with each increase of 10 mmHg in blood pressure [174]. A reduction in blood pressure slows the progression of CKD [175]. Normally multidrug therapy, such as a combination of calcium channel blockers, angiotensin converting enzyme inhibitors and angiotensin receptor blockers is recommended for treatment of hypertension in CKD patients [176]. However, it should be noted that low level of blood pressure has also been correlated to increased mortality in dialysis patients [177].

Dyslipidaemia

Dyslipidaemia commonly exists in patients with CKD and ESRD, characterised by increased concentrations of triglyceride, VLDL cholesterol, LDL cholesterol and Lp(a) lipoprotein, reduced levels of HDL cholesterol [171]. Dyslipidaemia is independently correlated with cardiovascular diseases in CKD patients [178]. In patients on haemodialysis, increased Lp(a) lipoprotein levels predicts a higher risk in developing CAD [179]. In patients on peritoneal dialysis, there is a strong relationship between the severity of coronary artery events and the lipid abnormalities [180]. Statins have been shown to significantly reduce plasma lipid levels and prevent cardiovascular events without side effects such as liver injury in CKD patients [181, 182]. However, in patients on dialysis, statins failed to improve cardiovascular endpoints despite the treatment significantly lowered LDL cholesterol concentrations [183].

Diabetes

Diabetes is a risk factor for the adverse outcomes in patients with all stages of CKD [184]. In patients on dialysis, high values of haemoglobin A_{1c} have been associated

with a greater risk of cardiovascular mortality [185]. However, contradictory results have also been reported that no association was found between haemoglobin A_{1c} levels and death in dialysis patients in a different epidemiological study [186]. Using haemoglobin A_{1c} as an index for glycaemic control can be unreliable in uraemic patients, due to the variable red blood cell survival and the interference of carbamylated haemoglobin in glycohaemoglobin assays [187].

Smoking, Older Age and Male Gender

Smoking has been associated with progression of CKD [188]. Smoking is also a risk factor for increased mortality and development of heart failure in patients on dialysis [189]. In dialysis patients, older age appears to be one of the strongest traditional risk factors for cardiovascular events [190]. Male gender is correlated with higher prevalence of both CAD and LVH in dialysis patients [191].

1.2.3.2.1 Non-traditional Risk Factors

Anaemia

Anaemia is a common complication in CKD patients due to a deficiency in renal erythropoietin production. Severe anaemia (haemoglobin less than 90 g/l) is an independent predictor of death, cardiovascular mortality and impaired quality of life in CKD patients [192]. Anaemia leads to reductions in plasma viscosity, systemic vascular resistance, and oxygen delivery capacity of blood, and increases in venous return and sympathetic activity. The increases of venous return and sympathetic activity subsequently lead to increases in both of the heart rate and the venous tone, thus, an increased cardiac output. The increased cardiac output consequently causes adaptive or maladaptive LVH due to the increase in LV wall tension, as well as vascular hypertrophy and atherosclerosis due to the increase in arterial tension [193].

Correction of anaemia by erythropoiesis-stimulating agents, e.g. recombinant human erythropoietin, has been shown to lower the cardiac output and partially reverse LVH [194]. Both normalisation of haemoglobin ($\geq$130 g/l) and partial correction of anaemia (haemoglobin levels of 100 g/l) significantly improved quality of life in patients on haemodialysis, while no difference was observed in survival rate or improvement of quality of life between two target groups [175, 192]. US drug labels

recommend target haemoglobin levels of 90-110 g/l for patients on dialysis with the use of erythropoiesis-stimulating agents, so that blood transfusions can be avoided, while higher target haemoglobin levels (100-120 g/l) is recommended by European standard [192].

Hyperparathyroidism, Calcium and Phosphate Metabolism

Abnormalities in serum levels of parathyroid hormone, phosphate and calcium-phosphate product are correlated with overall mortality in dialysis patients [195, 196]. Hyperparathyroidism is involved in the development of LVH. Increased plasma level of parathyroid hormone is implicated in the pathogenesis of myocardial fibrosis in uraemia [197]. Whereas parathyroidectomy improves LV function and partially reverses LV size in CKD patients [175]. In patients with stage 3-4 CKD, high phosphate levels predisposes to coronary artery calcification, myocardial infarction and death [198, 199]. Coronary artery calcification subsequently contributes, at least in part, to the development of atherosclerosis, which is a predictor of mortality in CKD patients [187]; and increases arterial stiffness, which leads to decreased coronary artery perfusion, systolic and diastolic blood pressure changes, LVH and adverse cardiovascular outcomes [200].

High calcium levels have been shown to stimulate coronary artery calcification and associated with cardiovascular mortality in patients on dialysis [201, 202]. Therefore, non-calcium-containing phosphate binders, e.g. sevelamer, have been studied for their potential therapeutic effects on controlling secondary hyperparathyroidism, without increasing calcium loads, in dialysis patients. A randomized clinical trial involved 127 patients on haemodialysis showed that all-cause mortality was less in the sevelamer group compared with patients treated with calcium containing phosphate binders [203]. However, a multicentre clinical trial involved 2,103 haemodialysis patients showed contradictory results that no difference was observed in either cardiovascular death or all-cause death between sevelamer group and calcium based agents group [204].

Left Ventricular Hypertrophy

The prevalence of LVH increases as the declination of renal function. LVH is a strong predictor of cardiovascular events and mortality [205, 206]. Factors contributing to

the pathogenesis of LVH in patients with CKD or ESRD include increased cardiac output, elevated blood pressure, extracellular fluid volume overload and vascular stiffness [187, 207].

A prospective clinical study has shown that activated vitamin D-calcitriol treatment regresses myocardial hypertrophy, parallels with the decreases in plasma levels of intact parathyroid hormone [208]. Compared with conventional haemolysis 3 times per week, frequent nocturnal haemolysis (6 times per week) has been shown to associate with significant decreased LV mass, improved mineral metabolism, reduced usage of medications for controlling blood pressure and oral phosphate binders [209].

Inflammation

Inflammation commonly exists in patients with all stages CKD, in dialysis patients, about 50% population showed biochemical evidence of inflammation [210, 211]. Many factors may contribute to the inflammatory response in CKD patients, which include impaired renal excretion of inflammatory substances, reduced half-life of inflammatory cytokines, concomitant infections or sepsis, and increased risk of exposure to endotoxin due to the routine dialysis procedure [187, 212].

Inflammation is a crucial factor contributing to the development of atherosclerosis [213]. Inflammation facilitates plague formation probably by causing endothelial cell injury, thus activating leukocytes and platelets, which subsequently adhere to the endothelium. Endothelial injury also leads to vascular smooth muscle cell proliferation favouring the development of atherosclerosis [213].

CRP, a marker of inflammation, predicts both cardiovascular mortality [214] and all-cause mortality in dialysis patients [215]. Elevated levels of CRP correlate with increased number of atherosclerotic plaques in the carotid arteries of haemodialysis patients [216]. CRP probabaly contributes to CVD by binding to injured endothelial cells and activating compliments [217]. Additionally, cardiovascular mortality and all-cause mortality are significantly increased in dialysis patients with elevated levels of inflammatory cytokines, such as IL-6 [218]. IL-6 can favour lipid formation and vascular smooth muscle cells proliferation by damaging endothelial cells [219].

In haemodialysis patients, simvastatin showed (in addition to its lipid-lowering effect)

an anti-inflammatory effect, demonstrated by a 47% reduction in serum CRP levels [220]. Therefore, it is reasonable to recommend the use of statins and aspirin in patients with high risk of developing CVD, due to their effects being designed as well as their effects in modulating inflammatory response [221].

Oxidative Stress

Oxidative stress is seen when there is an imbalance between generation of ROS and anti-oxidant mechanisms, e.g. with an increased pro-oxidant formation and deficiencies of anti-oxidant substances, or both. Formation of ROS is crucial in host response against inflammation and in tissue repair [222]. Major enzymatic anti-oxidant members for detoxifying ROS include dismutase and glutathione peroxidase. Non-enzymatic members include Vitamin C and E, zinc, and selenium [223]. Oxidative stress commonly exists in CKD/ESRD patients [207, 224], which is probably ascribed to both of the deficiencies of anti-oxidant substances [225] and increased pro-oxidant activity caused by blood-membrane interaction [226] as well as by the chronic inflammatory response and uraemic toxins [222, 227].

Oxidative stress is involved in atherosclerosis and CVD, as it induces peroxidation of lipids, which produces oxidised lipoproteins, such as oxidised LDL. Oxidized LDL plays crucial roles in foam cells formation, endothelial cells injury and vascular smooth muscle cells proliferation, favouring the development of atherosclerosis [221]. The serum concentration of oxidative stress markers has been shown to have a positive correlation with the incidence of CVD in haemodialysis patients [228, 229].

Supplementation with vitamin E reduces the susceptibility of LDL to oxidation in patients on dialysis, especially on peritoneal dialysis [230]. Supplementation with high-dose vitamin E to haemodialysis patients with pre-existing cardiovascular disease has been associated with improved CVD outcomes [231]. Supplementation of antioxidant acetylcysteine has been shown to decrease the incidence of cardiovascular events in ESRD patients on haemodialysis [232].

Hyperhomocysteinaemia

Plasma homocysteine level is mainly determined by the renal function, it increases as the renal function declines [233]. Hyperhomocysteinaemia is universally observed in

CKD patients, at least in part, due to the impaired renal clearance [234]. Hyperhomocysteinaemia has been reported to have a significant association with an increased incidence of cardiovascular accidents in patients with CKD [235]. High level of homocysteine promotes atherosclerosis probably by causing endothelial cells injury, enhancing LDL oxidation, inducing smooth muscle cell proliferation and enhancing thrombosis [221].

Treatment with folic acid and vitamins B6 and B12 reduces total homocysteine levels in patients undergoing dialysis [236], however, a random clinical trial has shown that high doses of folic acid and vitamins B6 and B12 fail to improve cardiovascular outcomes in patients with advanced renal failure [237].

1.2.4 Infection/Sepsis in Chronic Kidney Disease

1.2.4.1 Epidemiology and Outcomes

Infectious complications account for one third of all of the ICU admissions in patients with CKD [238]. The urinary tract is the primary source of infection in patients on dialysis, due to the reduction in urine output and increased risk of urinary obstructions. Pneumonia is the second most common infectious complication in CKD patients, followed by sepsis (Figure 1.4) [239]. Other infectious complications can result from an interruption of the skin barrier, contaminated dialysis machine or dialysate; these infections are at high risk of progressing to septicaemia [239]. A seven-year follow-up study shows that in patients on haemodialysis and peritoneal dialysis, the hospitalization rates for septicaemia are 11.7% and 9.4%, respectively [240]. When compared with the general population without CKD, the hospitalization rates for bacteraemia/sepsis are 4-times higher in CKD patients without dialysis, and nearly 10-times higher in patients on dialysis [241]. The microorganisms causing these infectious events are mainly bacteria and fungi, the device-related infections are mostly caused by Gram-positive bacteria, such as *Staphylococcus aureus* [242, 243], while other report shows that the most common pathogens causing bloodstream infections are Gram-negative bacteria, particularly *Escherichia coli* [244].
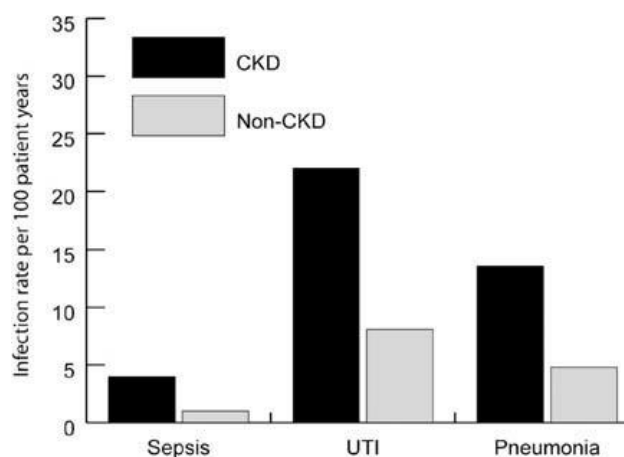
Figure 1.4 Raw infection rates in CKD and non-CKD populations. UTI = urinary tract infection. Figure modified from Sakina et al., 2006.

Among all of the causes of mortality in patients with CKD, infectious complications are the second leading cause, closely following CVD [239]. Compared with the general population with pneumonia and sepsis, in patients on dialysis, the annual mortality rates caused by these infectious complications are 10-fold and 100-300 fold higher, respectively [245, 246]. Despite refined transplant surgical techniques and more potent immunosuppressive therapies, the annual mortality rate following sepsis is 20-fold higher among recipients of kidney transplants as compared with general population with sepsis [245]. An observatory study associated with non-dialysis CKD patients showed that the 28- and 90-day mortality rates secondary to pneumonia were 29.6% and 37.4%, respectively. Moreover, the 28-day mortality rate following sepsis in this same cohort was 35.6% and 90-day mortality was 44.2% [247]. It has also been shown that among all chronic medical conditions, pre-existing CKD predisposes the septic patients to the highest 90-day mortality risk [248].

1.2.4.2 Risk Factors

Numerous potential risk factors (Figure 1.5) contribute to the increased risk of infection/sepsis in CKD and ESRD patients. These risk factors include older age, comorbidities (particularly diabetes), anaemia, nephrotic syndrome and low serum albumin, etc. Moreover, these factors further lead to the immune dysfunction among CKD and ESRD populations, characterised by defective neutrophil phagocytosis and deranged functions of lymphocytes [249]. Initiation of maintenance dialysis increases infection risk through inducing vascular access and membrane re-use, etc. [240].
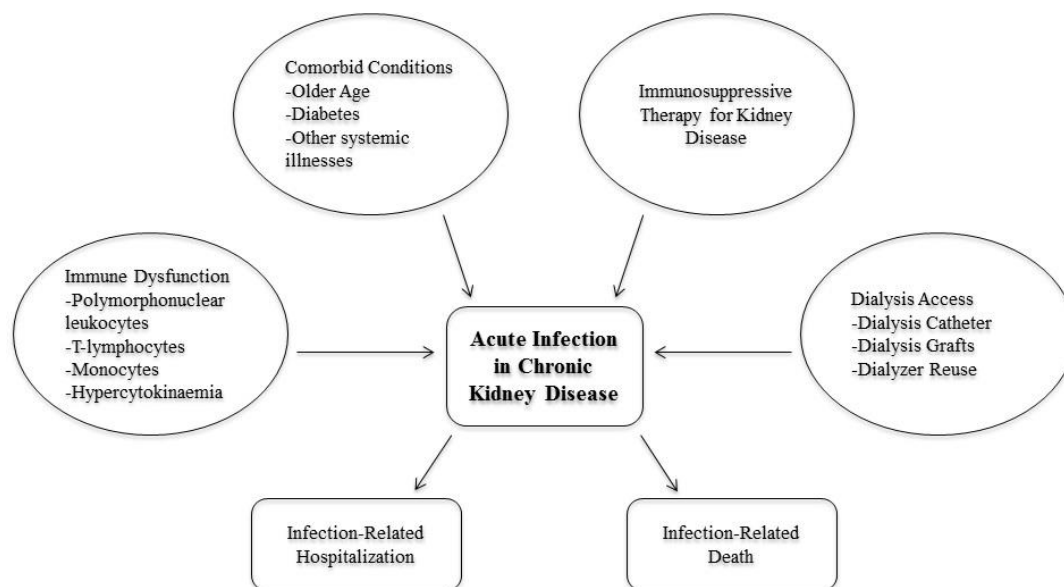
Figure 1.5 Risk factors and outcomes of infection in CKD. Figure modified from Dalrymple et al., 2008.

Older Age and Diabetes

CKD and ESRD populations are characterised by older age and coexisting diabetes [250]. Among ESRD patients, older patients and patients with diabetes are associated with higher risk for infection, regardless of dialysis-related complications [240]. Diabetes is a widely recognised risk factor that predisposes patients to infections, due to impaired phagocytosis and immune defensive mechanisms, which have been characterised in patients with diabetes without good metabolic control [251].

Nephrotic Syndrome and Immunosuppressive Therapy

Nephrotic syndrome in children has been reported to be closely correlated with bacterial sepsis and peritonitis [252]. This may be ascribed to deficient neutrophil and splenic functions and significant loss of factors of the alternative complement pathway in the urine in children with nephrotic syndrome [253]. Patients with autoimmune renal disorders normally receive immunosuppressive therapy, especially cytotoxic drugs, which are known to increase the risk for infection in these patients [254]. Immunosuppressive medications have also been strongly correlated with an increased incidence of bacteraemia in patients on haemodialysis [255].

Immune Dysfunction

In CKD patients, impaired polymorphonuclear leukocyte function is caused by variety of factors, such as uraemic toxins, anaemia, malnutrition, iron overload and bio-incompatibility of dialysis membrane, etc. [256]. LPS stimulated monocytes obtained from patients on peritoneal dialysis release less IL-1β and TNF-α when compared with those from normal populations [257]. Monocytes and monocyte-derived dendritic cells obtained from ESRD patients exhibit defective endocytosis and impaired terminal differentiation [258]. Moreover, uraemic serum blunts the response of T-cells to antigens [259].

Uraemic patients have elevated plasma levels of both pro-inflammatory (e.g. TNF-α and IL-6) and anti-inflammatory cytokines (e.g. IL-10) [260]. The major reasons for this hypercytokinemia in patients with CKD and ESRD is probably secondary to reduced excretion of cytokines due to impaired renal function, as well as increased generation of cytokines caused by uraemic toxins, oxidative stress and comorbidities

[261].

Dialysis Access

Repeated access to vascular fistulas or grafts or dialysis catheters increase the risk of infections, due to the disruption of the skin barrier [262]. Among these forms of dialysis access, vascular dialysis catheters and vascular grafts predispose to even higher risk for infections. Compared with native fistulas, vascular grafts are associated with increased risk of septicaemia among patients on haemodialysis [240]. Dialysis catheters conferred a nearly two-fold higher risk for sepsis as well as infection-related mortality as compared with native fistulas in dialysis patients [263, 264]. Several clinical studies show a positive relationship between dialyzer reuse and increased risk for infections [240, 265]. Dialyzer reuse has also been associated with a higher mortality rate in patients on haemodialysis [266].

1.2.4.3 Preventive Strategies

Due to the high morbidity and mortality rate of infection/sepsis in CKD and ESRD patients, effective approaches for preventing infections in this population are essential. However, many risk factors for infections cannot be altered, such as older age and nephrotic syndrome as the cause of CKD. It is unknown that whether the management of comorbidities, e.g., diabetes, is associated with a lower risk for infections in patients with CKD and ESRD. However, potentially effective strategies have been applied to reduce the risk for infections, such as vaccination. Early vaccination against infections by pneumococci is recommended in all CKD patients. Among patients on dialysis, pneumococcal vaccination correlates with a lower total mortality, demonstrating a protective role of vaccine-triggered anti-pneumococcal strategy in CKD patients [267]. Among patients with peritoneal dialysis, influenza A and B vaccination results in decreased all-cause mortality rate. In patients on haemodialysis, influenza vaccination reduces hospitalizations for infections, such as influenza and pneumonia, as well as decreases all-cause mortality rate [268].

However, it should be noted that because of the alterations of immune function in patients with ESRD, this population has a blunted response to vaccinations [267, 269]. Patients with renal disease have reduced responsiveness to vaccination, and once the antibody is generated after vaccination, the declination rate of antibody levels is more

rapid [270], which could limit the potential effectiveness of the preventive strategy of vaccination for reducing infections in patients with CKD and ESRD.

1.3 TRPV1

1.3.1 Properties of TRPV1

Transient receptor potential vanilloid 1 (TRPV1), or vanilloid receptor type 1 (VR1), is a non-selective calcium influx channel, was originally characterised as a noxious heat (>42°C) sensor [271]. The TRPV1 receptor can be activated by a variety of exogenous agonists, including capsaicin (the extract of hot chilli peppers), as well as capsaicin analogues (olvanil or plant toxin resiniferatoxin) [272] and low pH (<6.0 at room temperature) [273]. Endogenous agonists acting at the TRPV1 receptor *in vivo* include anandamide [274], protons [275], and several products of lipoxygenases, including 12-(S)-hydroperoxyeicosatetraenoic acid (12-(S)-HpETE) [276] and 20-hydroxyeicosatetraenoic acid (20-HETE) [277].

1.3.1.1 Molecular Structure, Expression and Functions of TRPV1

TRPV1 receptors have large cytosolic amino-(N-) and carboxy-(C-) termini and 6 transmembrane domains (TM1-6), with a pore-forming loop between TM5 and TM6 (Figure 1.6) [271]. In the N-terminus, there are at least three ankyrin repeats, which bind cytosolic proteins, such as calmodulin [278]. In the C-terminus, there is a TRP domain, which acts as molecular determinate of tetramerisation of TRPV1 [279]. The C-terminus also contains a binding site for phosphatidylinositol-4,5-bisphosphate (PIP2), and its location in the upper or lower leaflet of the cell membrane determines its function in up-regulating or down-regulating the activity of TRPV1 [280]. Additionally, there are multiple potential phosphorylation sites of protein kinase A and protein kinase C in the C-terminus, the N-terminus and the TM2-TM3 loop region.
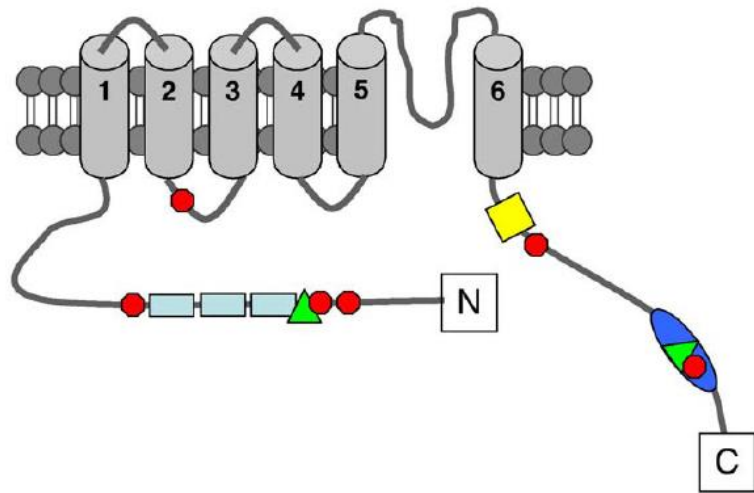
Figure 1.6 Molecular structure of the TRPV1 receptor. ▭ Ankyrin repeat domain; ▯ TRP domain; ⬭ PIP2-binding domain; ⬤ PKA/PKC phosphorylation sites; ▲ CaM binding sites. Figure adopted from K. Alawi and J. Keeble, 2010.

Intradermal injection of the TRPV1 agonist capsaicin causes intense pain in humans and animals [281]. Consistent with these findings, TRPV1 expression is localised in small- to medium-diameter primary afferents, mainly in unmyelinated C afferents and thinly myelinated Aδ afferents [271, 282]. These nociceptive fibres characteristically contain neuropeptides, including calcitonin gene-related peptide (CGRP), somatostatin and substance P [283]. Activation of TRPV1 through its agonists triggers influx of divalent cations (particularly $Ca2^+$) and nerve depolarisation, which in turn results in the conduction of painful afferent impulses and concomitant release of the neuropeptides [284].

TRPV1 is also expressed in non-neuronal tissues including liver [285], various regions of brain [286], bladder urothelium, smooth muscle cells, endothelium [287], keratinocytes [288] as well as immune cells such as polymorphonuclear granulocytes [289], macrophages [290] and lymphocytes [291]. However, the function of TRPV1 in these non-neuronal tissues remains the subject of current research.

1.3.2 Roles of TRPV1 in Inflammation and Sepsis

1.3.2.1 Neurogenic Inflammation

Neurogenic inflammation is caused by the release of neuropeptides from sensory nerve terminals upon the activation of TRPV1 channel receptor, resulting in increased blood flow, plasma extravasation and recruitment of inflammatory cells. Among these neuropeptides, substance P is largely considered pro-inflammatory. Activation of NK_1 receptors by substance P causes microvascular leukocyte accumulation [292] and keratinocyte-derived cytokine (KC; equivalent to IL-8 in human) production [293]. Substance P is also associated with oedema formation and increased blood flow [294]. All of the above processes play a key role in the pathogenesis of numerous conditions, such as joint inflammation, colitis, and neuropathic pain, to name, but a few [283]. On the other hand, there is good evidence that CGRP and somatostatin are anti-inflammatory. In LPS-injected mice, CGRP pre-treatment reduces TNF-α and KC generation, and attenuates recruitment of neutrophil; these beneficial effects are reverted by the CGRP receptor antagonist, CGRP8-37 [295]. The anti-inflammatory effects of CGRP are mediated by inhibiting of TLR activation, reducing the production of down-stream inflammatory mediators [296]. Somatostatin acts as an

anti-inflammatory neuropeptide in an auto-inhibitory manner, in which it not only inhibits its own release from sensory nerve terminals, but also prevents release of other pro-inflammatory neuropeptides [297]. Additionally, somatostatin inhibits the actions of pro-inflammatory mediators at their effector sites by binding to G-protein coupled receptors on vascular smooth muscle and immune cells [297].

1.3.2.2 Direct Stimulation of Inflammatory Cytokines Production

In addition to eliciting neurogenic inflammation, TRPV1 may also act as a direct stimulator of the formation of pro-inflammatory mediators from immune cells. In murine mast cells, TRPV1 activation leads to production and release of IL-4 [298]. Immunohistochemistry of human inflammatory skin samples revealed TRPV1 expression in all mast cells, whereas very few mast cells were TRPV1 positively stained in healthy skin samples [299]. Although TRPV1 has been considered as a pro-inflammatory receptor in the past, new evidence regarding its protective roles against some inflammatory conditions has emerged, particularly in sepsis.

1.3.2.3 Protect Roles of TRPV1 in Sepsis

The discoveries of increased plasma levels of CGRP in patients with sepsis [300] and of an aggravated inflammatory response in sensory denervated rats [301] raised the awareness of the importance of TRPV1 in sepsis. More recently, in rats with endotoxaemia, elevated TRPV1 was observed in the tongue tissue [302].

To investigate the potential involvement of TRPV1 in sepsis, both loss- and gain of TRPV1 function methodologies have been used. In rats treated with LPS, the TRPV1 antagonist (capsazepine) strongly inhibited the recovery of hypotension and tachycardia. Moreover, both 24- and 48-hour survival of endotoxaemic rats were significantly reduced by capsazepine treatment [303]. At 4 h after LPS injection, TRPV1$^{-/-}$ mice showed greater hypotension compared with WT mice, indicating a vascular protective role of TRPV1. Additionally, TRPV1$^{-/-}$ mice challenged with LPS also exhibited enhanced liver injury indicated by elevated levels of plasma AST and liver plasma extravasation, as well as aggravated acute inflammatory response indicated by increased production of TNF-α and nitric oxide in peritoneal lavage [304]. Aggravated hypotension, liver injury, renal and pancreatic dysfunction in TRPV1$^{-/-}$ mice were also confirmed in CLP-induced polymicrobial sepsis model

[290].

On the other hand, administration of the TRPV1 agonist capsaicin to septic rats significantly reduced the mortality rate and attenuated the catabolism of skeletal muscle [305]. Capsaicin treatment also reduced plasma concentrations of TNF-α and IL-6, but increased anti-inflammatory IL-10 levels in a rat model of CLP [306].

1.4 Aims of the Thesis

This thesis had the overall aim to (i) investigate the pathophysiology of the cardiac dysfunction associated with sepsis and to (ii) identify novel therapeutic approaches for improving cardiac function in preclinical models of sepsis.

Increasing evidence shows that gender determines the degree of inflammatory response of the host and that females tolerate sepsis better than males. However, it is unknown whether gender affects the cardiac dysfunction in animals or patients with sepsis. In this thesis, I will establish animal models of polymicrobial sepsis caused by CLP, and systemic hyper-inflammation induced by co-administration of LPS and PepG in both male and female mice (chapter II). Using these models, I will then investigate whether the severity of sepsis-induced cardiac dysfunction differs in male and female mice (chapter II).

Patients with CKD requiring dialysis have a higher risk of infection and sepsis. Once infected, dialysis patients with sepsis have an approximately 100-fold higher mortality rate compared with the general population with sepsis. However, the reasons for this higher mortality rate are unclear. Therefore, in chapter III, I will investigate (a) the roles of pre-existing CKD on cardiac function in mice with sepsis, and (b) the molecular mechanism underlying the cardiac dysfunction in CKD/sepsis, and (c) whether inhibition of NF-κB (with a specific IKK-inhibitor) reduces the cardiac dysfunction in CKD-sepsis.

Activation of TRPV1, which is highly expressed by neurons innervating the heart, improves outcome in sepsis/endotoxaemia. However, the identity of the endogenous activators of TRPV1 and the role of the channel in the cardiac function during sepsis/endotoxaemia is unknown. Therefore, in chapter IV, I will investigate (a) the roles of TRPV1 in the cardiac dysfunction caused by lipopolysaccharide (LPS; endotoxaemia), and (b) the involvements of 12-(S)-HpETE and 20-HETE (potent ligands of TRPV1) and neuropeptides (downstream mediators of TRPV1) in the cardioprotective effects afforded by TRPV1.

CHAPTER II | GENDER DIMORPHISM OF THE CARDIAC DYSFUNCTION IN MURINE SEPSIS: SIGNALLING MECHANISMS

2.1 Introduction

Sepsis is one of the most common causes of morbidity and mortality among admissions to the intensive care unit [307, 308]. Sepsis is a systemic dysregulated hyperinflammatory and/or anti-inflammatory response to infectious stimuli, such as bacteria, viruses and fungi, which, when excessive, may progress to organ failure and death [28]. Development of myocardial dysfunction is associated with increased morbidity and mortality of sepsis. More than 40% cases of sepsis have cardiovascular impairment [309] and the presence of myocardial dysfunction can increase the mortality rate of affected patients to 70% [16].

There is now good evidence that gender is a key determinant in the degree of the host inflammatory response and even of outcome in patients with sepsis. In a number of clinical and epidemiological studies, a significantly increased survival rate was reported in female patients when compared with male patients with sepsis [68, 310-312]. This may be associated with lower pro-inflammatory and higher anti-inflammatory cytokine levels in female patients [68]. Moreover, healthy female volunteers challenged with either lipopolysaccharide (LPS) or LTA showed less pro-inflammatory response than males as demonstrated by lower levels of TNF-α, IL-1β, IL-6 and IL-8 in blood [313]. In addition, severely injured male trauma-patients had a higher incidence of sepsis, multiple organ dysfunction syndrome and greater elevations in plasma procalcitonin and IL-6 compared with the equivalent group of females [73]. Further basic research studies also confirmed these clinical data on gender dimorphism following sepsis. These experimental studies suggested that females had immunologic advantage and showed a significantly increased survival rate compared with males following induction of polymicrobial sepsis by CLP [70].

However, little is known about the impact of gender dimorphism on cardiac dysfunction caused by sepsis. Moreover, the mechanisms underlying the gender

difference in susceptibility of the heart to a septic challenge are not understood. The present study was designed to determine whether the severity of myocardial dysfunction caused by either co-administration of LPS/ PepG or polymicrobial sepsis induced by CLP differs in male and female mice. Having found that the cardiac dysfunction associated with sepsis was less pronounced in female than in male mice, I have then investigated the potential signalling pathways that may have contributed to the observed differences.

2.1.1 Scientific Hypotheses and Aims of the Study Presented in Chapter II

My project was driven by the hypotheses that:

- Female mice subjected to sepsis have better cardiac function than male mice

- Cardiac activation of the Akt/eNOS survival pathway and decreased activation of NF-κB are essential to the protection of female hearts against the dysfunction associated with sepsis

My study had the following scientific objectives:

- To establish animal models of hyper-inflammation induced by co-administration of LPS and PepG in both male and female mice

- To investigate the gender dimorphism in the severity of cardiac dysfunction caused by co-administration of LPS/PepG

- To elucidate signalling mechanism (s) underlying the protection of female hearts against the dysfunction associated with sepsis

- To establish a clinically relevant model of polymicrobial sepsis caused by CLP (with antibiotic therapy and fluid-resuscitation) in both male and female mice

- To confirm the results obtained in the model of hyper-inflammation in polymicrobial sepsis model induced by CLP

2.2 Materials and Methods

2.2.1 Animals

The animal protocols followed in this study were approved by the Animal Welfare Ethics Review Board (AWERB) of Queen Mary University of London in accordance with the derivatives of both the Home Office guidance on the Operation of Animals (Scientific Procedures Act 1986) published by Her Majesty's Stationery Office and the Guide for the Care and Use of Laboratory Animals of the National Research Council. All surgery was performed under ketamine/xylazine anaesthesia and echocardiography was performed under inhalation anaesthesia of isoflurane, buprenorphine was administered before surgery as well as 6 h and 18 h after surgery to reduce postoperative pain, and all efforts were made to minimise suffering of the animals. This study was carried out on ten week-old male (n = 29) and age-matched female (n = 22) C57BL/6 mice, weighing 20-30 g, and eight month-old male (n = 12) and age-matched female (n = 12) C57BL/6 mice (Charles River Laboratories UK Ltd., Kent, UK), weighing 35-50 g. The animals were allowed to acclimatise to laboratory conditions for a period of at least one week before any experimental procedures were initiated. They were housed in individually ventilated cages lined with an absorbent bedding material with no more than 6 mice per cage. The room temperature and humidity was maintained at 19°C -23°C and 55%, respectively. All animals had free access to a standard diet and water *ad libitum*. The feeding boxes were cleaned and disinfected every 3 days, and the water was changed on a daily basis to prevent infectious diseases. Animals were inspected for signs of illness and/or unusual behaviour by research staff at least once per day. All studies involving animals are reported in accordance with the ARRIVE guidelines for reporting experiments involving animals [314, 315].

2.2.2 Model of LPS/PepG-induced cardiac dysfunction

Ten week-old male and female C57BL/6 mice received intraperitoneal administration of LPS/PepG (LPS (derived from *Escherichia coli* 0111:B4); 3 mg/kg and PepG; 0.1 mg/kg or LPS; 9 mg/kg and PepG; 1 mg/kg in PBS; 5 ml/kg i.p.) (Figure 2.1). Sham-treated mice were not subjected to LPS/PepG, but were otherwise treated the same way. Eighteen hours after LPS/PepG administration, cardiac function was assessed by

echocardiography *in vivo*. Mice were then deeply anaesthetised i.p. with ketamine (100 mg/kg) and xylazine (10 mg/kg), and were killed by removing the hearts. Heart samples were stored at -80 °C for further analyses. Mice were randomly allocated into eight different groups as indicated in Table 2.1.

At 18 hours post-LPS/PepG injection, a clinical score for monitoring the health of experimental mice was used to evaluate the symptoms consistent with murine sepsis. The maximum score of 6 comprised the presence of the following signs: lethargy, piloerection, tremors, periorbital exudates, respiratory distress, and diarrhea.
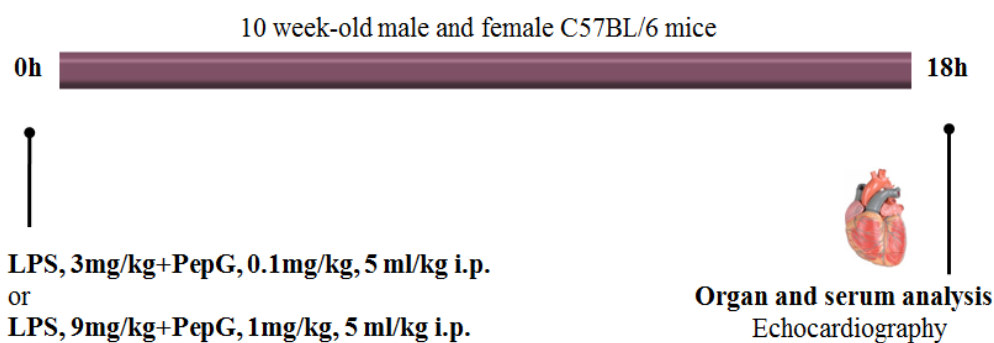
Figure 2.1 Co-administration of LPS/PepG-induced cardiac dysfunction. Scheme of animal experiments carried out in a model of co-administration of LPS/PepG-induced experimental sepsis in 10 week-old male and female C57BL/6 mice to investigate gender dimorphism of cardiac dysfunction and its underlying mechanism. Mice received intraperitoneal (i.p.) administration of LPS/PepG (LPS; 3 mg/kg and PepG; 0.1 mg/kg or LPS; 9 mg/kg and PepG; 1 mg/kg in PBS; 5 ml/kg i.p.). At 18 h cardiac function was assessed by echocardiography *in vivo* under anaesthesia with isoflurane. Mice were then euthanised; organs and blood samples were collected for quantification of organ dysfunction/injury.

Table 2.1 Experimental groups used to study gender dimorphism in murine model of LPS/PepG-induced cardiac dysfunction.

Study	Group	Number
Low dose LPS/PepG co-administration [LPS (3 mg/kg)/PepG (0.1 mg/kg)] study	Male + vehicle (5ml/kg PBS i.p.)	6
	Male + LPS/PepG	7
	Female + vehicle (5ml/kg PBS i.p.)	4
	Female + LPS/PepG	8
High dose LPS/PepG co-administration [LPS (9 mg/kg)/PepG (1 mg/kg)] study	Male + vehicle (5ml/kg PBS i.p.)	5
	Male + LPS/PepG	11
	Female + vehicle (5ml/kg PBS i.p.)	4
	Female + LPS/PepG	6

2.2.3 Model of polymicrobial sepsis caused by caecal ligation and puncture

In the model of polymicrobial sepsis-induced cardiac dysfunction (Figure 2.2), eight month-old male and female C57BL/6 mice were subjected to CLP. Sham-operated mice were not subjected to ligation or perforation of cecum but were otherwise treated the same way. I followed the original CLP protocol introduced by Wichterman and co-workers [26] with slight modifications including analgesia, antibiotic therapy and fluid resuscitation as described previously [15,21]. Based on previous evidence and preliminary data, an 18-G needle was used with the double puncture technique in order to generate reproducible cardiac dysfunction during the early phase of sepsis (24 h). Briefly, mice were anaesthetised i.p. with ketamine (100 mg/kg) and xylazine (10 mg/kg) prepared in the same solution by using 1.5ml/kg. Buprenorphine (0.05mg/kg i.p.) was injected additionally to provide adequate analgesia. The rectal temperature of the animals was maintained at 37°C with a homeothermic blanket. The abdomen was opened via a 1.5 cm midline incision, and the cecum exposed. The cecum was ligated just below the ileocaecal valve and punctured at both opposite ends. After a small amount of faecal matter was extruded from both ends, the cecum was placed back in its anatomical position and the abdomen was sutured. Ringer's solution was given s.c. for resuscitation directly after surgery (1 ml/mouse) and 6 h and 18 h after surgery (0.5 ml/mouse). Antibiotic (Imipenem/Cilastin; 20 mg/kg s.c.) and analgesia (buprenorphine; 0.05 mg/kg i.p.) was administered 6 h and 18 h after surgery. At 24 h after CLP, cardiac function was assessed by echocardiography *in vivo*. Mice were then deeply anaesthetised i.p. with ketamine/xylazine, and blood samples were taken by cardiac puncture under deep anaesthsia. Mice were killed by removing the hearts. Organs and blood samples were collected for quantification of organ dysfunction/injury. Mice were randomly allocated into four different groups as indicated in Table 2.2.

At 24 hours post-CLP, a clinical score for monitoring the health of experimental mice was used. The detailed score system is described in chapter 2.2.2.
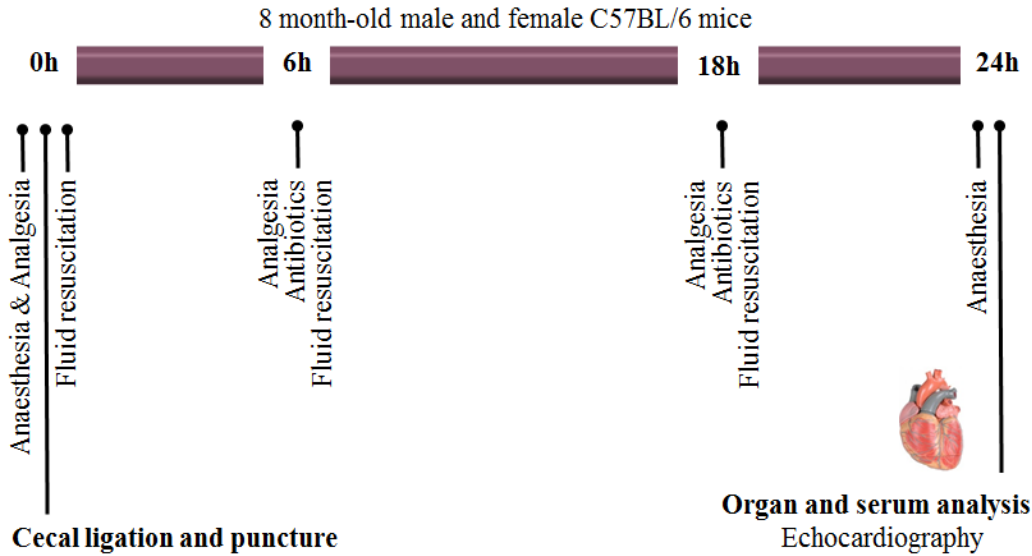
Figure 2.2 Polymicrobial sepsis-induced cardiac dysfunction. Scheme of animal experiments carried out in a model of polymicrobial sepsis induced by caecal ligation and puncture (CLP) in 8 month-old male and female C57BL/6 mice to investigate gender dimorphism of cardiac dysfunction and its underlying mechanism. Ringer's solution was given s.c. for resuscitation directly after CLP surgery (1 ml/mouse) and 6 h and 18 h after surgery (0.5 ml/mouse). Antibiotic (Imipenem/Cilastin; 20 mg/kg s.c.) and analgesia (buprenorphine; 0.05 mg/kg i.p.) was administered 6 h and 18 h after surgery. At 24 h after CLP, cardiac function was assessed by echocardiography *in vivo* under anaesthesia with isoflurane. Mice were then euthanised; organs and blood samples were collected for quantification of organ dysfunction/injury.

Table 2.2 Experimental groups used to study gender dimorphism in cardiac dysfunction in mice that underwent CLP.

Group	Number
Male + sham-operation	4
Female + sham-operation	4
Male + CLP	8
Female + CLP	8

2.2.4 Assessment of cardiac function *in vivo*

Cardiac function was assessed in mice by echocardiography *in vivo* as reported previously [316, 317]. At 18 h after LPS/PepG co-administration or 24 h after CLP, anaesthesia was induced with 3 % isofluorane and maintained at 0.5 to 0.7 % for the duration of the procedure. Before assessment of cardiac function, mice were allowed to stabilise for at least 10 min. During echocardiography the heart rate was obtained from ECG tracing and the temperature was monitored with a rectal thermometer. Two-dimensional B-mode and one-dimensional M-mode echocardiography images were recorded using a Vevo-770 imaging system (VisualSonics, Toronto, Ontario, Canada) (Figure 2.3). Percentage fractional area change (FAC) was assessed from a two-dimensional B-mode trace of LV (Figure 2.4), and was derived by 100 x [(LV end-diastolic area – LV end-systolic area)/ LV end-diastolic area]. The method involves tracing endocardial surface of the LV in the parasternal short axis view at the level of papillary muscles. Percentage EF and fractional shortening (FS) were calculated from the M-mode measurements in the parasternal short axis view at the level of the papillary muscles. Calculation of EF and FAC requires the measurements of LV internal dimension (LVID) in diastolic (d) and systolic (s) phase (Figure 2.5). Percentage EF was calculated from 100 x {[LVID (d) ^{3} – LVID (s) ^{3}]/ LVID (d)^3}; percentage FS was derived by 100 x {[LVID (d) – LVID (s)]/ LVID (d)}. The intra-observer variability of percentage EF, FS and FAC measurements over the course of one year was less than 4%, 4% and 5%, respectively. The inter-observer variability of percentage EF, FS and FAC measurements between two independent operators was all less than 4%.
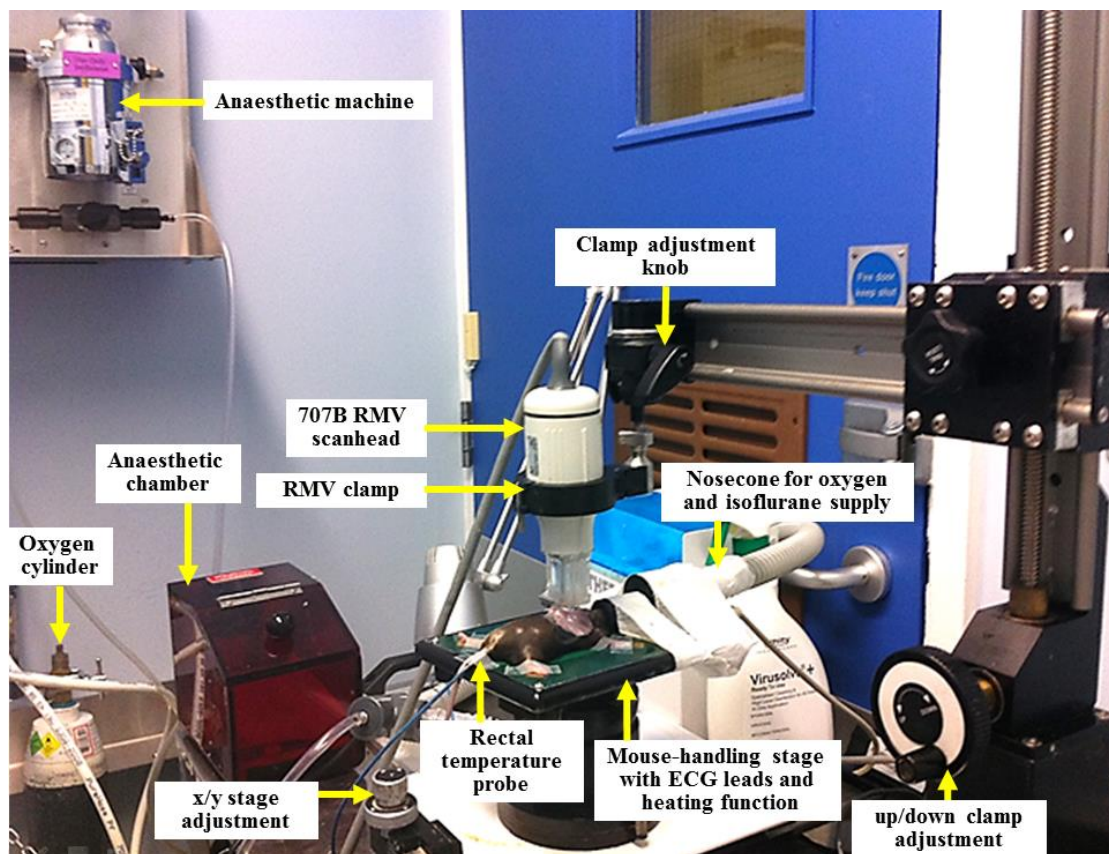
Figure 2.3 Set up of Vevo-770 imaging system. Echocardiography was conducted on a mouse under anaesthesia with isoflurane. Anaesthesia was induced in the anaesthetic chamber, and was maintained through a nosecone for oxygen and isoflurane supply. The mouse was placed on a mouse-handling stage with ECG leads and heating function, which could be adjusted by scrolling x/y stage adjustment. The heart rate was obtained from ECG tracing and the temperature was monitored through a rectal temperature probe. 707B RMV scanhead was connected to the RMV clamp. The clamp adjustment knob and up/down clamp adjustment scroll could be used to adjust orientation of the RMV clamp, thus the scanhead.
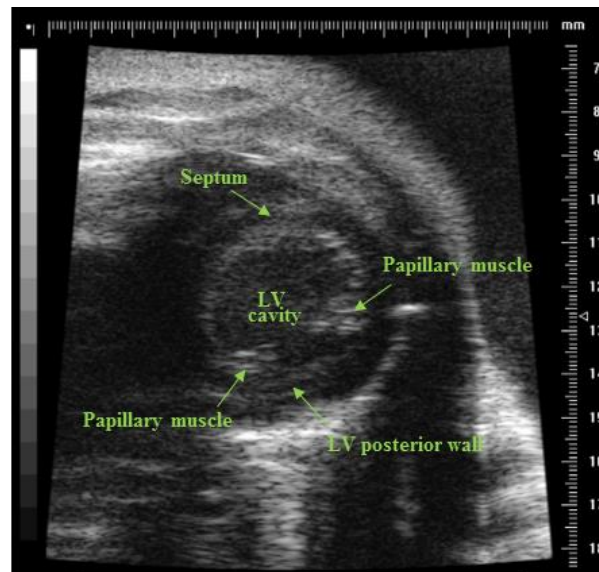
Figure 2.4 B-mode echocardiography image of the mouse heart. Representative B-mode echocardiography image shows the left ventricle (LV) in the parasternal short axis view at the level of the papillary muscles. Measurements of LV end-diastolic area and LV end-systolic area required for percentage fractional area change (FAC) calculation involve tracing endocardial surface of the LV in the parasternal short axis view at the level of papillary muscles.
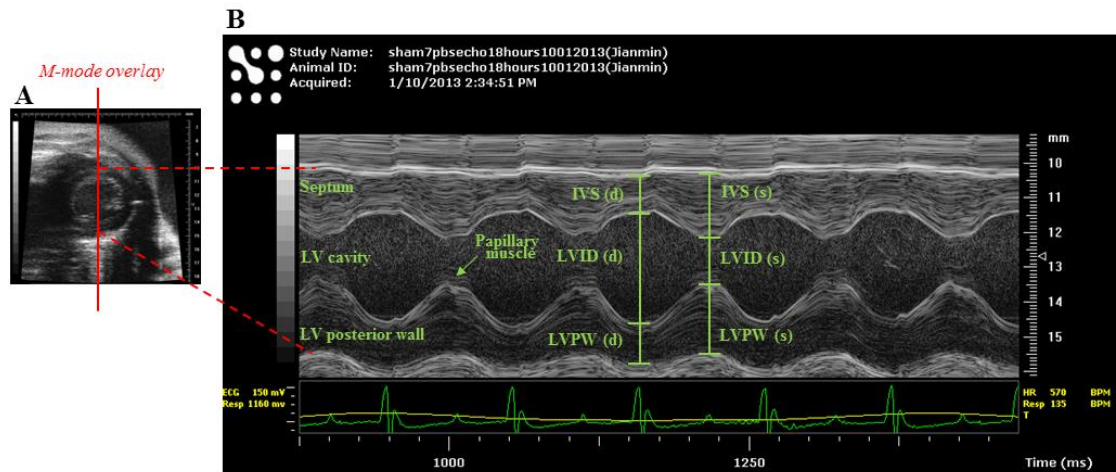
Figure 2.5 M-mode image of the mouse heart. M-mode imaging (B) shows the movement of tissue detected by one line of the B-mode image in the parasternal short axis view at the level of papillary muscles (A) throughout the cardiac cycle. Calculation of percentage ejection fraction (EF) and fractional shortening (FS) requires the measurements of left ventricle internal dimension (LVID) in diastolic (d) and systolic (s) phase. Measurements of LVID should be taken from the left surface of the interventricular septum (IVS) to the inner surface of the LV posterior wall (LVPW). In order to make accurate assessment, it is important to avoid the interference of papillary muscles on the endocardial surface of LVPW. Cardiac structures and the electrocardiogram (ECG) are closely related both temporally and spatially. LVID (d) should be taken at the end of diastole, which coincides with the peak of R wave on the ECG whereas LVID (s) at the end of systole which correlates with the T wave of ECG.

2.2.5 Quantification of renal dysfunction and hepatocellular injury

Renal dysfunction and hepatocellular injury were assessed in mice subjected to LPS/PepG at 18 h or CLP at 24 h. Mice were anaesthetised with 1.5 ml/kg i.p. of a ketamine (100 mg/ml)/xylazine (20 mg/ml) solution in a 2:1 ratio before being sacrificed. Approximately 0.7 ml of blood was collected by cardiac puncture into non-heparinised syringes and immediately decanted into serum gel S/1.3 tube (Sarstedt, Nürnbrecht, Germany), after which the heart was removed to terminate the experiment. The samples were centrifuged at 9900 g for 3 min to separate serum, which was sent to an independent laboratory (IDEXX Laboratories, Buckinghamshire, UK) for analyses of serum creatinine and ALT, markers of renal dysfunction and hepatocellular injury, respectively. Additionally, heart samples were taken and stored at 80 °C for further analyses.

2.2.6 Western Blot Analysis

Semi-quantitative western blot analyses were carried out in mouse heart tissues as described previously [27]. We assessed the degree of phosphorylation of Akt on Ser[473], eNOS on Ser[1177], inhibitor of κB (IκB) α on Ser[32/36], as well as the nuclear translocation of the p65 subunit of NF-κB (nucleus/cytosol ratio) and iNOS expression.

2.2.6.1 Solutions and Reagents

These solutions or buffers (Table 2.3) may be stored at 4°C for several weeks or for up to a year aliquoted and stored at -20°C.

Table 2.3 Protocols for making western blot solutions.

Solutions	Components
Homogenisation buffer	20 mM Hepes-KOH pH 7.9
	1 mM $MgCl_2$
	0.5 mM EDTA
	1 mM EGTA
	0.1% Triton X-100
	100 ml Distilled H_2O
	<u>Protease Inhibitors (add just before use):</u>
	0.1% Proteinase Inhibitor cocktail (PIC)
	0.5 mM PMSF
	0.1 mM DL-Dithiethrectol (DTT)
Extraction buffer	20 mM Hepes-KOH pH 7.9
	1.5 mM MgCl2
	0.2 mM EDTA
	1 mM EGTA
	20% Glycerol
	420 mM NaCl
	50 ml Distilled H_2O
	<u>Protease Inhibitors (add just before use):</u>
	0.1% PIC
	0.5 mM PMSF
	0.1 mM DTT
Loading buffer	4% SDS
	20% Glycerol
	0.004% Bromophenol blue
	0.125 M Tris-HCl
Running buffer	25 mM Tris base
	190 mM Glycine
	0.1% SDS
	Distilled H_2O
Transfer buffer	48 mM Tris
	39 mM Glycine
	15% Methanol
	0.04% SDS
	Distilled H_2O
Blocking buffer	0.1% Tween
	10% Milk
	PBS
Primary antibody solution	0.1% Tween
	5% Milk
	Dilution 1:200 or 1:1000 Primary antibody (rabbit anti-total Akt, dilution 1:1000; mouse anti-pAkt Ser473,

	dilution 1:1000; rabbit anti total eNOS, dilution 1:200; goat anti-peNOS Ser1177, dilution 1:200; mouse anti-total IκBα, dilution 1:1000; mouse anti-IκBα pSer32/36, dilution 1:1000; rabbit anti-NF-κB p65, dilution 1:1000; rabbit anti total iNOS, dilution 1:200)
	PBS
Secondary antibody solution	0.1% Tween
	5% Milk
	Dilution 1:10000 Secondary antibody conjugated with horseradish peroxidase (HRP)
	0.005% StrepTactin-HRP
	PBS
Washing buffer	0.002% Tween
	PBS

2.2.6.2 Procedures

Tissue Homogenisation and Cytosolic Protein Collection

(1) Take 40-50 µg tissue in a dish on ice, homogenise the tissue with homogenisation buffer in ice at concentrations of 1:10 (e.g. 30 ug of tissue in 300 ul of homogenisation buffer).

(2) Centrifuge at 4 000 RPM for 5 min at 4°C to separate cytosol from nuclei (Figure 2.6).

(3) Separate the supernatant (Supernatant 1) from the pellet (Pellet 1). Keep tubes with nuclear pellet (Pellet 1) on ice.

(4) Centrifuge the Supernatant 1 at 14000 RPM (16215g) for 40 min at 4°C. The obtained supernatant (Supernatant 2) containing the cytosolic proteins.

(5) Transfer the supernatants to fresh tubes kept on ice, and discard the pellet. Keep cytosol protein supernatants in 4°C fridge.

Nuclear Protein Extraction

(1) The pelleted nuclei (Pellet 1) were re-suspended in extraction buffer (1:3.3 tissue weight/ solution volume). Vortex for 40 sec. Incubate solutions in ice for 30 min, vortex once every 10 min (Figure 2.6).

(2) Centrifuge at 14 000 RPM for 20 min at 4°C to separate nuclear protein from DNA and nuclear membrane, etc. The obtained supernatant (Supernatant 3) containing the nuclear proteins. Keep supernatant in 4°C fridge. Or freeze Supernatant 2 (cytosolic proteins) and Supernatant 3 (nuclear proteins) at -80° C for future use.
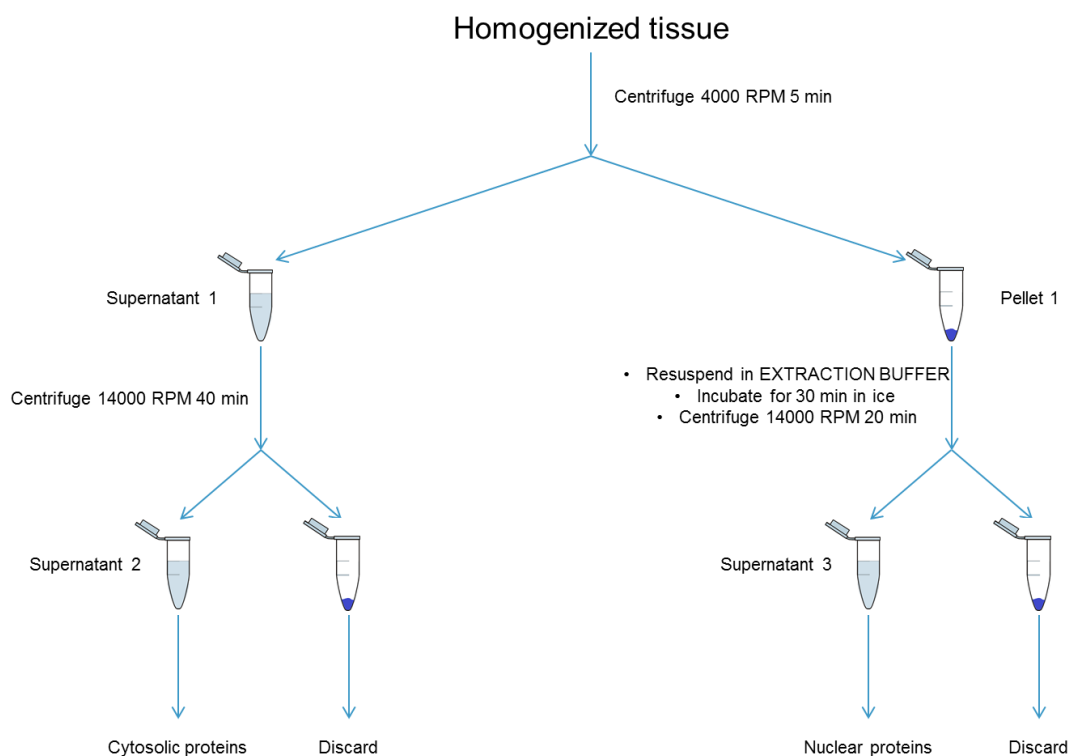
Figure 2.6 Protocols for cytosolic protein collection and nuclear protein extraction from homogenised tissue. Figure is kindly provided by Mr Fausto Chiaza.

Bicinchoninic Acid (BCA) Protein Assay

Protein content was determined on both nuclear and cytosolic extracts using a BCA protein assay following the manufacturer's directions (Therma Fisher Scientific, Rockford, IL).

(1) Make up BCA standard curve albumin.

(2) Make up BCA buffer by adding buffer A to buffer B at 50:1.

(3) Add 3 µl nuclear or cytosolic protein sample, 27 µl distilled water and 570 µl BCA solution per labelled well on plate.

(4) Add 30 µl distilled water and 570 µl BCA solution in one well as negative control.

(5) Incubate 37°C 30 min in dark for reaction (Figure 2.7).

(6) Read plate (Revelation programme, 560nm).

(7) Calculate protein concentrations.

Step 1:

Protein + Cu²⁺ $\xrightarrow{\text{OH}^-}$ Protein + Cu⁺

Step 2:

Cu⁺ + 2 BCA $\longrightarrow$
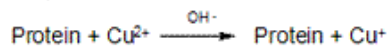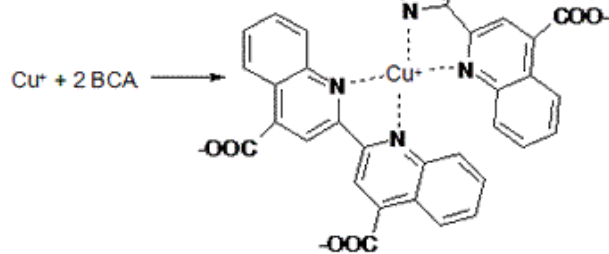
Figure 2.7 The BCA assay reaction procedure. Addition of copper (II) ions to a protein solution in an alkaline medium reduces the copper (II) ions to copper (I). Copper (I) forms coordination complex with BCA reagent in a 1:2 stoichiometry. The BCA-Copper (I) complex produces a strong purple color. (http://guweb2.gonzaga.edu/faculty/cronk/CHEM240/experiments.cfm?expt= 02)

Loading and Running the Gel

(1) Load 60 μg total cytosol protein samples or 30 μg total nuclear protein samples into the wells of the 8% sodium dodecyl sulphatepolyacrylamide gel electrophoresis (SDS-PAGE), along with 5 μl molecular weight markers. Empty wells were loaded with 5 μl sample buffer.

(2) Total loading volume for protein sample loaded well was 15 μl [eg. 4.96 μl protein sample + 7.04 μl distilled H_2O (12 μl in total) + 3 μl sample buffer)].

(3) Before loading the sample solution to the stacking gel, boil the solution (15 μl) for 5 min to accelerate the effect of SDS in breaking 3rd structure of protein.

(4) Run the gel for 30-35 min at 200 V (time depends on protein size, small proteins run faster).

Transferring the Protein from the Gel to Polyvinyldenedifluoride (PVDF) Paper Membrane

(1) Place membrane into methanol for 15 sec.

(2) Place membrane into Transfer buffer for 5 min.

(3) Make "transfer sandwich", ie: sponge/ 2-3 filter paper/ PVDF membrane/ gel/ 2-3 filter paper/ sponge (Figure 2.8).

(4) Place into transfer module 70 min/ 100 V.

Figure 2.8 Preparing the "transfer sandwich". (http://www.abcam.cn/index.html?pageconfig= resource&rid=1304)

Antibody Incubation and Visualisation

(1) Remove PVDF membrane and wash in washing buffer for 10 min.

(2) Block membrane for 2 h at 4°C.

(3) Wash membrane with washing buffer for 10 sec.

(4) Incubate membrane with appropriate dilutions of primary antibody in 5% blocking solution overnight at 4°C.

(5) Wash membrane with washing buffer 3 x 3 min.

(6) Incubate membrane with secondary antibody solution for 30 min at room temperature.

(7) Wash membrane with washing buffer 3 x 3 min.

(8) ECL: add buffer 1 to buffer 2, stand 1 min then pour the solution onto membrane. Leave 1 min then discard.

(9) Cover the membrane in transparent plastic wrap, place it into film cassette in dark room, and place a film on it.

(10) Place film into developing solution for 10 sec, then stop the reaction by placing it into water, fix film in fixing solution.

(11) Strip membrane (add Invitrogen Western stripping solu. Incubate 15 min/ RT/ shaking).

(12) Wash membrane in washing buffer 3 x 3 min.

(13) Incubate in blocking buffer for 2 h shaking at room temperature.

(14) Store in fridge or reprobe with another primary antibody.

(15) Densitometric analysis of the bands was performed using the Gel Pro Analyser 4.5, 2000 software (Media Cybernetics, Silver Spring, MD, USA). Each group was then adjusted against corresponding sham data to establish relative protein expression when compared with sham animals.

2.2.7 Quantitative Determination of Tissue TNF-α and IL-6 by ELISA

The expressions of TNF-α and IL-6 in mouse heart samples were determined using mouse TNF-α and IL-6 immunoassay kits (R&D Systems, Minneapolis, MN), respectively. The detailed tissue homogenisation procedure is described in chapter 2.2.6.2. ELISA was performed on tissue supernatant containing the cytosolic proteins. ELISA was performed by adding 100 µl of each sample (tested in duplicate) to wells

in a 96-well plate (12 strips x 8 wells) coated with anti-mouse TNF-α or IL-6. Wells were covered and samples were incubated for 2.5 h at room temperature, followed by rinsing 4 times in wash buffer. The samples were then incubated with 100 μl biotinylated anti-mouse TNF-α or IL-6 in each well for 1 h at room temperature. After washing 4 times in wash buffer, the wells were incubated with 100 μl HRP-conjugated streptavidin for 45 min at room temperature. The wells were then rinsed 4 times in wash buffer and the sites of HRP bing were visualised with a 3,3',5,5'-tetramethylbenzidine (TMB) solution, incubating for 30 min at room temperature in the dark. Adding 0.2 M sulfuric acid solution to the wells stopped the reaction. The expressions of TNF-α and IL-6 have been normalized to the protein content.

2.2.8 Statistics

All values described in the text and figures are presented as mean ± standard error of the mean (SEM) of n observations, where n represents the number of animals studied. Statistical analysis was performed using GraphPad Prism 6.0 (GraphPad Software, San Diego, California, USA). Two-way ANOVA followed by Sidak's multiple comparisons test was used to compare intergroup differences. Comparing results were considered statistically significant when $P < 0.05$.

2.2.9 Materials

Unless otherwise stated, all compounds in this study were purchased from Sigma-Aldrich Company Ltd (Poole, Dorset, UK). All solutions were prepared using non-pyrogenic saline [0.9% (w/v) NaCl; Baxter Healthcare Ltd, Thetford, Norfolk, UK]. Antibodies for immunoblot analysis were purchased from Santa Cruz Biotechnology, Inc. (Heidelberg, Germany).

2.3 Results

2.3.1 Gender dimorphism of cardiac dysfunction and clinical score in response to LPS (3 mg/kg)/PepG (0.1 mg/kg) co-administration.

To determine the gender difference of cardiac dysfunction caused by LPS/PepG, left ventricular function was assessed using echocardiography at 18 h after intraperitoneal injection of LPS (3 mg/kg)/PepG (0.1 mg/kg) or PBS (5mg/kg). Mice injected with LPS/PepG had a lower body temperature and a lower heart rate in comparison to sham-treated mice (male sham/female sham versus male + LPS/PepG/female + LPS/PepG; $P<0.05$; Table 2.4). In sham-treated mice, there was no difference of EF, FS or FAC between male and female mice ($P>0.05$; Figure 2.9A - D). When compared to sham-treated mice, LPS/PepG caused a significant reduction in EF ($P<0.05$; Figure 2.9A, 2.9B), FS ($P<0.05$; Figure 2.9A, 2.9C) and FAC ($P<0.05$; Figure 2.9A, 2.9D) in both male and female mice, indicating the development of cardiac dysfunction *in vivo*. However, female mice subjected to LPS/PepG exhibited significantly higher EF, FS and FAC in comparison with male mice ($P<0.05$; Figure 2.9A - D), indicating the cardiac dysfunction caused by LPS/PepG was less pronounced in female than in male animals. Additionally, when compared with male mice subjected to LPS/PepG injection, female mice yielded attenuated clinical scores ($P<0.05$; Figure 2.9E).

Table 2.4 Gender dimorphism of heart rate and temperature of mice responses to septic insults.

Parameter	Male		Female	
	Sham	LPS (3 mg/kg)/ PepG (0.1 mg/kg)	Sham	LPS (3 mg/kg)/ PepG (0.1 mg/kg)
Number	6	7	4	8
Heart Rate (bpm)	543.33 ± 23.23	486.14 ± 15.07*	569.25 ± 16.44	505.75 ± 12.16*
Temperature (°C)	35.38 ± 0.31	30.38 ± 0.87*	35.62 ± 0.46	32.24 ± 0.94*
	Sham	CLP	Sham	CLP
Number	4	8	4	8
Heart Rate (bpm)	537.25 ± 25.76	481.13 ± 11.98*	546.75 ± 10.06	494.25 ± 18.69*
Temperature (°C)	35.02 ± 0.52	31.19 ± 0.67*	35.45 ± 0.32	32.08 ± 0.81*
	Sham	LPS (9 mg/kg)/ PepG (1 mg/kg)	Sham	LPS (9 mg/kg)/ PepG (1 mg/kg)
Number	5	11	4	6
Heart Rate (bpm)	550.50 ± 26.34	456.72±12.08*	570.75 ± 20.14	448.17 ± 28.53*
Temperature (°C)	35.52 ± 0.44	29.16 ± 0.63*	35.90 ± 0.48	29.70 ± 1.03*

Heart rate and temperature were recorded at 18 h in mice subjected to LPS/PepG co-administration and at 24 h in mice that underwent CLP. Bpm, beats per min. Data are expressed as means ± SEM for n number of observations. *$P < 0.05$ versus the respective sham group, #$P < 0.05$ versus male LPS/PepG or CLP group.
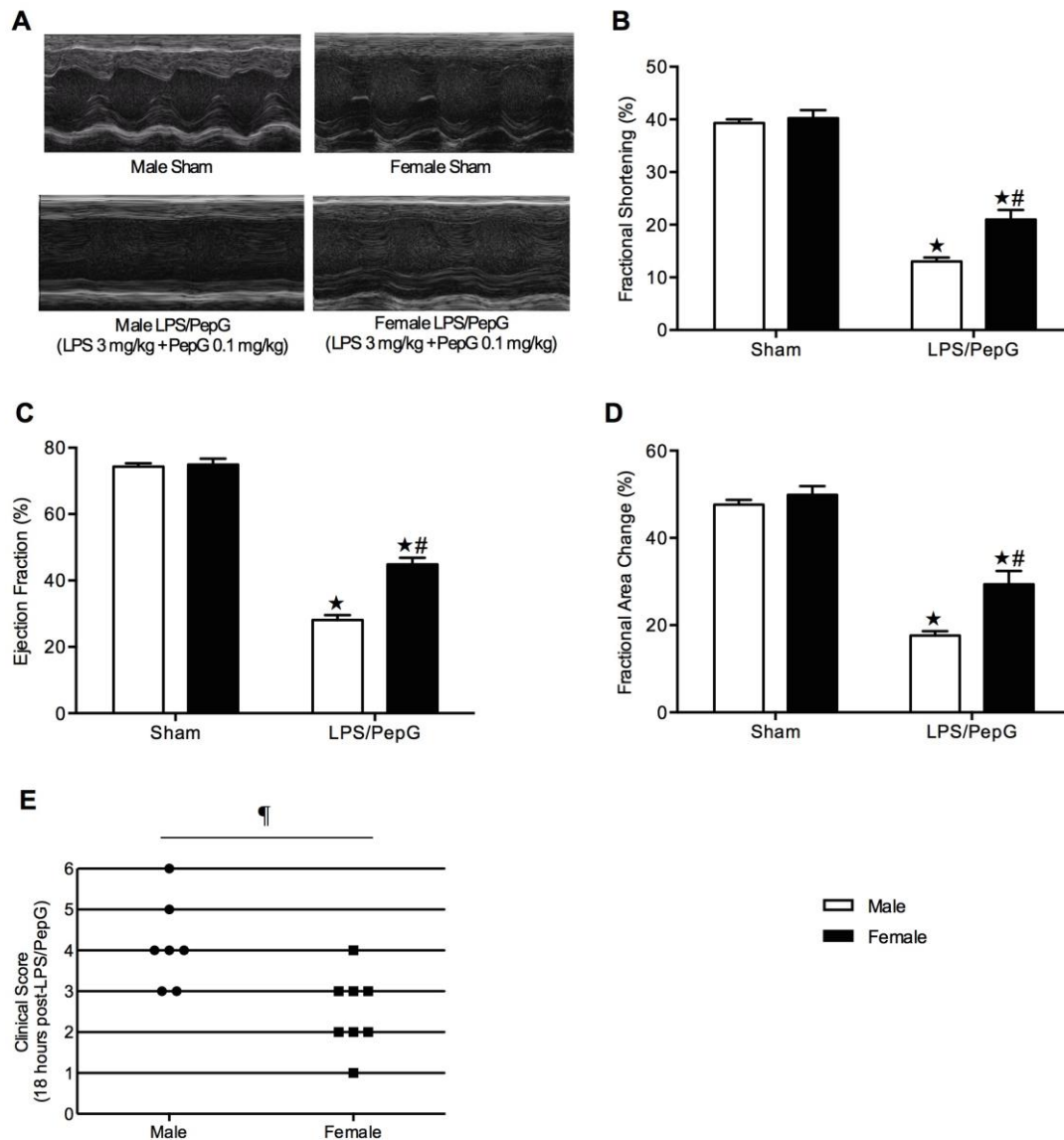
Figure 2.9 Gender dimorphism of cardiac dysfunction and clinical score in mice subjected to LPS (3 mg/kg)/PepG (0.1 mg/kg) co-administration. Male or female mice received LPS (3 mg/kg)/PepG (0.1 mg/kg) or PBS intraperitoneally. Cardiac function was assessed at 18 h. (**A**) Representative M-mode echocardiograms; percentage (%) (**B**) ejection fraction (EF); (**C**) fractional shortening (FS); (**D**) fractional area of change (FAC); and (**E**) clinical score: At 18 hours post-LPS/PepG, mice were scored for the presence or absence of six different macroscopic signs of sepsis. The following groups were studied: Male + vehicle (n = 6); Female + vehicle (n = 4); Male + LPS/PepG (n = 7); Female + LPS/PepG (n = 8). Panel **B – D**: Data are expressed as means ± SEM for n number of observations. ★$P < 0.05$ versus sham group, #$P < 0.05$ versus male LPS/PepG group, ¶ $P < 0.05$ versus male LPS/PepG group.

2.3.2 Gender dimorphism of cardiac dysfunction and clinical score in response to CLP-induced polymicrobial sepsis.

The murine model of CLP with fluid resuscitation and antibiotic treatment offers a clinically relevant model of abdominal polymicrobial human sepsis. Cardiac dysfunction induced by polymicrobial sepsis caused by CLP was only observed in 8 month-old male mice [317]. We sought to confirm the above observed gender difference of cardiac dysfunction in the CLP animal model in 8 month-old male and female mice. Left ventricular function was assessed using echocardiography at 24 h after CLP or sham surgery. Mice that underwent CLP had a lower body temperature and a lower heart rate in comparison to sham-operated mice (male sham/female sham versus male + CLP/female + CLP; $P<0.05$; Table 2.4). In sham-operated mice, there was no difference of EF, FS or FAC between male and female mice ($P>0.05$; Figure 2.10A - D). When compared to sham-treated mice, polymicrobial sepsis induced by CLP caused a significant reduction in EF ($P<0.05$; Figure 2.10A, 2.10B), FS ($P<0.05$; Figure 2.10A, 2.10C) and FAC ($P<0.05$; Figure 2.10A, 2.10D) in both male and female mice, indicating the development of cardiac dysfunction *in vivo*. However, female mice that underwent CLP exhibited significantly higher EF, FS and FAC in comparison with male mice ($P<0.05$; Figure 2.10A - D), indicating the cardiac dysfunction induced by CLP was less pronounced in female than in male animals. Additionally, when compared with male mice subjected to CLP, female mice yielded attenuated clinical scores ($P<0.05$; Figure 2.10E).
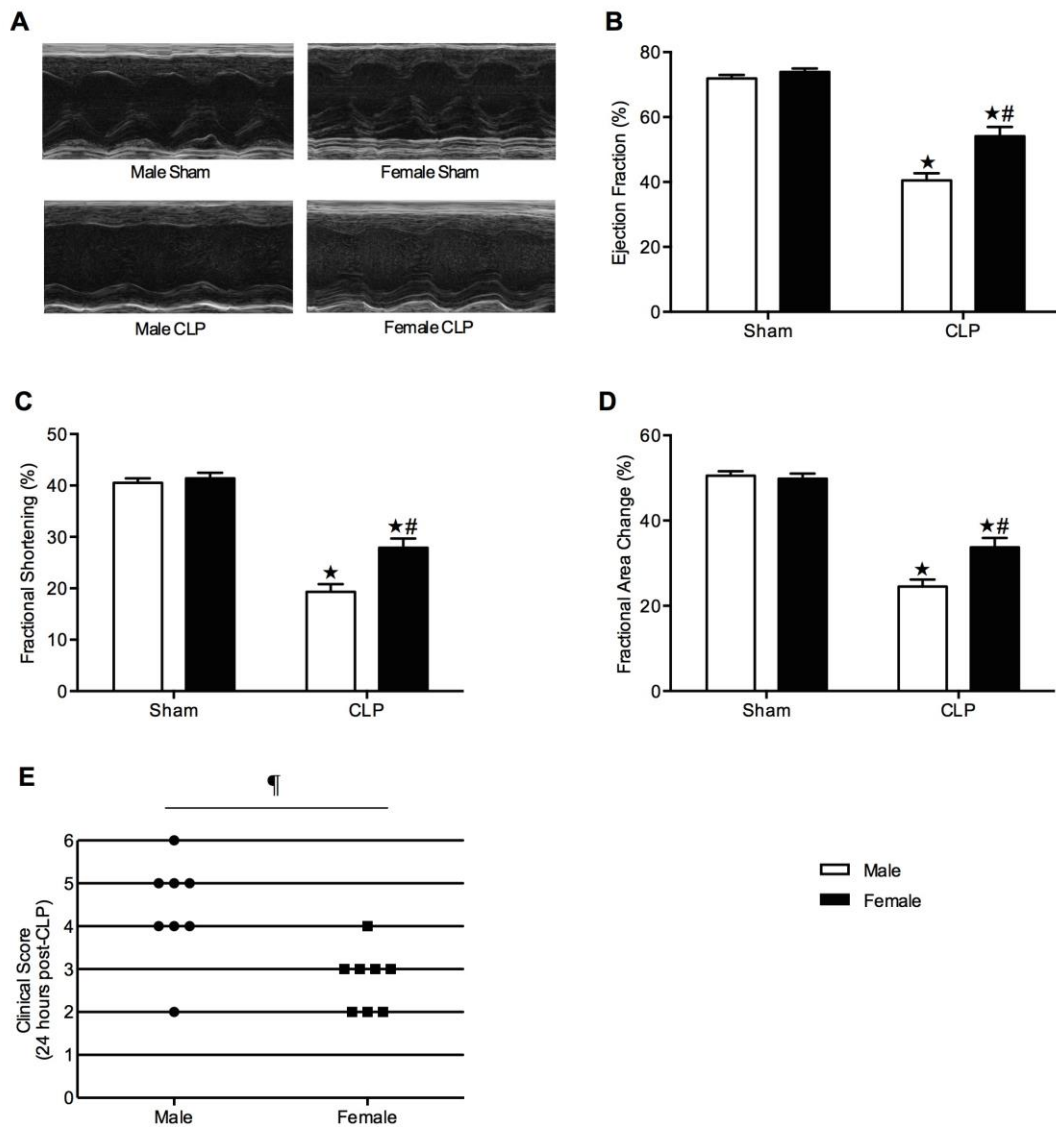
Figure 2.10 Gender dimorphism of cardiac dysfunction and clinical score in mice that underwent CLP. Male or female mice were subjected to CLP or sham-operation. Cardiac function was assessed at 24 h. (**A**) Representative M-mode echocardiograms; % (**B**) EF; (**C**) FS; (**D**) FAC; and (**E**) clinical score: At 24 hours post-CLP, mice were scored for the presence or absence of six different macroscopic signs of sepsis. The following groups were studied: Male + sham-operation (n = 4); Female + sham-operation (n = 4); Male + CLP (n = 8); Female + CLP (n = 8). Panel **B – D**: Data are expressed as means ± SEM for n number of observations. ★$P < 0.05$ versus sham group, #$P < 0.05$ versus male CLP group, ¶ $P < 0.05$ versus male CLP group.

2.3.3 Gender dimorphism of the phosphorylation of Akt in the hearts of mice subjected to LPS (3 mg/kg)/PepG (0.1 mg/kg) co-administration.

The potential underlying mechanisms behind the observed gender dimorphism of cardiac dysfunction were investigated by semi-quantitative western blot analysis of the mouse heart subjected to LPS/PepG at 18 h. When compared to male sham-treated mice, female sham-treated mice showed a higher degree of phosphorylation of Akt on Ser^{473} in heart tissue, but these data were not significant ($P{>}0.05$; Figure 2.11A). Exposure of male mice to LPS/PepG for 18 h caused a small and non-significant increase in the phosphorylation of Akt on Ser^{473} ($P{>}0.05$; Figure 2.11A). However, exposure of female mice to LPS/PepG for 18 h induced a significant increase in the phosphorylation of Akt on Ser^{473} compared with either female sham-treated mice or male LPS/PepG-treated mice ($P{<}0.05$; Figure 2.11A).

2.3.4 Gender dimorphism of the phosphorylation of eNOS in the hearts of mice subjected to LPS (3 mg/kg)/PepG (0.1 mg/kg) co-administration.

When compared to male sham-treated mice, female sham-treated mice showed a higher degree of phosphorylation of eNOS on Ser^{1177} in heart tissue, but these data were not significant ($P{>}0.05$; Figure 2.11B). Exposure of male mice to LPS/PepG for 18 h caused a small and not significant increase in the phosphorylation of eNOS on Ser^{1177} ($P{>}0.05$; Figure 2.11B). However, exposure of female mice to LPS/PepG for 18 h induced a significant increase in the phosphorylation of eNOS on Ser^{1177} compared with either female sham-treated mice or male LPS/PepG-treated mice ($P{<}0.05$; Figure 2.11B).
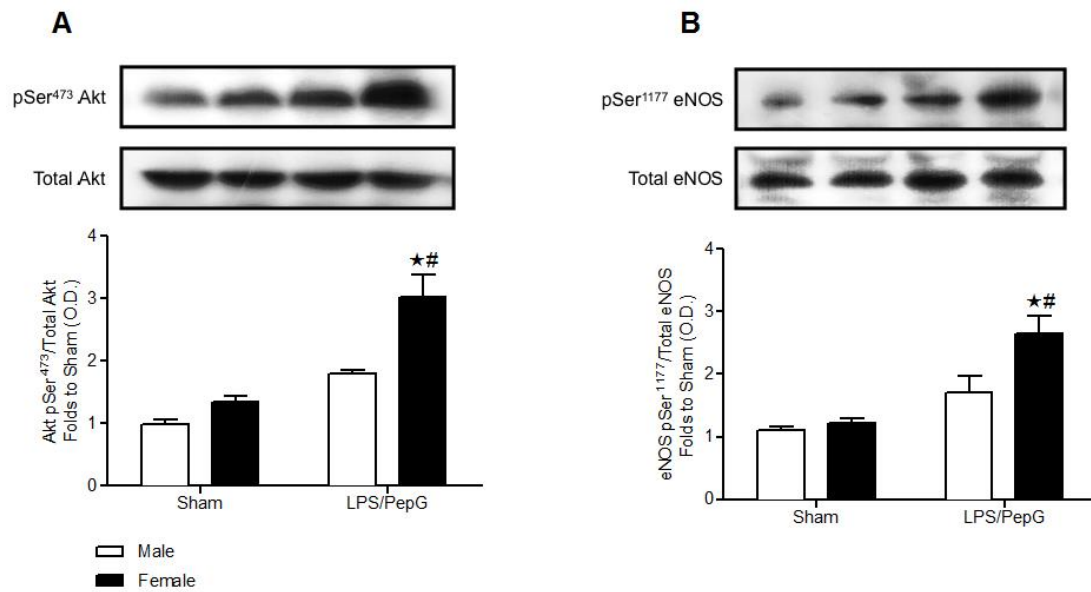
Figure 2.11 Gender dimorphism of the phosphorylation of Akt and eNOS in the hearts of mice subjected to LPS (3 mg/kg)/PepG (0.1 mg/kg) co-administration. Male or female mice received LPS (3 mg/kg)/PepG (0.1 mg/kg) or PBS. Signalling events in heart tissue were assessed at 18 h. Densitometric analysis of the bands is expressed as relative optical density (O.D.) of (**A**) phosphorylated Akt (pSer^{473}) corrected for the corresponding total Akt content and normalized using the related sham band; (**B**) phosphorylated eNOS (pSer^{1177}), corrected for the corresponding total eNOS content and normalized using the related sham band. Each analysis (**A - B**) is from a single experiment and is representative of three to four separate experiments. Data are expressed as means ± SEM for n number of observations. ★P < 0.05 versus the respective sham group, #P < 0.05 versus male LPS/PepG group.

2.3.5 Gender dimorphism of the phosphorylation of IκBα in the hearts of mice subjected to LPS (3 mg/kg)/PepG (0.1 mg/kg) co-administration.

In sham-treated mice, there was no difference in the phosphorylation of IκBα on $Ser^{32/36}$ between male and female hearts ($P>0.05$; Figure 2.12A). When compared to sham-treated mice, both male and female mice subjected to LPS/PepG demonstrated significant increases in the phosphorylation of IκBα on $Ser^{32/36}$ in heart tissue ($P<0.05$; Figure 2.12A). However, the increase in IκBα phosphorylation on $Ser^{32/36}$ caused by LPS/PepG was significantly less pronounced in hearts obtained from female than male mice ($P<0.05$; Figure 2.12A).

2.3.6 Gender dimorphism of nuclear translocation of the p65 NF-κB subunit in the hearts of mice subjected to LPS (3 mg/kg)/PepG (0.1 mg/kg) co-administration.

In sham-treated mice, there was no difference of nuclear translocation of the p65 NF-κB subunit between male and female hearts ($P>0.05$; Figure 2.12B). When compared to sham-treated mice, both male and female mice subjected to LPS/PepG demonstrated significant increases in the nuclear translocation of the p65 NF-κB subunit in heart tissue ($P<0.05$; Figure 2.12B). However, female mice subjected to LPS/PepG exhibited a significantly attenuated response in the nuclear translocation of the p65 NF-κB subunit in comparison with male mice ($P<0.05$; Figure 2.12B), indicating an important role of gender in LPS/PepG induced activation of NF-κB.

2.3.7 Gender dimorphism of the expression of iNOS in the hearts of mice subjected to LPS (3 mg/kg)/PepG (0.1 mg/kg) co-administration.

In sham-treated mice, we detected a faint expression of iNOS protein, but there was no difference of iNOS expression between male and female hearts ($P>0.05$; Figure 2.12C). When compared to sham-treated mice, LPS/PepG caused significant increases in the expression of iNOS protein in the heart ($P<0.05$; Figure 2.12C). However, in hearts from female mice subjected to LPS/PepG, the levels of iNOS protein were significantly lower than in hearts from male mice subjected to LPS/PepG ($P<0.05$; Figure 2.12C).
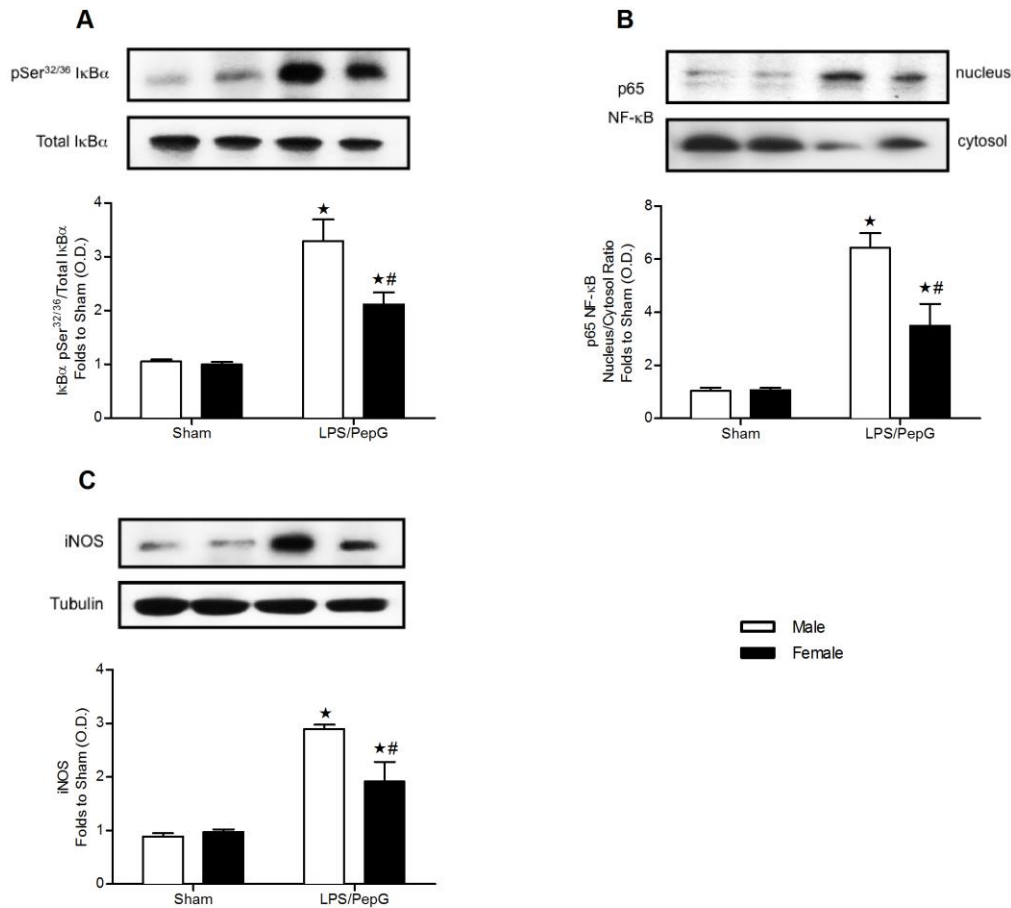
Figure 2.12 Gender dimorphism of the phosphorylation of IκBα, nuclear translocation of the p65 NF-κB subunit and expression of iNOS in the hearts of mice subjected to LPS (3 mg/kg)/PepG (0.1 mg/kg) co-administration. Male or female mice received LPS (3 mg/kg)/PepG (0.1 mg/kg) or PBS. Signalling events in heart tissue were assessed at 18 h. Densitometric analysis of the bands is expressed as relative optical density (O.D.) of (**A**) phosphorylated IκBα (pSer$^{32/36}$) corrected for the corresponding total IκBα content and normalized using the related sham band; (**B**) NF-κB p65 subunit levels in both, cytosolic and nuclear fractions expressed as a nucleus/cytosol ratio normalized using the related sham bands and (**C**) iNOS expression corrected for the corresponding tubulin band. Each analysis is from a single experiment and is representative of three to four separate experiments. Data are expressed as means ± SEM for n number of observations. ★$P < 0.05$ versus the respective sham group, #$P < 0.05$ versus male LPS/PepG group.

2.3.8 Gender dimorphism of the expression of TNF-α and IL-6 in the hearts of mice subjected to LPS (3 mg/kg)/PepG (0.1 mg/kg) co-administration.

When compared to male sham-treated mice, female sham-treated mice showed a lower TNF-α and IL-6 expressions in heart tissue, but these data were not significant ($P>0.05$; Figure 2.13A, 2.13B). When compared to sham-treated mice, both male and female mice subjected to LPS/PepG demonstrated significant increases in the expression of TNF-α and IL-6 in heart tissue ($P<0.05$; Figure 2.13A, 2.13B). However, female mice subjected to LPS/PepG exhibited a significantly attenuated response in the expression of TNF-α and IL-6 in comparison with male mice after LPS/PepG challenge ($P<0.05$; Figure 2.13A, 2.13B).
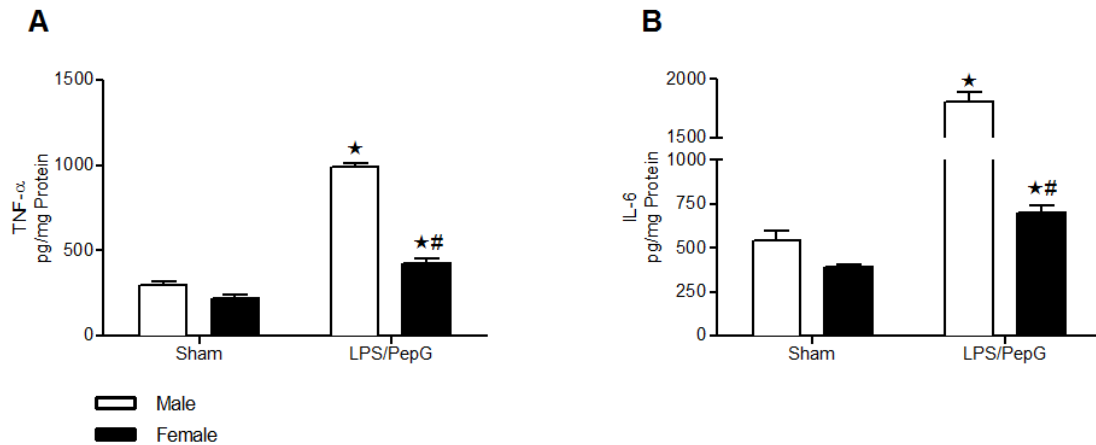
Figure 2.13 Gender dimorphism of the expression of TNF-α and IL-6 in the hearts of mice subjected to LPS (3 mg/kg)/PepG (0.1 mg/kg) co-administration. Male or female mice received either LPS (3 mg/kg)/PepG (0.1 mg/kg) or PBS. Signalling events in heart tissue were assessed at 18 h. (**A**) TNF-α expression and (**B**) IL-6 expression in heart tissue of mice subjected to LPS/PepG. Each analysis is from a single experiment and is representative of three to four separate experiments. Data are expressed as means ± SEM for n number of observations. ★$P < 0.05$ versus the respective sham group, #$P < 0.05$ versus male LPS/PepG group.

2.3.9 Gender dimorphism of cardiac dysfunction was blunted in response to high dose of LPS (9 mg/kg)/PepG (1 mg/kg) co-administration.

To further investigate whether the gender dimorphism still exists under increased inflammatory stimulus, left ventricular function was assessed using echocardiography at 18 h after intraperitoneal injection of LPS (9 mg/kg)/PepG (1 mg/kg) or vehicle. Mice injected with LPS/PepG had a lower body temperature and a lower heart rate in comparison to sham-treated mice (male sham/female sham versus male + LPS/PepG/female + LPS/PepG; $P<0.05$; Table 2.4). In sham-treated mice, there was no difference in EF, FS or FAC between male and female mice ($P>0.05$; Figure 2.14A - D). When compared to sham-treated mice, LPS/PepG caused a significant reduction in EF ($P<0.05$; Figure 2.14A, 2.14B), FS ($P<0.05$; Figure 2.14A, 2.14C) and FAC ($P<0.05$; Figure 2.14A, 2.14D) in both male and female mice, indicating the development of cardiac dysfunction *in vivo*. When compared to male LPS/PepG-treated mice, female mice subjected to LPS/PepG showed a significant increase in FAC ($P<0.05$; Figure 2.14A, 2.14D), but this was not significant for EF ($P>0.05$; Figure 2.14A, 2.14B) and FS ($P>0.05$; Figure 2.14A, 2.14C), indicating that gender dimorphism of the cardiac dysfunction after septic insult was abrogated by the severe injury induced by high dose of LPS (9 mg/kg)/PepG (1 mg/kg) co-administration.
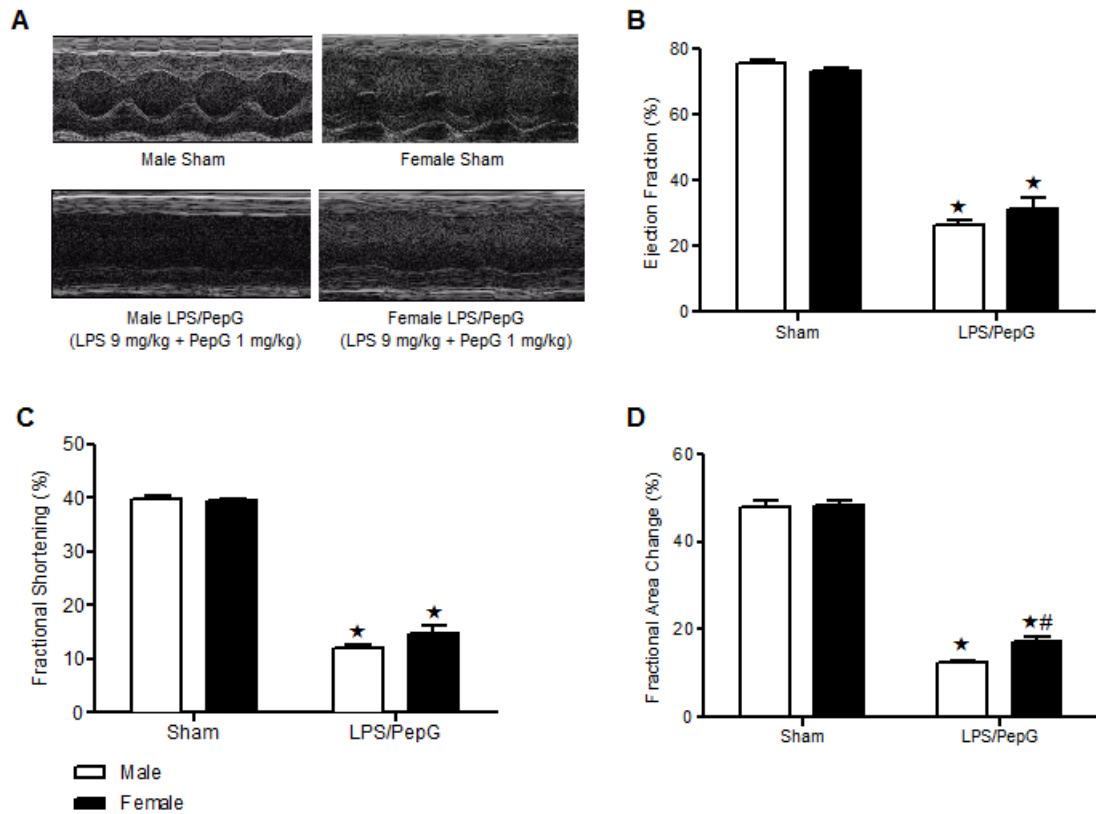
Figure 2.14 Gender dimorphism of cardiac dysfunction was blunted in response to high dose of LPS (9 mg/kg)/PepG (1 mg/kg) co-administration. Male or female mice received either LPS (9 mg/kg)/PepG (1 mg/kg) or PBS intraperitoneally. Cardiac function was assessed at 18 h. (**A**) Representative M-mode echocardiograms; percentage (%) (**B**) ejection fraction (EF); (**C**) fractional shortening (FS); and (**D**) fractional area of change (FAC). The following groups were studied: Male + vehicle (n = 5); Female + vehicle (n = 4); Male + LPS/PepG (n = 11); Female + LPS/PepG (n = 6). Data are expressed as means ± SEM for n number of observations. ★$P < 0.05$ versus the respective sham group, #$P < 0.05$ versus male LPS/PepG group.

2.3.10 Gender dimorphism of renal dysfunction and hepatocellular injury in mice subjected to LPS/PepG co-administration or polymicrobial sepsis.

In sham-treated mice, there was no difference of serum creatinine and serum ALT levels between male and female mice ($P>0.05$; Table 2.5). When compared to sham-operated mice, both male and female mice subjected to septic insults induced either by co-administration of LPS (3 mg/kg)/PepG (0.1 mg/kg), CLP or co-administration of LPS (9 mg/kg)/PepG (1 mg/kg) exhibited significant increases in serum creatinine ($P<0.05$) and ALT ($P<0.05$) (Table 2.5), indicating the development of renal dysfunction and hepatocellular injury, respectively. There appeared to be no difference in serum creatinine and, hence, renal dysfunction between male and female mice subjected to septic insults ($P>0.05$; Table 2.5). However, the rise in serum ALT was significantly less in female than in male mice subjected to CLP or co-administration of LPS (9 mg/kg)/PepG (1 mg/kg), indicating that females developed less hepatocellular injury than male mice ($P<0.05$; Table 2.5).

Table 2.5 Gender dimorphism of the renal dysfunction and hepatocellular injury in mice subjected to septic insults.

Parameter	Male		Female	
	Sham	LPS (3 mg/kg)/ PepG (0.1 mg/kg)	Sham	LPS (3 mg/kg)/ PepG (0.1 mg/kg)
Creatinine (μmol/L)	32.08 ± 0.67	48.60 ± 0.93*	29.07 ± 0.81	39.37 ± 4.24*
ALT (U/L)	29.36 ± 2.14	74.46 ± 10.95*	28.85 ± 1.67	86.26 ± 7.45*
	Sham	CLP	Sham	CLP
Creatinine (μmol/L)	29.62 ± 0.40	46.44 ± 2.96*	29.15 ± 0.78	43.39 ± 3.76*
ALT (U/L)	24.98 ± 1.70	224.15 ± 22.35*	23.88 ± 2.86	148.60 ± 19.11*#
	Sham	LPS (9 mg/kg)/ PepG (1 mg/kg)	Sham	LPS (9 mg/kg)/ PepG (1 mg/kg)
Creatinine (μmol/L)	31.46 ± 0.58	43.97 ± 2.59*	28.73 ± 0.69	42.86 ± 3.60*
ALT (U/L)	28.06 ± 2.52	165.50 ± 21.12*	29.82 ± 1.75	104.78 ± 9.63*#

Serum creatinine levels and serum alanine aminotransferase (ALT) levels were assessed at 18 h in mice subjected to LPS/PepG co-administration and at 24 h in mice that underwent CLP. Data are expressed as means ± SEM for *n* number of observations. *$P < 0.05$ versus the respective sham group, #$P < 0.05$ versus male LPS/PepG or CLP group.

2.4 Discussion

We describe here for the first time that the myocardial dysfunction caused by LPS/PepG is less pronounced in female than in male mice *in vivo*. This finding is in agreement with the previous reports showing that the cardiac dysfunction caused by myocardial ischaemia/reperfusion injury [318], trauma-haemorrhage [319] and burns [320] is also less pronounced in females than in males. Oestrogen modulates a number of acute injury-related myocardial responses; specifically oestrogen protects the heart against the injury and dysfunction caused by trauma-haemorrhage [321] and ischaemia/reperfusion injury (in isolated hearts subjected to global ischaemia and in hearts undergoing left anterior descending coronary artery (LAD) occlusion *in vivo*) [322, 323]. Although we provide clear evidence that female hearts show less dysfunction than male murine hearts when challenged with LPS/PepG, we wished to confirm this finding by using a more clinically relevant model of polymicrobial sepsis with antibiotic therapy and fluid-resuscitation caused by CLP in middle-aged mice (8 month-old) [316, 317]. The age of mice was selected based on the knowledge that 8 month-old female C57BL/6 mice are pre-ovarian failure and still have an active oestrus cycle [324]. Most notably, we demonstrate here that the cardiac function in female mice subjected to polymicrobial sepsis induced by CLP was significantly less pronounced than the cardiac dysfunction observed in male mice. Taken together, these findings indicate that the hearts of young or older female mice exhibit less cardiac dysfunction in response to polymicrobial sepsis or co-administration of LPS/PepG.

To obtain a better insight into the mechanisms underlying the observed gender dimorphism of the cardiac response to sepsis, we investigated the phosphorylation of Akt, eNOS and IκBα, nuclear translocation of NF-κB subunit p65, iNOS expression, as well as TNF-α and IL-6 expression in murine hearts; When compared to the hearts of male mice subjected to LPS/PepG, hearts of female mice subjected to LPS/PepG showed i) profound increases in phosphorylation of Akt and eNOS; ii) reductions in phosphorylation of IκBα and nuclear translocation of the NF-κB subunit p65, iii) reduced expression of the pro-inflammatory cytokines TNF-α and IL-6, and iv) reduced expression of iNOS.

Akt is a member of the phosphoinositide 3-kinases (PI3K) signal transduction enzyme family, activation of which protects the heart against injury [325, 326]. Here we

demonstrate that co-administration of LPS/PepG to female rather than male mice leads to a greater increase in Akt-phosphorylation and, hence, activity in the heart of female animals. Indeed, a greater increase in cardiac Akt phosphorylation in female when compared to male hearts also accounts for the reduced cardiac injury caused by ischaemia-reperfusion in female mice [327]. Most notably, when the Akt-pathway is blocked, the degree of cardiac injury in male and female mice was identical. Thus, activation of cardiac Akt (presumably by oestradiol) protects female hearts against cardiac injury and dysfunction [327]. Oestradiol activates cardiac Akt, which in turn also leads to a reduction in the cardiac dysfunction caused by trauma-haemorrhage [321, 326]. Blockade of the Akt pathway also abrogated the salutary effects of oestradiol on cardiac function following trauma-haemorrhage [321]. Moreover, activation of Akt mediates the inhibition by oestradiol of the TNF-α expression and NF-κB activation caused by LPS in cardiomyocytes [328]. In the present study, we found a small increase in cardiac Akt activity in female but not in male sham hearts. In line with this finding, one previous study showed that young women possess higher levels of Akt in the myocardium compared to comparably aged men or postmenopausal women, and that sexually mature female mice have elevated Akt kinase activity in nuclear extracts of hearts than male mice [329]. The hypothesis that cardiac Akt activity is modulated by oestrogen is also supported by the finding that the Akt activation in cardiomyocytes was reduced in ovariectomised rats [330]. In addition, activation of the PI3K/Akt signalling cascade by oestrogen was observed in rat cardiomyocytes [326]. A few studies have been conducted to explain the exact mechanism by which oestrogen induces Akt activation. Oestrogen receptor α has been shown to bind with the p85 α regulatory subunit of PI3K in a ligand-dependent manner in human endothelial cells; increased oestrogen receptor associated PI3K activity induced by oestrogen leads to the activation of Akt and eNOS in human endothelial cells [331]. Another study has shown that the direct interaction between oestrogen receptor and the PI3K regulatory subunit p85 in a time-dependent manner was consistent with the temporal profile for Akt phosphorylation in neurons [332]. Additionally, in cardiomyocytes, oestrogen stimulated Akt activation and prevented DNA fragmentation [326]. Thus, we propose that the higher cardiac activation of Akt in female mice importantly contributes to the improvement in cardiac dysfunction in sepsis.

Activation of Akt is known to modulate eNOS activity through phosphorylation of eNOS at Ser^{1177} [333, 334]. Indeed, the present study reported an increase in eNOS phosphorylation in female than in male hearts, which was correlated with the expression pattern of Akt. Augmentation of eNOS activity was shown to decrease sepsis-related increases in neutrophil-endothelial cell interaction and potentially maintain microvascular patency in sepsis [335]. There is good evidence that oestrogen modulates activation of eNOS. Oestrogen receptor α has been implicated in increased PI3K/Akt and eNOS activation induced by oestrogen in human endothelial cells [331]. Another study demonstrated that oestrogen stimulation of the eNOS promoter was mediated via increased activity of the transcription factor Sp1 (which is essential for the activity of the human eNOS promoter) [336]. Moreover, oestradiol treatment in guinea pigs increased eNOS mRNA in skeletal muscle, suggesting an increase in eNOS activity [337]. In line with these findings, data from the present study indicate that less vulnerability of female hearts to sepsis may be mediated in part by an increased activity of eNOS, secondary to the activation of PI3K/Akt pathway.

NF-κB controls the transcription of a large number of genes, particularly those involved in inflammatory and acute stress responses, such as cytokines, chemokines, cell adhesion molecules, apoptotic factors, and other mediators [338]. IκBα inactivates NF-κB by masking the nuclear localisation signals of the NF-κB proteins and by sequestering NF-κB as an inactive complex in the cytoplasm [338, 339]. Phosphorylation of IκBα by IKK leads to the dissociation of IκBα from NF-κB, which liberates NF-κB to enter the nucleus and activates the expression of NF-κB target genes [338]. Up-regulation of NF-κB has been linked to the development of myocardial dysfunction following the onset of sepsis [317, 340]. Inhibition of NF-κB activation results in improved myocardial function after septic challenge [316]. Additionally, the dimer of oestrogen and its receptor can bind to NF-κB in osteoblasts following IL-1β exposure, further, NF-κB is proved to be one of the targets for oestrogen receptor, resulting in reduced IL-6 promoter activity [341]. In murine splenic macrophages, oestradiol inhibited TNF-α and IL-6 production was associated with a decreased LPS-induced NF-κB-binding activity [341]. Thus, our present results indicate that less myocardial dysfunction in females subjected to LPS/PepG could be importantly due to the decreased activation of NF-κB (secondary to the reduced activation of IκBα and, hence, nuclear translocation) in murine hearts.

Activation of NF-κB may also mediate myocardial dysfunction through induction of expression of its target gene iNOS, which plays an important role in sepsis-related hypotension and impaired left ventricular function [125, 129]. Indeed, in the present study, iNOS expression was increased in male hearts, which correlates with their exacerbated cardiac dysfunction under septic insult.

In addition to causing the expression of iNOS, NF-κB activation also leads to a pronounced increase in production of inflammatory mediators such as TNF-α and IL-6 [342]. In turn, TNF also activates NF-κB through TNF-receptor-associated factors, this increases cytokine production, thus forming a feed-forward mechanism and amplifying the inflammatory reaction [343]. There is good evidence that those inflammatory cytokines play a significant role in the pathogenesis of sepsis-induced cardiac dysfunction [108, 344]. Moreover, clinical studies showed that stimulation of healthy females with LPS or LTA led to lower TNF-α and IL-6 levels in blood than males [313]. Female patients with sepsis had a higher survival rate, which was correlated with lower TNF-α and higher IL-10 levels [68], while male trauma-patients showed higher IL-6 level than females [73]. In experimental studies, cardiomyocyte TNF-α and IL-6 release was markedly lower in female than male rats following burn injury [320]. In addition, female hearts expressed less myocardial TNF-α in isolated hearts subjected to ischaemia/reperfusion injury [318] or LPS treatment [345]. Others have suggested that elevated plasma TNF-α and IL-6 induced by trauma-haemorrhage was prevented by oestradiol treatment in rats [321, 346]. Consistent with these findings, in our study, female mice, which had better cardiac function following septic insult, expressed less myocardial TNF-α and IL-6 than male mice subjected to LPS/PepG co-administration.

In addition to the protective roles of oestrogen against inflammation, the observed gender dimorphism in our study might also be due to the pro-inflammatory effects of testosterone in male mice. Testosterone induces activation of NF-κB, macrophage chemotactic protein-1 (MCP-1) and IL-6 expression in 3T3-L1 adipocytes; the effect of testosterone on the expression of IL-6 and MCP-1 is inhibited by NF-κB inhibitor [347]. Additionally, testosterone injection for 2 weeks in rats caused NF-κB and iNOS upregulation in prostate tissue [348]. However, contradictory findings have shown also that testosterone inhibited TNF-α-induced nuclear translocation of NF-κB in

human aortic endothelial cells [349].

Our study demonstrated that the gender dimorphism of cardiac dysfunction in response to septic insults was abolished by the severe injury induced by high dose of LPS (9 mg/kg)/PepG (1 mg/kg) co-administration. This is in line with a report that the inflammatory cytokine response differed more strongly between blood from men and women after low-concentration of LPS stimulation compared with a higher stimulus concentration [313]. Population-based studies on sex dimorphism in mortality after sepsis showed inconsistent results. Some studies reported increased mortality in males [311, 312], while other studies demonstrated mortality from severe sepsis/sepsis was not affected by gender [350]. The inconsistency may have resulted from multiple factors such as pre-existing co-morbidities. More importantly, our observations of gender dimorphism in cardiac dysfunction responses to different severities of injury may partially explain the conflicting clinical data.

The present study reported less hepatocellular injury in female than in male mice subjected to CLP or with injection of high dose of LPS (9 mg/kg)/PepG (1 mg/kg). This is consistent with the previous study in rats that females showed less liver tissue damage than males demonstrated by less liver congestion, and that oestrogen/progesterone treatment attenuated congestion, portal inflammation, and focal necrosis of the liver in male rats underwent CLP [351]. Additionally, administration of oestrogen significantly improved hepatocellular function assessed by serum AST, ALT levels and ameliorated oxidative organ damage in septic rats [77]. However, in the present study, no gender dimorphism of liver dysfunction was observed in mice subjected to low-dose LPS (3 mg/kg)/PepG (0.1 mg/kg) co-administration. We propose that this may be secondary to the small therapeutic window in liver dysfunction induced by low-dose LPS (3 mg/kg)/PepG (0.1 mg/kg) may be not sufficient to show the gender dimorphism. In addition, the present study appears to show no difference in renal dysfunction between the two genders subjected to septic insults. This finding is line with a clinical study illustrating that mortality of acute kidney injury is independent of gender and age [352]. However, it has been suggested that the female gender is associated with slower progression of chronic kidney disease and better renal survival in chronic renal failure [353].

It could be argued that the present study did not provide information about proestrus/oestrus or dioestrus state of oestrus cycle in female mice subjected to septic insults. In this regard, a recent study showed that female mice with CLP survived better than male mice that underwent CLP, but the higher survival in females did not correspond to any specific oestrus phase [71]. Furthermore, it has been demonstrated vaginal cytology does not reflect changes of circulating oestrogens in females and that the oestrus cycle cannot be predicted by vaginal smears [354]. Moreover, we did not notice a lot of variations in data obtained from female mice in our study. Therefore, oestrus cycle phases were not monitored in this study.

2.4.1 Conclusion

In this chapter, my findings provide for the first time a very clear indication of a gender dimorphism in the sepsis-induced cardiac dysfunction *in vivo* and we have shown that female mice have less cardiac dysfunction than male mice subjected to either co-administration of LPS/PepG in young mice or CLP in older mice. I report here that female hearts subjected to sepsis have a greater activation of Akt/eNOS, and less activation of NF-κB, which in turn results in reduced expression of the proinflammatory cytokines TNF-α and IL-6 as well as iNOS. I propose that the above pro-survival and anti-inflammatory signalling events contribute to the reduced cardiac dysfunction in female mice with sepsis.

CHAPTER III | IκB KINASE INHIBITOR ATTENUATES SEPSIS-INDUCED CARDIAC DYSFUNCTION IN MICE WITH CHRONIC KIDNEY DISEASE

3.1 Introduction

The lack of translatability of preclinical findings (e.g. efficacy of new interventions) to patients with sepsis has many possible reasons including: interventions given relatively late, a great degree of heterogeneity in the patient population (older patients of either gender) which often have a prior insult (trauma, burns) and very frequently co-morbidities including diabetes and CKD, or both [11, 307, 355, 356]. CKD is a growing public health burden with increasing number of patients receiving maintenance dialysis [357]. Cardiovascular disease is the leading cause of death in patients with CKD [358]. The cardiac injury caused by ischaemia-reperfusion is greater in uraemic rats compared to non-uraemic controls [359]. Moreover, patients with CKD requiring dialysis have a higher risk of infection and sepsis [360] due to uraemia-induced immune deficiency [262, 361, 362], significant co-morbidities and the dialysis procedure itself [363]. Once infected, dialysis patients with sepsis have an approximately 100-fold higher mortality rate compared with the general population with sepsis [245]. However, the reasons for this higher mortality rate are unclear; the detrimental role of cardiac dysfunction in sepsis and the higher mortality in septic patients following CKD together raise the possibility that alterations in cardiac function (at baseline, in response to sepsis or both) might play a crucial role in the increased risk of death in CKD patients followed by sepsis.

Up-regulation of NF-κB (Figure 3.1) has been linked to the development of cardiac dysfunction following the onset of sepsis [317, 340]. Physiologically, IκBα inactivates NF-κB by sequestering NF-κB as an inactive complex in the cytoplasm [338, 339]. Phosphorylation of IκBα by IKK dissociates IκBα from NF-κB, which liberates NF-κB to enter the nucleus and activates the expression of NF-κB target genes [338]. Recently, we showed that a specific IKK inhibitor, IKK 16 (Figure 3.1, Figure 3.2)

[364] significantly attenuated the impairment in sepsis-induced multiple organ dysfunction/injury in mice [316].
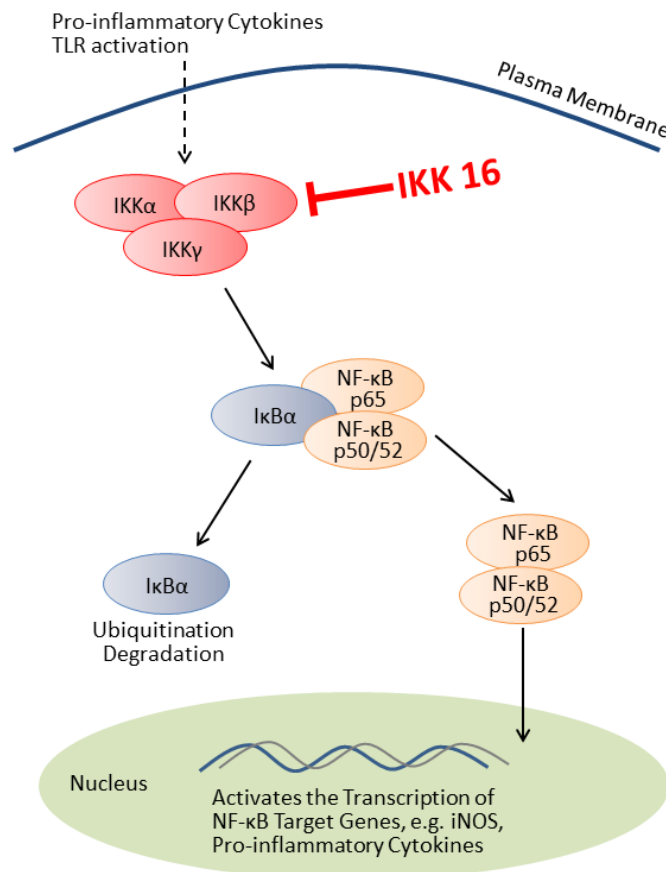
Figure 3.1 Schematic overview of the NF-κB signalling and IKK 16. Stimuli such as pro-inflammatory cytokines or activation of Toll-like receptor (TLR) results in downstream activation of inhibitor of IκB kinase (IKK). Activated IKK phosphorylates IκBα, causing the degradation of IκBα. NF-κB is then released and translocated to the nucleus, activating the expression of NF-κB target genes. IKK 16 selectively inhibits IKK.
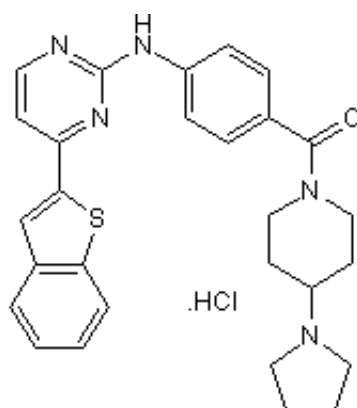
Figure 3.2 Chemical structure of IKK 16. Compound IKK 16 [N-(4-Pyrrolidin-1-yl-piperidin-1-yl-)-[4-(4-benzo [b]thiophen-2-yl-pyrimidin-2-ylamino)-phenyl] carboxamide hydrochloride] is a selective inhibitor of IKK. It was discovered by Waelchli et al by screening the Novaritis compound archive, IKK 16 was found to hit with IKK inhibitor motifs (2-anilino-pyrimidines and 2,4-disubstituted quinazolines). The tertiary amines structure of IKK16 enables it to be potently active in the low-nanomolar range, with IC_{50} values of 40, 70 and 200 nM for IKK-β, IKK complex and IKK-α inhibitiuon, respectively. Figure adapted from Waelchli et al., 2006.

It is, however, unknown whether pre-existing CKD augments the cardiac dysfunction in sepsis, and whether excessive activation of NF-κB drives cardiac dysfunction in animals with CKD and sepsis. This study investigates (a) the effects of pre-existing CKD on cardiac function in murine models of endotoxaemia and polymicrobial sepsis, and (b) the molecular mechanism underlying the cardiac dysfunction in CKD/sepsis, and (c) whether inhibition of NF-κB (with a specific IKK-inhibitor) improves cardiac performance and reduces systemic inflammation in mice with CKD and sepsis.

3.1.1 Scientific Hypotheses and Aims of the Study Presented in Chapter III

My project was driven by the hypotheses that:

- Pre-existing CKD aggravates the cardiac dysfunction caused by sepsis in mice

- IKK 16 (a specific IKK-inhibitor) protects against cardiac dysfunction in CKD mice with sepsis

My study had the following scientific objectives:

- To investigate the effects of pre-exiting CKD on cardiac dysfunction induced by low dose LPS

- To elucidate signalling events underlying the aggravated cardiac dysfunction in CKD mice subjected to low dose LPS

- To investigate the effects of pre-exiting CKD on cardiac dysfunction in a clinically relevant model of polymicrobial sepsis caused by CLP (with antibiotic therapy and fluid-resuscitation)

- To elucidate signalling events underlying the aggravated cardiac dysfunction in CKD mice subjected to CLP

- To investigate the effects of treatment with IKK16 on cardiac performance and systemic inflammation in mice with CKD and polymicrobial sepsis induced by CLP

- To elucidate signalling events underlying the observed protective effects of IKK16 on cardiac function in CKD mice subjected to CLP

3.2 Materials and Methods

3.2.1 Animals

This study was carried out on 86 four to six week-old male C57BL/6 mice (Charles River, Kent, UK), receiving a standard diet and water *ad libitum*. The ethical statement is provided in chapter 2.2.1.

3.2.2 Animal models of subtotal (5/6th) nephrectomy (SNX)

Mice were subjected to a two-stage, SNX or sham surgery under ketamine (100 mg/kg)/xylazine (10 mg/kg) anaesthesia. We followed the original SNX protocol introduced by Gagnon et al. [365] with slight modifications. Briefly, in the first stage of the SNX, the upper and lower poles of the left kidney (2/6th NX) were removed by electrocoagulation knife, the mice were allowed to recover for 2 weeks, then the right kidney (3/6th NX) was removed. After the second stage of the surgery, the mice were kept for 8 weeks to develop CKD (Figure 3.3). Mice subjected to sham operations were operated on without removing kidney. To avoid adrenal gland injury, the renal capsule was peeled away carefully before partial or total nephrectomy.
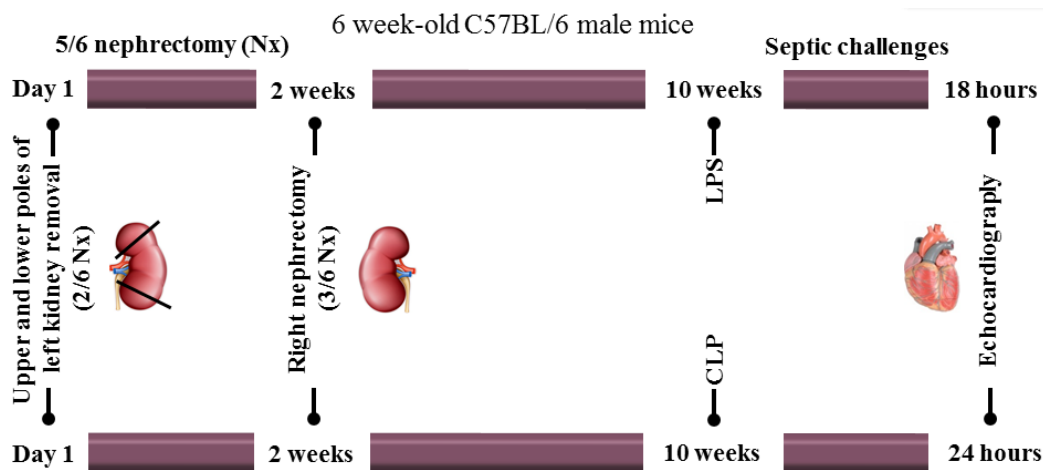
Figure 3.3 Scheme of inducing animal model of CKD by subtotal (5/6th) SNX, and inducing organ dysfunction in CKD mice by LPS administration or CLP. Mice were subjected to a two-stage SNX to develop CKD. In the first stage, the upper and lower poles of the left kidney were removed (2/6th NX), 2 weeks after the first stage, the right kidney (3/6th NX) was removed. Then the mice were kept for 8 weeks to develop CKD. The mice with CKD were further used for LPS or CLP study. Cardiac function was assessed by echocardiography *in vivo* under anaesthesia with isoflurane at 18 h after LPS injection or 24 h after CLP surgery.

3.2.3 Model of LPS-induced organ dysfunctions

Mice with CKD and without CKD (CKD Sham) received *i.p.* injection of low dose LPS (2 mg/kg) or its vehicle (PBS) (Figure 3.3). Sham-treated mice were not subjected to LPS, but were otherwise treated the same way. Mice were randomly allocated into four different groups as indicated in Table 3.1.

At 18 hours post-LPS injection, a clinical score for monitoring the health of experimental mice was used. The detailed score system is described in chapter 2.2.2.

Table 3.1 Experimental groups used to study LPS (2mg/kg)-induced cardiac dysfunction in CKD mice.

Group	Number
CKD sham + PBS (5 ml/kg i.p.)	6
CKD + PBS (5 ml/kg i.p.)	7
CKD sham + LPS	7
CKD + LPS	7

3.2.4 Model of polymicrobial sepsis caused by CLP

Polymicrobial sepsis was induced by CLP (18-G needle, double puncture) in mice (Figure 3.3). Mice received volume resuscitation and antibiotic and analgesic therapy [366, 367]. The detailed CLP procedure is described in chapter 2.2.3 and depicted in Figure 2.2. Sham-operated mice were not subjected to ligation or perforation of cecum but were otherwise treated the same way. One hour after CLP, CKD mice were treated either with IKK 16 (1 mg/kg *i.v.* Tocris Bioscience, Bristol, UK) or vehicle (2 % DMSO) (Figure 3.4). Mice were randomly allocated into four different groups for investigating CLP-induced cardiac dysfunction in CKD mice as indicated in Table 3.2; into three different groups for studying the effects of IKK 16 on cardiac function in CKD mice underwent CLP as indicated in Table 3.3.

At 24 hours post-CLP, a clinical score for monitoring the health of experimental mice was used. The detailed score system is described in chapter 2.2.2.
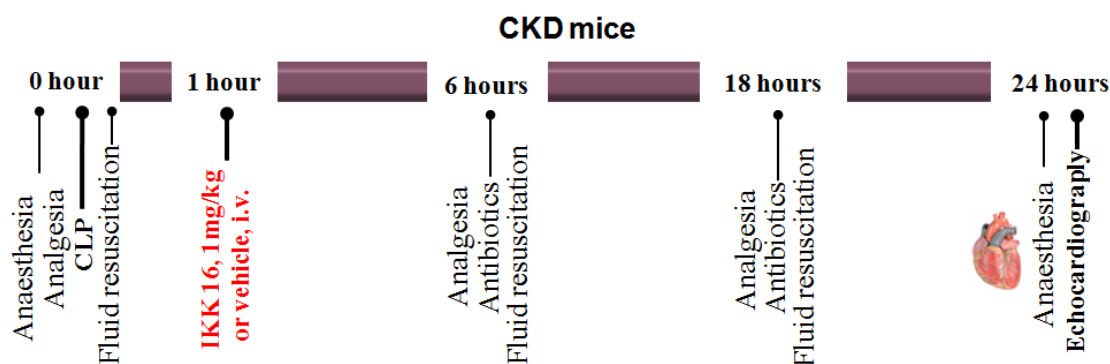
Figure 3.4 Experimental protocol for IKK 16 treatment in CKD mice underwent CLP. IKK 16 (1 mg/kg, *i.v.*) was given to CKD mice at one hour after the CLP surgery. Cardiac function was assessed by echocardiography in vivo under anaesthesia with isoflurane at 24 h after CLP surgery.

Table 3.2 Experimental groups used to study CLP-induced cardiac dysfunction in CKD mice.

Group	Number
CKD sham + sham-operation	6
CKD + sham-operation	7
CKD sham + CLP	7
CKD + CLP	7

Table 3.3 Experimental groups used to study the effects of IKK 16 on cardiac function in CKD mice underwent CLP.

Group	Number
CKD + sham-operation	7
CKD + CLP + 2% DMSO	7
CKD + CLP + IKK 16	7

3.2.5 Quantification of organ dysfunction/injury

Cardiac function was assessed in mice subjected to LPS at 18 h or CLP at 24 h, respectively, by echocardiography using a Vevo-770 imaging system (Visual Sonics, Toronto, Canada) (Figure 3.3) [367, 368]. Then, the experiment was terminated and organ and blood samples were collected for quantification of organ dysfunction/injury. Details are described in chapter 2.2.4 and 2.2.5, and depicted in Figure 2.3, Figure 2.4 and Figure 2.5.

3.2.6 Western blot analysis

We analysed the degree of phosphorylation of IκBα on $Ser^{32/36}$, Akt on Ser^{473} and ERK1/2, the nuclear translocation of the p65 subunit of NF-κB and the expression of iNOS. Semi-quantitative western blot analyses were carried out in mouse heart tissues as described previously [369] and details are described in chapter 2.2.6.

3.2.7 Determination of myeloperoxidase (MPO) activity in lung tissue

MPO was extracted from the tissue as described by Barone et al. [370] with slight modifications. MPO activity, used as a marker for neutrophil accumulation in tissues, was determined as previously described [371]. Details for solutions and reagents, and analysis procedure are described as below.

3.2.7.1 Solutions and Reagents for MPO assay

Table 3.4 Protocols for making solutions for MPO assay.

Solutions	Components
Homogenisation buffer, 5 mmol/L pH 6.0	2.17g K_2HPO_4 per 250ml H_2O (solution A) 1.7g KH_2PO_4 per 250ml H_2O (solution B) Add 0.307ml solution A and 2.19ml solution B in 200ml H_2O <u>Protease Inhibitors (add just before use):</u> 0.1% Proteinase Inhibitor cocktail (PIC) 0.5 mM PMSF 0.1 mM DL-Dithiethrectol (DTT)
Extraction buffer, 50 mmol/L pH 6.0	2.17g K_2HPO_4 per 250ml H_2O (solution A) 1.7g KH_2PO_4 per 250ml H_2O (solution B) Add 3.075ml solution A and 21.9ml solution B in 200ml H_2O 0.5% Hexadecyltrimethylammonium bromide <u>Protease Inhibitors (add just before use):</u> 0.1% PIC 0.5 mM PMSF 0.1 mM DTT
Substrate buffer	50 mmol/L pH 6.0 phosphate buffer 0.167 mg/ml O-Dianisidine HCl 0.005% H_2O_2

3.2.7.2 Procedures for MPO assay

(1) Homogenise tissue (30-40 μg tissue per mouse) in 5 mmol/L homogenisation buffer (1:20 tissue weight/ solution volume).

(2) Centrifuge at 13 000 g for 30 min at 4°C.

(3) Supernatants were removed and the pellets were re-suspended in preheated 25°C 50 mmol/L extraction buffer (1:5 tissue weight/ solution volume), then vortex the solutions and keep them in ice for 2 min.

(4) Three cycles of the following procedures to release MPO from the tissue: keep samples in -80°C freezer for 3 min; keep samples in 37°C water bath for 3 min and sonicating samples for 10 sec.

(5) Incubate samples for 20 min at 4°C.

(6) Centrifuge at 12 500 g for 15 min at 4°C.

(7) Keep supernatants, and discard the pellets.

(8) Add 5 μl sample in 145 μl substrate buffer (150 μl in total for each well). Add 150 μl substrate buffer in one well as negative control.

(9) Read the absorbance at 460 nm every 15 sec for a time span of 2 min.

(10) uMPO = the quantity of enzyme which degrades 1 μmol/ min of peroxide at 25°C.

(11) Values of μUMPO/ tissue weight were calculated and compared.

3.2.8 Measurement of cytokines by ELISA

Concentrations of cytokines in culture supernatants and plasma were measured using a commercially available cytometric bead array (BD Bioscience Hatfield, UK) as described in the manufacturer's instructions.

3.2.9 Bacteria counting

Accurate enumeration of bacteria in peritoneal lavages was performed by flow cytometry using the SYTO BC bacteria counting kit (Invitrogen, UK) according to the manufacturer's instructions.

3.2.10 Primary macrophage cultures

CKD and CKD sham mice were injected with 1 mL of 2% Bio-Gel (Bio-Rad) i.p., and 4 days later, peritoneal lavages were harvested with 4 mL of EDTA (3 mM) in PBS. Cells (2×10^6) were plated in 24-well plates in RPMI medium 1640 containing 10% (vol/vol) FCS and 50 mg/mL of gentamicin. After 2 h at 37 °C, non-adherent cells were washed and adherent cells (>90% macrophages) were incubated in RPMI 1640 1% FCS and treated with different concentrations of LPS (0.1 ng/ml, 1 ng/ml and 10 ng/ml) or vehicle (sterile PBS) for 6 h at 37 °C. Supernatants were harvested and cytokine production was determined by CBA (eBioscience, Hatfield, UK).

3.2.11 Statistics

Values are presented as mean ± SEM of n observations. Data were assessed by a one-way ANOVA followed by Bonferroni's post hoc test (multiple comparison), unpaired Student's t-test or Mann-Whitney U test using GraphPad Prism 5.0 (GraphPad Software, San Diego, CA, USA). $P < 0.05$ was considered to be statistically significant.

3.2.12 Materials

Reagents and compounds were purchased from Sigma Aldrich (Poole, Dorset, UK), unless otherwise stated. Antibodies for immunoblot analysis were purchased from Santa Cruz Biotechnology (Heidelberg, Germany).

3.3 Results

3.3.1 Characterisation of organ dysfunctions and blood tests in mice that underwent SNX.

When compared to a sham procedure, SNX resulted in significantly higher plasma urea and creatinine concentrations, this was paralleled by a mild cardiomyopathy indicated by slight, but significant, reductions in % EF, FS and FAC, as well as greater heart weights and heart weight to body weight ratio (a surrogate marker for myocardial hypertrophy [372]) ($P<0.05$; Table 3.5).

CKD mice exhibited significantly increased plasma levels of IL-1β and KC ($P<0.05$; Table 3.5), but other inflammatory cytokines, such as TNF-α, IL-6 and IL-10 were not detected. Additionally, full blood analysis indicated the development of anaemia and an increase in neutrophil-to-lymphocyte ratio in CKD mice ($P<0.05$; Table 3.5).

Table 3.5 Combined data sets from all groups studied prior to the intervention of endotoxaemia/sepsis for the characterisation of mice with CKD induced by subtotal (5/6th) SNX.

Parameter	CKD Sham	CKD
Urea (mmol/L)	8.18 ±0.41 (n=12)	17.43 ±0.61 (n=14)*
Creatinine (µmol/L)	29.72 ±0.38 (n=12)	45.96 ±1.76 (n=14)*
Ejection Fraction (%)	72.78 ±0.56 (n=11)	65.25 ±0.89 (n=23)*
Fractional Shortening (%)	41.25 ±0.48 (n=11)	35.85 ±0.67 (n=23)*
Fractional Area Change (%)	50.64 ±0.64 (n=11)	44.34 ±0.91 (n=23)*
Alanine Aminotransferase (U/L)	27.57 ±1.78 (n=12)	37.30 ±4.45 (n=14)
Body Weight (g)	31.11 ±0.82 (n=5)	29.13 ±0.41 (n=8)*
Heart Weight (g)	0.135 ±0.006 (n=5)	0.154 ±0.004 (n=8)*
Heart Weight Index[a]	4.34 ±0.10 (n=5)	5.29 ±0.19 (n=8)*
Plasma IL-1β (pg/ml)	15.83 ±4.85 (n=3)	78.08 ±19.36 (n=6)*
Plasma KC (pg/ml)	25.55 ±25.45 (n=3)	105.4 ±12.78 (n=6)*
Haemoglobin (g/dL)	13.41 ±0.37 (n=8)	10.97 ±0.34 (n=6)*
Haematocrit (%)	42.83 ±1.50 (n=8)	33.38 ±1.14 (n=6)*
White Blood Cells (K/uL)	6.57 ±0.76 (n=8)	7.75 ±1.14 (n=5)
Neutrophils (K/uL)	0.64 ±0.08 (n=8)	0.24 ±0.07 (n=5)*
Lymphocytes (K/uL)	5.80 ±0.68 (n=8)	5.20 ±0.82 (n=5)
Monocytes (K/uL)	0.03 ±0.01 (n=8)	0.13 ±0.02 (n=5)*
Neutrophil-to-Lymphocyte Ratio[b]	0.11 ±0.01 (n=8)	0.45 ±0.09 (n=5)*
Neutrophils (%)	9.73 ±0.53 (n=8)	30.44 ±3.20 (n=5)*
Lymphocytes (%)	88.3 ±0.57 (n=8)	66.44 ±3.69 (n=5)*
Monocytes (%)	0.55 ±0.19 (n=8)	1.68 ±0.26 (n=5)*

Mice underwent a two-stage SNX were compared with mice which underwent sham surgery. All data are expressed as means ± SEM for *n* number of observations. Data were analysed by unpaired Student's t-test, or Mann-Whitney *U* test when *n* number of the group equals 3. *$P<0.05$ versus the CKD sham group. [a]Heart Weight Index was calculated by dividing the weight of the heart in grams by the weight of the animal in kilograms. [b]Neutrophil-to-lymphocyte ratio was calculated as the ratio of the neutrophils to lymphocytes. IL, interleukin; KC, keratinocyte-derived cytokine.

3.3.2 Pre-existing CKD augmented the cardiac dysfunction and worsened clinical score caused by low dose LPS administration.

In CKD sham animals, low dose LPS (2 mg/kg) had no effect on % EF, FAC and FS ($P>0.05$; Figure 3.5A - D), however, in CKD mice, low dose LPS induced significant reductions in % EF, FAC and FS ($P<0.05$; Figure 3.5A - D), indicating the development of a clear and significant cardiac dysfunction *in vivo*. Additionally, when compared with CKD sham mice subjected to low dose LPS injection, CKD mice yielded worse clinical scores ($P<0.05$; Figure 3.5E).
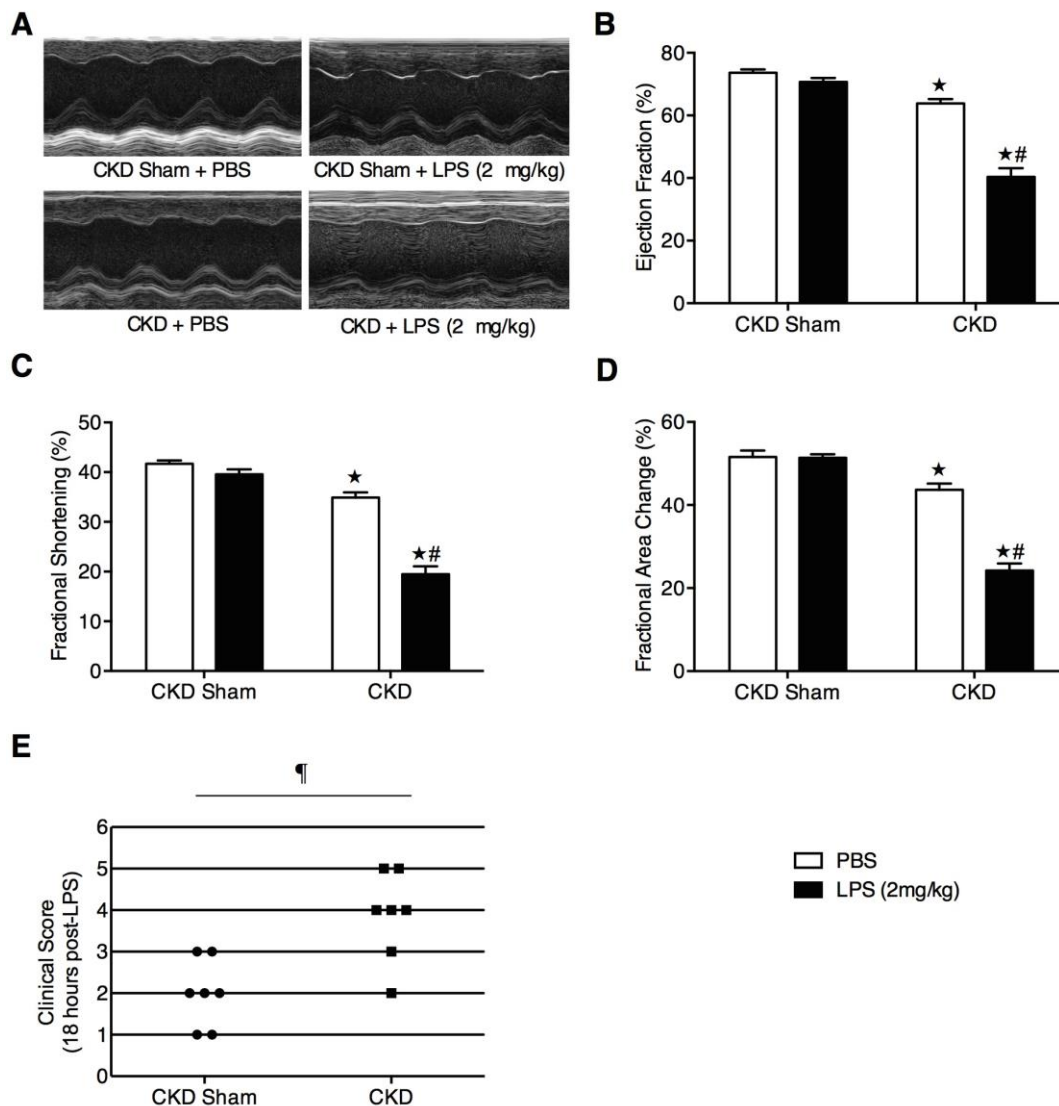
Figure 3.5 Effects of low dose of LPS (2 mg/kg) administration on cardiac function and

clinical score in mice with CKD. CKD sham or CKD mice received either LPS (2 mg/kg) or PBS (5 ml/kg) intraperitoneally. Cardiac function was assessed at 18 h. (**A**) Representative M-mode echocardiograms; percentage (%) (**B**) ejection fraction (EF); (**C**) fractional area change (FAC); (**D**) fractional shortening (FS); and (**E**) clinical score: At 18 hours post-LPS, mice were scored for the presence or absence of six different macroscopic signs of sepsis.. The following groups were studied: CKD sham + PBS (n = 6); CKD + PBS (n = 7); CKD sham + LPS (2 mg/kg) (n = 7); CKD + LPS (2 mg/kg) (n = 7). Panel **B** – **D**: Data are represented as mean ± SEM. ★*P*<0.05 versus the CKD sham group with respective treatment, #*P*<0.05 versus repective PBS group, ¶ *P* < 0.05 versus CKD sham group.

3.3.3 Pre-existing CKD augmented the cardiac dysfunction and worsened clinical score caused by CLP.

The murine model of CLP with fluid resuscitation and antibiotics treatment offers a clinically relevant model of abdominal polymicrobial human sepsis. CLP induced-cardiac dysfunction was only observed in 8 month-old mice, but not in young mice [317]. As previously reported [317], CLP had no significant effect on cardiac parameters in young mice (*P*>0.05; Figure 3.6A - D). However, in CKD mice, CLP caused significant reductions in % EF, FAC and FS (*P*<0.05; Figure 3.6A - D), indicating the development of a pronounced cardiac dysfunction *in vivo.* The degree of systolic dysfunction in young CKD mice with CLP was similar to the cardiac dysfunction reported prevously in old (8 months) mice with CLP [317]. Additionally, when compared with CKD sham mice subjected to CLP, CKD mice yielded worse clinical scores (*P*<0.05; Figure 3.6E).
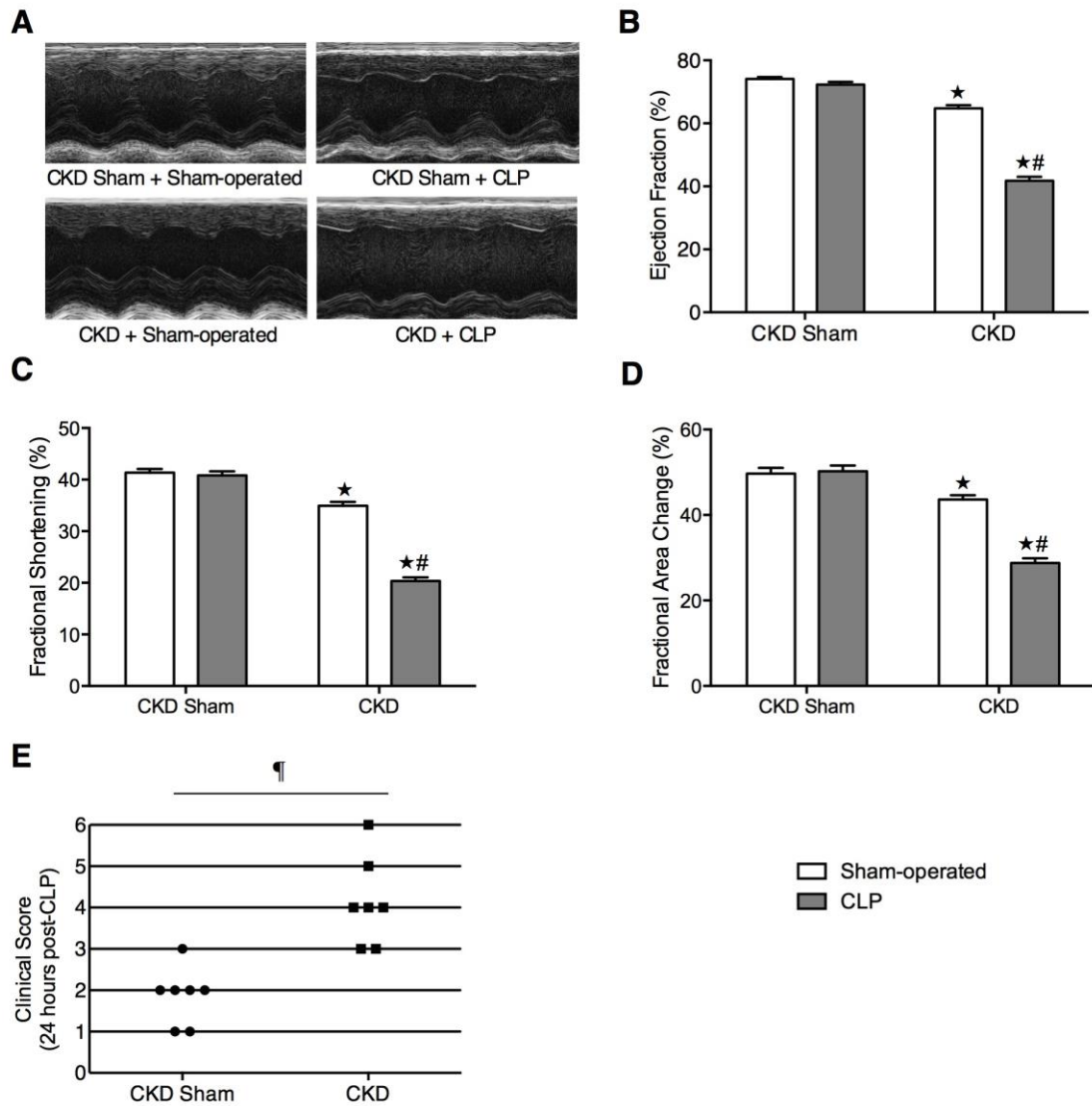
Figure 3.6 Effects of polymicrobial sepsis induced by CLP on cardiac function and clinical score in mice with CKD. CKD sham or CKD mice were subjected to CLP or sham-operated surgery. Cardiac function was assessed at 24 h. (**A**) Representative M-mode echocardiograms; percentage (%) (**B**) ejection fraction (EF); (**C**) fractional area change (FAC); (**D**) fractional shortening (FS); and (**E**) clinical score: At 18 hours post-CLP, mice were scored for the presence or absence of six different macroscopic signs of sepsis. The following groups were studied: CKD sham + sham-operated (n = 6); CKD + sham-operated (n = 7); CKD sham + CLP (n = 7); CKD + CLP (n = 7). Panel **B** – **D**: Data are represented as mean ± SEM. ★$P<0.05$ versus the CKD sham group with respective treatment, #$P<0.05$ versus the respective sham-operated group, ¶ $P < 0.05$ versus CKD sham group.

3.3.4 Increases in the phosphorylation of IκBα, the nuclear translocation of p65 NF-κB and the iNOS expression in hearts of mice with CKD subjected to low dose LPS administration.

To gain a better mechanical insight into the augmented sepsis-associated cardiac dysfunction in CKD mice, we investigated the effects of pre-existing CKD on signalling events in mouse hearts subjected to LPS. When compared to PBS-treated CKD sham mice, PBS-treated CKD mice exhibited significantly higher degrees of cardiac phosphorylation of IKKα/β on $Ser^{176/180}$, subsequent phosphorylation of IκBα on $Ser^{32/36}$, subsequent nuclear translocation of p65 NF-κB, and iNOS expression ($P<0.05$; Figure 3.7A - D). Exposure of CKD sham mice to low dose LPS had no significant effect on any of the above signalling pathways ($P>0.05$; Figure 3.7A - D). However, LPS further increased cardiac phosphorylation of IKKα/β and IκBα, nuclear translocation of p65, and iNOS expression ($P<0.05$; Figure 3.7A - D) to profound degrees in CKD mice.

Figure 3.7 Effects of pre-existing CKD on NF-κB signalling pathways in hearts of mice subjected to low dose of LPS (2 mg/kg) administration. CKD sham or CKD mice received either LPS (2 mg/kg) or PBS (5 ml/kg) intraperitoneally. Signalling events in heart tissue were assessed at 18 h. Densitometric analysis of the bands is expressed as relative optical density (O.D.) of (**A**) phosphorylated inhibitor of kappa B (IκB) kinase (IKK) α/β (pSer$^{176/180}$) corrected for the corresponding total IKKα/β content and normalized using the related sham band; (**B**) phosphorylated inhibitor of kappa B (IκB) α (pSer$^{32/36}$) corrected for the corresponding total IκBα content and normalized using the related sham band; (**C**) NF-κB p65 subunit levels in both, cytosolic and nuclear fractions expressed as a nucleus/cytosol ratio normalized using the related sham bands; (**D**) inducible nitric oxide synthase (iNOS) expression corrected for the corresponding tubulin band. Each analysis (**A - D**) is from a single experiment and is representative of three separate experiments. Data are expressed as mean ± SEM for *n* number of observations. Data were analysed by one-way ANOVA followed by Bonferroni's post hoc test. ★$P<0.05$ versus the CKD sham group with respective treatment, #$P<0.05$ versus the respective PBS group.

3.3.5 Increases in the phosphorylation of IκBα, the nuclear translocation of p65

NF-κB and the iNOS expression in hearts of mice with CKD subjected to CLP.

When compared to sham-operated CKD sham mice, sham-operated CKD mice exhibited significantly higher degrees of cardiac phosphorylation of IKKα/β on Ser$^{176/180}$, subsequent phosphorylation of IκBα on Ser$^{32/36}$, subsequent nuclear translocation of p65 NF-κB, and iNOS expression ($P<0.05$; Figure 3.8A - D). Exposure of CKD sham mice to CLP had no significant effect on any of the above signalling pathways ($P>0.05$; Figure 3.8A - D). However, CLP further increased cardiac phosphorylation of IKKα/β and IκBα, nuclear translocation of p65, and iNOS expression ($P<0.05$; Figure 3.8A - D) to profound degrees in CKD mice.
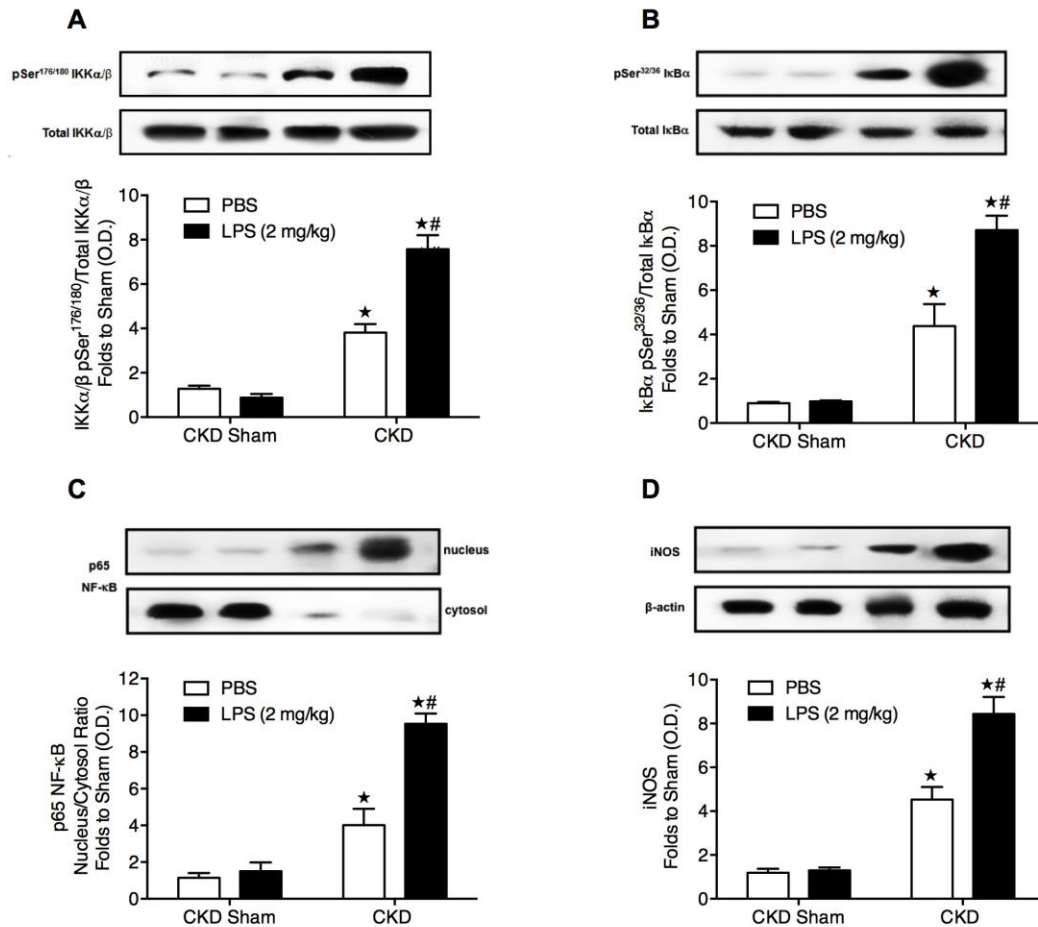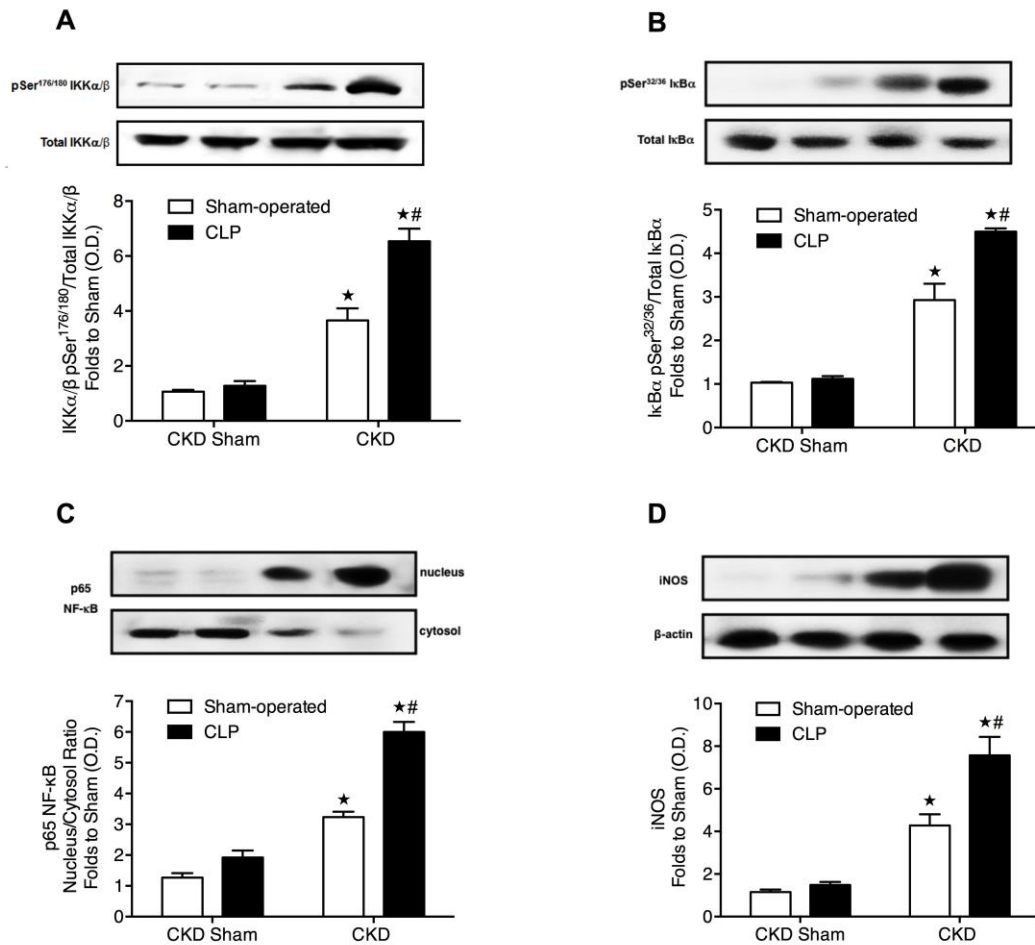
Figure 3.8 Effects of pre-existing CKD on NF-κB signalling pathways in hearts of mice subjected to polymicrobial sepsis induced by CLP. CKD sham or CKD mice were subjected to CLP or sham-operated surgery. Signalling events in heart tissue were assessed at 24 h. Densitometric analysis of the bands is expressed as relative optical density (O.D.) of (**A**) phosphorylated inhibitor of kappa B (IκB) kinase (IKK) α/β (pSer$^{176/180}$) corrected for the corresponding total IKKα/β content and normalized using the related sham band; (**B**) phosphorylated inhibitor of kappa B (IκB) α (pSer$^{32/36}$) corrected for the corresponding total IκBα content and normalized using the related sham band; (**C**) nuclear factor (NF)-κB p65 subunit levels in both, cytosolic and nuclear fractions expressed as a nucleus/cytosol ratio normalized using the related sham bands; (**D**) inducible nitric oxide synthase (iNOS) expression corrected for the corresponding tubulin band. Each analysis (**A - D**) is from a single experiment and is representative of three separate experiments. Data are expressed as mean ± SEM for *n* number of observations. Data were analysed by one-way ANOVA followed by Bonferroni's post hoc test. ★$P < 0.05$ versus the CKD sham group with respective treatment, #$P < 0.05$ versus the respective sham-operated group.

3.3.6 Effects of low dose LPS administration on the phosphorylation of Akt and ERK1/2 in hearts of mice with CKD.

When compared to PBS-treated CKD sham mice, PBS-treated CKD mice demonstrated significantly higher degrees of cardiac phosphorylation of Akt on Ser^{473} and ERK1/2 on Tyr^{202} and Tyr^{204}, respectively ($P<0.05$; Figure 3.9A, 3.9B). CKD sham or CKD mice subjected to LPS demonstrated no significant change in the degree of phosphorylation of Akt or ERK1/2 ($P>0.05$; Figure 3.9A, 3.9B).
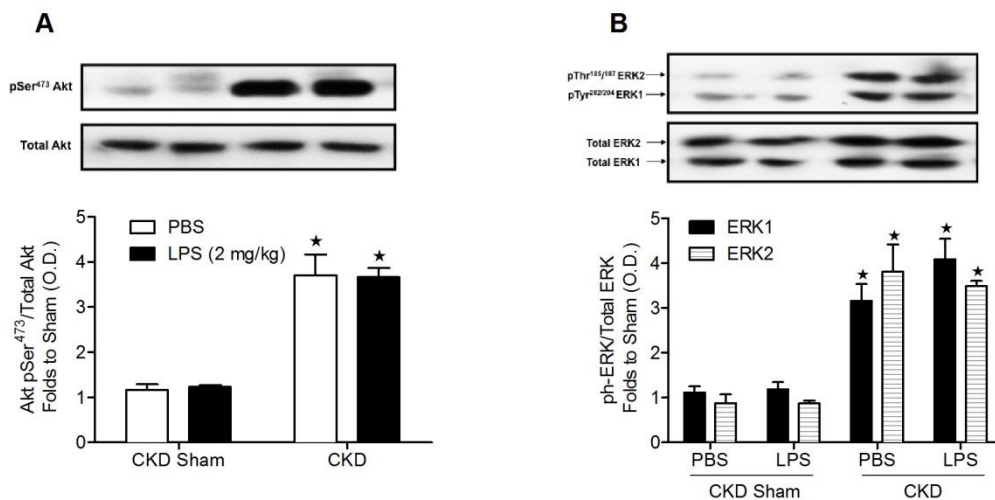
Figure 3.9 Effects of pre-existing CKD on Akt and ERK1/2 phosphorylation in hearts of mice subjected to low dose of LPS (2 mg/kg) administration. CKD sham or CKD mice received either LPS (2 mg/kg) or PBS (5 ml/kg) intraperitoneally. Signalling events in heart tissue were assessed at 18 h. Densitometric analysis of the bands is expressed as relative optical density (O.D.) of (**A**) phosphorylated Akt ($pSer^{473}$) corrected for the corresponding total Akt content and normalized using the related sham band; (**B**) ERK1/2 phosphorylation, corrected for the corresponding total ERK1/2 content and normalized using the related sham band. Each analysis (**A, B**) is from a single experiment and is representative of three separate experiments. Data are expressed as mean ± SEM for *n* number of observations. Data were analysed by one-way ANOVA followed by Bonferroni's post hoc test. ★$P<0.05$ versus the CKD sham group with respective treatment, #$P<0.05$ versus the respective PBS group.

3.3.7 Effects of CLP on the phosphorylation of Akt and ERK1/2 in hearts of mice with CKD.

When compared to sham-operated CKD sham mice, sham-operated CKD mice demonstrated significantly higher degrees of cardiac phosphorylation of Akt on Ser^{473} and ERK1/2 on Tyr^{202} and Tyr^{204}, respectively ($P<0.05$; Figure 3.10A, 3.10B). CKD sham or CKD mice subjected to CLP demonstrated no significant change in the degree of phosphorylation of Akt or ERK1/2 ($P>0.05$; Figure 3.10A, 3.10B).
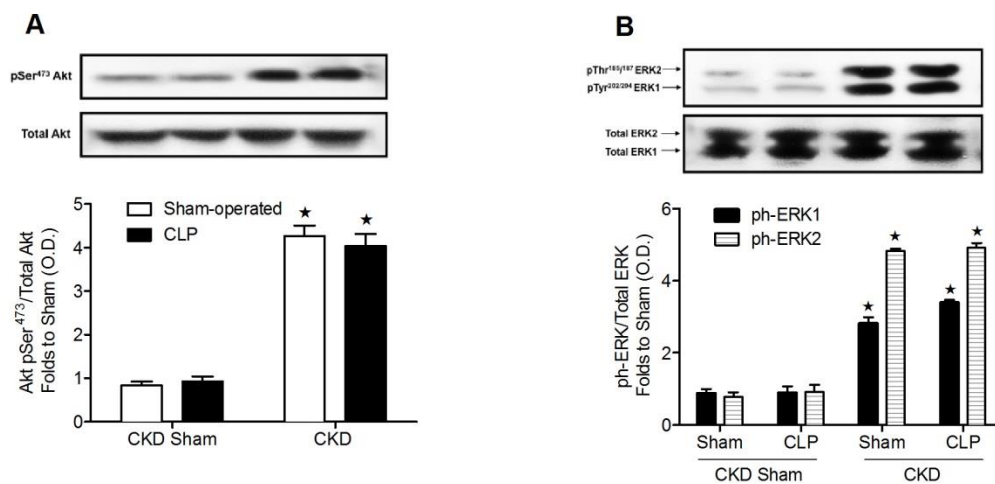
Figure 3.10 Effects of pre-existing CKD on Akt and ERK1/2 phosphorylation in hearts of mice subjected to polymicrobial sepsis induced by CLP. CKD sham or CKD mice were subjected to CLP or sham-operated surgery. Signalling events in heart tissue were assessed at 24 h. Densitometric analysis of the bands is expressed as relative optical density (O.D.) of (**A**) phosphorylated Akt ($pSer^{473}$) corrected for the corresponding total Akt content and normalized using the related sham band; (**B**) ERK1/2 phosphorylation, corrected for the corresponding total ERK1/2 content and normalized using the related sham band. Each analysis (**A, B**) is from a single experiment and is representative of three separate experiments. Data are expressed as mean ± SEM for n number of observations. Data were analysed by one-way ANOVA followed by Bonferroni's post hoc test. ★$P<0.05$ versus the CKD sham group with respective treatment, #$P<0.05$ versus the respective sham-operated group.

3.3.8 Pre-existing CKD increases severity of renal dysfunction and hepatocellular injury caused by low dose LPS administration or CLP.

In CKD sham animals, septic insults induced either by low dose LPS or CLP had no significant effect on plasma urea, creatinine or ALT level ($P>0.05$; Table 3.6), however, in CKD mice, low dose LPS further increased plasma urea, creatinine and ALT levels to profound degrees ($P<0.05$; Table 3.6); CLP resulted in significant increases in plasma urea and ALT levels ($P<0.05$; Table 3.6), indicating the augmentation of renal dysfunction and hepatocellular injury, respectively.

Table 3.6 Effects of low dose of LPS (2 mg/kg) administration or polymicrobial sepsis induced by CLP on renal dysfunction and hepatocellular injury in mice with CKD.

Parameter	CKD Sham		CKD	
	PBS	LPS (2mg/kg)	PBS	LPS (2mg/kg)
Number	6	7	7	7
Urea (mmol/L)	8.26 ± 0.47	16.13 ± 3.88	17.24 ± 1.09*	38.56 ± 2.11*†
Creatinine (µmol/L)	30.22 ± 0.55	30.23 ± 2.35	45.47 ± 2.42*	58.43 ± 2.55*†
ALT (U/L)	27.23 ± 3.01	52.06 ± 2.11	32.16 ± 3.34	83.35 ± 14.11*†
	Sham-operated	CLP	Sham-operated	CLP
Number	6	6	7	7
Urea (mmol/L)	8.08 ± 0.72	13.08 ± 087	17.61 ± 0.66	37.60 ± 6.91*†
Creatinine (µmol/L)	29.22 ± 0.50	27.30 ± 0.93	46.44 ± 2.75	67.43 ± 12.92*
ALT (U/L)	23.62 ± 2.90	103.52 ± 15.31	42.44 ± 8.10	287.10 ± 49.86*†

Plasma urea, creatinine and alanine aminotransferase (ALT) levels were assessed at 18 h in mice subjected to LPS administration and at 24 h in mice that underwent CLP. All data are represented as mean ± SEM. Data were analysed by one-way ANOVA followed by Bonferroni's post hoc test. *$P<0.05$ versus the CKD sham group with respective treatment, †$P<0.05$ versus the respective PBS or sham-operated group.

3.3.9 Pre-existing CKD increased lung inflammation and systemic inflammatory

response caused by CLP.

In CKD sham animals, CLP had no significant effect on lung MPO activity or plasma inflammatory cytokine levels (TNF-α, IL-1β, IL-6, IL-10 or KC) ($P>0.05$; Figure 3.11A - F), however, in CKD mice, CLP resulted in significant increases in lung MPO activity and inflammatory cytokine levels ($P<0.05$; Figure 3.11A - E), indicating an increased neutrophil infiltration in the lung and an enhanced systemic inflammatory response, respectively. No alteration was detected in peritoneal bacteria content between CKD and CKD sham mice following CLP ($P>0.05$; Figure 3.12).
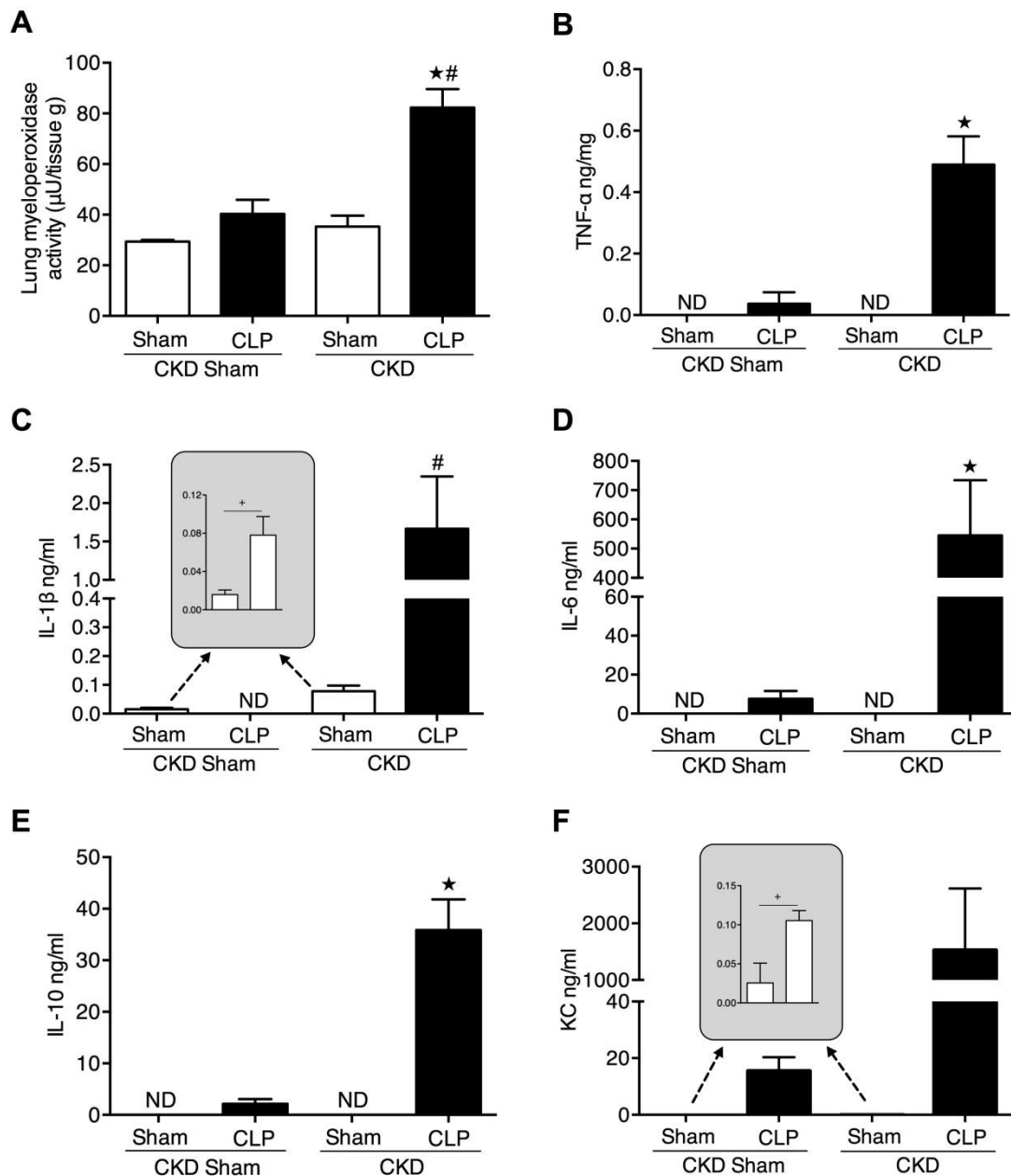
Figure 3.11 Effects of polymicrobial sepsis induced by CLP on lung inflammation and systemic response in mice with CKD. Markers of lung inflammation and systemic response were assessed at 24 h in mice that underwent CLP. (**A**) Myeloperoxidase (MPO) activity in lung tissue; (**B**) plasma tumor necrosis factor (TNF)-α concentration; (**C**) plasma interleukin (IL)-1β concentration; (**D**) plasma IL-6 concentration; (**E**) plasma IL-10 concentration; and (**F**) plasma keratinocyte-derived cytokine (KC) concentration. Panel **A**: n=3 per group; Panel **B** – **F**: n=3 for CKD Sham + Sham-operated group, n=5-6 for other groups. All data are represented as mean ± SEM. Data were analysed by one-way ANOVA followed by Bonferroni's post hoc test for multiple comparisons or by Student's t-test for comparisons between two groups. ★$P<0.05$ versus the CKD sham group with respective treatment, #$P<0.05$ versus the respective sham-operated group, +$P<0.05$ versus the CKD sham group with sham operation. ND, not detected.
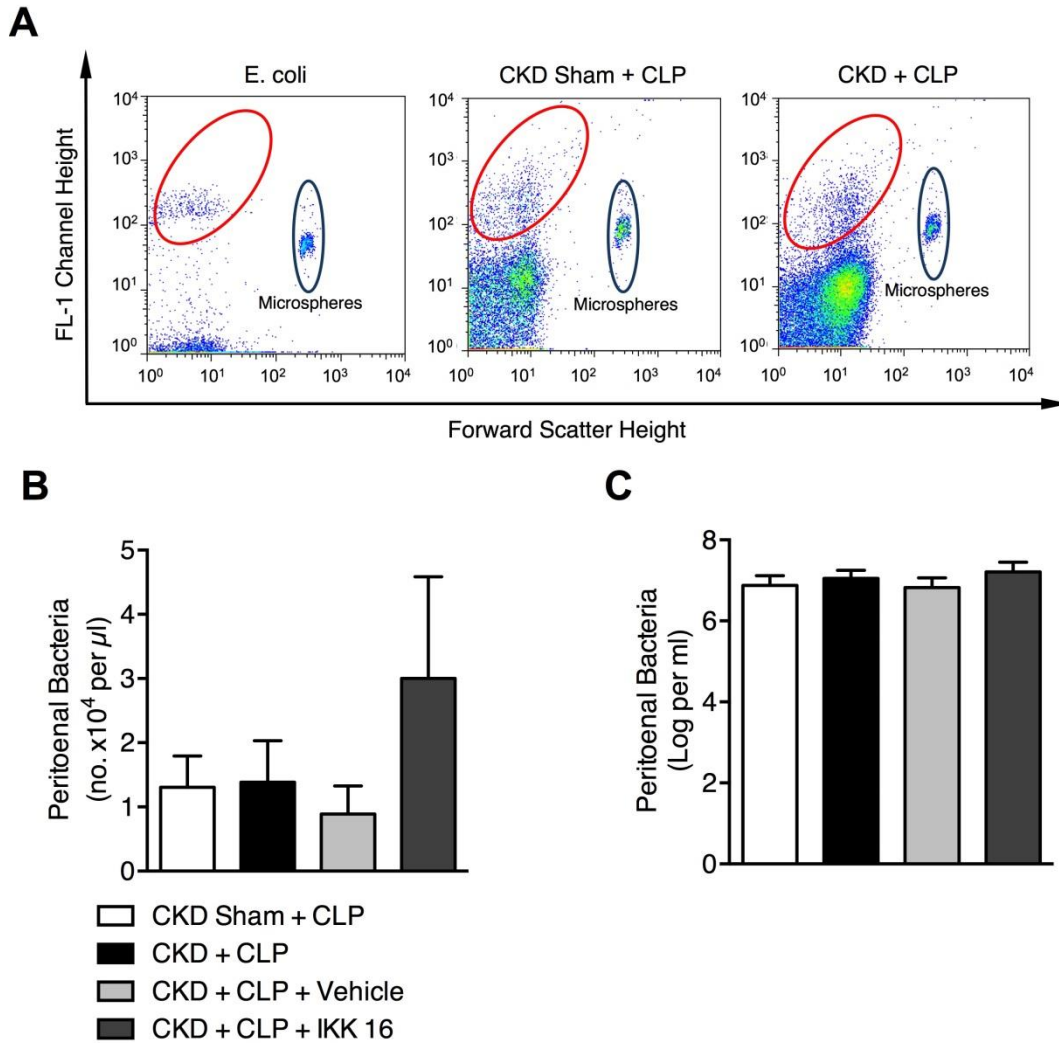
Figure 3.12 Peritoneal bacterial loads following CLP and IKK 16 treatment in CKD mice. Mice underwent CLP surgery. One hour after CLP, two groups of CKD control mice were treated with either IKK 16 (1 mg/kg *i.v.*) or vehicle (2% DMSO). (**A**) Representative flow cytometry scattergrams illustrating bacteria (SYTO BC bacteria dye) positive events in E. coli suspension (Left) as well as 24 h post-CLP peritoneal exudates from CKD sham and CKD control mice. The density of bacteria in the experimental samples was determined from the ratio of bacterial to microsphere signals. (**B - C**) Bacteria levels in peritoneal lavages from CKD sham and CKD control mice. N=3-6 per group. All data are represented as mean ± SEM. Data were analysed by one-way ANOVA followed by Bonferroni's post hoc test.

To determine whether the observed higher levels of inflammatory cytokines in CLP challenged CKD mice were due to increased cytokine production, macrophages isolated from either CKD sham or CKD mice were incubated with different concentrations of LPS (0.1 ng/ml, 1 ng/ml and 10 ng/ml). Untreated CKD-derived macrophages released significantly higher levels of IL-1β in the supernatant ($P<0.05$; Figure 3.13B). Yet significantly increased TNF-α released by CKD-derived macrophages in comparison with CKD sham-derived macrophages was solely induced by a low dose LPS (0.1 ng/ml) stimulation ($P<0.05$; Figure 3.13A), no other significant difference was detected in the cytokine production levels in response to LPS stimulation ($P>0.05$; Figure 3.13).
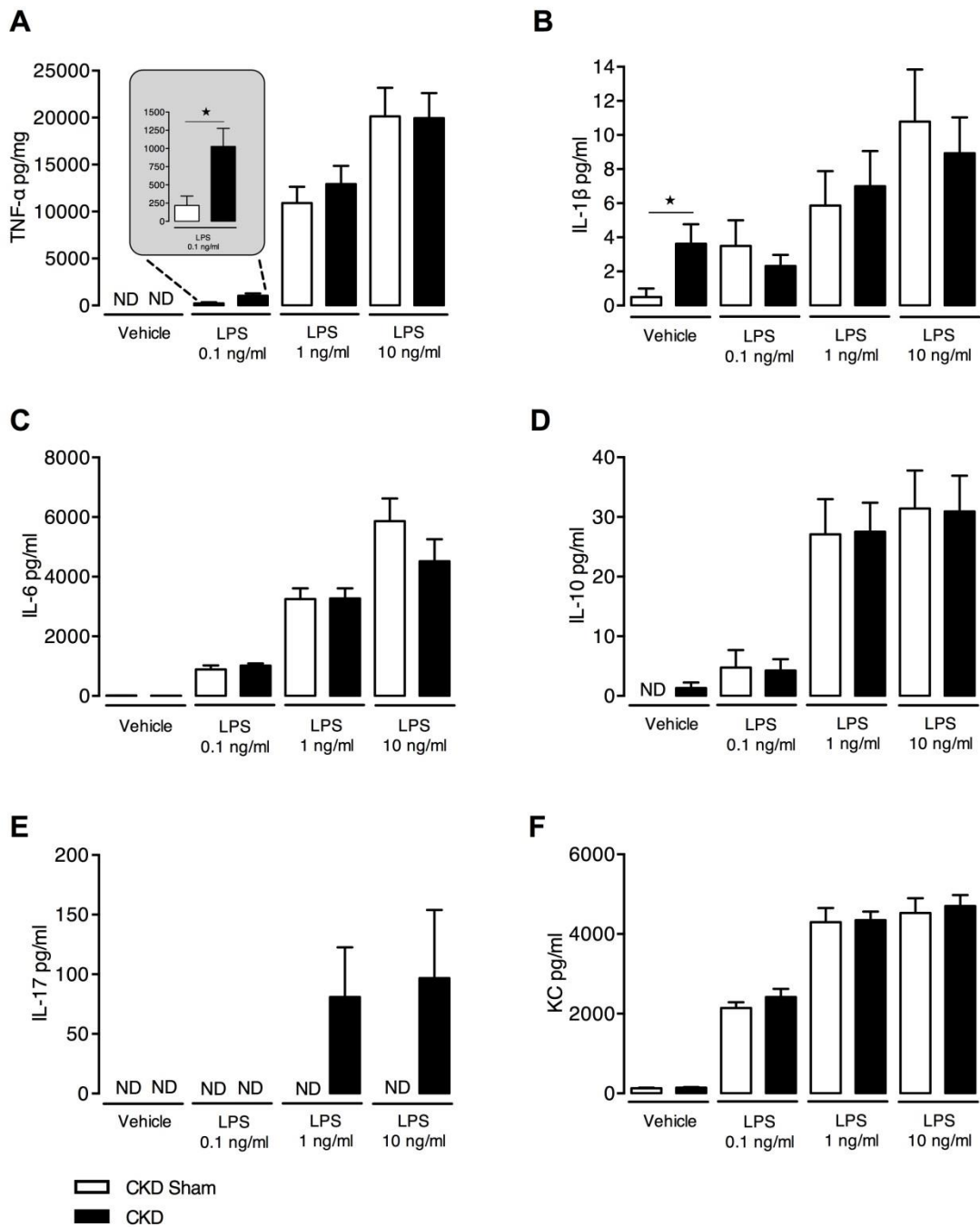
Figure 3.13 Cytokine production by macrophages derived from CKD sham and CKD mice following LPS incubation. Biogel-elicited macrophages from CKD sham and CKD mice were incubated with the indicated concentrations of LPS or vehicle (sterile PBS) for 6 h at 37 °C before assessment of cytokine production in supernatants by CBA. (**A**) Supernatant tumour necrosis factor (TNF)-α concentration; (**B**) supernatant interleukin (IL)-1β concentration; (**C**) supernatant IL-6 concentration; (**D**) supernatant IL-10 concentration; (**E**) supernatant IL-17 concentration; and (**F**) supernatant keratinocyte-derived cytokine (KC) concentration. N=4-7 per group. All data are represented as mean ± SEM. Data were analysed by unpaired Student's t-test for comparisons between two groups with the same PBS or LPS treatment. ★$P<0.05$ versus corresponding CKD sham group. ND, not detected.

3.3.10 Inhibition of IκB kinase attenuated CLP-induced cardiac dysfunction and reduced clinical score in mice with CKD.

When compared to sham-operated CKD mice, CKD mice that underwent CLP with vehicle treatment developed significant cardiac dysfunction ($P<0.05$; Figure 3.14A - D); this was significantly attenuated by delayed administration of IKK 16 one hour after CLP ($P<0.05$; Figure 3.14A - D). Additionally, when compared with vehicle-treated CKD/CLP mice, IKK16 treatment significantly attenuated clinical scores ($P<0.05$; Figure 3.14E). No significant change in plasma urea, creatinine or ALT level was seen with IKK 16 administration ($P>0.05$; Table 3.7).
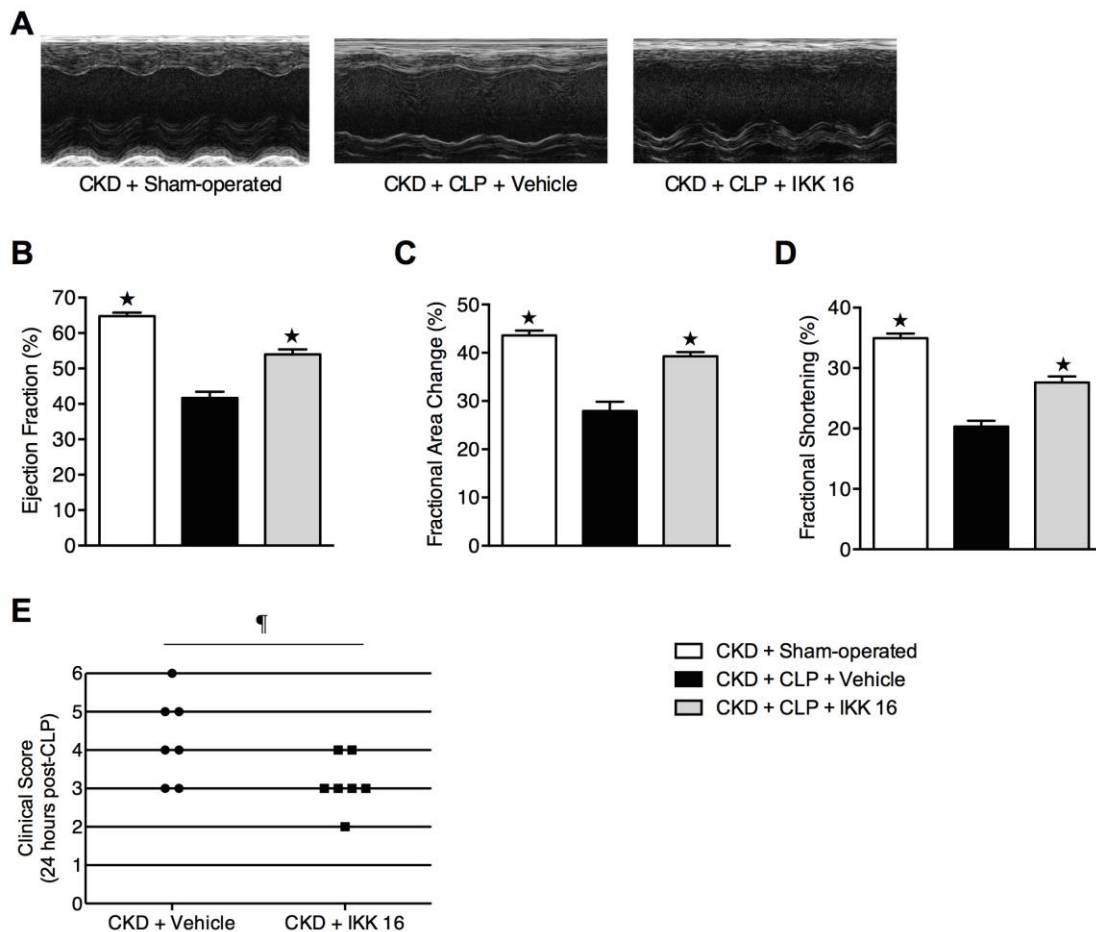
Figure 3.14 Effects of IκB kinase inhibitor on cardiac dysfunction and clinical score induced by polymicrobial sepsis in mice with CKD. CKD mice underwent sham-operated surgery or caecal ligation and puncture (CLP). One hour after CLP, mice were treated with either IKK 16 (1 mg/kg *i.v.*) or vehicle (2% DMSO). Cardiac function was assessed at 24 h.

(**A**) Representative M-mode echocardiograms; percentage (%) (**B**) ejection fraction; (**C**) fractional area change; (**D**) fractional shortening (FS); and (**E**) clinical score: At 18 hours post-CLP, mice were scored for the presence or absence of six different macroscopic signs of sepsis. The following groups were studied: CKD + sham-operated (n = 7); CKD + CLP + Vehicle (n = 7); CKD + CLP + IKK 16 (n = 7). Panel **B** – **D**: Data are represented as mean ± SEM. ★P<0.05 versus the CKD + CLP + Vehicle group, ¶ P < 0.05 versus CKD + CLP + Vehicle group.

Table 3.7 Effects of IκB kinase inhibitor on renal dysfunction and hepatocellular injury induced by polymicrobial sepsis in mice with CKD.

Parameter	CKD		
	Sham-operated	**CLP + Vehicle**	**CLP + IKK 16**
Number	7	7	7
Urea (mmol/L)	17.61 ± 0.66*	34.01 ± 6.41	21.90 ± 1.85
Creatinine (µmol/L)	46.44 ± 2.75	62.17 ± 5.69	52.59 ± 4.78
ALT (U/L)	42.44 ± 8.10*	240.7 ± 36.78	626.0 ± 308.2[a]

CKD mice underwent sham-operated surgery or caecal ligation and puncture (CLP). One hour after CLP, mice were treated with either IKK 16 (1 mg/kg *i.v.*) or vehicle (2% DMSO). Plasma urea, creatinine and alanine aminotransferase (ALT) levels were assessed at 24 h after CLP. All data are represented as mean ± SEM. Data were analysed by one-way ANOVA followed by Bonferroni's post hoc test. *P<0.05 versus the CKD + CLP + Vehicle group. [a]Two extremely high ALT values were detected in CKD + CLP + IKK 16 group, further research needs to be conducted to study the effects of IKK 16 on potential liver toxicity.

3.3.11 Effects of IκB kinase inhibitor on signalling events induced by CLP in hearts of CKD mice.

When compared to septic CKD mice with vehicle treatment, delayed administration of IKK 16 significantly attenuated the increases in cardiac phosphorylation of IKKα/β and IκBα, nuclear translocation of p65 and iNOS expression ($P<0.05$; Figure 3.15A - D). Moreover, IKK 16 treatment significantly reduced cardiac phosphorylation of Akt and ERK1/2 ($P<0.05$; Figure 3.16A, 3.16B) in septic CKD mice.
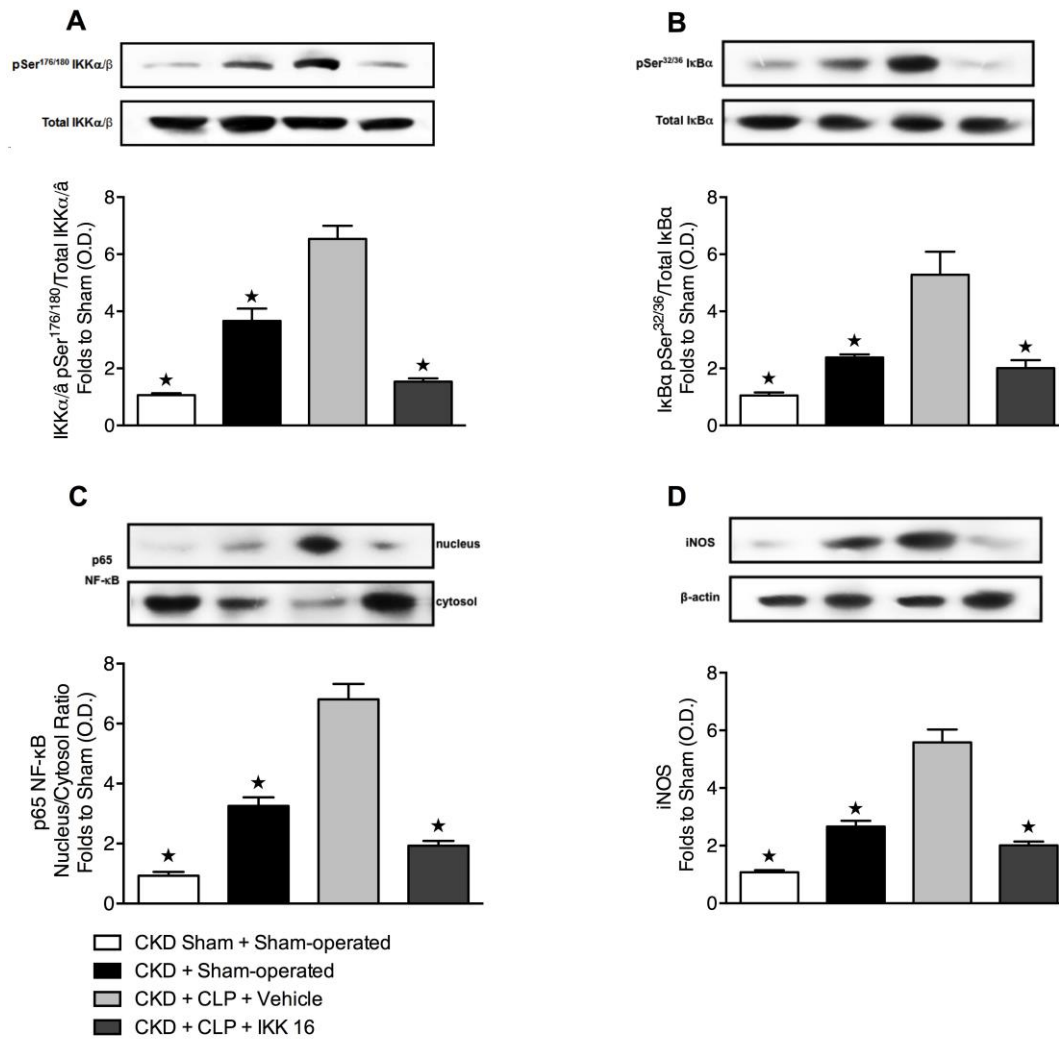
Figure 3.15 Effects of IκB kinase inhibitor on NF-κB signalling pathways in hearts of mice with CKD subjected to polymicrobial sepsis induced by CLP. CKD sham underwent sham-operated surgery, CKD mice were subjected to CLP or sham-operated surgery. One hour after CLP, CKD mice were treated with either IKK 16 (1 mg/kg i.v.) or vehicle (2% DMSO). Signalling events in heart tissue were assessed at 24 h. Densitometric analysis of the bands is expressed as relative optical density (O.D.) of (**A**) phosphorylated inhibitor of kappa B (IκB) kinase (IKK) α/β (pSer$^{176/180}$) corrected for the corresponding total IKKα/β content and normalized using the related sham band; (**B**) phosphorylated inhibitor of kappa B (IκB) α (pSer$^{32/36}$) corrected for the corresponding total IκBα content and normalized using the related sham band; (**C**) NF-κB p65 subunit levels in both, cytosolic and nuclear fractions expressed as a nucleus/cytosol ratio normalized using the related sham bands; (**D**) inducible nitric oxide synthase (iNOS) expression corrected for the corresponding tubulin band. Each analysis (**A - D**) is from a single experiment and is representative of three separate experiments. Data are expressed as mean ± SEM. Data were analysed by one-way ANOVA followed by Bonferroni's post hoc test. ★$P < 0.05$ versus the CKD + CLP + Vehicle group.

Figure 3.16 Effects of IκB kinase inhibitor on Akt and ERK1/2 phosphorylation in hearts of mice with CKD subjected to polymicrobial sepsis induced by CLP. CKD sham underwent sham-operated surgery, CKD mice were subjected to CLP or sham-operated surgery. One hour after CLP, CKD mice were treated with either IKK 16 (1 mg/kg i.v.) or vehicle (2% DMSO). Signalling events in heart tissue were assessed at 24 h. Densitometric analysis of the bands is expressed as relative optical density (O.D.) of (**A**) phosphorylated Akt (pSer^{473}) corrected for the corresponding total Akt content and normalized using the related sham band; (**B**) ERK1/2 phosphorylation, corrected for the corresponding total ERK1/2 content and normalized using the related sham band. Each analysis (**A, B**) is from a single experiment and is representative of three separate experiments. Data are expressed as mean ± SEM for *n* number of observations. Data were analysed by one-way ANOVA followed by Bonferroni's post hoc test. ★*P* <0.05 versus the CKD + CLP + Vehicle group.

3.3.12 Inhibition of IκB kinase attenuated lung inflammation and systemic inflammatory response caused by CLP.

Treatment of septic CKD mice with IKK 16 one hour after CLP significantly reduced the increases in lung MPO activity and plasma inflammatory cytokine levels ($P<0.05$; Figure 3.17A - E). However, IKK 16 treatment had no effect on peritoneal bacteria content in CKD mice following CLP ($P>0.05$; Figure 3.12).
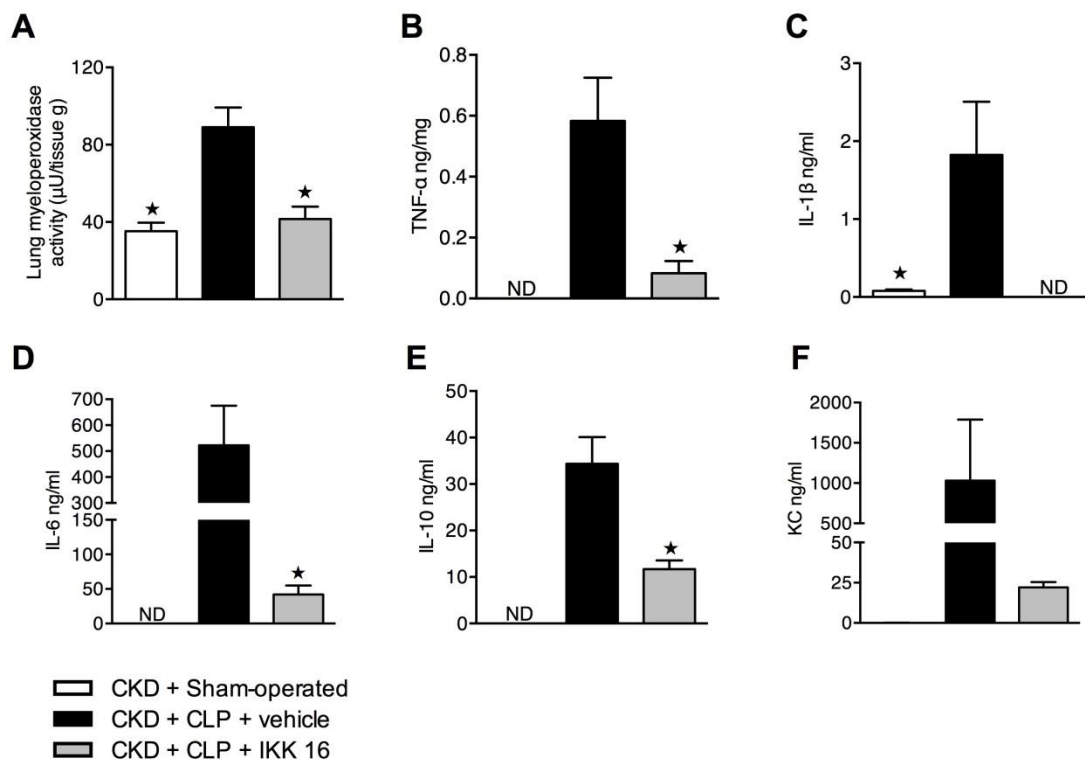
Figure 3.17 Effects of IκB kinase inhibitor on lung inflammation and systemic response in mice with CKD subjected to polymicrobial sepsis induced by CLP. CKD mice underwent CLP or sham-operated surgery. One hour after CLP, CKD mice were treated with either IKK 16 (1 mg/kg i.v.) or vehicle (2% DMSO). Markers of lung inflammation and systemic response were assessed at 24 h. (**A**) Myeloperoxidase (MPO) activity in lung tissue; (**B**) plasma tumour necrosis factor (TNF)-α concentration n; (**C**) plasma interleukin (IL)-1β concentration; (**D**) plasma IL-6 concentration; (**E**) plasma IL-10 concentration; and (**F**) plasma keratinocyte-derived cytokine (KC) concentration. Panel **A**: n=3 per group; Panel **B –F**: n=5-6 per group. All data are represented as mean ± SEM. Data were analysed by one-way ANOVA followed by Bonferroni's post hoc test. ★P <0.05 versus the CKD + CLP + Vehicle group. ND, not detected.

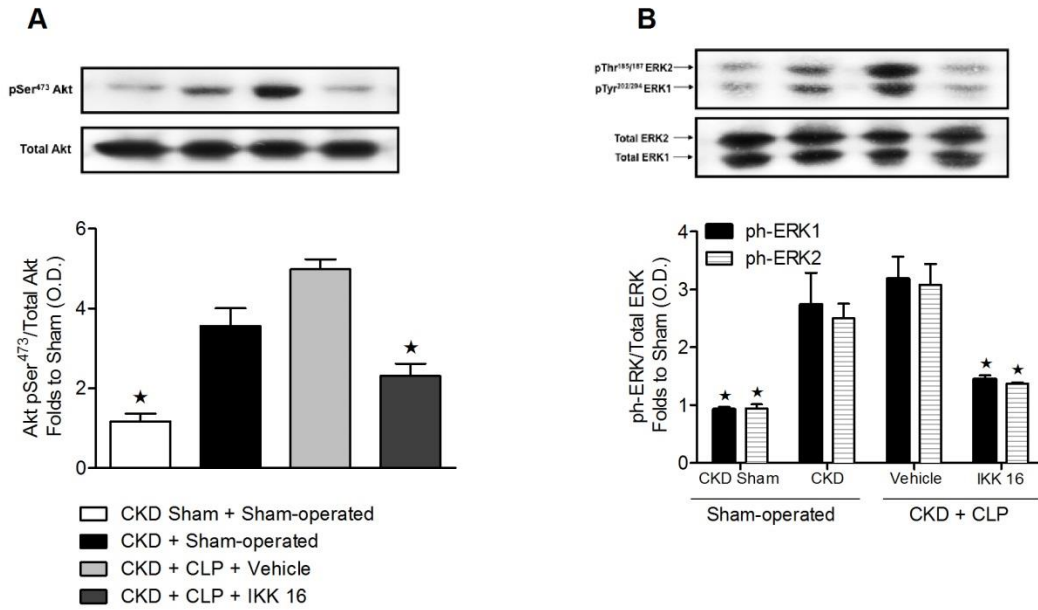## 3.4 Discussion

The presence of cardiac dysfunction in septic patients has been linked to a significantly raised mortality rate [16]. Patients with CKD also have a significantly higher risk of death followed by sepsis [363, 373], however, the reasons for this higher risk is unclear. The current study was designed to elucidate whether pre-existing CKD worsens cardiac performance in mice with sepsis, to identify (some of) the molecular mechanisms responsible in order to target/test new therapeutic interventions in order to reduce cardiac dysfunction in mice with CKD and sepsis.

In mice with SNX for 8 weeks (without sepsis), I found a small, but significant, impairment in systolic function (EF) and cardiac hypertrophy. This result is consistent with a previous study revealing the presence of impaired cardiac function, indicated by a reduced %FS in SNX-induced mouse model of CKD [374]. Indeed, systolic dysfunction, cardiac hypertrophy and left ventricular dilation are present in patients with end-stage renal disease, and only 16% of new dialysis patients present with normal cardiac findings on echocardiography [375, 376]. These structural and functional alterations may contribute to the increased risk of cardiac death in patients with renal failure [205, 376].

Notably, we report here for the first time that the presence of CKD increases the severity of LPS-induced cardiac dysfunction, using a "two-hit" animal model that consists of pre-existing CKD followed by LPS injection. This is in agreement with the clinical findings that the pre-existing CKD worsens outcome in patients with infection or sepsis [245, 377]. We have recently reported that CLP-sepsis does not cause a significant cardiac (and indeed multiple organ) dysfunction in young mice, when these animals are treated with fluids and antibiotics, while older animals (8 month-old) do develop cardiac (multiple organ) dysfunction despite fluid resuscitation and antibiotics [316, 317]. We demonstrate here that young mice with CKD do develop a profound cardiac (systolic) dysfunction in response to CLP, which is similar to the cardiac dysfunction in aged mice with CLP. Like CKD, ageing is associated with a mild systemic inflammation, characterised by elevated plasma concentrations of IL-6, IL-1β and TNF [378]; this pro-inflammatory phenotype in ageing (or CKD) may be secondary to a) the observed activation of NF-κB, which is one of the signatures of ageing [378]; b) impaired excretion of cytokines by the kidneys due to decreased

renal function (due to reduced number of functional glomeruli and lower glomerular filtration rate) [379].

NF-κB is one of the most important pro-inflammatory transcription factors, consisting of heterodimer-subunits p50 and p65 [338]. CKD caused cardiac phosphorylation of Ser$^{176/180}$ on IKKα/β, indicating IKK activation, which in turn led to phosphorylation of IκBα and activation of NF-κB. Additionally, phosphorylation of IκBα, and the subsequent activation of NF-κB, can be induced by the exposure to pro-inflammatory cytokines, such as IL-1β [380]. Accordingly, plasma IL-1β and KC levels were increased in CKD mice, paralleled by the increased cardiac phosphorylation of IκBα. The cardiac activation of NF-κB in CKD mice may also be attributable to the potential hypertensive state (indicated by the presence of myocardial hypertrophy); this assumption is strengthened by a study showing that NF-κB is significantly activated in rat cardiomyocytes subjected to cyclic mechanical stretch, which mimics some aspects of the pathophysiological changes associated with hypertension in cardiac myocytes [381]. It is possible that the activation of NF-κB has (at least in part) contributed to the cardiomyopathy through induction of expression of its target gene iNOS. Cardiac activation of NF-κB and the subsequent iNOS expression contribute to both sepsis-related hypotension and impaired left ventricular function [125, 129, 317]. Indeed, in the present study, nuclear translocation of p65 and iNOS expression were augmented in hearts of CKD mice with sepsis, and this was associated with a worsened cardiac dysfunction. As neither low dose LPS nor CLP had a significant effect on any of the above signalling pathways in mice without CKD, it is likely that the baseline cardiac activation of NF-κB during CKD acts as the prime driver of the observed excessive activation of NF-κB (and expression of NF-κB dependent genes) and the associated cardiac dysfunction in CKD/sepsis.

In addition to inducing iNOS expression, NF-κB activation also leads to a pronounced increase in other pro-inflammatory cytokines [342]. Here we report a dramatic increase in plasma levels of TNF-α, IL-1β, IL-6 and IL-10, in CKD mice with CLP. More than 70% of inflammatory cytokines are excreted by the kidney [212]; and the half-lifes of TNF-α, IL-6 and IL-10 are 2-3-fold prolonged in CKD mice compared with normal mice [212]. Therefore, impaired renal function resulting in a prolonged half-life of cytokines in CKD mice may amplify systemic inflammation, which in turn

may contribute to the excessive cardiac dysfunction in CKD-mice with sepsis [108, 344].

Having found the significant roles of phosphorylation of IKKα/β and the subsequent activation of NF-κB in the augmented cardiac dysfunction induced by sepsis in CKD mice, we have then investigated the role of the selective inhibition of IKK complex *in vivo* in CKD mice that underwent CLP. The treatment protocol for IKK 16 used in the current study reduces systemic inflammation and organ injury in mice with sepsis without CKD [316]. We found for the first time that a single dose of IKK 16 started one hour after CLP attenuated sepsis-induced cardiac dysfunction in CKD mice corresponded to significant attenuated cardiac activation of NF-κB and iNOS expression. Additionally, the systemic inflammatory cytokine levels in CKD mice with CLP were reduced by IKK 16, presumably by inhibiting the production of inflammatory cytokines mediated by NF-κB activation and their release into plasma [364]. The attenuated lung inflammation with IKK 16 treatment in CKD mice with CLP was in line with previous studies, which showed therapeutic benefits of IKK 16 on sepsis-induced lung inflammation in normal mice [316] and on ventilation-induced lung injury [382].

Sustained high levels activation of the PI3K/Akt and the ERK1/2 pathways have been involved in cardiomyocyte growth and the development of cardiac hypertrophy [383]. In the present study, the cardiac phosphorylation of Akt and ERK1/2 may contribute to the CKD-associated cardiac hypertrophy and cardiomyopathy. Similar to our results, the ERK1/2 pathway was also activated in rat hearts with adenine-induced CKD [384]. The activation of Akt and ERK1/2 was not changed by the exposure to septic insults but was reduced by the administration of IKK 16 in septic CKD animals, presumably through the down-regulation of NF-κB activation and the decreased expression of inflammatory cytokines, such as TNF-α [385, 386]. In turn, down-regulated Akt and ERK1/2 phosphorylation may lead to less NF-κB activation, decreasing cytokine production, thus forming a feed-forward mechanism and further reducing the inflammatory reaction [385, 387].

3.4.1 Conclusions

In this chapter, I have discovered that pre-existing CKD augments the cardiac dysfunction caused by sepsis. CKD alone resulted in moderate systemic inflammation and activation of NF-κB (and iNOS expression) in the heart, while sepsis (second hit) in animals with pre-existing CKD resulted in a dramatic rise in a number of pro-inflammatory cytokines (in the plasma) as well as a dramatic increase in the activation of NF-κB (and iNOS expression) in the heart. Most notably, selective inhibition of IKK (by administration of IKK 16 after the onset of sepsis) abolished the systemic inflammation and cardiac dysfunction caused by sepsis in animals with CKD. Thus, inhibition of IKK may be useful to treat the excessive inflammation and systolic cardiac dysfunction associated with sepsis in patients with CKD.

CHAPTER IV | ACTIVATION OF TRPV1 BY 12-(S)-HPETE AND 20-HETE RELEASES CGRP AND PROTECTS THE HEART AGAINST THE CARDIAC DYSFUNCTION CAUSED BY LPS

4.1 Introduction

Recently, TRPV1 has been proposed to exhibit anti-inflammatory properties and protective roles in sepsis [388]. TRPV1 is a non-selective cation channel that is predominantly localised on nociceptive C and Aδ fibers [271, 282]. TRPV1-positive sensory nerves innervate predominantly cardiovascular and renal tissues [389, 390]. TRPV1 can be activated by the chilli extract capsaicin, noxious heat, low pH [283], and multiple endogenous agonists including the arachidonic acid metabolites 12-(S)-HpETE [276] and 20-HETE [277]. Influx of divalent cations (particularly Ca^{2+}) through TRPV1 results in nerve depolarisation and concomitant release of the neuropeptides CGRP, somatostatin and substance P from the sensory nerve terminals [391]. CGRP [295] and somatostatin [392] are anti-inflammatory, while substance P is pro-inflammatory [393].

Both loss- and gain of function studies have revealed a protective role of TRPV1 in the onset of sepsis. In rats challenged with LPS, the TRPV1 antagonist (capsazepine) strongly inhibited the recovery of hypotension and tachycardia, and increased mortality [303]. When challenged with LPS, TRPV1$^{-/-}$ mice exhibited greater hypotension, hypothermia, liver injury [304], renal dysfunction and elevated serum pro-inflammatory cytokine levels [394] than wild-type (WT) mice. Similarly, sepsis-induced by CLP in TRPV1$^{-/-}$ mice also caused enhanced hypotension and significant elevations in plasma markers of liver injury, renal and pancreas dysfunction compared with WT [290]. On the other hand, TRPV1 agonist (capsaicin) improved survival [305] and reduced the systemic inflammatory response in septic rats [306].

However, the identity of the endogenous activators of TRPV1 and the role of the

channel in the cardiac function during sepsis/endotoxaemia is unknown. As cardiovascular tissues are heavily innervated by primary efferent neurons that highly express TRPV1 [389, 390]; and TRPV1 activation improves the outcome in endotoxaemia, I hypothesised that TRPV1 may play a pivotal role in protecting against the endotoxaemia-induced cardiac dysfunction. Therefore, this study (a) investigates the impact of TRPV1 deletion upon the cardiac dysfunction caused by lipopolysaccharide (LPS; endotoxemia), and (b) identifies the endogenous mediators, which trigger TRPV1 in endotoxaemia, and (c) identifies CGRP as the downstream neuropeptide, which mediates the cardioprotection afforded by TRPV1 in endotoxaemia.

4.1.1 Scientific Hypotheses and Aims of the Study Presented in Chapter IV

My project was driven by the hypotheses that:

- TRPV1 activation protects against cardiac dysfunction caused by endotoxaemia

- 12-(S)-HpETE and 20-HETE (potent ligands of TRPV1) and CGRP (downstream mediator of TRPV1) are essential for the cardioprotective effects afforded by TRPV1

My study had the following scientific objectives:

- To study the impact of TRPV1 activation on cardiac function in TRPV1$^{-/-}$ mice and WT mice with endotoxaemia induced by low dose LPS (2 mg/kg)

- To determine the cardiac TRPV1 phosphorylation in WT mice subjected to low dose LPS

- To investigate the effects of 12-(S)-HpETE biosynthesis inhibitor CDC and/or the 20-HETE biosynthesis inhibitor 17ODYA on cardiac function in WT mice subjected to low dose LPS

- To determine plasma CGRP levels in WT mice subjected to low dose LPS

- To investigate the effects of CGRP receptor antagonist CGRP8-37 on cardiac function in WT mice subjected to low dose LPS

4.2 Materials and Methods

4.2.1 Animals

TRVR1 knockout mice (TRPV1$^{-/-}$) [395] on a C57BL/6 background were from Jackson Laboratories (Bar Harbor, ME, USA) and bred in-house. WT littermates and C57BL/6 WT mice purchased from Charles River (Kent, UK) were used as controls. This study was carried out on 9-13 week-old TRPV1$^{-/-}$ (n=13) and WT (n=104) mice, receiving a standard diet and water *ad libitum*. The ethical statement is provided in chapter 2.2.1.

4.2.2 Models of LPS or LPS/PepG co-administration-induced cardiac dysfunction

TRPV1$^{-/-}$ and/or WT mice received low dose LPS (2 mg/kg) in PBS (5 ml/kg) intraperitoneally. Some WT mice received intraperitoneal co-administration of high dose LPS/PepG (LPS; 6 mg/kg and PepG; 0.1 mg/kg). Sham-treated mice received PBS only (Figure 4.1). Mice were randomly allocated into five different groups for investigating LPS-induced cardiac dysfunction in TRPV1$^{-/-}$ mice as indicated in Table 4.1.

At 18 hours post-LPS injection, a clinical score for monitoring the health of experimental mice was used. The detailed score system is described in chapter 2.2.2.
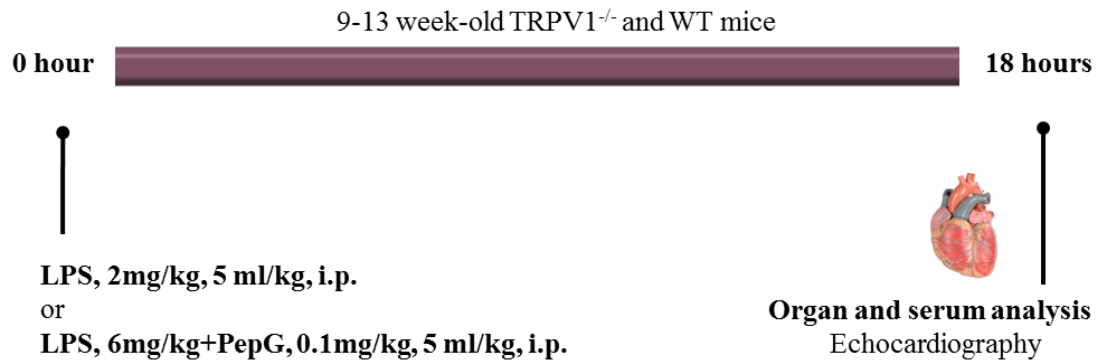
Figure 4.1 Experimental protocol for inducing cardiac dysfunction in TRPV1^{-/-} and WT mice by LPS or LPS/PepG co-administration. Mice received intraperitoneal (i.p.) administration of LPS (2 mg/kg) or LPS/PepG (LPS; 6 mg/kg and PepG; 0.1 mg/kg in PBS; 5 ml/kg i.p.). At 18 h cardiac function was assessed by echocardiography under anaesthesia with isoflurane.

Table 4.1 Experimental groups used to study LPS or LPS/PepG-induced cardiac dysfunction in TRPV1^{-/-} and WT mice.

Group	Number
WT + PBS (5 ml/kg i.p.)	9
TRPV1^{-/-} + PBS (5 ml/kg i.p.)	5
WT + LPS (2 mg/kg i.p.)	8
TRPV1^{-/-} + LPS (2 mg/kg i.p.)	7
WT + LPS (6 mg/kg)/PepG (0.1 mg/kg)	7

4.2.3 Quantification of organ dysfunction/injury

Cardiac function was assessed in mice subjected to LPS at 18 h by echocardiography using a Vevo-770 imaging system (Visual Sonics, Toronto, Canada) [367, 368]. During echocardiography the heart rate was obtained from ECG tracing and the temperature was monitored with a rectal thermometer. Then, the experiment was terminated and blood, hearts and dorsal root ganglions were collected for quantification of organ dysfunction/injury and further analysis. Details are described in chapter 2.2.4 and 2.2.5, and depicted in Figure 2.3, Figure 2.4 and Figure 2.5.

4.2.4 Blockade of 12-(S)-HpETE and 20-HETE biosynthesis

In some experiments, 12-(S)-HpETE biosynthesis was blocked with a potent pharmacological inhibitor of 12-lipoxygenase and to a lesser extend of 15-lipoxygenase [396] (Cinnamyl-3, 4-dihydroxy-a-cyanocinnamate, CDC; Enzo Life Sciences, UK), and 20-HETE biosynthesis was blocked by a specific cytochrome P450 inhibitor [397] (17 octadecynoic acid, 17ODYA; Enzo Life Sciences, UK). WT mice were co-injected with 0.7 mg/mouse 17ODYA and/or 0.2 mg/mouse CDC intraperitoneally together with LPS (2 mg/kg) at 18 h before echocardiography and sample collection (Figure 4.2). WT mice were randomly allocated into four different groups as indicated in Table 4.2.
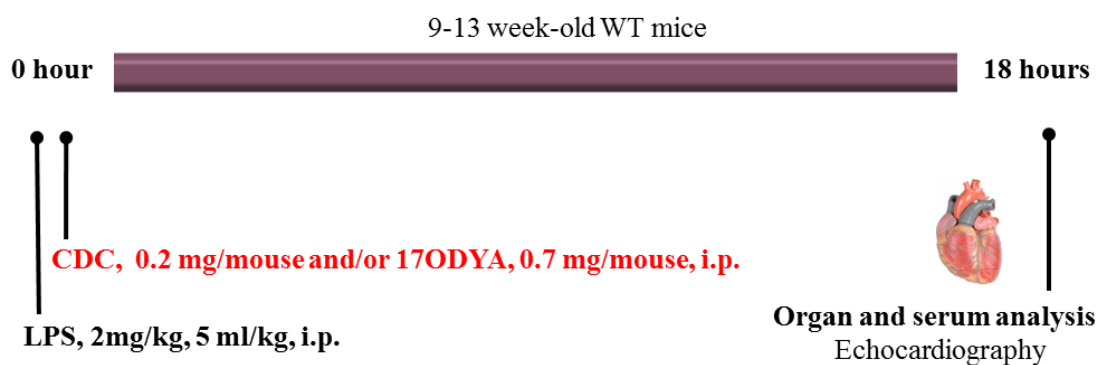
Figure 4.2 Experimental protocol for CDC and/or 17ODYA administration in WT mice with LPS (2 mg/kg) injection. WT mice received either low dose LPS (2 mg/kg i.p.). Together with LPS administration, mice were treated with CDC (a 12-lipoxygenase inhibitor to block 12-(S)-HpETE biosynthesis, 0.2 mg/mouse), 17ODYA (cytochrome P450 inhibitor to block 20-HETE biosynthesis, 0.7 mg/mouse), CDC/17ODYA or vehicle (70% ethanol, 20 μl; i.p.). Cardiac function was analysed at 18 h after LPS injection.

Table 4.2 Experimental groups used to study the effects of CDC and/or 17ODYA on cardiac dysfunction in WT mice with LPS (2 mg/kg) administration.

Group	Number
WT + LPS + Vehicle	5
WT + LPS + CDC (0.2 mg/mouse i.p.)	8
WT + LPS + 17ODYA (0.7 mg/mouse i.p.)	8
WT + LPS + CDC/17ODYA	8

4.2.5 Blockade of CGRP receptor and somatostatin receptor

In some experiments, WT mice were treated intravenously with the CGRP receptor antagonist CGRP8-37 [398] (150 µg/kg, BACHEM, Switzerland), somatostatin receptor antagonist cyclo-somatostatin [399] (C-SOM; 250 µg/kg, BACHEM, Switzerland) or 50 µl PBS as vehicle at 30 min before the administration of LPS (2 mg/kg, i.p.), as well as 1 h and 2 h after LPS injection. Echocardiography was analysed at 18 h after LPS injection (Figure 4.3). WT mice were randomly allocated into three different groups as indicated in Table 4.3.
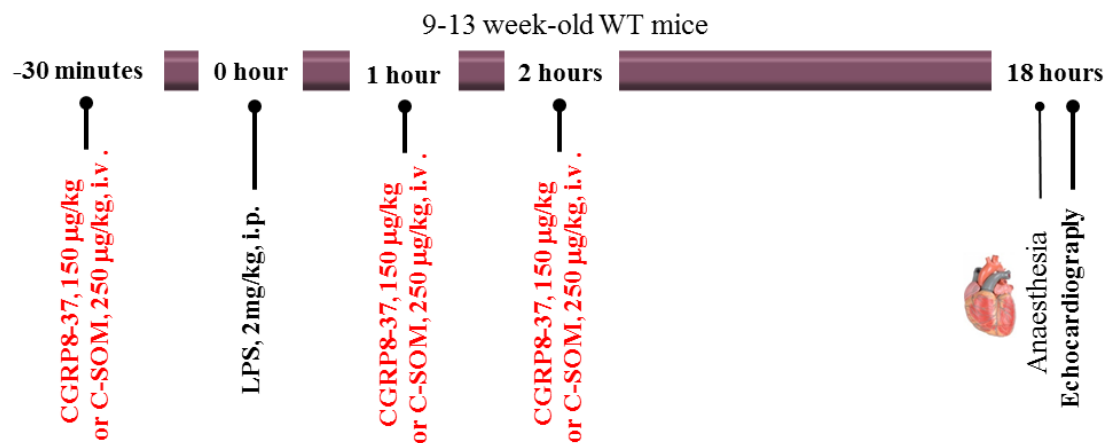
Figure 4.3 Scheme for CGRP8-37 or C-SOM administration in WT mice with LPS (2 mg/kg) injection. WT mice were treated introvenously with CGRP8-37 (CGRP receptor antagonist, 150 µg/kg), C-SOM (somatostatin receptor antagonist, 250 µg/kg), or vehicle (PBS, 50 µl) 30 min before the administration of LPS (2 mg/kg, i.p.), as well as 1 h and 2 h after LPS injection. Cardiac function, body temperature and heart rate were analysed at 18 h after LPS administration.

Table 4.3 Experimental groups used to study the effects of CGRP8-37 or C-SOM on cardiac function in WT mice underwent LPS (2 mg/kg) injection.

Group	Number
WT + LPS + Vehicle	8
WT + LPS + CGRP8-37 (150 µg/kg i.v.)	7
WT + LPS + C-SOM (250 µg/kg i.v.)	7

4.2.6 ELISA

Serum neuropeptide concentrations were assessed using specific ELISA kits following the manufacturer's instruction (CGRP-EIA kit, Cayman Chemical Company, Ann Arbor, MI, USA; substance P- and somatostatin-EIA kits, Phoenix Pharmaceuticals, Inc., Burlingame, CA, USA).

4.2.7 Western blot analysis

Hearts and dorsal root ganglions were processed for protein extraction and immunoblotting as previously described [277]. Due to low protein concentrations obtained from dorsal root ganglions of a single mouse, samples from 3-4 mice were pooled to obtain sufficient protein for immunoblotting. Therefore, analysis of dorsal root ganglions involved a relatively low n-number. TRPV1 and TRPV1 pSer^{800} polyclonal antibodies were from Cosmo Bio Co Ltd. (Japan), and actin monoclonal antibody (C4) was from Millipore (CA, USA). Detection was carried out with horseradish peroxidase-conjugated secondary antibodies (goat anti -rabbit or goat anti-mouse, respectively; Dako, Denmark) and enhanced chemiluminescence detection reagents (Cell Signalling Technology, MA, USA). Intensity of bands were analysed on the software provided with FluorChemE imaging system (Protein Simple, CA, USA). Each group was then adjusted against corresponding sham data to establish relative protein expression when compared with sham animals. Details are described in chapter 2.2.6.

4.2.8 Statistics

Values are presented as mean ± SEM of n observations. Data were assessed by a one-way ANOVA followed by Bonferroni's post hoc test (multiple comparison), unpaired Student's t-test or Mann-Whitney U test using GraphPad Prism 5.0 (GraphPad Software, San Diego, CA, USA). $P<0.05$ was considered to be statistically significant.

4.2.9 Materials

Reagents and compounds were purchased from Sigma Aldrich (Poole, Dorset, UK), unless otherwise stated.

4.3 Results

4.3.1 Low dose LPS (2 mg/kg) administration induces cardiac dysfunction and worsens clinical score in TRPV1 deficient mice

Under basal condition (PBS-treatment), WT and TRPV1$^{-/-}$ mice showed similar levels of cardiac function as measured by % EF, FS, FAC and left ventricular end-diastolic volume (LVEDV), as well as body temperature and heart rate (P>0.05; Figure 4.4A - G). In WT mice, low dose LPS (2 mg/kg) had no effect on % EF, FAC and FS (P>0.05; Figure 4.4A - D). In TRPV1$^{-/-}$ mice, however, low dose LPS induced significant reductions in % EF, FAC and FS (P<0.05; Figure 4.4A - D) indicating the development of a clear and significant cardiac dysfunction. Additionally, TRPV1$^{-/-}$ mice treated with low dose LPS exhibited significant hypothermia (P<0.05; Figure 4.4F), and bradycardia (P<0.05; Figure 4.4G) compared with low dose LPS-treated WT mice. Interestingly, the degrees of systolic dysfunction, hypothermia and bradycardia observed in TRPV1$^{-/-}$ mice challenged with low dose LPS (2 mg/kg) were similar to those in WT mice challenged with high dose LPS (LPS; 6 mg/kg and PepG; 0.1 mg/kg) (P>0.05; Figure 4.4A - D, 4.4F, 4.4G). Additionally, when compared with WT mice subjected to low dose LPS injection, TRPV1$^{-/-}$ yielded worse clinical scores (P<0.05; Figure 4.4H). No significant difference was observed in LVEDV among any of the animal groups studied (P>0.05; Figure 4.4E).

Figure 4.4 TRPV1⁻ᐟ⁻ mice exhibit reduced cardiac function and worse clinical score in endotoxaemia. Cardiac function, body temperature, heart rate and clinical score were analysed at 18 h after either low dose LPS (2 mg/kg), high dose LPS (6 mg/kg)/PepG (0.1 mg/kg) or PBS (5

ml/kg) intraperitoneally administration in WT and TRPV1^{-/-} mice. (**A**) Representative M-mode echocardiograms; percentage (%) (**B**) ejection fraction (EF); (**C**) fractional shortening (FS); (**D**) fractional area change (FAC); (**E**) left ventricular end-diastolic volume (LVEDV); (**F**) body temperature; (**G**) heart rate and (**H**) clinical score: At 18 hours post-LPS, mice were scored for the presence or absence of six different macroscopic signs of sepsis. The following groups were studied: WT + PBS (n=9); TRPV1^{-/-} + PBS (n=5); WT + LPS (2 mg/kg) (n=8); TRPV1^{-/-} + LPS (2 mg/kg) (n=7); WT + LPS (6 mg/kg)/PepG (0.1 mg/kg) (n=7). Panel **B** – **G**: Data are represented as mean ± SEM. ★P < 0.05 versus either PBS-treated groups or WT + LPS (2 mg/kg) group, ¶ P < 0.05 versus WT + LPS (2 mg/kg) group.

4.3.2 Low dose LPS (2 mg/kg) administration increases TRPV1 phosphorylation in heart tissue and dorsal root ganglions (DRGs) in WT mice

To determine that whether the activation of TRPV1 is involved in the protected cardiac function in WT mice with low dose LPS administration, we investigated the effect of low dose LPS on TRPV1 phosphorylation on Ser^{800} in hearts and DRGs (areas of primary TRPV1 expression) in WT mice. When compared with PBS-treated WT mice, low dose LPS significantly increased the phosphorylation of TRPV1 on Ser^{800} both in heart tissue (P<0.05; Figure 4.5A - D) and in DRGs (P<0.05; Figure 4.5E - H), indicating that the protected cardiac function in WT mice is dependent on the TRPV1 activation in hearts and DRGs.

A

PBS   LPS

pSer^{800} TRPV1

Total TRPV1

β-actin

B

Total TRPV1/Actin
Folds to sham (O.D.)

2.5
2.0
1.5
1.0
0.5
0.0

PBS   LPS

C

TRPV1 pSer^{800}/Actin
Folds to sham (O.D.)

2.5
2.0
1.5
1.0
0.5
0.0

★

PBS   LPS

D

TRPV1 pSer^{800}/Total TRPV1
Folds to sham (O.D.)

5.0

2.5

0.0

★

PBS   LPS

E

PBS   LPS

pSer^{800} TRPV1

Total TRPV1

β-actin

F

Total TRPV1/Actin
Folds to sham (O.D.)

0.6

0.4

0.2

0.0

PBS   LPS

G

TRPV1 pSer^{800}/Actin
Folds to sham (O.D.)

0.5
0.4
0.3
0.2
0.1
0.0

PBS   LPS

H

TRPV1 pSer^{800}/Total TRPV1
Folds to sham (O.D.)

2.0

1.5

1.0

0.5

0.0

★

PBS   LPS

Figure 4.5 LPS administration leads to TRPV1 activation in WT mouse heart and DRG. Heart (**A** - **D**) and DRG samples (**E** - **H**) were collected from WT mice at 18 h after LPS (2 mg/kg) or PBS (5 ml/kg i.p.). Total TRPV1, TRPV1 phosphorylation at Ser^{800} and β-actin protein expression were analysed. Panel **A**, **E**: Representative immunoblots of a single experiment of three (heart) or two (DRGs) independent experiments are shown. Each band represents an individual sample. Bands for DRGs represent pooled samples from 3-4 mice each. Panel **B** - **D**, **F** - **H**: Densitometric quantification of TRPV1 protein and phosphorylated protein relative to β-actin (**B**, **C**, **F**, **G**) and phosphorylated TRPV1 protein relative to total TRPV1 protein (**D**, **H**) in hearts

(**B** - **D**) and DRGs (**F** - **H**). Data are expressed as mean ± SEM of n=20 PBS-treated or n=7 LPS-treated mice (hearts) or n=4 pooled samples of 3-4 mice each (DRGs). Panel **B** - **D**: Data were analysed by unpaired Student's t-test. ★*P* < 0.05 versus PBS group. Panel **F** - **H**: Data were analysed by Mann-Whitney *U* test. ★*P* < 0.05 versus PBS group.

4.3.3 Blockade of 12-(S)-HpETE and/or 20-HETE biosynthesis diminishes TRPV1-dependent cardioprotective effects in WT mice challenged with low dose LPS (2 mg/kg)

Previous studies have identified 12-(S)-HpETE [276] and 20-HETE [277] as potent endogenous TRPV1 agonists. To investigate the role of these mediators in triggering the TRPV1-dependent cardioprotective effects in endotoxaemia, WT mice challenged with low dose LPS were co-treated with CDC (a 12-lipoxygenase inhibitor to block 12-(S)-HpETE biosynthesis), 17ODYA (a cytochrome P450 inhibitor to block 20-HETE biosynthesis), or both. When compared with the low dose LPS and drug vehicle-treated WT mice, co-administration of CDC or/and 17ODYA with LPS caused a significant reduction in % EF, FAC and FS (*P*<0.05; Figure 4.6A - D), indicating a further decline in systolic contractility. These data support the view that 12-(S)-HpETE and 20-HETE, as endogenous agonists, trigger TRPV1 activation, which, in turn, protects against the LPS-induced cardiac dysfunction. No significant difference was observed in LVEDV, body temperature or heart rate among any of the different animal groups studied (*P*>0.05; Figure 4.6E - G).
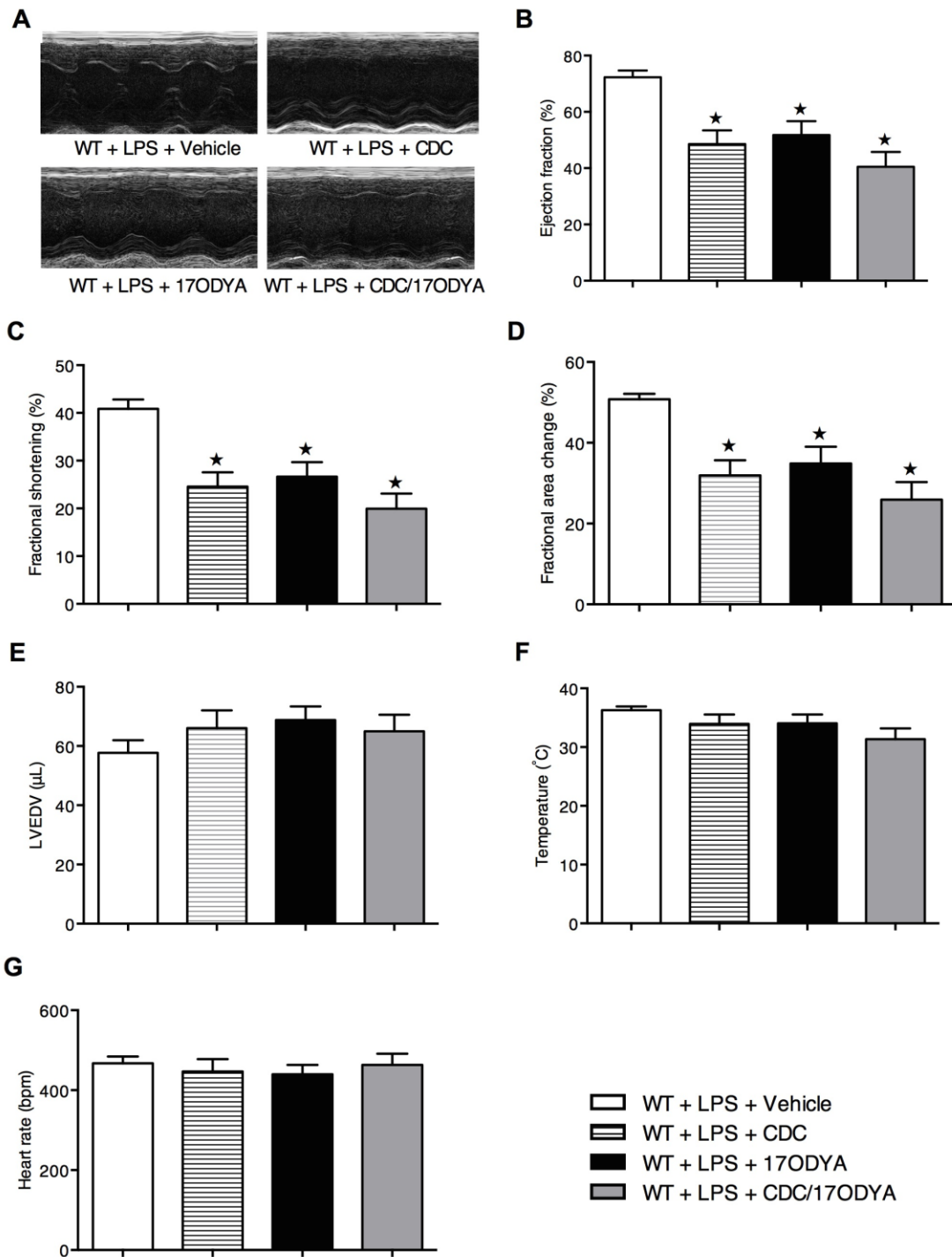
Figure 4.6 Blockade of 12-(S)-HpETE or/and 20-HETE biosynthesis worsens cardiac function in endotoxaemia. WT mice received low dose LPS (2 mg/kg) intraperitoneally. Together with LPS administration, mice were treated with CDC (a 12-lipoxygenase inhibitor to block 12-(S)-HpETE biosynthesis, 0.2 mg/mouse), 17ODYA (cytochrome P450 inhibitor to block 20-HETE biosynthesis, 0.7 mg/mouse), CDC/17ODYA or vehicle (70% ethanol, 20 µl) intraperitoneally. Cardiac function, body temperature and heart rate were analysed at 18 h after LPS injection. (**A**) Representitive M-mode echocardiograms; percentage (%) (**B**) ejection fraction

(EF); (**C**) fractional shortening (FS); (**D**) fractional area change (FAC); (**E**) left ventricular end-diastolic volume (LVEDV); (**F**) body temperature and (**G**) heart rate. The following groups were studied: WT + LPS + Vehicle (n=5); WT + LPS + CDC (n=8); WT + LPS + 17ODYA (n=8); WT + LPS + CDC/17ODYA (n=8). All data are represented as mean ± SEM and were analysed by one-way ANOVA followed by Bonferroni's post hoc test. ★$P < 0.05$ versus WT + LPS + Vehicle group. 12-(S)-HpETE: 12-(S)-hydroperoxyeicosatetraenoic acid; 20-HETE: 20-Hydroxyeicosatetraenoic acid; CDC: cinnamyl-3, 4-dihydroxy-a-cyanocinnamate; 17ODYA: 17 octadecynoic acid.

4.3.4 Plasma CGRP level is up-regulated by low dose LPS (2 mg/kg) administration, but down-regulated by blocking 12-(S)-HpETE and/or 20-HETE biosynthesis in WT mice

Activation of TRPV1 triggers the release of neuropeptides including CGRP, somatostatin and substance P [391]. To gain a better understanding of the mechanism underlying the observed cardioprotective effects of TRPV1 in endotoxemia, we measured the levels of these mediators in endotoxemia. When compared with PBS-treated WT mice, plasma CGRP and substance P levels were increased at 18 hours after low dose LPS injection ($P<0.05$; Figure 4.7A, 4.7E), while plasma somatostatin level was decreased ($P<0.05$; Figure 4.7C). 17ODYA or co-administration of CDC and 17ODYA significantly decreased plasma CGRP and somatostatin levels in low dose LPS-treated WT mice ($P<0.05$; Figure 4.7B, 4.7D); these decreases in plasma CGRP and somatostatin levels were associated with the cardiac dysfunction observed in these mice. CDC treatment resulted in non-significant decreases in plasma CGRP and somatostatin levels ($P>0.05$; Figure 4.7B, 4.7D). Neither 17ODYA nor CDC had any effect on plasma substance P level ($P>0.05$; Figure 4.7F). Notably, low dose LPS injection caused an increase in CGRP level in heart tissues of WT mice ($P<0.05$; Figure 4.7G). These data indicate that CGRP and/or somatostatin as downstream mediators may play a role in the cardioprotection afforded by TRPV1.
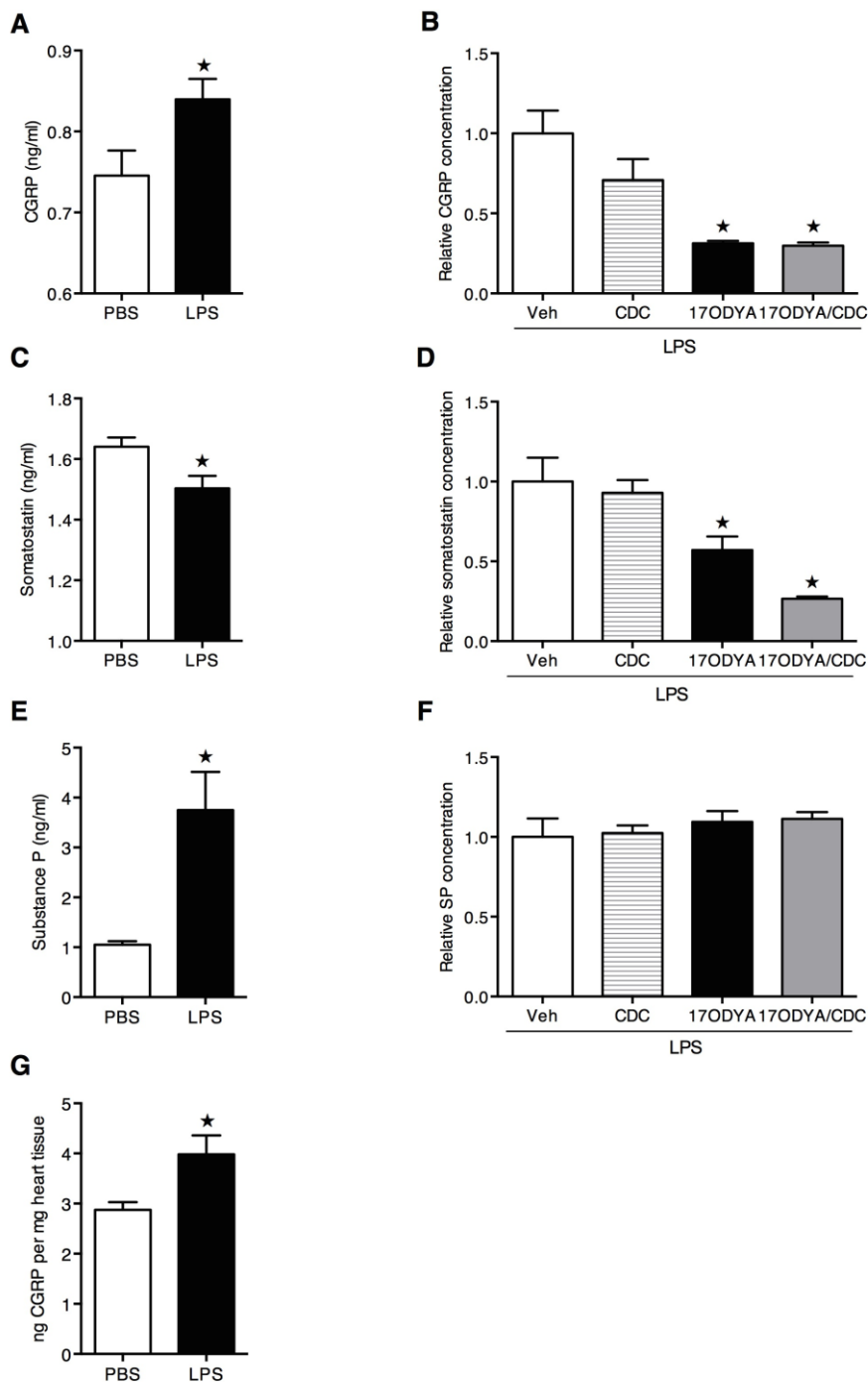
Figure 4.7 Plasma CGRP level is up-regulated after LPS administration, but is down-regulated with 20-HETE and 12-(S)-HpETE inhibition. Plasma samples were collected at 18 hours after LPS administration. Panel **A, C, E, G:** (**A**) Plasma CGRP; (**C**) somatostatin; (**E**) substance P and (**G**) CGRP levels in the heart. WT mice received either low dose LPS (2 mg/kg) or PBS (5 ml/kg) intraperitoneally. The following groups were studied: WT + PBS (n=14); WT + LPS (n=13). Panel **B**, **D**, **F**: (**B**) Plasma CGRP; (**D**) somatostatin and (**F**) substance P. Together with LPS (2 mg/kg) administration, WT mice were treated with CDC (a 12-lipoxygenase inhibitor to block 12(s)-HpETE biosynthesis, 0.2 mg/mouse), 17ODYA (cytochrome P450 inhibitor to block 20-HETE biosynthesis, 0.7 mg/mouse), CDC/17ODYA or vehicle (70%

ethanol, 20 μl) intraperitoneally. The following groups were studied: WT + LPS + Vehicle (n=5); WT + LPS + CDC (n=8); WT + LPS + 17ODYA (n=8); WT + LPS + CDC/17ODYA (n=8). Data are shown as mean ± SEM. Panel **A, C, E, G**: Data were analyzed by unpaired Student's t-test. ★$P < 0.05$ versus PBS group. Panel **B**, **D, F**: Data were analyzed by one-way ANOVA followed by Bonferroni's post hoc test. ★$P < 0.05$ versus WT + LPS + Vehicle group. CGRP: calcitonin gene-related peptide; 12(s)-HpETE: 12-(S)-hydroperoxyeicosatetraenoic acid; 20-HETE: 20-Hydroxyeicosatetraenoic acid; CDC: cinnamyl-3, 4-dihydroxy-a-cyanocinnamate; 17ODYA: 17 octadecynoic acid.

4.3.5 Blockade of CGRP receptor, but not somatostatin receptor, aggravates cardiac dysfunction in WT mice subjected to low dose LPS (2 mg/kg)

To further identity the neuropeptide(s) that contributes to or even mediates the cardioprotective effects of TRPV1, WT mice challenged with low dose LPS were treated with CGRP8-37 (CGRP receptor antagonist) or C-SOM (somatostatin receptor antagonist) at 30 min before and 1 h and 2 h after LPS injection. When compared with the low dose LPS and drug vehicle-treated WT mice, mice subjected to co-administration of CGRP8-37 with LPS demonstrated a significant reduction of % EF, FAC and FS, as well as an increased LVEDV ($P<0.05$; Figure 4.8A - E), indicating impaired systolic contractility and dilated left ventricle, respectively. Administration of C-SOM did not affect % EF, FAC, FS and LVEDV in mice challenged with low dose LPS. These results suggest that CGRP, but not somatostatin, mediates the cardioprotective effects of TRPV1. No significant difference was observed in body temperature or heart rate ($P>0.05$; Figure 4.8F, 4.8G).
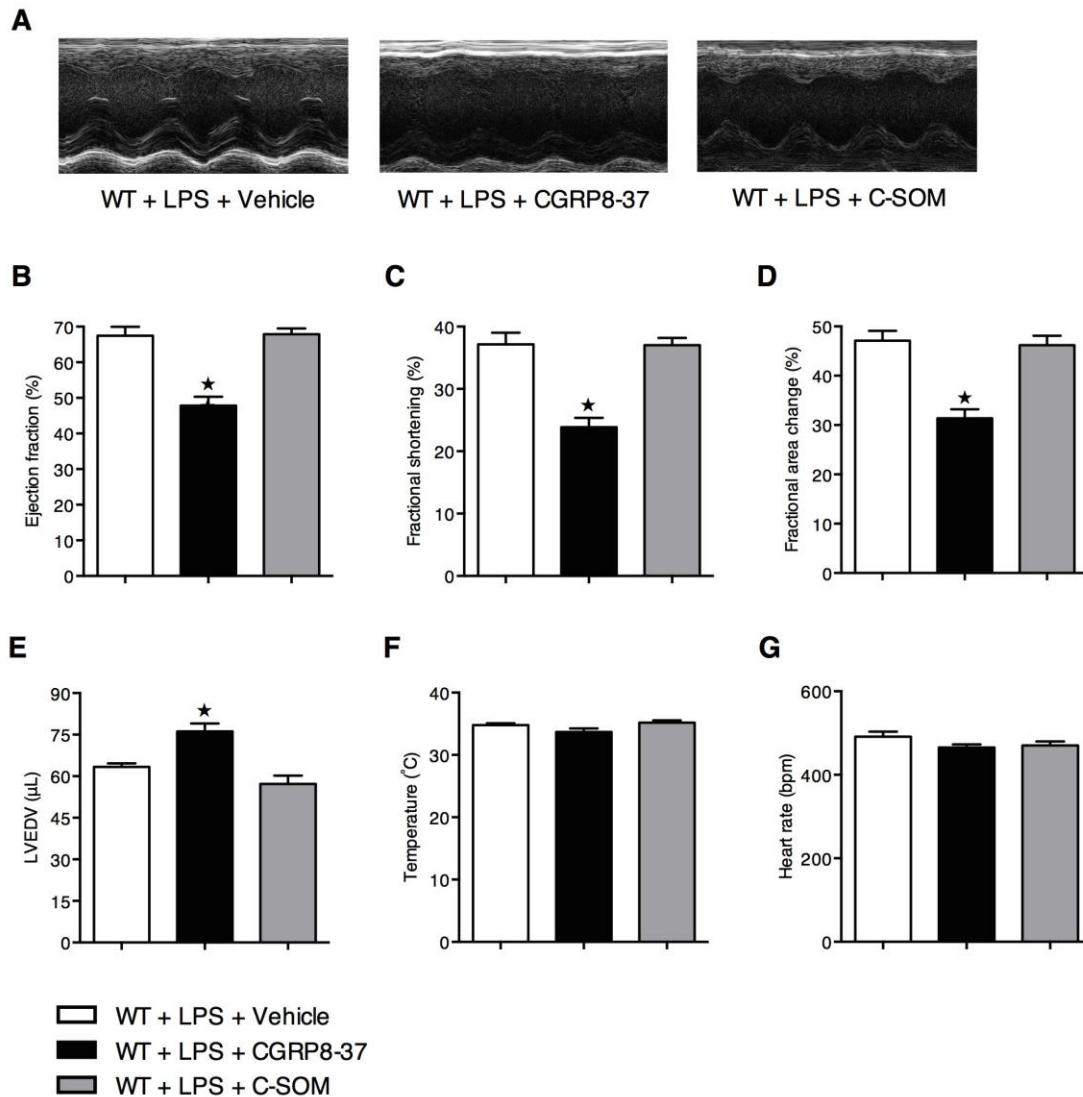
Figure 4.8 Blockade of CGRP receptor, but not somatostatin receptor, aggravates cardiac dysfunction in endotoxaemia. WT mice were treated introvenously with CGRP8-37 (CGRP receptor antagonist, 150 μg/kg), C-SOM (somatostatin receptor antagonist, 250 μg/kg), or vehicle (PBS, 50 μl) 30 min before the administration of LPS (2 mg/kg, i.p.), as well as 1 h and 2 h after LPS injection. Cardiac function, body temperature and heart rate were analysed at 18 h after LPS administration. (**A**) Representitive M-mode echocardiograms; percentage (%) (**B**) ejection fraction (EF); (**C**) fractional shortening (FS); (**D**) fractional area change (FAC); (**E**) left ventricular end-diastolic volume (LVEDV); (**F**) body temperature and (**G**) heart rate. The following groups were studied: WT + LPS + Vehicle (n=8); WT + LPS + CGRP8-37 (n=7); WT + LPS + C-SOM (n=7). All data are represented as mean ± SEM and was analysed by one-way ANOVA followed by Bonferroni's post hoc test. ★$P < 0.05$ versus WT + LPS + Vehicle group. CGRP: calcitonin gene-related peptide; C-SOM: cyclo-somatostatin.

4.4 Discussion

In addition to causing high morbidity and mortality, sepsis is associated with a significant financial burden [400], highlighting the need for improving pharmacological strategies to target specific aspects of the pathophysiology of sepsis. The cardiovascular system is frequently compromised both early and severely during sepsis and always affected in septic shock, and therefore has been studied with regards to this pathology in clinical and basic research for more than 50 years [401]. However, the precise mechanism causing myocardial dysfunction in sepsis/endotoxaemia is still unknown. The present study shows for the first time a protective role of TRPV1 signalling on cardiac function in endotoxaemia (Figure 4.9).
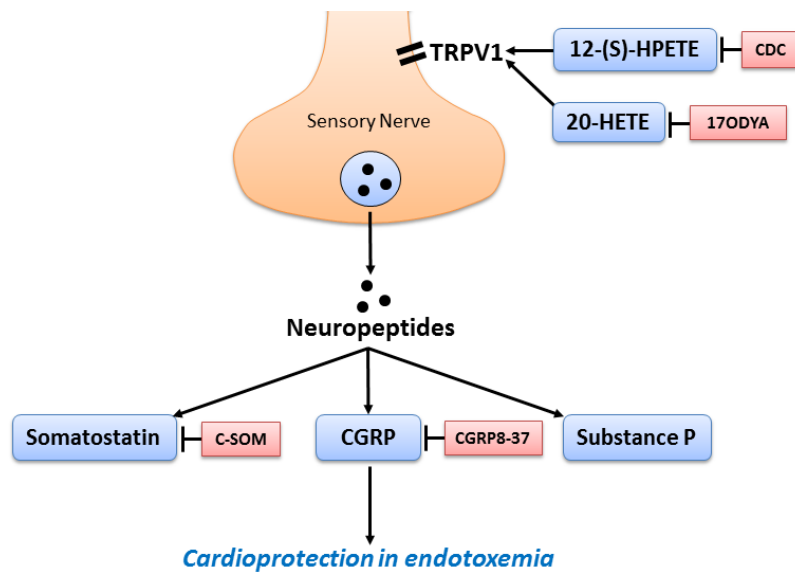
Figure 4.9. TRPV1 signalling modulates cardioprotection in endotoxaemia. Endogenous agonists 12-(S)-HpETE and/or 20-HETE activate TRPV1, leading to the release of downstream neuropeptides, including CGRP, somatostatin and substance P. Blockade of 12-(S)-HpETE, 20-HETE or CGRP increased the susceptibility to LPS-induced cardiac dysfunction. Therefore, cardioprotective effects of TRPV1 in endotoxaemia are dependent on its ligands 12-(S)-HpETE and 20-HETE, as well as the release of CGRP. CDC: 12-(S)-HpETE inhibitor; 17ODYA: 20-HETE inhibitor; C-SOM: somatostatin receptor antagonist; CGRP8-37: CGRP receptor antagonist. Abbreviations: CGRP: calcitonin gene-related peptide; C-SOM: cyclo-somatostatin; 12-(S)-HpETE: 12-(S)-hydroperoxyeicosatetraenoic acid; 20-HETE: 20-Hydroxyeicosatetraenoic acid; CDC: cinnamyl-3, 4-dihydroxy-a-cyanocinnamate; 17ODYA: 17 octadecynoic acid.

In contrast to WT mice, TRPV1$^{-/-}$ animals developed a significant reduction in systolic contractility at 18 h after administration of a relatively low dose of LPS. In addition to impaired systolic contractility, heart rate and body temperature were also reduced in TRPV1$^{-/-}$ mice challenged with low dose LPS. Collectively, these results indicate that the severity of key aspects of the pathophysiology (cardiac performance, temperature regulation) of endotoxaemia are exacerbated in the absence of TRPV1 signalling. Notably, basal levels of all measured parameters were not different in mice lacking TRPV1 receptors as compared to WT animals, indicating that TRPV1-deficiency has no impact on cardiac function under physiological conditions. Studies in humans using echocardiography showed decreased contractility and impaired myocardial compliances in patients with severe sepsis and septic shock [402-404], which is similar to our results observed in TRPV1$^{-/-}$ mice challenged with LPS.

I also discovered increased levels of TRPV1 phosphorylation in heart and dorsal root ganglion biopsies obtained from WT mice subjected to LPS (when compared to control mice). This supports the hypothesis that TRPV1 activation occurs during endotoxaemia. Although previous studies did not investigate the effects of endotoxaemia/sepsis on TRPV1 activation, our results are in line with data showing decreased mortality rates in rats treated with the TRPV1 agonist capsaicin [305].

Deletion or blockade of TRPV1 is associated with reduced organ function in the liver, lung and kidney [304, 394, 399, 405]. To our knowledge, this study provides the first evidence of a cardio-protective role of TRPV1 signalling in endotoxaemia. What then are the endogenous ligands which activate TRPV1 during endotoxaemia? The arachidonic acid metabolites, 20-HETE and 12-(S)-HpETE, are well-known ligands of TRPV1. Indeed, when treated with inhibitors of 12-(S)-HpETE and/or 20-HETE biosynthesis (with CDC and 17ODYA, respectively), mice exhibited similar levels of cardiac dysfunction as observed in TRPV$^{-/-}$ mice. Blocking 20-HETE and 12-(S)-HpETE synthesis simultaneously caused a small additive effect on cardiac dysfunction. Indeed, 12-(S)-HpETE protects the heart against ischaemia or hypoxia [406-408]. 20-HETE and 12-(S)-HpETE are potent vasoactive factors and previous studies from our group showed a close link between TRPV1 and an increase in blood pressure caused by 20-HETE [277]. Increased cardiac output was observed in patients with sepsis, which is believed to play a compensatory role in maintaining blood

pressure in the presence of systemic vasodilation. In contrast, septic patients with contractile dysfunction show a diminished blood pressure response to intravenous fluids and reduced ability to augment cardiac output despite increased levels of circulating catecholamines, an effect that is fully reversible in survivors [409]. By signalling through TRPV1, 20-HETE and 12-(S)-HpETE might participate in the regulation of blood pressure in endotoxaemia. Indeed, previous studies demonstrated that deletion or blockade of TRPV1 exacerbates/prolongs hypotension in sepsis/endotoxaemia [303, 304]. TRPV1 is a polymodal receptor and hence might be activated by multiple stimuli. An acidic extracellular milieu, which develops in sepsis/endotoxaemia might further potentiate ligand-evoked channel gating.

In addition, we demonstrated that plasma CGRP levels are increased in WT mice with LPS administration. CGRP is a vasodilator and downstream mediator of TRPV1 with important roles in the physiological function and homeostatic maintenance of the cardiovascular system. Thus, CGRP might play a role in mediating TRPV1-dendent effect on cardiac function in endotoxaemia. Indeed, mice treated with CGRP receptor antagonist (CGRP8-37) exhibited an increased susceptibility to cardiac dysfunction induced by LPS. In line with our study, pre-treatment of synthetic CGRP reduces TNF-α and KC generation, and indirectly attenuates neutrophils recruitment induced by LPS injection in mice, which is reverted by the co-administration with CGRP8-37 [295]. *In vitro* studies suggest that CGRP inhibits TLR-stimulated production of inflammatory mediators, such as TNF-α, by dendritic cells [296], and inhibits release of TNF-α from macrophages [295]. Interestingly, inflammatory responses in liver induced by ischaemia/reperfusion are exaggerated in CGRP^{-/-} mice [410]. Elevated levels in C-fibre-derived neuropeptides, including CGRP have been suggested also to limit tissue damage during myocardial infarction [411] and both TRPV1 and CGRP levels are reduced in diabetes mellitus patients, a disease associated with impaired recovery of mice hearts following global ischaemia [412].

4.4.1 Conclusions

In this chapter, I showed for the first time that activation of TRPV1 by 12-(S)-HpETE and 20-HETE leads to the release of CGRP, which protects the heart against the cardiac dysfunction caused by LPS. Therefore, we propose the TRPV1 signalling pathway as a potential pharmaceutical target in patients with sepsis/endotoxaemia to improve the outcome of these patients by maintaining cardiac function.

CHAPTER V | CONCLUDING REMARKS AND FUTURE DIRECTIONS

Sepsis is the leading cause of death in non-coronary intensive care units [307] and among the top 10 causes of death in the United States [413]. One in two patients with sepsis develop cardiac dysfunction [309], and the presence of cardiac dysfunction increases the mortality rate from 40% to 70% [16]. Several inflammatory mediators including cytokines, nitric oxide and factors of the coagulation cascade are associated with cardiac dysfunction in sepsis, however, clinical studies targeting these factors were overall disappointing and the survival of patients remains poor [22, 401, 414]. This thesis had the overall aim to (i) investigate the pathophysiology of the cardiac dysfunction in sepsis and (ii) to identify novel therapeutic approaches for improving sepsis-associated cardiac dysfunction in preclinical models of sepsis.

One potential reason for the lack of translatability of preclinical findings (e.g. efficacy of new interventions) to patients with sepsis is that animal models of sepsis do not sufficiently mimic human sepsis. Laboratory animals may often be inbred strains, and are young, healthy and (often) male animals, and most importantly, do not have comorbidities. However, a cohort of patients with sepsis has a great degree of heterogeneity: Patients are often older and of either gender, they frequently have a prior insult (trauma, burns), pre-existing medication or immunosuppression, and very frequently co-morbidities including diabetes, hypertension and CKD [11, 307, 355, 356].

Currently there is no single animal model of sepsis which mimics all components of human sepsis, but rather a number of animal models which recapitulate some individual aspects of human sepsis and the various animal models complement each other. In this thesis, two different and complementary animal models of sepsis have been established and used to study both pathophysiology and novel therapies for sepsis-associated cardiac dysfunction.

In chapter II and III, a clinically relevant model of polymicrobial sepsis caused by CLP was established in both male and female mice. In this CLP protocol, antibiotic therapy and fluid-resuscitation was given both at 6 h and 18 h after the surgery, which

recapitulates some aspects of the clinical, supportive interventions in septic patients (outlined in chapter I). In young mice, CLP-sepsis with both antibiotic therapy and fluid-resuscitation did not cause cardiac dysfunction (chapter III), but in older mice (8-month-old), it caused a significant cardiac dysfunction (chapter II) indicating that the degree of cardiac dysfunction caused by CLP is age-dependent. In chapter II, a model of systemic hyper-inflammation, which was induced by co-administration of LPS (Gram-negative bacterial cell wall component) and PepG (Gram-positive bacterial cell wall component), was established in both male and female mice. LPS triggers a systemic inflammatory response by activating TLR4 and TLR2, while PepG targets TLR2 and NOD receptors. NODs synergise with TLRs to augment the inflammatory response [43, 66], through which a stable and reproducible hyper-inflammation model can be obtained. In chapter III, I developed a "two-hit" animal model that consists of pre-existing CKD (secondary to 5/6th nephrectomy) followed by LPS injection or CLP surgery, with the aim to study whether a pre-existing renal dysfunction affects the severity of sepsis-associated cardiac dysfunction, and also to test new therapeutic interventions in order to reduce cardiac dysfunction in mice with CKD/sepsis.

In chapter II, apart from successfully establishing the experimental model, my results show for the first time a gender dimorphism in the cardiac dysfunction induced *in vivo* by either co-administration of LPS/PepG (in young mice) or by polymicrobial sepsis caused by CLP (in middle-aged mice). Female mice had less cardiac dysfunction than male mice in both experimental settings. These findings suggest that the observed protection of female hearts against the dysfunction caused by systemic inflammation and sepsis is associated with (and may well be secondary to) the activation in the heart of the well-known Akt/eNOS survival pathway, the inhibition of inflammatory signalling via NF-κB/iNOS, as well the reduction in cardiac inflammatory cytokine production. Interestingly, a gender dimorphism in the cardiac dysfunction to sepsis was not observed when a strong inflammatory stimulus (high dose of LPS/PepG) was used.

In both pre-clinical and clinical studies, different responses among genders have been found in sepsis, and females have a better outcome than males, which may be attributable to sex steroid-associated immunologic advantages in females. Oestrogen

protects against the cardiac dysfunction that occurs in response to a number of insults, such as trauma-haemorrhage and ischaemia/reperfusion injury. Therefore, characterisation of gender dimorphism in sepsis-induced cardiac dysfunction will hopefully enable the development of individualised and sex-based treatment strategies in male and female patients with sepsis. Future studies are warranted to test this hypothesis, e.g. by evaluating whether oestrogen does indeed improve cardiac function and outcome in patients with sepsis. Issues such as adverse effects of hormone therapy should also be addressed before its translation to clinical settings.

Having established animal models of hyper-inflammation and sepsis, I aimed in chapter III to elucidate the impact of the pre-existing CKD on sepsis-associated cardiac dysfunction. Infection and sepsis in CKD patients are one of the major causes of their hospitalisation and death [245]. Moreover, patients with CKD have a significantly higher mortality when developing sepsis [363, 373], however, the reasons for this higher risk is unclear.

The results in chapter III showed for the first time that pre-existing CKD augments the cardiac dysfunction caused by sepsis. CKD alone resulted in moderate systemic inflammation and activation of NF-κB (and iNOS expression) in the heart, while sepsis (second hit) in animals with pre-existing CKD resulted in a dramatic rise in a number of pro-inflammatory cytokines (in the plasma) as well as a dramatic increase in the activation of NF-κB (and iNOS expression) in the heart. Most notably, selective inhibition of IKK (by administration of IKK 16 at 1 h after the onset of CLP-sepsis) abolished the cardiac dysfunction caused by sepsis in animals with CKD; this attenuated cardiac dysfunction was associated with (or secondary to) the decreases in the cardiac activation of NF-κB (and iNOS expression) and the systemic inflammation caused by CLP in the CKD mice. Therefore, inhibition of IKK may be useful to treat the excessive inflammation and systolic cardiac dysfunction associated with sepsis in patients with CKD.

In addition to the heterogeneity of the patient population, another important reason for the failed translation from preclinical findings to bedside might be that the interventions are normally given relatively late in patients with sepsis. Many other experimental approaches with therapeutic effects also inhibit the activation of NF-κB, however, most of these interventions have to be given at the very early phase of

sepsis, thus, are unlikely to be suitable for clinical settings where the interventions are often relatively late. The treatment protocol of IKK16 used in this study may be translatable to clinical settings in CKD patients followed by sepsis, with a relatively low dose of IKK 16, administrated intravenously at one hour after the induction of polymicrobial sepsis (although this time point is still relatively early in the pathophysiology). Targeting the IKK complex has the advantage that it might still be effective even when achieved relatively late in the course of sepsis, as it inhibits one of the final steps leading to the activation of NF-κB. However, further studies are needed to investigate how late after the onset of sepsis the administration of IKK16 can still improve outcome (e.g. cardiac systolic function, cardiac damage markers, neutrophils recruitment to heart tissues and mortality rate) of the CKD animals. Additionally, more experiments are needed to evaluate the safety of IKK16 (e.g. liver toxicity) in CKD animals.

Anti-inflammatory properties and protective roles of TRPV1 activation in sepsis have recently emerged [388]. The results presented in chapter IV highlight, for the first time, that the activation of TRPV1 helps to maintain cardiac function in endotoxaemia. The main findings outlined in chapter IV are that TRPV1 phosphorylation was increased in the heart in WT mice subjected to low dose LPS (2 mg/kg) injection. Low dose LPS did not affect the cardiac function in WT mice, but caused a significant reduction in EF in TRPV1$^{-/-}$ mice, which was similar to the degree of cardiac dysfunction caused by high dose LPS (6 mg/kg) plus PepG (0.1 mg/kg) in WT mice. The 12-(S)-HpETE inhibitor CDC or the 20-HETE inhibitor 17ODYA augmented the cardiac dysfunction caused by LPS (2 mg/kg) in WT mice. LPS (2 mg/kg) caused significant increases in plasma CGRP levels in WT mice; and this effect was significantly attenuated by either 17ODYA or co-administration of CDC together with 17ODYA. The CGRP-receptor antagonist CGRP8-37 increased the cardiac dysfunction induced by LPS (2 mg/kg), suggesting that the release of endogenous CGRP mediates the cardioprotective action of TRPV1. Western blot analysis confirmed activation of TRPV1 with low dose LPS treatment in WT mice with increased expression of phosphorylated TRPV1 relative to total TRPV1 relative to vehicle control, reflecting increased TRPV1 activation.

TRPV1 has been shown to regulate vascular tone, inhibit neutrophil activation,

oxidative stress, cardiac TNF production and preservation of endothelial function [388]. In chapter IV, we showed for the first time that activation of TRPV1 by 12-(S)-HpETE and 20-HETE leads to the release of CGRP, which protects the heart against the cardiac dysfunction caused by LPS. Therefore, I propose the TRPV1 signalling pathway as a potential pharmaceutical target in patients with sepsis/endotoxaemia and that activation of TRPV1 may improve the outcome of these patients by maintaining cardiac function. To further elucidate the protective roles of TRPV1/CGRP, more experimental studies are needed to investigate whether delayed treatment of septic animals with CGRP improves sepsis-associated cardiac dysfunction in both hyper-inflammation model induced by co-administration of LPS and PepG, and the polymicrobial sepsis induced by CLP.

Hypothermia was observed in both polymicrobial sepsis model and endotoxaemia model, which recapitulates the clinical aspect that critically ill patients with endotoxaemia/sepsis often experience hypothermia [415]. The hypothermia in septic mice may be caused by reduced peripheral vascular resistance and redistribution of body heat from core tissues to periphery tissues [416]. The altered tissue perfusion in the gut is more evident than that in skin and skeletal muscles during septic shock [417]. Hypothermia in septic animals may contribute to decreased heart rate and cardiac conduction, which in turn lead to reduced cardiac output and tissue perfusion [418]. However, it should be noted that minimising the potential variant, body temperature, by heating or cooling the septic mice externally might change the pro- and anti-inflammatory pathways [415, 419]. Therefore, in current studies, no procedure was carried out to change the body temperature of the septic mice.

CHAPTER VI | REFERENCES

1.	Geroulanos, S. and E.T. Douka, *Historical perspective of the word "sepsis".* Intensive Care Med, 2006. **32**(12): p. 2077.
2.	Ewald, P.W., *Evolution of virulence.* Infect Dis Clin North Am, 2004. **18**(1): p. 1-15.
3.	Vincent, J.L., *Clinical sepsis and septic shock--definition, diagnosis and management principles.* Langenbecks Arch Surg, 2008. **393**(6): p. 817-24.
4.	Strieter, R.M., et al., *Host responses in mediating sepsis and adult respiratory distress syndrome.* Semin Respir Infect, 1990. **5**(3): p. 233-47.
5.	Bone, R.C., et al., *Definitions for sepsis and organ failure and guidelines for the use of innovative therapies in sepsis. The ACCP/SCCM Consensus Conference Committee. American College of Chest Physicians/Society of Critical Care Medicine.* Chest, 1992. **101**(6): p. 1644-55.
6.	Levy, M.M., et al., *2001 SCCM/ESICM/ACCP/ATS/SIS International Sepsis Definitions Conference.* Crit Care Med, 2003. **31**(4): p. 1250-6.
7.	Vincent, J.L., et al., *Use of the SOFA score to assess the incidence of organ dysfunction/failure in intensive care units: results of a multicenter, prospective study. Working group on "sepsis-related problems" of the European Society of Intensive Care Medicine.* Crit Care Med, 1998. **26**(11): p. 1793-800.
8.	Padkin, A., et al., *Epidemiology of severe sepsis occurring in the first 24 hrs in intensive care units in England, Wales, and Northern Ireland.* Critical care medicine, 2003. **31**(9): p. 2332-8.
9.	Harrison, D.A., C.A. Welch, and J.M. Eddleston, *The epidemiology of severe sepsis in England, Wales and Northern Ireland, 1996 to 2004: secondary analysis of a high quality clinical database, the ICNARC Case Mix Programme Database.* Crit Care, 2006. **10**(2): p. R42.
10.	Angus, D.C., et al., *Epidemiology of severe sepsis in the United States: analysis of incidence, outcome, and associated costs of care.* Critical care medicine, 2001. **29**(7): p. 1303-10.
11.	Martin, G.S., et al., *The epidemiology of sepsis in the United States from 1979 through 2000.* N Engl J Med, 2003. **348**(16): p. 1546-54.
12.	Vincent, J.L., et al., *Sepsis in European intensive care units: results of the SOAP study.* Crit Care Med, 2006. **34**(2): p. 344-53.
13.	Annane, D., et al., *Current epidemiology of septic shock: the CUB-Rea Network.* Am J Respir Crit Care Med, 2003. **168**(2): p. 165-72.
14.	Silva, E., et al., *Brazilian Sepsis Epidemiological Study (BASES study).* Crit Care, 2004. **8**(4): p. R251-60.
15.	Mayr, F.B., S. Yende, and D.C. Angus, *Epidemiology of severe sepsis.* Virulence, 2014. **5**(1): p. 4-11.
16.	Blanco, J., et al., *Incidence, organ dysfunction and mortality in severe sepsis: a Spanish multicentre study.* Crit Care, 2008. **12**(6): p. R158.
17.	Danai, P.A., et al., *The epidemiology of sepsis in patients with malignancy.* Chest, 2006. **129**(6): p. 1432-40.
18.	Esper, A.M., et al., *The role of infection and comorbidity: Factors that influence disparities in sepsis.* Crit Care Med, 2006. **34**(10): p. 2576-82.
19.	Angus, D.C., C.A. Pereira, and E. Silva, *Epidemiology of severe sepsis around the world.* Endocr Metab Immune Disord Drug Targets, 2006. **6**(2): p. 207-12.
20.	Linde-Zwirble, W.T. and D.C. Angus, *Severe sepsis epidemiology: sampling, selection, and society.* Crit Care, 2004. **8**(4): p. 222-6.
21.	Dellinger, R.P., et al., *Surviving Sepsis Campaign guidelines for management of severe sepsis and septic shock.* Crit Care Med, 2004. **32**(3): p. 858-73.
22.	Dellinger, R.P., et al., *Surviving Sepsis Campaign: international guidelines for management of severe sepsis and septic shock: 2008.* Intensive Care Med, 2008. **34**(1): p. 17-60.
23.	Dellinger, R.P., et al., *Surviving Sepsis Campaign: International Guidelines for Management of Severe Sepsis and Septic Shock, 2012.* Intensive Care Medicine, 2013. **39**(2): p. 165-228.
24.	Levy, M.M., et al., *The Surviving Sepsis Campaign: results of an international guideline-based performance improvement program targeting severe sepsis.* Crit Care Med, 2010.

38(2): p. 367-74.

25.   Ferrer, R., et al., *Improvement in process of care and outcome after a multicenter severe sepsis educational program in Spain.* JAMA, 2008. **299**(19): p. 2294-303.

26.   Bernard, G.R., et al., *Efficacy and safety of recombinant human activated protein C for severe sepsis.* N Engl J Med, 2001. **344**(10): p. 699-709.

27.   Abraham, E., et al., *Drotrecogin alfa (activated) for adults with severe sepsis and a low risk of death.* N Engl J Med, 2005. **353**(13): p. 1332-41.

28.   Hotchkiss, R.S., G. Monneret, and D. Payen, *Immunosuppression in sepsis: a novel understanding of the disorder and a new therapeutic approach.* Lancet Infect Dis, 2013. **13**(3): p. 260-8.

29.   Kopterides, P. and M.E. Falagas, *Statins for sepsis: a critical and updated review.* Clinical microbiology and infection : the official publication of the European Society of Clinical Microbiology and Infectious Diseases, 2009. **15**(4): p. 325-34.

30.   Buerke, U., et al., *Apoptosis contributes to septic cardiomyopathy and is improved by simvastatin therapy.* Shock, 2008. **29**(4): p. 497-503.

31.   Eisen, D.P., D. Reid, and E.S. McBryde, *Acetyl salicylic acid usage and mortality in critically ill patients with the systemic inflammatory response syndrome and sepsis.* Critical care medicine, 2012. **40**(6): p. 1761-7.

32.   Vincent, J.L., et al., *International study of the prevalence and outcomes of infection in intensive care units.* JAMA, 2009. **302**(21): p. 2323-9.

33.   Cohen, J., et al., *New method of classifying infections in critically ill patients.* Crit Care Med, 2004. **32**(7): p. 1510-26.

34.   Janeway, C.A., Jr. and R. Medzhitov, *Innate immune recognition.* Annu Rev Immunol, 2002. **20**: p. 197-216.

35.   Rietschel, E.T. and H. Brade, *Bacterial endotoxins.* Sci Am, 1992. **267**(2): p. 54-61.

36.   Majcherczyk, P.A., et al., *Digestion of Streptococcus pneumoniae cell walls with its major peptidoglycan hydrolase releases branched stem peptides carrying proinflammatory activity.* J Biol Chem, 1999. **274**(18): p. 12537-43.

37.   Morath, S., A. Geyer, and T. Hartung, *Structure-function relationship of cytokine induction by lipoteichoic acid from Staphylococcus aureus.* J Exp Med, 2001. **193**(3): p. 393-7.

38.   Annane, D., E. Bellissant, and J.M. Cavaillon, *Septic shock.* Lancet, 2005. **365**(9453): p. 63-78.

39.   De Kimpe, S.J., et al., *The cell wall components peptidoglycan and lipoteichoic acid from Staphylococcus aureus act in synergy to cause shock and multiple organ failure.* Proc Natl Acad Sci U S A, 1995. **92**(22): p. 10359-63.

40.   Fraser, J.D. and T. Proft, *The bacterial superantigen and superantigen-like proteins.* Immunol Rev, 2008. **225**: p. 226-43.

41.   Kumar, H., T. Kawai, and S. Akira, *Pathogen recognition by the innate immune system.* Int Rev Immunol, 2011. **30**(1): p. 16-34.

42.   Kumar, S., et al., *Recognition of bacterial infection by innate immune sensors.* Crit Rev Microbiol, 2013. **39**(3): p. 229-46.

43.   Takeuchi, O. and S. Akira, *Pattern recognition receptors and inflammation.* Cell, 2010. **140**(6): p. 805-20.

44.   Franchi, L., et al., *Function of Nod-like receptors in microbial recognition and host defense.* Immunol Rev, 2009. **227**(1): p. 106-28.

45.   Medzhitov, R., *TLR-mediated innate immune recognition.* Semin Immunol, 2007. **19**(1): p. 1-2.

46.   Ranjan, P., et al., *Cytoplasmic nucleic acid sensors in antiviral immunity.* Trends Mol Med, 2009. **15**(8): p. 359-68.

47.   Figdor, C.G., Y. van Kooyk, and G.J. Adema, *C-type lectin receptors on dendritic cells and Langerhans cells.* Nat Rev Immunol, 2002. **2**(2): p. 77-84.

48.   Netea, M.G. and J.W. van der Meer, *Immunodeficiency and genetic defects of pattern-recognition receptors.* N Engl J Med, 2011. **364**(1): p. 60-70.

49.   Kawai, T. and S. Akira, *Toll-like receptors and their crosstalk with other innate receptors in infection and immunity.* Immunity, 2011. **34**(5): p. 637-50.

50.   Chuenchor, W., et al., *Structures of pattern recognition receptors reveal molecular mechanisms of autoinhibition, ligand recognition and oligomerization.* Curr Opin Immunol, 2014. **26**: p. 14-20.

51.   Anderson, K.V., L. Bokla, and C. Nusslein-Volhard, *Establishment of dorsal-ventral polarity*

in the Drosophila embryo: the induction of polarity by the Toll gene product. Cell, 1985. **42**(3): p. 791-8.

52. Lemaitre, B., et al., *The dorsoventral regulatory gene cassette spatzle/Toll/cactus controls the potent antifungal response in Drosophila adults.* Cell, 1996. **86**(6): p. 973-83.

53. Bowie, A., et al., *A46R and A52R from vaccinia virus are antagonists of host IL-1 and toll-like receptor signaling.* Proc Natl Acad Sci U S A, 2000. **97**(18): p. 10162-7.

54. Suresh, R. and D.M. Mosser, *Pattern recognition receptors in innate immunity, host defense, and immunopathology.* Adv Physiol Educ, 2013. **37**(4): p. 284-91.

55. Poltorak, A., et al., *Defective LPS signaling in C3H/HeJ and C57BL/10ScCr mice: mutations in Tlr4 gene.* Science, 1998. **282**(5396): p. 2085-8.

56. Shimazu, R., et al., *MD-2, a molecule that confers lipopolysaccharide responsiveness on Toll-like receptor 4.* J Exp Med, 1999. **189**(11): p. 1777-82.

57. Kawagoe, T., et al., *Sequential control of Toll-like receptor-dependent responses by IRAK1 and IRAK2.* Nat Immunol, 2008. **9**(6): p. 684-91.

58. Lim, K.H. and L.M. Staudt, *Toll-like receptor signaling.* Cold Spring Harb Perspect Biol, 2013. **5**(1): p. a011247.

59. Ting, J.P., et al., *The NLR gene family: a standard nomenclature.* Immunity, 2008. **28**(3): p. 285-7.

60. Sutterwala, F.S., Y. Ogura, and R.A. Flavell, *The inflammasome in pathogen recognition and inflammation.* J Leukoc Biol, 2007. **82**(2): p. 259-64.

61. Ogura, Y., et al., *Nod2, a Nod1/Apaf-1 family member that is restricted to monocytes and activates NF-kappaB.* J Biol Chem, 2001. **276**(7): p. 4812-8.

62. Hisamatsu, T., et al., *CARD15/NOD2 functions as an antibacterial factor in human intestinal epithelial cells.* Gastroenterology, 2003. **124**(4): p. 993-1000.

63. Harder, J., et al., *Activation of the Nlrp3 inflammasome by Streptococcus pyogenes requires streptolysin O and NF-kappa B activation but proceeds independently of TLR signaling and P2X7 receptor.* J Immunol, 2009. **183**(9): p. 5823-9.

64. Paul-Clark, M.J., et al., *Pharmacology and therapeutic potential of pattern recognition receptors.* Pharmacol Ther, 2012. **135**(2): p. 200-15.

65. Hsu, Y.M., et al., *The adaptor protein CARD9 is required for innate immune responses to intracellular pathogens.* Nat Immunol, 2007. **8**(2): p. 198-205.

66. Masumoto, J., et al., *Nod1 acts as an intracellular receptor to stimulate chemokine production and neutrophil recruitment in vivo.* J Exp Med, 2006. **203**(1): p. 203-13.

67. Mahmood, K., K. Eldeirawi, and M.M. Wahidi, *Association of gender with outcomes in critically ill patients.* Crit Care, 2012. **16**(3): p. R92.

68. Schroder, J., et al., *Gender differences in human sepsis.* Arch Surg, 1998. **133**(11): p. 1200-5.

69. Kisat, M., et al., *Predictors of sepsis in moderately severely injured patients: an analysis of the National Trauma Data Bank.* Surg Infect (Larchmt), 2013. **14**(1): p. 62-8.

70. Zellweger, R., et al., *Females in proestrus state maintain splenic immune functions and tolerate sepsis better than males.* Crit Care Med, 1997. **25**(1): p. 106-10.

71. Drechsler, S., et al., *Relationship between age/gender-induced survival changes and the magnitude of inflammatory activation and organ dysfunction in post-traumatic sepsis.* PLoS One, 2012. **7**(12): p. e51457.

72. Frink, M., et al., *Influence of sex and age on mods and cytokines after multiple injuries.* Shock, 2007. **27**(2): p. 151-6.

73. Oberholzer, A., et al., *Incidence of septic complications and multiple organ failure in severely injured patients is sex specific.* J Trauma, 2000. **48**(5): p. 932-7.

74. Wang, H.E., et al., *Inflammatory and endothelial activation biomarkers and risk of sepsis: a nested case-control study.* J Crit Care, 2013. **28**(5): p. 549-55.

75. Li, P., et al., *Mice deficient in IL-1 beta-converting enzyme are defective in production of mature IL-1 beta and resistant to endotoxic shock.* Cell, 1995. **80**(3): p. 401-11.

76. Scotland, R.S., et al., *Sex differences in resident immune cell phenotype underlie more efficient acute inflammatory responses in female mice.* Blood, 2011. **118**(22): p. 5918-27.

77. Sener, G., et al., *Estrogen protects the liver and intestines against sepsis-induced injury in rats.* J Surg Res, 2005. **128**(1): p. 70-8.

78. Angele, M.K., et al., *Testosterone receptor blockade after hemorrhage in males. Restoration of the depressed immune functions and improved survival following subsequent sepsis.* Arch Surg, 1997. **132**(11): p. 1207-14.

79. Hsieh, Y.C., et al., *Flutamide restores cardiac function after trauma-hemorrhage via an estrogen-dependent pathway through upregulation of PGC-1.* Am J Physiol Heart Circ Physiol, 2006. **290**(1): p. H416-23.

80. Shimizu, T., et al., *Flutamide attenuates pro-inflammatory cytokine production and hepatic injury following trauma-hemorrhage via estrogen receptor-related pathway.* Ann Surg, 2007. **245**(2): p. 297-304.

81. Fernandes, C.J., Jr., N. Akamine, and E. Knobel, *Cardiac troponin: a new serum marker of myocardial injury in sepsis.* Intensive care medicine, 1999. **25**(10): p. 1165-8.

82. Parker, M.M., et al., *Profound but reversible myocardial depression in patients with septic shock.* Annals of internal medicine, 1984. **100**(4): p. 483-90.

83. MacLean, L.D., et al., *Patterns of septic shock in man--a detailed study of 56 patients.* Annals of surgery, 1967. **166**(4): p. 543-62.

84. Clowes, G.H., Jr., M. Vucinic, and M.G. Weidner, *Circulatory and metabolic alterations associated with survival or death in peritonitis: clinical analysis of 25 cases.* Annals of surgery, 1966. **163**(6): p. 866-85.

85. Wilson, R.F., E.J. Sarver, and P.L. LeBlanc, *Factors affecting hemodynamics in clinical shock with sepsis.* Annals of surgery, 1971. **174**(6): p. 939-43.

86. Abraham, E., et al., *Sequential cardiorespiratory patterns in septic shock.* Critical care medicine, 1983. **11**(10): p. 799-803.

87. Dellinger, R.P., *Cardiovascular management of septic shock.* Critical care medicine, 2003. **31**(3): p. 946-55.

88. Zanotti-Cavazzoni, S.L., et al., *Fluid resuscitation influences cardiovascular performance and mortality in a murine model of sepsis.* Intensive care medicine, 2009. **35**(4): p. 748-54.

89. Price, S., et al., *Myocardial dysfunction in sepsis: mechanisms and therapeutic implications.* European heart journal, 1999. **20**(10): p. 715-24.

90. Belcher, E., J. Mitchell, and T. Evans, *Myocardial dysfunction in sepsis: no role for NO?* Heart, 2002. **87**(6): p. 507-9.

91. Flierl, M.A., et al., *Molecular events in the cardiomyopathy of sepsis.* Mol Med, 2008. **14**(5-6): p. 327-36.

92. Bruni, F.D., et al., *Endotoxin and myocardial failure: role of the myofibril and venous return.* The American journal of physiology, 1978. **235**(2): p. H150-6.

93. Cunnion, R.E., et al., *The coronary circulation in human septic shock.* Circulation, 1986. **73**(4): p. 637-44.

94. Dhainaut, J.F., et al., *Coronary hemodynamics and myocardial metabolism of lactate, free fatty acids, glucose, and ketones in patients with septic shock.* Circulation, 1987. **75**(3): p. 533-41.

95. Rabuel, C. and A. Mebazaa, *Septic shock: a heart story since the 1960s.* Intensive care medicine, 2006. **32**(6): p. 799-807.

96. ver Elst, K.M., et al., *Cardiac troponins I and T are biological markers of left ventricular dysfunction in septic shock.* Clinical chemistry, 2000. **46**(5): p. 650-7.

97. Romero-Bermejo, F.J., et al., *Sepsis-induced cardiomyopathy.* Curr Cardiol Rev, 2011. **7**(3): p. 163-83.

98. Groeneveld, A.B., et al., *Maldistribution of heterogeneous coronary blood flow during canine endotoxin shock.* Cardiovascular research, 1991. **25**(1): p. 80-8.

99. Solomon, M.A., et al., *Myocardial energy metabolism and morphology in a canine model of sepsis.* The American journal of physiology, 1994. **266**(2 Pt 2): p. H757-68.

100. Madorin, W.S., et al., *Cardiac myocytes activated by septic plasma promote neutrophil transendothelial migration: role of platelet-activating factor and the chemokines LIX and KC.* Circulation research, 2004. **94**(7): p. 944-51.

101. Tavener, S.A. and P. Kubes, *Is there a role for cardiomyocyte toll-like receptor 4 in endotoxemia?* Trends in cardiovascular medicine, 2005. **15**(5): p. 153-7.

102. Ward, P.A., *Sepsis, apoptosis and complement.* Biochemical pharmacology, 2008. **76**(11): p. 1383-8.

103. Lancel, S., et al., *Ventricular myocyte caspases are directly responsible for endotoxin-induced cardiac dysfunction.* Circulation, 2005. **111**(20): p. 2596-604.

104. Neviere, R., et al., *Caspase inhibition prevents cardiac dysfunction and heart apoptosis in a rat model of sepsis.* American journal of respiratory and critical care medicine, 2001. **163**(1): p. 218-25.

105. Takasu, O., et al., *Mechanisms of cardiac and renal dysfunction in patients dying of sepsis.* American journal of respiratory and critical care medicine, 2013. **187**(5): p. 509-17.

106. Lovett, W.L., et al., *Presence of a myocardial depressant factor in patients in circulatory shock.* Surgery, 1971. **70**(2): p. 223-31.

107. Johnston, G.R. and N.R. Webster, *Cytokines and the immunomodulatory function of the vagus nerve.* British journal of anaesthesia, 2009. **102**(4): p. 453-62.

108. Natanson, C., et al., *Endotoxin and tumor necrosis factor challenges in dogs simulate the cardiovascular profile of human septic shock.* J Exp Med, 1989. **169**(3): p. 823-32.

109. Goldhaber, J.I., et al., *Effects of TNF-alpha on [Ca2+]i and contractility in isolated adult rabbit ventricular myocytes.* The American journal of physiology, 1996. **271**(4 Pt 2): p. H1449-55.

110. Kumar, A., et al., *Tumor necrosis factor alpha and interleukin 1beta are responsible for in vitro myocardial cell depression induced by human septic shock serum.* The Journal of experimental medicine, 1996. **183**(3): p. 949-58.

111. Finkel, M.S., et al., *Negative inotropic effects of cytokines on the heart mediated by nitric oxide.* Science, 1992. **257**(5068): p. 387-9.

112. Julian, M.W., et al., *Intestinal epithelium is more susceptible to cytopathic injury and altered permeability than the lung epithelium in the context of acute sepsis.* International journal of experimental pathology, 2011. **92**(5): p. 366-76.

113. Niederbichler, A.D., et al., *An essential role for complement C5a in the pathogenesis of septic cardiac dysfunction.* The Journal of experimental medicine, 2006. **203**(1): p. 53-61.

114. Rittirsch, D., M.A. Flierl, and P.A. Ward, *Harmful molecular mechanisms in sepsis.* Nature reviews. Immunology, 2008. **8**(10): p. 776-87.

115. Reilly, J.M., et al., *A circulating myocardial depressant substance is associated with cardiac dysfunction and peripheral hypoperfusion (lactic acidemia) in patients with septic shock.* Chest, 1989. **95**(5): p. 1072-80.

116. Suffredini, A.F., et al., *The cardiovascular response of normal humans to the administration of endotoxin.* The New England journal of medicine, 1989. **321**(5): p. 280-7.

117. Frantz, S., et al., *Toll4 (TLR4) expression in cardiac myocytes in normal and failing myocardium.* The Journal of clinical investigation, 1999. **104**(3): p. 271-80.

118. Knuefermann, P., et al., *CD14-deficient mice are protected against lipopolysaccharide-induced cardiac inflammation and left ventricular dysfunction.* Circulation, 2002. **106**(20): p. 2608-15.

119. Schuetz, P., et al., *Circulating precursor levels of endothelin-1 and adrenomedullin, two endothelium-derived, counteracting substances, in sepsis.* Endothelium : journal of endothelial cell research, 2007. **14**(6): p. 345-51.

120. Gardiner, S.M., et al., *Effects of the novel selective endothelin ET(A) receptor antagonist, SB 234551, on the cardiovascular responses to endotoxaemia in conscious rats.* Br J Pharmacol, 2001. **133**(8): p. 1371-7.

121. Brady, A.J. and P.A. Poole-Wilson, *Circulatory failure in septic shock. Nitric oxide: too much of a good thing?* British heart journal, 1993. **70**(2): p. 103-5.

122. Julou-Schaeffer, G., et al., *Loss of vascular responsiveness induced by endotoxin involves L-arginine pathway.* Am J Physiol, 1990. **259**(4 Pt 2): p. H1038-43.

123. Kilbourn, R.G., et al., *NG-methyl-L-arginine inhibits tumor necrosis factor-induced hypotension: implications for the involvement of nitric oxide.* Proc Natl Acad Sci U S A, 1990. **87**(9): p. 3629-32.

124. Szabo, C., G.J. Southan, and C. Thiemermann, *Beneficial effects and improved survival in rodent models of septic shock with S-methylisothiourea sulfate, a potent and selective inhibitor of inducible nitric oxide synthase.* Proc Natl Acad Sci U S A, 1994. **91**(26): p. 12472-6.

125. Thiemermann, C. and J. Vane, *Inhibition of nitric oxide synthesis reduces the hypotension induced by bacterial lipopolysaccharides in the rat in vivo.* Eur J Pharmacol, 1990. **182**(3): p. 591-5.

126. Schulz, R., et al., *Recent advances in the understanding of the role of nitric oxide in cardiovascular homeostasis.* Pharmacology & therapeutics, 2005. **108**(3): p. 225-56.

127. Poelaert, J., et al., *Left ventricular systolic and diastolic function in septic shock.* Intensive care medicine, 1997. **23**(5): p. 553-60.

128. Ullrich, R., et al., *Congenital deficiency of nitric oxide synthase 2 protects against endotoxin-induced myocardial dysfunction in mice.* Circulation, 2000. **102**(12): p. 1440-6.

129. Barth, E., et al., *Role of inducible nitric oxide synthase in the reduced responsiveness of the myocardium to catecholamines in a hyperdynamic, murine model of septic shock.* Crit Care Med, 2006. **34**(2): p. 307-13.

130. Ichinose, F., et al., *Cardiomyocyte-specific overexpression of nitric oxide synthase 3 prevents myocardial dysfunction in murine models of septic shock.* Circulation research, 2007. **100**(1): p. 130-9.

131. Xie, Y.W., P.M. Kaminski, and M.S. Wolin, *Inhibition of rat cardiac muscle contraction and mitochondrial respiration by endogenous peroxynitrite formation during posthypoxic reoxygenation.* Circulation research, 1998. **82**(8): p. 891-7.

132. Ishida, H., et al., *Peroxynitrite-induced cardiac myocyte injury.* Free radical biology & medicine, 1996. **20**(3): p. 343-50.

133. Ferdinandy, P., et al., *Peroxynitrite is a major contributor to cytokine-induced myocardial contractile failure.* Circulation research, 2000. **87**(3): p. 241-7.

134. Lancel, S., et al., *Peroxynitrite decomposition catalysts prevent myocardial dysfunction and inflammation in endotoxemic rats.* Journal of the American College of Cardiology, 2004. **43**(12): p. 2348-58.

135. Zhong, J., et al., *Reduced L-type calcium current in ventricular myocytes from endotoxemic guinea pigs.* The American journal of physiology, 1997. **273**(5 Pt 2): p. H2312-24.

136. Dong, L.W., et al., *Impairment of the ryanodine-sensitive calcium release channels in the cardiac sarcoplasmic reticulum and its underlying mechanism during the hypodynamic phase of sepsis.* Shock, 2001. **16**(1): p. 33-9.

137. Tavernier, B., et al., *Myofilament calcium sensitivity is decreased in skinned cardiac fibres of endotoxin-treated rabbits.* Cardiovascular research, 1998. **38**(2): p. 472-9.

138. Brealey, D., et al., *Association between mitochondrial dysfunction and severity and outcome of septic shock.* Lancet, 2002. **360**(9328): p. 219-23.

139. Crouser, E.D., *Mitochondrial dysfunction in septic shock and multiple organ dysfunction syndrome.* Mitochondrion, 2004. **4**(5-6): p. 729-41.

140. Suliman, H.B., et al., *Lipopolysaccharide induces oxidative cardiac mitochondrial damage and biogenesis.* Cardiovascular research, 2004. **64**(2): p. 279-88.

141. Levy, R.J., *Mitochondrial dysfunction, bioenergetic impairment, and metabolic down-regulation in sepsis.* Shock, 2007. **28**(1): p. 24-8.

142. Larche, J., et al., *Inhibition of mitochondrial permeability transition prevents sepsis-induced myocardial dysfunction and mortality.* Journal of the American College of Cardiology, 2006. **48**(2): p. 377-85.

143. Rudiger, A. and M. Singer, *Mechanisms of sepsis-induced cardiac dysfunction.* Crit Care Med, 2007. **35**(6): p. 1599-608.

144. Fishbane, S., et al., *Challenges and opportunities in late-stage chronic kidney disease.* Clin Kidney J, 2015. **8**(1): p. 54-60.

145. Stevens, L.A., et al., *Assessing kidney function--measured and estimated glomerular filtration rate.* N Engl J Med, 2006. **354**(23): p. 2473-83.

146. Coresh, J., B. Astor, and M.J. Sarnak, *Evidence for increased cardiovascular disease risk in patients with chronic kidney disease.* Curr Opin Nephrol Hypertens, 2004. **13**(1): p. 73-81.

147. National Kidney, F., *K/DOQI clinical practice guidelines for chronic kidney disease: evaluation, classification, and stratification.* Am J Kidney Dis, 2002. **39**(2 Suppl 1): p. S1-266.

148. Stevens, L.A. and A.S. Levey, *Measurement of kidney function.* Med Clin North Am, 2005. **89**(3): p. 457-73.

149. Berglund, F., J. Killander, and R. Pompeius, *Effect of trimethoprim-sulfamethoxazole on the renal excretion of creatinine in man.* J Urol, 1975. **114**(6): p. 802-8.

150. Levey, A.S., *Measurement of renal function in chronic renal disease.* Kidney Int, 1990. **38**(1): p. 167-84.

151. Jha, V., et al., *Chronic kidney disease: global dimension and perspectives.* Lancet, 2013. **382**(9888): p. 260-72.

152. Barsoum, R.S., *Chronic kidney disease in the developing world.* N Engl J Med, 2006. **354**(10): p. 997-9.

153. Zhang, Q.L. and D. Rothenbacher, *Prevalence of chronic kidney disease in population-based studies: systematic review.* BMC Public Health, 2008. **8**: p. 117.

154. Centers for Disease, C. and Prevention, *Prevalence of chronic kidney disease and associated risk factors--United States, 1999-2004.* MMWR Morb Mortal Wkly Rep, 2007.

56(8): p. 161-5.

155.   Martins, D., et al., *The association of poverty with the prevalence of albuminuria: data from the Third National Health and Nutrition Examination Survey (NHANES III).* Am J Kidney Dis, 2006. **47**(6): p. 965-71.

156.   Merkin, S.S., et al., *Individual and neighborhood socioeconomic status and progressive chronic kidney disease in an elderly population: The Cardiovascular Health Study.* Soc Sci Med, 2007. **65**(4): p. 809-21.

157.   Annual Data Report: Atlas of Chronic Kidney Disease and End-Stage Renal Disease in the United States. 2013. Available from: URL: http:// www.usrds.org/atlas.aspx.) (Accessed December 5, 2013)

158.   Levey, A.S., et al., *Chronic kidney disease as a global public health problem: approaches and initiatives - a position statement from Kidney Disease Improving Global Outcomes.* Kidney Int, 2007. **72**(3): p. 247-59.

159.   El Nahas, M., *The global challenge of chronic kidney disease.* Kidney Int, 2005. **68**(6): p. 2918-29.

160.   Murray, C.J., et al., *The state of US health, 1990-2010: burden of diseases, injuries, and risk factors.* JAMA, 2013. **310**(6): p. 591-608.

161.   Foley, R.N., P.S. Parfrey, and M.J. Sarnak, *Clinical epidemiology of cardiovascular disease in chronic renal disease.* Am J Kidney Dis, 1998. **32**(5 Suppl 3): p. S112-9.

162.   Sarnak, M.J., et al., *Kidney disease as a risk factor for development of cardiovascular disease: a statement from the American Heart Association Councils on Kidney in Cardiovascular Disease, High Blood Pressure Research, Clinical Cardiology, and Epidemiology and Prevention.* Circulation, 2003. **108**(17): p. 2154-69.

163.   Herzog, C.A., *Poor long-term survival of dialysis patients after acute myocardial infarction: bad treatment or bad disease?* Am J Kidney Dis, 2000. **35**(6): p. 1217-20.

164.   Sarnak, M.J. and A.S. Levey, *Epidemiology, diagnosis, and management of cardiac disease in chronic renal disease.* J Thromb Thrombolysis, 2000. **10**(2): p. 169-80.

165.   Parfrey, P.S., et al., *Outcome and risk factors for left ventricular disorders in chronic uraemia.* Nephrol Dial Transplant, 1996. **11**(7): p. 1277-85.

166.   Foley, R.N., et al., *Blood pressure and long-term mortality in United States hemodialysis patients: USRDS Waves 3 and 4 Study.* Kidney Int, 2002. **62**(5): p. 1784-90.

167.   Harnett, J.D., et al., *The reliability and validity of echocardiographic measurement of left ventricular mass index in hemodialysis patients.* Nephron, 1993. **65**(2): p. 212-4.

168.   de Lemos, J.A. and L.D. Hillis, *Diagnosis and management of coronary artery disease in patients with end-stage renal disease on hemodialysis.* J Am Soc Nephrol, 1996. **7**(10): p. 2044-54.

169.   Boudreau, R.J., et al., *Perfusion thallium imaging of type I diabetes patients with end stage renal disease: comparison of oral and intravenous dipyridamole administration.* Radiology, 1990. **175**(1): p. 103-5.

170.   Rostand, S.G., K.A. Kirk, and E.A. Rutsky, *Dialysis-associated ischemic heart disease: insights from coronary angiography.* Kidney Int, 1984. **25**(4): p. 653-9.

171.   Lisowska, A. and W.J. Musial, *Heart failure in patients with chronic kidney disease.* Rocz Akad Med Bialymst, 2004. **49**: p. 162-5.

172.   Muntner, P., et al., *Traditional and nontraditional risk factors predict coronary heart disease in chronic kidney disease: results from the atherosclerosis risk in communities study.* J Am Soc Nephrol, 2005. **16**(2): p. 529-38.

173.   Foley, R.N., *Cardiac disease in chronic uremia: can it explain the reverse epidemiology of hypertension and survival in dialysis patients?* Semin Dial, 2004. **17**(4): p. 275-8.

174.   Foley, R.N., et al., *Impact of hypertension on cardiomyopathy, morbidity and mortality in end-stage renal disease.* Kidney Int, 1996. **49**(5): p. 1379-85.

175.   Foley, R.N., *Clinical epidemiology of cardiac disease in dialysis patients: left ventricular hypertrophy, ischemic heart disease, and cardiac failure.* Semin Dial, 2003. **16**(2): p. 111-7.

176.   Uhlig, K., A.S. Levey, and M.J. Sarnak, *Traditional cardiac risk factors in individuals with chronic kidney disease.* Semin Dial, 2003. **16**(2): p. 118-27.

177.   Port, F.K., et al., *Predialysis blood pressure and mortality risk in a national sample of maintenance hemodialysis patients.* Am J Kidney Dis, 1999. **33**(3): p. 507-17.

178.   Jungers, P., et al., *Incidence and risk factors of atherosclerotic cardiovascular accidents in predialysis chronic renal failure patients: a prospective study.* Nephrol Dial Transplant, 1997. **12**(12): p. 2597-602.

179. Kronenberg, F., et al., *The low molecular weight apo(a) phenotype is an independent predictor for coronary artery disease in hemodialysis patients: a prospective follow-up.* J Am Soc Nephrol, 1999. **10**(5): p. 1027-36.

180. Webb, A.T. and E.A. Brown, *Prevalence of symptomatic arterial disease and risk factors for its development in patients on continuous ambulatory peritoneal dialysis.* Perit Dial Int, 1993. **13 Suppl 2**: p. S406-8.

181. Sharp Collaborative, G., *Study of Heart and Renal Protection (SHARP): randomized trial to assess the effects of lowering low-density lipoprotein cholesterol among 9,438 patients with chronic kidney disease.* Am Heart J, 2010. **160**(5): p. 785-794 e10.

182. Strippoli, G.F., et al., *Effects of statins in patients with chronic kidney disease: meta-analysis and meta-regression of randomised controlled trials.* BMJ, 2008. **336**(7645): p. 645-51.

183. Wanner, C., et al., *Atorvastatin in patients with type 2 diabetes mellitus undergoing hemodialysis.* N Engl J Med, 2005. **353**(3): p. 238-48.

184. Tonelli, M., et al., *Effect of pravastatin in people with diabetes and chronic kidney disease.* J Am Soc Nephrol, 2005. **16**(12): p. 3748-54.

185. Kalantar-Zadeh, K., et al., *A1C and survival in maintenance hemodialysis patients.* Diabetes Care, 2007. **30**(5): p. 1049-55.

186. Williams, M.E., et al., *Hemodialyzed type I and type II diabetic patients in the US: Characteristics, glycemic control, and survival.* Kidney Int, 2006. **70**(8): p. 1503-9.

187. Rucker, D. and M. Tonelli, *Cardiovascular risk and management in chronic kidney disease.* Nat Rev Nephrol, 2009. **5**(5): p. 287-96.

188. Orth, S.R. and S.I. Hallan, *Smoking: a risk factor for progression of chronic kidney disease and for cardiovascular morbidity and mortality in renal patients--absence of evidence or evidence of absence?* Clin J Am Soc Nephrol, 2008. **3**(1): p. 226-36.

189. Combe, C., et al., *Kidney Disease Outcomes Quality Initiative (K/DOQI) and the Dialysis Outcomes and Practice Patterns Study (DOPPS): nutrition guidelines, indicators, and practices.* Am J Kidney Dis, 2004. **44**(5 Suppl 2): p. 39-46.

190. United States Renal Data System. 1998 Annual Data Report. The National Institutes of Health. The National Institute of Diabetes and Digestive and Kidney Disease. Division of Kidney, Urologic, and Hematologic Diseases. Bethesda 1998.

191. Bloembergen, W.E., et al., *Causes of death in dialysis patients: racial and gender differences.* J Am Soc Nephrol, 1994. **5**(5): p. 1231-42.

192. Horl, W.H., *Anaemia management and mortality risk in chronic kidney disease.* Nat Rev Nephrol, 2013. **9**(5): p. 291-301.

193. Sarnak, M.J., *Cardiovascular complications in chronic kidney disease.* Am J Kidney Dis, 2003. **41**(5 Suppl): p. 11-7.

194. London, G.M., *Cardiovascular disease in chronic renal failure: pathophysiologic aspects.* Semin Dial, 2003. **16**(2): p. 85-94.

195. Block, G.A., et al., *Association of serum phosphorus and calcium x phosphate product with mortality risk in chronic hemodialysis patients: a national study.* Am J Kidney Dis, 1998. **31**(4): p. 607-17.

196. London, G.M., et al., *Arterial media calcification in end-stage renal disease: impact on all-cause and cardiovascular mortality.* Nephrol Dial Transplant, 2003. **18**(9): p. 1731-40.

197. Amann, K., et al., *A role of parathyroid hormone for the activation of cardiac fibroblasts in uremia.* J Am Soc Nephrol, 1994. **4**(10): p. 1814-9.

198. Kestenbaum, B., et al., *Serum phosphate levels and mortality risk among people with chronic kidney disease.* J Am Soc Nephrol, 2005. **16**(2): p. 520-8.

199. Kramer, H., et al., *Association between chronic kidney disease and coronary artery calcification: the Dallas Heart Study.* J Am Soc Nephrol, 2005. **16**(2): p. 507-13.

200. Guerin, A.P., et al., *Arterial stiffening and vascular calcifications in end-stage renal disease.* Nephrol Dial Transplant, 2000. **15**(7): p. 1014-21.

201. Goodman, W.G., et al., *Coronary-artery calcification in young adults with end-stage renal disease who are undergoing dialysis.* N Engl J Med, 2000. **342**(20): p. 1478-83.

202. Tentori, F., et al., *Mortality risk for dialysis patients with different levels of serum calcium, phosphorus, and PTH: the Dialysis Outcomes and Practice Patterns Study (DOPPS).* Am J Kidney Dis, 2008. **52**(3): p. 519-30.

203. Block, G.A., et al., *Mortality effect of coronary calcification and phosphate binder choice in incident hemodialysis patients.* Kidney Int, 2007. **71**(5): p. 438-41.

204. Suki, W.N., et al., *Effects of sevelamer and calcium-based phosphate binders on mortality in*

hemodialysis patients. Kidney Int, 2007. **72**(9): p. 1130-7.

205. Shlipak, M.G., et al., *Cardiovascular mortality risk in chronic kidney disease: comparison of traditional and novel risk factors.* JAMA, 2005. **293**(14): p. 1737-45.

206. Stack, A.G. and R. Saran, *Clinical correlates and mortality impact of left ventricular hypertrophy among new ESRD patients in the United States.* Am J Kidney Dis, 2002. **40**(6): p. 1202-10.

207. Schlieper, G., et al., *The vulnerable patient with chronic kidney disease.* Nephrol Dial Transplant, 2015.

208. Park, C.W., et al., *Intravenous calcitriol regresses myocardial hypertrophy in hemodialysis patients with secondary hyperparathyroidism.* Am J Kidney Dis, 1999. **33**(1): p. 73-81.

209. Culleton, B.F., et al., *Effect of frequent nocturnal hemodialysis vs conventional hemodialysis on left ventricular mass and quality of life: a randomized controlled trial.* JAMA, 2007. **298**(11): p. 1291-9.

210. Stenvinkel, P., *Malnutrition and chronic inflammation as risk factors for cardiovascular disease in chronic renal failure.* Blood Purif, 2001. **19**(2): p. 143-51.

211. Stenvinkel, P. and A. Alvestrand, *Inflammation in end-stage renal disease: sources, consequences, and therapy.* Semin Dial, 2002. **15**(5): p. 329-37.

212. Leelahavanichkul, A., et al., *Chronic kidney disease worsens sepsis and sepsis-induced acute kidney injury by releasing High Mobility Group Box Protein-1.* Kidney Int, 2011. **80**(11): p. 1198-211.

213. Ross, R., *Atherosclerosis--an inflammatory disease.* N Engl J Med, 1999. **340**(2): p. 115-26.

214. Yeun, J.Y. and G.A. Kaysen, *C-reactive protein, oxidative stress, homocysteine, and troponin as inflammatory and metabolic predictors of atherosclerosis in ESRD.* Curr Opin Nephrol Hypertens, 2000. **9**(6): p. 621-30.

215. Iseki, K., et al., *Serum C-reactive protein (CRP) and risk of death in chronic dialysis patients.* Nephrol Dial Transplant, 1999. **14**(8): p. 1956-60.

216. *C-reactive protein and atherosclerosis in dialysis patients.* Nephrol Dial Transplant, 1998. **13**(10): p. 2710-1.

217. Griselli, M., et al., *C-reactive protein and complement are important mediators of tissue damage in acute myocardial infarction.* J Exp Med, 1999. **190**(12): p. 1733-40.

218. Pecoits-Filho, R., et al., *Interleukin-6 is an independent predictor of mortality in patients starting dialysis treatment.* Nephrol Dial Transplant, 2002. **17**(9): p. 1684-8.

219. Stenvinkel, P., *Endothelial dysfunction and inflammation-is there a link?* Nephrol Dial Transplant, 2001. **16**(10): p. 1968-71.

220. Chang, J.W., et al., *Effects of simvastatin on high-sensitivity C-reactive protein and serum albumin in hemodialysis patients.* Am J Kidney Dis, 2002. **39**(6): p. 1213-7.

221. Madore, F., *Uremia-related metabolic cardiac risk factors in chronic kidney disease.* Semin Dial, 2003. **16**(2): p. 148-56.

222. Locatelli, F., et al., *Oxidative stress in end-stage renal disease: an emerging threat to patient outcome.* Nephrol Dial Transplant, 2003. **18**(7): p. 1272-80.

223. Sies, H., *Oxidative stress: oxidants and antioxidants.* Exp Physiol, 1997. **82**(2): p. 291-5.

224. Canaud, B., et al., *Imbalance of oxidants and antioxidants in haemodialysis patients.* Blood Purif, 1999. **17**(2-3): p. 99-106.

225. Descamps-Latscha, B., T. Drueke, and V. Witko-Sarsat, *Dialysis-induced oxidative stress: biological aspects, clinical consequences, and therapy.* Semin Dial, 2001. **14**(3): p. 193-9.

226. Nguyen, A.T., et al., *Hemodialysis membrane-induced activation of phagocyte oxidative metabolism detected in vivo and in vitro within microamounts of whole blood.* Kidney Int, 1985. **28**(2): p. 158-67.

227. Yu, M., Y.J. Kim, and D.H. Kang, *Indoxyl sulfate-induced endothelial dysfunction in patients with chronic kidney disease via an induction of oxidative stress.* Clin J Am Soc Nephrol, 2011. **6**(1): p. 30-9.

228. Boaz, M., et al., *Serum malondialdehyde and prevalent cardiovascular disease in hemodialysis.* Kidney Int, 1999. **56**(3): p. 1078-83.

229. Usberti, M., et al., *Oxidative stress and cardiovascular disease in dialyzed patients.* Nephron, 2002. **91**(1): p. 25-33.

230. Islam, K.N., et al., *Alpha-tocopherol supplementation decreases the oxidative susceptibility of LDL in renal failure patients on dialysis therapy.* Atherosclerosis, 2000. **150**(1): p. 217-24.

231. Boaz, M., et al., *Secondary prevention with antioxidants of cardiovascular disease in*

endstage renal disease (SPACE): randomised placebo-controlled trial. Lancet, 2000. **356**(9237): p. 1213-8.

232. Tepel, M., et al., *The antioxidant acetylcysteine reduces cardiovascular events in patients with end-stage renal failure: a randomized, controlled trial.* Circulation, 2003. **107**(7): p. 992-5.

233. van Guldener, C., F. Stam, and C.D. Stehouwer, *Homocysteine metabolism in renal failure.* Kidney Int Suppl, 2001. **78**: p. S234-7.

234. Menon, V., et al., *Relationship between homocysteine and mortality in chronic kidney disease.* Circulation, 2006. **113**(12): p. 1572-7.

235. Robinson, K., E. Mayer, and D.W. Jacobsen, *Homocysteine and coronary artery disease.* Cleve Clin J Med, 1994. **61**(6): p. 438-50.

236. Bostom, A.G., et al., *High dose-B-vitamin treatment of hyperhomocysteinemia in dialysis patients.* Kidney Int, 1996. **49**(1): p. 147-52.

237. Jamison, R.L., et al., *Effect of homocysteine lowering on mortality and vascular disease in advanced chronic kidney disease and end-stage renal disease: a randomized controlled trial.* JAMA, 2007. **298**(10): p. 1163-70.

238. Contou, D., et al., *Description and predictive factors of infection in patients with chronic kidney disease admitted to the critical care unit.* J Infect, 2014. **68**(2): p. 105-15.

239. Naqvi, S.B. and A.J. Collins, *Infectious complications in chronic kidney disease.* Adv Chronic Kidney Dis, 2006. **13**(3): p. 199-204.

240. Powe, N.R., et al., *Septicemia in dialysis patients: incidence, risk factors, and prognosis.* Kidney Int, 1999. **55**(3): p. 1081-90.

241. U.S. Renal Data System: USRDS 2003 Annual Data Report. Bethesda MD, National Institutes of Health, National Institute of Diabetes and Digestive and Kidney Diseases, 2003

242. Aslam, S., et al., *Systematic review and meta-analysis on management of hemodialysis catheter-related bacteremia.* J Am Soc Nephrol, 2014. **25**(12): p. 2927-41.

243. Ghali, J.R., et al., *Microbiology and outcomes of peritonitis in Australian peritoneal dialysis patients.* Perit Dial Int, 2011. **31**(6): p. 651-62.

244. Rojas, L., et al., *Bloodstream infections in patients with kidney disease: risk factors for poor outcome and mortality.* J Hosp Infect, 2013. **85**(3): p. 196-205.

245. Sarnak, M.J. and B.L. Jaber, *Mortality caused by sepsis in patients with end-stage renal disease compared with the general population.* Kidney Int, 2000. **58**(4): p. 1758-64.

246. Sarnak, M.J. and B.L. Jaber, *Pulmonary infectious mortality among patients with end-stage renal disease.* Chest, 2001. **120**(6): p. 1883-7.

247. McDonald, H.I., et al., *Are pre-existing markers of chronic kidney disease associated with short-term mortality following acute community-acquired pneumonia and sepsis? A cohort study among older people with diabetes using electronic health records.* Nephrol Dial Transplant, 2015. **30**(6): p. 1002-9.

248. Mansur, A., et al., *Chronic kidney disease is associated with a higher 90-day mortality than other chronic medical conditions in patients with sepsis.* Sci Rep, 2015. **5**: p. 10539.

249. Francis, A., Y. Cho, and D.W. Johnson, *Honey in the Prevention and Treatment of Infection in the CKD Population: A Narrative Review.* Evid Based Complement Alternat Med, 2015. **2015**: p. 261425.

250. Go, A.S., et al., *Chronic kidney disease and the risks of death, cardiovascular events, and hospitalization.* N Engl J Med, 2004. **351**(13): p. 1296-305.

251. Carton, J.A., et al., *Diabetes mellitus and bacteraemia: a comparative study between diabetic and non-diabetic patients.* Eur J Med, 1992. **1**(5): p. 281-7.

252. Tain, Y.L., G. Lin, and T.W. Cher, *Microbiological spectrum of septicemia and peritonitis in nephrotic children.* Pediatr Nephrol, 1999. **13**(9): p. 835-7.

253. McIntyre, P. and J.C. Craig, *Prevention of serious bacterial infection in children with nephrotic syndrome.* J Paediatr Child Health, 1998. **34**(4): p. 314-7.

254. Langford, C.A., et al., *Use of cytotoxic agents and cyclosporine in the treatment of autoimmune disease. Part 1: rheumatologic and renal diseases.* Ann Intern Med, 1998. **128**(12 Pt 1): p. 1021-8.

255. Hoen, B., et al., *EPIBACDIAL: a multicenter prospective study of risk factors for bacteremia in chronic hemodialysis patients.* J Am Soc Nephrol, 1998. **9**(5): p. 869-76.

256. Cohen, G. and W.H. Horl, *Immune dysfunction in uremia—an update.* Toxins (Basel), 2012. **4**(11): p. 962-90.

257. Ando, M., et al., *Impairment of innate cellular response to in vitro stimuli in patients on continuous ambulatory peritoneal dialysis.* Nephrol Dial Transplant, 2005. **20**(11): p. 2497-503.

258. Verkade, M.A., et al., *Functional impairment of monocyte-derived dendritic cells in patients with severe chronic kidney disease.* Nephrol Dial Transplant, 2007. **22**(1): p. 128-38.

259. Stachowski, J., et al., *Signalling via the TCR/CD3 antigen receptor complex in uremia is limited by the receptors number.* Nephron, 1993. **64**(3): p. 369-75.

260. Kato, S., et al., *Aspects of immune dysfunction in end-stage renal disease.* Clin J Am Soc Nephrol, 2008. **3**(5): p. 1526-33.

261. Stenvinkel, P., et al., *IL-10, IL-6, and TNF-alpha: central factors in the altered cytokine network of uremia--the good, the bad, and the ugly.* Kidney Int, 2005. **67**(4): p. 1216-33.

262. Vanholder, R. and S. Ringoir, *Infectious morbidity and defects of phagocytic function in end-stage renal disease: a review.* J Am Soc Nephrol, 1993. **3**(9): p. 1541-54.

263. Allon, M., et al., *Impact of dialysis dose and membrane on infection-related hospitalization and death: results of the HEMO Study.* J Am Soc Nephrol, 2003. **14**(7): p. 1863-70.

264. Ishani, A., et al., *Septicemia, access and cardiovascular disease in dialysis patients: the USRDS Wave 2 study.* Kidney Int, 2005. **68**(1): p. 311-8.

265. Flaherty, J.P., et al., *An outbreak of gram-negative bacteremia traced to contaminated O-rings in reprocessed dialyzers.* Ann Intern Med, 1993. **119**(11): p. 1072-8.

266. Galvao, T.F., et al., *Dialyzer reuse and mortality risk in patients with end-stage renal disease: a systematic review.* Am J Nephrol, 2012. **35**(3): p. 249-58.

267. Vandecasteele, S.J., et al., *The ABC of pneumococcal infections and vaccination in patients with chronic kidney disease.* Clin Kidney J, 2015. **8**(3): p. 318-24.

268. Gilbertson, D.T., et al., *Influenza vaccine delivery and effectiveness in end-stage renal disease.* Kidney Int, 2003. **63**(2): p. 738-43.

269. Pesanti, E.L., *Immunologic defects and vaccination in patients with chronic renal failure.* Infect Dis Clin North Am, 2001. **15**(3): p. 813-32.

270. Kausz, A.T. and D.T. Gilbertson, *Overview of vaccination in chronic kidney disease.* Adv Chronic Kidney Dis, 2006. **13**(3): p. 209-14.

271. Caterina, M.J., et al., *The capsaicin receptor: a heat-activated ion channel in the pain pathway.* Nature, 1997. **389**(6653): p. 816-24.

272. Piper, A.S., et al., *A study of the voltage dependence of capsaicin-activated membrane currents in rat sensory neurones before and after acute desensitization.* J Physiol, 1999. **518 (Pt 3)**: p. 721-33.

273. Jordt, S.E., M. Tominaga, and D. Julius, *Acid potentiation of the capsaicin receptor determined by a key extracellular site.* Proc Natl Acad Sci U S A, 2000. **97**(14): p. 8134-9.

274. Smart, D., et al., *The endogenous lipid anandamide is a full agonist at the human vanilloid receptor (hVR1).* Br J Pharmacol, 2000. **129**(2): p. 227-30.

275. Chuang, H.H., et al., *Bradykinin and nerve growth factor release the capsaicin receptor from PtdIns(4,5)P2-mediated inhibition.* Nature, 2001. **411**(6840): p. 957-62.

276. Hwang, S.W., et al., *Direct activation of capsaicin receptors by products of lipoxygenases: endogenous capsaicin-like substances.* Proc Natl Acad Sci U S A, 2000. **97**(11): p. 6155-60.

277. Bubb, K.J., et al., *Activation of neuronal transient receptor potential vanilloid 1 channel underlies 20-hydroxyeicosatetraenoic acid-induced vasoactivity: role for protein kinase A.* Hypertension, 2013. **62**(2): p. 426-33.

278. Lishko, P.V., et al., *The ankyrin repeats of TRPV1 bind multiple ligands and modulate channel sensitivity.* Neuron, 2007. **54**(6): p. 905-18.

279. Garcia-Sanz, N., et al., *Identification of a tetramerization domain in the C terminus of the vanilloid receptor.* J Neurosci, 2004. **24**(23): p. 5307-14.

280. Senning, E.N., et al., *Regulation of TRPV1 ion channel by phosphoinositide (4,5)-bisphosphate: the role of membrane asymmetry.* J Biol Chem, 2014. **289**(16): p. 10999-1006.

281. Baumann, T.K., et al., *Neurogenic hyperalgesia: the search for the primary cutaneous afferent fibers that contribute to capsaicin-induced pain and hyperalgesia.* J Neurophysiol, 1991. **66**(1): p. 212-27.

282. Cavanaugh, D.J., et al., *Trpv1 reporter mice reveal highly restricted brain distribution and functional expression in arteriolar smooth muscle cells.* J Neurosci, 2011. **31**(13): p. 5067-77.

283. Alawi, K. and J. Keeble, *The paradoxical role of the transient receptor potential vanilloid 1*

receptor in inflammation. Pharmacol Ther, 2010. **125**(2): p. 181-95.

284. Holzer, P., *The pharmacological challenge to tame the transient receptor potential vanilloid-1 (TRPV1) nocisensor.* Br J Pharmacol, 2008. **155**(8): p. 1145-62.

285. Reilly, C.A., et al., *Capsaicinoids cause inflammation and epithelial cell death through activation of vanilloid receptors.* Toxicol Sci, 2003. **73**(1): p. 170-81.

286. Mezey, E., et al., *Distribution of mRNA for vanilloid receptor subtype 1 (VR1), and VR1-like immunoreactivity, in the central nervous system of the rat and human.* Proc Natl Acad Sci U S A, 2000. **97**(7): p. 3655-60.

287. Lazzeri, M., et al., *Immunohistochemical evidence of vanilloid receptor 1 in normal human urinary bladder.* Eur Urol, 2004. **46**(6): p. 792-8.

288. Southall, M.D., et al., *Activation of epidermal vanilloid receptor-1 induces release of proinflammatory mediators in human keratinocytes.* J Pharmacol Exp Ther, 2003. **304**(1): p. 217-22.

289. Heiner, I., et al., *Expression profile of the transient receptor potential (TRP) family in neutrophil granulocytes: evidence for currents through long TRP channel 2 induced by ADP-ribose and NAD.* Biochem J, 2003. **371**(Pt 3): p. 1045-53.

290. Fernandes, E.S., et al., *TRPV1 deletion enhances local inflammation and accelerates the onset of systemic inflammatory response syndrome.* J Immunol, 2012. **188**(11): p. 5741-51.

291. Saunders, C.I., et al., *Expression of transient receptor potential vanilloid 1 (TRPV1) and 2 (TRPV2) in human peripheral blood.* Mol Immunol, 2007. **44**(6): p. 1429-35.

292. Costa, S.K., et al., *How important are NK1 receptors for influencing microvascular inflammation and itch in the skin? Studies using Phoneutria nigriventer venom.* Vascul Pharmacol, 2006. **45**(4): p. 209-14.

293. Zhao, D., et al., *Substance P-stimulated interleukin-8 expression in human colonic epithelial cells involves Rho family small GTPases.* Biochem J, 2002. **368**(Pt 2): p. 665-72.

294. Lembeck, F. and P. Holzer, *Substance P as neurogenic mediator of antidromic vasodilation and neurogenic plasma extravasation.* Naunyn Schmiedebergs Arch Pharmacol, 1979. **310**(2): p. 175-83.

295. Gomes, R.N., et al., *Calcitonin gene-related peptide inhibits local acute inflammation and protects mice against lethal endotoxemia.* Shock, 2005. **24**(6): p. 590-4.

296. Harzenetter, M.D., et al., *Negative regulation of TLR responses by the neuropeptide CGRP is mediated by the transcriptional repressor ICER.* J Immunol, 2007. **179**(1): p. 607-15.

297. Pinter, E., Z. Helyes, and J. Szolcsanyi, *Inhibitory effect of somatostatin on inflammation and nociception.* Pharmacol Ther, 2006. **112**(2): p. 440-56.

298. Biro, T., et al., *Characterization of functional vanilloid receptors expressed by mast cells.* Blood, 1998. **91**(4): p. 1332-40.

299. Stander, S., et al., *Expression of vanilloid receptor subtype 1 in cutaneous sensory nerve fibers, mast cells, and epithelial cells of appendage structures.* Exp Dermatol, 2004. **13**(3): p. 129-39.

300. Joyce, C.D., et al., *Calcitonin gene-related peptide levels are elevated in patients with sepsis.* Surgery, 1990. **108**(6): p. 1097-101.

301. Bowden, J.J., et al., *Sensory denervation by neonatal capsaicin treatment exacerbates Mycoplasma pulmonis infection in rat airways.* Am J Physiol, 1996. **270**(3 Pt 1): p. L393-403.

302. Orliac, M.L., et al., *Increases in vanilloid TRPV1 receptor protein and CGRP content during endotoxemia in rats.* Eur J Pharmacol, 2007. **566**(1-3): p. 145-52.

303. Wang, Y., et al., *TRPV1-mediated protection against endotoxin-induced hypotension and mortality in rats.* Am J Physiol Regul Integr Comp Physiol, 2008. **294**(5): p. R1517-23.

304. Clark, N., et al., *The transient receptor potential vanilloid 1 (TRPV1) receptor protects against the onset of sepsis after endotoxin.* FASEB J, 2007. **21**(13): p. 3747-55.

305. Bryant, P., et al., *Capsaicin-sensitive nerves regulate the metabolic response to abdominal sepsis.* J Surg Res, 2003. **112**(2): p. 152-61.

306. Demirbilek, S., et al., *Small-dose capsaicin reduces systemic inflammatory responses in septic rats.* Anesth Analg, 2004. **99**(5): p. 1501-7; table of contents.

307. Angus, D.C., et al., *Epidemiology of severe sepsis in the United States: analysis of incidence, outcome, and associated costs of care.* Crit Care Med, 2001. **29**(7): p. 1303-10.

308. Padkin, A., et al., *Epidemiology of severe sepsis occurring in the first 24 hrs in intensive care units in England, Wales, and Northern Ireland.* Crit Care Med, 2003. **31**(9): p. 2332-8.

309. Fernandes, C.J., Jr., N. Akamine, and E. Knobel, *Cardiac troponin: a new serum marker of myocardial injury in sepsis.* Intensive Care Med, 1999. **25**(10): p. 1165-8.

310. Bone, R.C., *Toward an epidemiology and natural history of SIRS (systemic inflammatory response syndrome).* JAMA, 1992. **268**(24): p. 3452-5.

311. Ghuman, A.K., C.J. Newth, and R.G. Khemani, *Impact of gender on sepsis mortality and severity of illness for prepubertal and postpubertal children.* J Pediatr, 2013. **163**(3): p. 835-40 e1.

312. Melamed, A. and F.J. Sorvillo, *The burden of sepsis-associated mortality in the United States from 1999 to 2005: an analysis of multiple-cause-of-death data.* Crit Care, 2009. **13**(1): p. R28.

313. Aulock, S.V., et al., *Gender difference in cytokine secretion on immune stimulation with LPS and LTA.* J Interferon Cytokine Res, 2006. **26**(12): p. 887-92.

314. Kilkenny, C., et al., *Improving bioscience research reporting: the ARRIVE guidelines for reporting animal research.* PLoS Biol, 2010. **8**(6): p. e1000412.

315. McGrath, J.C., et al., *Guidelines for reporting experiments involving animals: the ARRIVE guidelines.* Br J Pharmacol, 2010. **160**(7): p. 1573-6.

316. Coldewey, S.M., et al., *Inhibition of IkappaB kinase reduces the multiple organ dysfunction caused by sepsis in the mouse.* Dis Model Mech, 2013. **6**(4): p. 1031-42.

317. Khan, A.I., et al., *Erythropoietin attenuates cardiac dysfunction in experimental sepsis in mice via activation of the beta-common receptor.* Dis Model Mech, 2013. **6**(4): p. 1021-30.

318. Wang, M., et al., *Sex differences in the myocardial inflammatory response to ischemia-reperfusion injury.* Am J Physiol Endocrinol Metab, 2005. **288**(2): p. E321-6.

319. Szalay, L., et al., *Estradiol improves cardiac and hepatic function after trauma-hemorrhage: role of enhanced heat shock protein expression.* American journal of physiology. Regulatory, integrative and comparative physiology, 2006. **290**(3): p. R812-8.

320. Horton, J.W., D.J. White, and D.L. Maass, *Gender-related differences in myocardial inflammatory and contractile responses to major burn trauma.* Am J Physiol Heart Circ Physiol, 2004. **286**(1): p. H202-13.

321. Hsu, J.T., et al., *Mechanism of salutary effects of estrogen on cardiac function following trauma-hemorrhage: Akt-dependent HO-1 up-regulation.* Crit Care Med, 2009. **37**(8): p. 2338-44.

322. Kim, Y.D., et al., *17 beta-Estradiol prevents dysfunction of canine coronary endothelium and myocardium and reperfusion arrhythmias after brief ischemia/reperfusion.* Circulation, 1996. **94**(11): p. 2901-8.

323. Kolodgie, F.D., et al., *Myocardial protection of contractile function after global ischemia by physiologic estrogen replacement in the ovariectomized rat.* J Mol Cell Cardiol, 1997. **29**(9): p. 2403-14.

324. Nelson, J.F., et al., *A longitudinal study of estrous cyclicity in aging C57BL/6J mice: I. Cycle frequency, length and vaginal cytology.* Biol Reprod, 1982. **27**(2): p. 327-39.

325. Rajesh, K.G., et al., *Hydrophilic bile salt ursodeoxycholic acid protects myocardium against reperfusion injury in a PI3K/Akt dependent pathway.* J Mol Cell Cardiol, 2005. **39**(5): p. 766-76.

326. Yu, H.P., et al., *The PI3K/Akt pathway mediates the nongenomic cardioprotective effects of estrogen following trauma-hemorrhage.* Ann Surg, 2007. **245**(6): p. 971-7.

327. Bae, S. and L. Zhang, *Gender differences in cardioprotection against ischemia/reperfusion injury in adult rat hearts: focus on Akt and protein kinase C signaling.* J Pharmacol Exp Ther, 2005. **315**(3): p. 1125-35.

328. Liu, C.J., et al., *Akt mediates 17beta-estradiol and/or estrogen receptor-alpha inhibition of LPS-induced tumor necrosis factor-alpha expression and myocardial cell apoptosis by suppressing the JNK1/2-NFkappaB pathway.* J Cell Mol Med, 2009. **13**(9B): p. 3655-67.

329. Camper-Kirby, D., et al., *Myocardial Akt activation and gender: increased nuclear activity in females versus males.* Circ Res, 2001. **88**(10): p. 1020-7.

330. Ren, J., et al., *Impact of estrogen replacement on ventricular myocyte contractile function and protein kinase B/Akt activation.* Am J Physiol Heart Circ Physiol, 2003. **284**(5): p. H1800-7.

331. Simoncini, T., et al., *Interaction of oestrogen receptor with the regulatory subunit of phosphatidylinositol-3-OH kinase.* Nature, 2000. **407**(6803): p. 538-41.

332. Mannella, P. and R.D. Brinton, *Estrogen receptor protein interaction with phosphatidylinositol 3-kinase leads to activation of phosphorylated Akt and extracellular*

signal-regulated kinase 1/2 in the same population of cortical neurons: a unified mechanism of estrogen action. J Neurosci, 2006. **26**(37): p. 9439-47.

333. Dimmeler, S., et al., *Activation of nitric oxide synthase in endothelial cells by Akt-dependent phosphorylation.* Nature, 1999. **399**(6736): p. 601-5.

334. Fulton, D., et al., *Regulation of endothelium-derived nitric oxide production by the protein kinase Akt.* Nature, 1999. **399**(6736): p. 597-601.

335. Khan, R., et al., *Augmentation of platelet and endothelial cell eNOS activity decreases sepsis-related neutrophil-endothelial cell interactions.* Shock, 2010. **33**(3): p. 242-6.

336. Kleinert, H., et al., *Estrogens increase transcription of the human endothelial NO synthase gene: analysis of the transcription factors involved.* Hypertension, 1998. **31**(2): p. 582-8.

337. Weiner, C.P., et al., *Induction of calcium-dependent nitric oxide synthases by sex hormones.* Proc Natl Acad Sci U S A, 1994. **91**(11): p. 5212-6.

338. Senftleben, U. and M. Karin, *The IKK/NF-kappa B pathway.* Crit Care Med, 2002. **30**(1 Suppl): p. S18-26.

339. Jacobs, M.D. and S.C. Harrison, *Structure of an IkappaBalpha/NF-kappaB complex.* Cell, 1998. **95**(6): p. 749-58.

340. Kapoor, A., et al., *Protective role of peroxisome proliferator-activated receptor-beta/delta in septic shock.* Am J Respir Crit Care Med, 2010. **182**(12): p. 1506-15.

341. Stein, B. and M.X. Yang, *Repression of the interleukin-6 promoter by estrogen receptor is mediated by NF-kappa B and C/EBP beta.* Mol Cell Biol, 1995. **15**(9): p. 4971-9.

342. Brown, M.A. and W.K. Jones, *NF-kappaB action in sepsis: the innate immune system and the heart.* Front Biosci, 2004. **9**: p. 1201-17.

343. Miyamoto, S. and I.M. Verma, *Rel/NF-kappa B/I kappa B story.* Adv Cancer Res, 1995. **66**: p. 255-92.

344. Parrillo, J.E., et al., *A circulating myocardial depressant substance in humans with septic shock. Septic shock patients with a reduced ejection fraction have a circulating factor that depresses in vitro myocardial cell performance.* J Clin Invest, 1985. **76**(4): p. 1539-53.

345. Zhu, H., L. Shan, and T. Peng, *Rac1 mediates sex difference in cardiac tumor necrosis factor-alpha expression via NADPH oxidase-ERK1/2/p38 MAPK pathway in endotoxemia.* J Mol Cell Cardiol, 2009. **47**(2): p. 264-74.

346. Hsieh, Y.C., et al., *Downregulation of migration inhibitory factor is critical for estrogen-mediated attenuation of lung tissue damage following trauma-hemorrhage.* Am J Physiol Lung Cell Mol Physiol, 2007. **292**(5): p. L1227-32.

347. Su, C., et al., *Testosterone enhances lipopolysaccharide-induced interleukin-6 and macrophage chemotactic protein-1 expression by activating the extracellular signal-regulated kinase 1/2/nuclear factor-kappaB signalling pathways in 3T3-L1 adipocytes.* Mol Med Rep, 2015. **12**(1): p. 696-704.

348. Atawia, R.T., et al., *Modulatory effect of silymarin on inflammatory mediators in experimentally induced benign prostatic hyperplasia: emphasis on PTEN, HIF-1alpha, and NF-kappaB.* Naunyn Schmiedebergs Arch Pharmacol, 2014. **387**(12): p. 1131-40.

349. Hatakeyama, H., et al., *Testosterone inhibits tumor necrosis factor-alpha-induced vascular cell adhesion molecule-1 expression in human aortic endothelial cells.* FEBS Lett, 2002. **530**(1-3): p. 129-32.

350. Wichmann, M.W., et al., *Incidence and mortality of severe sepsis in surgical intensive care patients: the influence of patient gender on disease process and outcome.* Intensive Care Med, 2000. **26**(2): p. 167-72.

351. Erikoglu, M., et al., *Effects of gender on the severity of sepsis.* Surg Today, 2005. **35**(6): p. 467-72.

352. Obialo, C.I., A.K. Crowell, and E.C. Okonofua, *Acute renal failure mortality in hospitalized African Americans: age and gender considerations.* J Natl Med Assoc, 2002. **94**(3): p. 127-34.

353. Eriksen, B.O. and O.C. Ingebretsen, *The progression of chronic kidney disease: a 10-year population-based study of the effects of gender and age.* Kidney Int, 2006. **69**(2): p. 375-82.

354. Weixelbaumer, K.M., et al., *Estrus cycle status defined by vaginal cytology does not correspond to fluctuations of circulating estrogens in female mice.* Shock, 2014. **41**(2): p. 145-53.

355. Esmon, C.T., *Why do animal models (sometimes) fail to mimic human sepsis?* Crit Care Med, 2004. **32**(5 Suppl): p. S219-22.

356. Rittirsch, D., L.M. Hoesel, and P.A. Ward, *The disconnect between animal models of sepsis and human sepsis.* J Leukoc Biol, 2007. **81**(1): p. 137-43.

357. Coresh, J., et al., *Prevalence of chronic kidney disease in the United States.* JAMA, 2007. **298**(17): p. 2038-47.

358. Moradi, H., D.A. Sica, and K. Kalantar-Zadeh, *Cardiovascular burden associated with uremic toxins in patients with chronic kidney disease.* Am J Nephrol, 2013. **38**(2): p. 136-48.

359. Dikow, R., et al., *Increased infarct size in uremic rats: reduced ischemia tolerance?* J Am Soc Nephrol, 2004. **15**(6): p. 1530-6.

360. Collins, A.J., et al., *US Renal Data System 2010 Annual Data Report.* Am J Kidney Dis, 2011. **57**(1 Suppl 1): p. A8, e1-526.

361. Cohen, G., M. Haag-Weber, and W.H. Horl, *Immune dysfunction in uremia.* Kidney Int Suppl, 1997. **62**: p. S79-82.

362. Lim, W.H., et al., *Uremia impairs monocyte and monocyte-derived dendritic cell function in hemodialysis patients.* Kidney Int, 2007. **72**(9): p. 1138-48.

363. Dalrymple, L.S. and A.S. Go, *Epidemiology of acute infections among patients with chronic kidney disease.* Clin J Am Soc Nephrol, 2008. **3**(5): p. 1487-93.

364. Waelchli, R., et al., *Design and preparation of 2-benzamido-pyrimidines as inhibitors of IKK.* Bioorg Med Chem Lett, 2006. **16**(1): p. 108-12.

365. Gagnon, R.F. and B. Gallimore, *Characterization of a mouse model of chronic uremia.* Urol Res, 1988. **16**(2): p. 119-26.

366. Coldewey, S.M., et al., *Erythropoietin attenuates acute kidney dysfunction in murine experimental sepsis by activation of the beta-common receptor.* Kidney Int, 2013. **84**(3): p. 482-90.

367. Gobbetti, T., et al., *Nonredundant protective properties of FPR2/ALX in polymicrobial murine sepsis.* Proc Natl Acad Sci U S A, 2014. **111**(52): p. 18685-90.

368. Chen, J., et al., *Gender dimorphism of the cardiac dysfunction in murine sepsis: signalling mechanisms and age-dependency.* PLoS One, 2014. **9**(6): p. e100631.

369. Collino, M., et al., *Beneficial effect of prolonged heme oxygenase 1 activation in a rat model of chronic heart failure.* Dis Model Mech, 2013. **6**(4): p. 1012-20.

370. Barone, F.C., et al., *Polymorphonuclear leukocyte infiltration into cerebral focal ischemic tissue: myeloperoxidase activity assay and histologic verification.* J Neurosci Res, 1991. **29**(3): p. 336-45.

371. Collino, M., et al., *Effects of a semi-synthetic N-,O-sulfated glycosaminoglycan K5 polysaccharide derivative in a rat model of cerebral ischaemia/reperfusion injury.* Thromb Haemost, 2009. **102**(5): p. 837-45.

372. Rambausek, M., et al., *Myocardial hypertrophy in rats with renal insufficiency.* Kidney Int, 1985. **28**(5): p. 775-82.

373. McDonald, H.I., et al., *Are pre-existing markers of chronic kidney disease associated with short-term mortality following acute community-acquired pneumonia and sepsis? A cohort study among older people with diabetes using electronic health records.* Nephrol Dial Transplant, 2015.

374. Li, Y., et al., *Molecular signaling mediated by angiotensin II type 1A receptor blockade leading to attenuation of renal dysfunction-associated heart failure.* J Card Fail, 2007. **13**(2): p. 155-62.

375. Curtis, B.M. and P.S. Parfrey, *Congestive heart failure in chronic kidney disease: disease-specific mechanisms of systolic and diastolic heart failure and management.* Cardiol Clin, 2005. **23**(3): p. 275-84.

376. Foley, R.N., et al., *Clinical and echocardiographic disease in patients starting end-stage renal disease therapy.* Kidney Int, 1995. **47**(1): p. 186-92.

377. Shmuely, H., et al., *Prediction of mortality in patients with bacteremia: the importance of pre-existing renal insufficiency.* Ren Fail, 2000. **22**(1): p. 99-108.

378. Chuang, S.Y., C.H. Lin, and J.Y. Fang, *Natural compounds and aging: between autophagy and inflammasome.* Biomed Res Int, 2014. **2014**: p. 297293.

379. Denic, A., R.J. Glassock, and A.D. Rule, *Structural and Functional Changes With the Aging Kidney.* Adv Chronic Kidney Dis, 2016. **23**(1): p. 19-28.

380. Henkel, T., et al., *Rapid proteolysis of I kappa B-alpha is necessary for activation of transcription factor NF-kappa B.* Nature, 1993. **365**(6442): p. 182-5.

381. Leychenko, A., et al., *Stretch-induced hypertrophy activates NFkB-mediated VEGF secretion*

in adult cardiomyocytes. PLoS One, 2011. **6**(12): p. e29055.

382. Shu, Y.S., et al., *Improvement of ventilation-induced lung injury in a rodent model by inhibition of inhibitory kappaB kinase.* J Trauma Acute Care Surg, 2014. **76**(6): p. 1417-24.

383. Kehat, I. and J.D. Molkentin, *Molecular pathways underlying cardiac remodeling during pathophysiological stimulation.* Circulation, 2010. **122**(25): p. 2727-35.

384. Diwan, V., et al., *Gender differences in adenine-induced chronic kidney disease and cardiovascular complications in rats.* Am J Physiol Renal Physiol, 2014. **307**(11): p. F1169-78.

385. Kaminska, B., *MAPK signalling pathways as molecular targets for anti-inflammatory therapy--from molecular mechanisms to therapeutic benefits.* Biochim Biophys Acta, 2005. **1754**(1-2): p. 253-62.

386. Meng, F., et al., *Akt is a downstream target of NF-kappa B.* J Biol Chem, 2002. **277**(33): p. 29674-80.

387. Ozes, O.N., et al., *NF-kappaB activation by tumour necrosis factor requires the Akt serine-threonine kinase.* Nature, 1999. **401**(6748): p. 82-5.

388. Devesa, I., et al., *Role of the transient receptor potential vanilloid 1 in inflammation and sepsis.* J Inflamm Res, 2011. **4**: p. 67-81.

389. Szallasi, A. and P.M. Blumberg, *Vanilloid (Capsaicin) receptors and mechanisms.* Pharmacol Rev, 1999. **51**(2): p. 159-212.

390. Wang, D.H., *The vanilloid receptor and hypertension.* Acta Pharmacol Sin, 2005. **26**(3): p. 286-94.

391. Holzer, P., *Local effector functions of capsaicin-sensitive sensory nerve endings: involvement of tachykinins, calcitonin gene-related peptide and other neuropeptides.* Neuroscience, 1988. **24**(3): p. 739-68.

392. Suto, B., et al., *Plasma somatostatin-like immunoreactivity increases in the plasma of septic patients and rats with systemic inflammatory reaction: experimental evidence for its sensory origin and protective role.* Peptides, 2014. **54**: p. 49-57.

393. Puneet, P., et al., *Preprotachykinin-A gene products are key mediators of lung injury in polymicrobial sepsis.* J Immunol, 2006. **176**(6): p. 3813-20.

394. Wang, Y. and D.H. Wang, *TRPV1 ablation aggravates inflammatory responses and organ damage during endotoxic shock.* Clin Vaccine Immunol, 2013. **20**(7): p. 1008-15.

395. Caterina, M.J., et al., *Impaired nociception and pain sensation in mice lacking the capsaicin receptor.* Science, 2000. **288**(5464): p. 306-13.

396. Cho, H., et al., *Novel caffeic acid derivatives: extremely potent inhibitors of 12-lipoxygenase.* J Med Chem, 1991. **34**(4): p. 1503-5.

397. Muerhoff, A.S., et al., *Prostaglandin and fatty acid omega- and (omega-1)-oxidation in rabbit lung. Acetylenic fatty acid mechanism-based inactivators as specific inhibitors.* J Biol Chem, 1989. **264**(2): p. 749-56.

398. De Winter, B.Y., et al., *Involvement of afferent neurons in the pathogenesis of endotoxin-induced ileus in mice: role of CGRP and TRPV1 receptors.* Eur J Pharmacol, 2009. **615**(1-3): p. 177-84.

399. Helyes, Z., et al., *Role of transient receptor potential vanilloid 1 receptors in endotoxin-induced airway inflammation in the mouse.* Am J Physiol Lung Cell Mol Physiol, 2007. **292**(5): p. L1173-81.

400. Wang, H.E., et al., *National estimates of severe sepsis in United States emergency departments.* Crit Care Med, 2007. **35**(8): p. 1928-36.

401. Merx, M.W. and C. Weber, *Sepsis and the heart.* Circulation, 2007. **116**(7): p. 793-802.

402. Munt, B., et al., *Diastolic filling in human severe sepsis: an echocardiographic study.* Crit Care Med, 1998. **26**(11): p. 1829-33.

403. Parker, M.M., et al., *Profound but reversible myocardial depression in patients with septic shock.* Ann Intern Med, 1984. **100**(4): p. 483-90.

404. Poelaert, J., et al., *Left ventricular systolic and diastolic function in septic shock.* Intensive Care Med, 1997. **23**(5): p. 553-60.

405. Ang, S.F., S.M. Moochhala, and M. Bhatia, *Hydrogen sulfide promotes transient receptor potential vanilloid 1-mediated neurogenic inflammation in polymicrobial sepsis.* Crit Care Med, 2010. **38**(2): p. 619-28.

406. Chen, W., et al., *Lipoxygenase metabolism of arachidonic acid in ischemic preconditioning and PKC-induced protection in heart.* Am J Physiol, 1999. **276**(6 Pt 2): p. H2094-101.

407. Patel, H.H., et al., *12-lipoxygenase in opioid-induced delayed cardioprotection: gene array,*

mass spectrometric, and pharmacological analyses. Circ Res, 2003. **92**(6): p. 676-82.

408. Tsutsumi, Y.M., et al., *Role of 12-lipoxygenase in volatile anesthetic-induced delayed preconditioning in mice.* Am J Physiol Heart Circ Physiol, 2006. **291**(2): p. H979-83.

409. Flynn, A., B. Chokkalingam Mani, and P.J. Mather, *Sepsis-induced cardiomyopathy: a review of pathophysiologic mechanisms.* Heart Fail Rev, 2010. **15**(6): p. 605-11.

410. Harada, N., et al., *Antithrombin reduces reperfusion-induced liver injury in mice by enhancing sensory neuron activation.* Thromb Haemost, 2006. **95**(5): p. 788-95.

411. Lechleitner, P., et al., *Calcitonin gene-related peptide in patients with and without early reperfusion after acute myocardial infarction.* Am Heart J, 1992. **124**(6): p. 1433-9.

412. Wei, Z., et al., *Decreased expression of transient receptor potential vanilloid 1 impaires the postischemic recovery of diabetic mouse hearts.* Circ J, 2009. **73**(6): p. 1127-32.

413. Hoyert, D.L., et al., *Deaths: final data for 1999.* Natl Vital Stat Rep, 2001. **49**(8): p. 1-113.

414. Zaky, A., et al., *Characterization of cardiac dysfunction in sepsis: an ongoing challenge.* Shock, 2014. **41**(1): p. 12-24.

415. Kanakura, H. and T. Taniguchi, *The antiinflammatory effects of propofol in endotoxemic rats during moderate and mild hypothermia.* J Anesth, 2007. **21**(3): p. 354-60.

416. Tao, W., et al., *Hemodynamic and cardiac contractile function during sepsis caused by cecal ligation and puncture in mice.* Shock, 2004. **21**(1): p. 31-7.

417. Mulder, M.F., et al., *The fall of cardiac output in endotoxemic rats cannot explain all changes in organ blood flow: a comparison between endotoxin and low venous return shock.* Shock, 1996. **5**(2): p. 135-40.

418. Hoover, D.B., et al., *Impaired heart rate regulation and depression of cardiac chronotropic and dromotropic function in polymicrobial sepsis.* Shock, 2015. **43**(2): p. 185-91.

419. Sarcia, P.J., et al., *Hypothermia induces interleukin-10 and attenuates injury in the lungs of endotoxemic rats.* Shock, 2003. **20**(1): p. 41-5.